

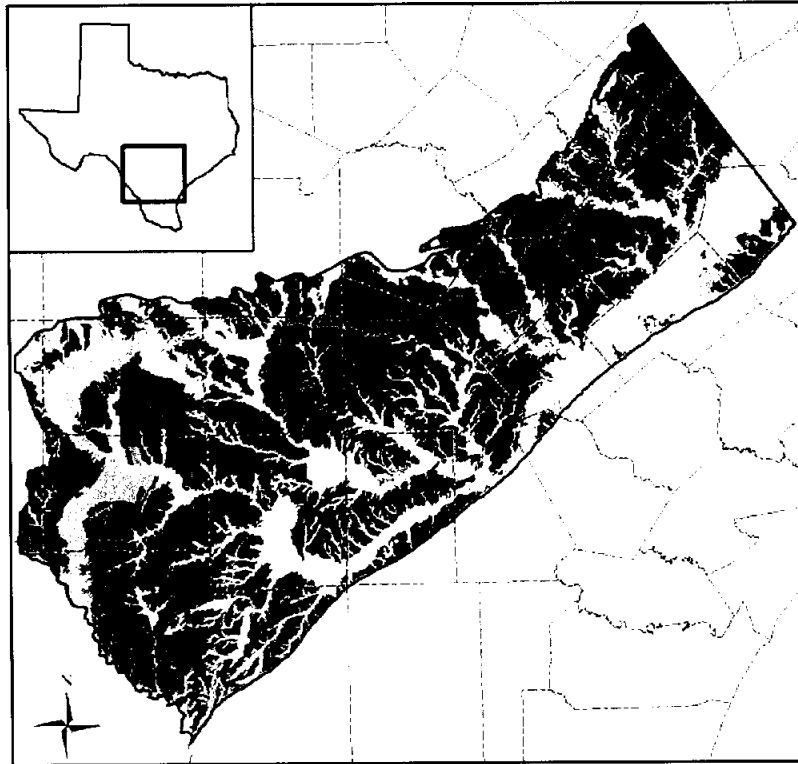
REVISIONS

3/21/03

FINAL REPORT

FWDB R&PF
GRANTS MANAGEMENT

Groundwater Availability Model for the Southern Carrizo-Wilcox Aquifer



Prepared for the:

Texas Water Development Board

Prepared by:

**Neil Deeds, Van Kelley,
Dennis Fryar, Toya Jones**

INTERA

Art J. Whallon, and Kirk E. Dean

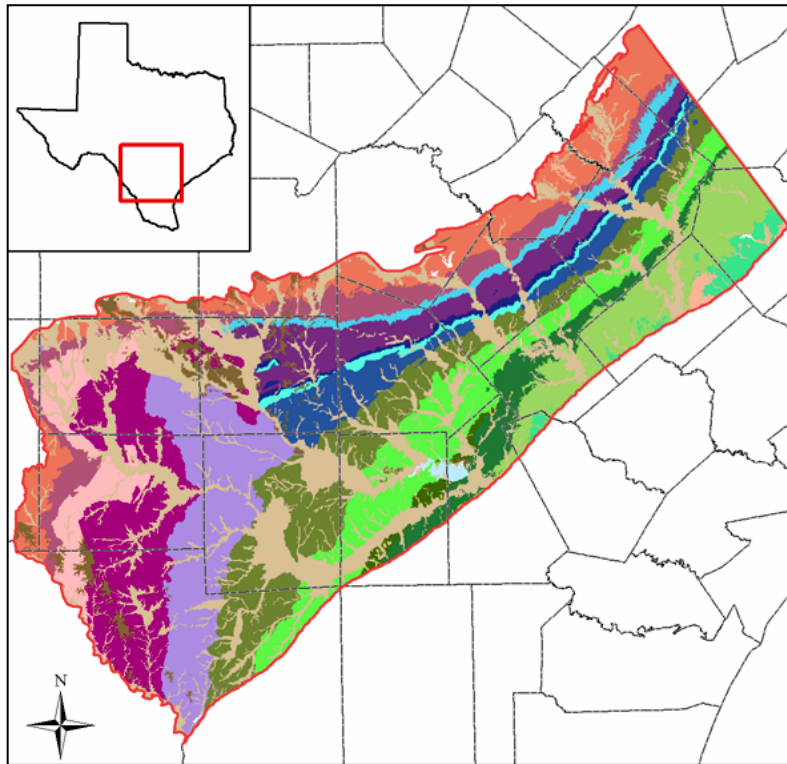
PARSONS

January 31, 2003

2001-483-381

FINAL REPORT

Groundwater Availability Model for the Southern Carrizo-Wilcox Aquifer



Prepared for the:

Texas Water Development Board

Prepared by:

**Neil Deeds, Van Kelley,
Dennis Fryar, Toya Jones**



Art J. Whallon, and Kirk E. Dean

PARSONS

January 31, 2003

TABLE OF CONTENTS

ABSTRACT	xi
1.0 INTRODUCTION.....	1-1
2.0 STUDY AREA.....	2-1
2.1 Physiography and Climate.....	2-10
2.2 Geology	2-18
3.0 PREVIOUS INVESTIGATIONS	3-1
4.0 HYDROGEOLOGIC SETTING	4-1
4.1 Hydrostratigraphy	4-1
4.2 Structure	4-5
4.3 Hydraulic Properties.....	4-25
4.3.1 Processing of the Hydraulic Property Database	4-26
4.3.2 Statistical Analysis of the Hydraulic Property Data	4-27
4.3.3 Spatial Distribution of Hydraulic Property Data	4-27
4.3.4 Relationship between Hydraulic Property and Sand Distribution.....	4-30
4.3.5 Vertical Hydraulic Conductivity.....	4-32
4.3.6 Storativity	4-33
4.4 Water Levels and Regional Groundwater Flow	4-46
4.4.1 Predevelopment Conditions for the Carrizo Sand and the Wilcox Group....	4-47
4.4.2 Pressure versus Depth Analysis.....	4-49
4.4.3 Predevelopment Conditions in the Queen City/Bigford Formations.....	4-50
4.4.4 Transient Water Levels	4-50
4.4.5 Water-Level Elevations for Model Calibration and Verification.....	4-52
4.5 Recharge	4-86
4.6 Natural Aquifer Discharge.....	4-91
4.7 Aquifer Discharge Through Pumping	4-100
4.8 Water Quality.....	4-110
5.0 CONCEPTUAL MODEL OF GROUNDWATER FLOW IN THE AQUIFER.....	5-1
6.0 MODEL DESIGN	6-1
6.1 Code and Processor.....	6-1
6.2 Model Layers and Grid.....	6-2
6.3 Boundary Condition Implementation.....	6-5
6.3.1 Lateral Model Boundaries	6-6
6.3.2 Vertical Boundaries	6-6
6.3.3 Surface Water Implementation	6-7
6.3.4 Implementation of Recharge	6-9
6.3.5 Implementation of Pumping Discharge	6-11
6.4 Model Hydraulic Parameters	6-18
6.4.1 Hydraulic Conductivity	6-18
6.4.2 Storativity	6-21

TABLE OF CONTENTS (CONTINUED)

7.0	MODELING APPROACH.....	7-1
7.1	Calibration	7-1
7.2	Calibration Target Uncertainty	7-5
7.3	Sensitivity Analyses	7-6
7.4	Predictions	7-6
8.0	STEADY-STATE MODEL.....	8-1
8.1	Calibration	8-1
8.1.1	Horizontal and Vertical Hydraulic Conductivities	8-1
8.1.2	Recharge.....	8-3
8.1.3	Groundwater Evapotranspiration.....	8-3
8.1.4	General Head Boundaries.....	8-4
8.1.5	Streams	8-5
8.2	Results	8-17
8.2.1	Heads.....	8-17
8.2.2	Streams.....	8-18
8.2.3	Water Budget.....	8-18
8.3	Sensitivity Analysis.....	8-30
9.0	TRANSIENT MODEL.....	9-1
9.1	Calibration	9-1
9.2	Results	9-6
9.2.1	Hydraulic Heads	9-6
9.2.2	Stream-Aquifer Interaction.....	9-9
9.2.3	Water Budget.....	9-10
9.3	Sensitivity Analysis.....	9-31
10.0	MODEL PREDICTIVE SIMULATIONS.....	10-1
10.1	Drought of Record	10-1
10.2	Predictive Simulation Results.....	10-8
10.3	Predictive Simulation Water Budget.....	10-37
11.0	LIMITATIONS OF THE MODEL.....	11-1
11.1	Limitations of Supporting Data	11-1
11.2	Limiting Assumptions	11-3
11.3	Limits for Model Applicability.....	11-5
12.0	FUTURE IMPROVEMENTS.....	12-1
12.1	Supporting Data	12-1
12.2	Future Model Improvements	12-2
13.0	CONCLUSIONS.....	13-1
14.0	ACKNOWLEDGEMENTS	14-1
15.0	REFERENCES.....	15-1

LIST OF FIGURES

Figure 2.1	Location of the three Carrizo-Wilcox GAMs.....	2-4
Figure 2.2	Location of study area showing county boundaries, cities, lakes, and rivers.	2-5
Figure 2.3	Areal extent of the major aquifers in the study area.	2-6
Figure 2.4	Location of Regional Water Planning Groups in the study area.	2-7
Figure 2.5	Location of Groundwater Conservation Districts in the study area.....	2-8
Figure 2.6	Major river basins in the study area.	2-9
Figure 2.7	Topographic map of the study area.....	2-12
Figure 2.8	Ecological regions within the study area.....	2-13
Figure 2.9	Average annual net pan evaporation rate in inches per year.	2-14
Figure 2.10	Location of precipitation gages in the study area (Period of Record is 1900 to 1999).	2-15
Figure 2.11	Average annual precipitation (1961-1990) over the study area in inches per year (Source: Oregon Climate Service, Oregon State University, PRISM data set).	2-16
Figure 2.12	Annual precipitation time series for gages in Bexar, Fayette, Frio, Karnes, and Webb counties.....	2-17
Figure 2.13	Surface geology of the study area.	2-20
Figure 2.14	Generalized stratigraphic section for the Carrizo-Wilcox aquifer in Texas (after Ayers and Lewis, 1985; Hamlin, 1988; Kaiser et al., 1978).	2-21
Figure 2.15	Structural cross-sections in the study area (after Hamlin, 1988).	2-22
Figure 3.1	Southern Carrizo-Wilcox GAM model boundary with previous modeling study boundaries which have included the Carrizo-Wilcox aquifer.	3-5
Figure 4.1.1	Hydrostratigraphy and model layers.	4-4
Figure 4.2.1	Structural setting of the study area.....	4-10
Figure 4.2.2	Structure contour map of the base of the Wilcox Group.....	4-11
Figure 4.2.3	Structure contour map of the top of the lower Wilcox.....	4-12
Figure 4.2.4	Structure contour map of the top of the middle Wilcox.....	4-13
Figure 4.2.5	Structure contour map of the top of the Wilcox Group.....	4-14
Figure 4.2.6	Structure contour map of the top of the Carrizo.	4-15
Figure 4.2.7	Structure contour map of the top of the Reklaw/Bigford formations.	4-16
Figure 4.2.8	Structure contour map of the top of the Queen City/El Pico.....	4-17
Figure 4.2.9	Thickness map of the lower Wilcox.....	4-18
Figure 4.2.10	Thickness map of the middle Wilcox.....	4-19
Figure 4.2.11	Thickness map of the upper Wilcox.....	4-20
Figure 4.2.12	Thickness map of the Carrizo.	4-21
Figure 4.2.13	Thickness map of the Reklaw/Bigford.....	4-22
Figure 4.2.14	Thickness map of the Queen City/El Pico.....	4-23
Figure 4.2.15	Thickness map of younger sediments overlying the Queen City.	4-24
Figure 4.3.1	Screening of hydraulic conductivity data.	4-35

LIST OF FIGURES (CONTINUED)

Figure 4.3.2	CDF curves of hydraulic conductivity for the modeled aquifer units.....	4-36
Figure 4.3.3	Variogram for hydraulic conductivity data for the lower Wilcox.	4-37
Figure 4.3.4	Variogram and kriged map of hydraulic conductivity for the lower Wilcox.....	4-38
Figure 4.3.5	Variogram and kriged map of hydraulic conductivity for the middle Wilcox.....	4-39
Figure 4.3.6	Variogram and kriged map of hydraulic conductivity for the Carrizo.....	4-40
Figure 4.3.7	Variogram and kriged map of hydraulic conductivity for the Queen- City.	4-41
Figure 4.3.8	Histogram of net-sand thickness for the Carrizo-upper Wilcox and maximum sand thickness of the Carrizo-upper Wilcox and hydraulic conductivity (Log K).	4-42
Figure 4.3.9	Histogram of sand percent for the Carrizo- upper Wilcox and the log of hydraulic conductivity (Log K).....	4-43
Figure 4.3.10	Percent sand for the Carrizo.	4-44
Figure 4.3.11	Percent sand for the upper Wilcox.	4-45
Figure 4.4.1	Water-level measurement locations for the Carrizo-Wilcox aquifer.	4-70
Figure 4.4.2	Predevelopment water-level elevations for the Carrizo-Wilcox aquifer.	4-71
Figure 4.4.3	Difference in predevelopment water-level elevation contours between adjusted and not adjusted water levels.....	4-72
Figure 4.4.4	Water-level measurement locations used for pressure-depth analysis.....	4-73
Figure 4.4.5	Pressure versus depth analysis results.	4-74
Figure 4.4.6	Predevelopment water-level elevation contours for the Queen City/Bigford formations.....	4-75
Figure 4.4.7	Water-level decline in the Carrizo –upper Wilcox from predevelopment to 1980.....	4-76
Figure 4.4.8	Model layer for locations with transient water-level data.	4-77
Figure 4.4.9	Example hydrographs for wells located in Bastrop, Caldwell, Gonzales, Guadalupe, and northern Wilson counties.....	4-78
Figure 4.4.10	Example hydrographs for wells in southern Wilson County and Karnes and Live Oak counties.	4-79
Figure 4.4.11	Example hydrographs for wells in the outcrop areas of Atascosa, Medina, Frio, Zavala, Maverick, and Dimmit counties.....	4-80
Figure 4.4.12	Example hydrographs for wells in the downdip areas of Atascosa, Frio, and Zavala counties.	4-81
Figure 4.4.13	Example hydrographs for wells in McMullen, La Salle, Webb, and the downdip area of Dimmit counties.....	4-82
Figure 4.4.14	Water-level elevation contours for the Carrizo-Wilcox aquifer at the start of model calibration (January 1980).	4-83
Figure 4.4.15	Water-level elevation contours for the Carrizo-Wilcox aquifer at the end model calibration (December 1989).	4-84
Figure 4.4.16	Water-level elevation contours for the Carrizo-Wilcox aquifer at the end model verification (December 1999).	4-85
Figure 4.5.1	Hydrographs for reservoirs in the Carrizo-Wilcox outcrop.....	4-90
Figure 4.6.1	Stream gain/loss studies in the study area (after Slade et al. 2002).....	4-98

LIST OF FIGURES (CONTINUED)

Figure 4.6.2	Documented spring locations in the study area.	4-99
Figure 4.7.1	Rural population density in the study area.	4-106
Figure 4.7.2	Younger (Layer 1) Pumpage, 1990 (AFY).....	4-107
Figure 4.7.3	Reklaw (Layer 2) Pumpage, 1990 (AFY).	4-107
Figure 4.7.4	Carrizo (Layer 3) Pumpage, 1990 (AFY).....	4-108
Figure 4.7.5	Upper Wilcox (Layer 4) Pumpage, 1990 (AFY).	4-108
Figure 4.7.6	Middle Wilcox (Layer 5) Pumpage, 1990 (AFY).....	4-109
Figure 4.7.7	Lower Wilcox (Layer 6) Pumpage, 1990 (AFY).....	4-109
Figure 5.1	Conceptual groundwater flow model for the Southern Carrizo- Wilcox GAM.	5-5
Figure 5.2	Schematic diagram of transient relationships between recharge rates, discharge rates, and withdrawal rates (from Freeze, 1971).	5-6
Figure 6.2.1	Southern Carrizo-Wilcox GAM model grid.	6-4
Figure 6.3.1	Layer 1 (Queen City) boundary conditions and active/inactive cells.	6-12
Figure 6.3.2	Layer 2 (Reklaw) boundary conditions and active/inactive cells.	6-13
Figure 6.3.3	Layer 3 (Carrizo) boundary conditions and active/inactive cells.	6-14
Figure 6.3.4	Layer 4 (upper Wilcox) boundary conditions and active/inactive cells.	6-15
Figure 6.3.5	Layer 5 (middle Wilcox) boundary conditions and active/inactive cells.	6-16
Figure 6.3.6	Layer 6 (lower Wilcox) boundary conditions and active/inactive cells.	6-17
Figure 8.1.1	Calibrated horizontal hydraulic conductivity field for the El Pico/Queen City (Layer 1).	8-7
Figure 8.1.2	Calibrated horizontal hydraulic conductivity field for Bigford/Reklaw (Layer 2).....	8-8
Figure 8.1.3	Calibrated horizontal hydraulic conductivity field for the Carrizo (Layer 3).....	8-9
Figure 8.1.4	Calibrated horizontal hydraulic conductivity field for the upper Wilcox (Layer 4).	8-10
Figure 8.1.5	Calibrated horizontal hydraulic conductivity field for middle Wilcox (Layer 5).....	8-11
Figure 8.1.6	Calibrated horizontal hydraulic conductivity field for the lower Wilcox (Layer 6).	8-12
Figure 8.1.7	Comparison between initial recharge and the calibrated recharge.	8-13
Figure 8.1.8	Steady-state calibrated recharge (in/year).	8-14
Figure 8.1.9	Steady-state groundwater ET maximum (in/year).	8-15
Figure 8.1.10	Steady-state calibrated GHB conductance.	8-16
Figure 8.2.1	Simulated steady-state head surface, residuals and scatterplot for the Queen City/El Pico (Layer 1).....	8-21
Figure 8.2.2	Simulated steady-state head surface and posted residuals for the Reklaw/Bigford (Layer 2).....	8-22
Figure 8.2.3	Simulated steady-state head surface, residuals and scatterplot for the Carrizo (Layer 3).	8-23
Figure 8.2.4	Simulated (a) and observed (b) steady-state head surfaces for the Carrizo (Layer 3).....	8-24

LIST OF FIGURES (CONTINUED)

Figure 8.2.5	Simulated steady-state head surface and posted residuals for the upper Wilcox (Layer 4).....	8-25
Figure 8.2.6	Simulated steady-state head surface and posted residuals for the middle Wilcox (Layer 5).....	8-26
Figure 8.2.7	Simulated steady-state head surface and posted residuals for the lower Wilcox (Layer 6).....	8-27
Figure 8.2.8	Steady-state model stream gain/loss (negative value denotes gaining stream).	8-28
Figure 8.2.9	Steady-state particle travel path and travel time (20,000 years) compared to the groundwater age dating study of Pearson and White (1967).....	8-29
Figure 8.3.1	Steady-state sensitivity results for the Carrizo (Layer 3) using target locations.	8-33
Figure 8.3.2	Steady-state sensitivity results for the Carrizo (Layer 3) using all active gridblocks.....	8-33
Figure 8.3.3	Steady-state sensitivity results for the Queen City/El Pico (Layer 1) using all active gridblocks.	8-34
Figure 8.3.4	Steady-state sensitivity results for the Reklaw/Bigford (Layer 2) using all active gridblocks.	8-34
Figure 8.3.5	Steady-state sensitivity results where GHB conductivity is varied.	8-35
Figure 8.3.6	Steady-state sensitivity results for the middle Wilcox (Layer 5) using all active gridblocks.....	8-35
Figure 8.3.7	Steady-state sensitivity results for the lower Wilcox (Layer 6) using all active gridblocks.....	8-36
Figure 8.3.8	Steady-state sensitivity results where recharge is varied.	8-36
Figure 9.1.1	Example of head sensitivity to Reklaw vertical hydraulic conductivity.....	9-4
Figure 9.1.2	Example of head sensitivity to specific storage.....	9-4
Figure 9.1.3	Storativity in the Carrizo Formation (Layer 3).....	9-5
Figure 9.2.1	Comparison between 1989 measured (a) and simulated (b) heads in the Carrizo formation (Layer 3).	9-16
Figure 9.2.2	Comparison between 1999 measured (a) and simulated (b) heads in the Carrizo formation (Layer 3).	9-17
Figure 9.2.3	Locations of hydrograph wells for the transient model.....	9-18
Figure 9.2.4	Calibration period (a) and verification period (b) crossplots for the Carrizo formation (Layer 3) in the calibrated transient model.	9-19
Figure 9.2.5	Calibration period crossplots for the calibrated transient model.	9-20
Figure 9.2.6	Verification period crossplots for the calibrated transient model.....	9-21
Figure 9.2.7	Transient model hydrographs from the Queen City/El Pico (Layer 1).....	9-22
Figure 9.2.8	Transient model hydrographs from the Carrizo (Layer 3), West.....	9-23
Figure 9.2.9	Transient model hydrographs from the Carrizo (Layer 3), Central.	9-24
Figure 9.2.10	Transient model hydrographs from the Carrizo (Layer 3), East.....	9-25
Figure 9.2.11	Transient model hydrographs from the upper Wilcox (Layer 4).....	9-26
Figure 9.2.12	Transient model hydrographs from the middle Wilcox (Layer 5).....	9-27
Figure 9.2.13	Transient model hydrographs from the lower Wilcox (Layer 6).....	9-28

LIST OF FIGURES (CONTINUED)

Figure 9.2.14	Average residuals for the verification period (1990-1999) in the Carrizo Formation (Layer 3).	9-29
Figure 9.2.15	Comparison of Slade et al. (2002) with average simulated stream gain/loss.	9-30
Figure 9.3.1	Transient sensitivity results for the Carrizo (Layer 3) using target locations.	9-34
Figure 9.3.2	Transient sensitivity results for the Carrizo (Layer 3) using all active gridblocks.	9-34
Figure 9.3.3	Transient sensitivity results for the Queen City/El Pico (Layer 1) using all active gridblocks.	9-35
Figure 9.3.4	Transient sensitivity results for the Reklaw/Bigford (Layer 2) using all active gridblocks.	9-35
Figure 9.3.5	Transient sensitivity results for the upper Wilcox (Layer 4) using all active gridblocks.	9-36
Figure 9.3.6	Transient sensitivity results for the middle Wilcox (Layer 5) using all active gridblocks.	9-36
Figure 9.3.7	Transient sensitivity results for the lower Wilcox (Layer 6) using all active gridblocks.	9-37
Figure 9.3.8	Transient sensitivity results where the horizontal hydraulic conductivities for all layers are varied.	9-37
Figure 9.3.9	Transient sensitivity results where recharge is varied.	9-38
Figure 9.3.10	Transient sensitivity results where specific yield is varied.	9-38
Figure 9.3.11	Transient sensitivity hydrographs from the Carrizo (Layer 3) where the horizontal hydraulic conductivities for all layers are varied.	9-39
Figure 9.3.12	Transient sensitivity hydrographs from the Carrizo (Layer 3) where pumping rate is varied.	9-40
Figure 10.1.1	Standard precipitation index (SPI) curves for the Dilley rain gage (#412458-Frio Co.) for 1 month, 1 year, 2 year, and 3 year time periods.	10-5
Figure 10.1.2	Standardized precipitation indices for precipitation gages in the region.	10-6
Figure 10.1.3	Standardized precipitation index averaged for all gages in the region from 1950-1960.	10-7
Figure 10.2.1	Simulated 2000 (a) and 2050 (b) head surfaces, Queen City/El Pico (Layer 1).	10-12
Figure 10.2.2	Difference between 2000 and 2050 simulated head surfaces, Queen City/El Pico (Layer 1).	10-13
Figure 10.2.3	Simulated 2000 (a) and 2050 (b) head surfaces, Carrizo (Layer 3).	10-14
Figure 10.2.4	Difference between 2000 and 2050 simulated head surfaces, Carrizo (Layer 3).	10-15
Figure 10.2.5	Simulated 2000 (a) and 2050 (b) head surfaces, upper Wilcox (Layer 4).	10-16
Figure 10.2.6	Difference between 2000 and 2050 simulated head surfaces, upper Wilcox (Layer 4).	10-17
Figure 10.2.7	Simulated 2000 (a) and 2050 (b) head surfaces, middle Wilcox (Layer 5).	10-18

LIST OF FIGURES (CONTINUED)

Figure 10.2.8	Difference between 2000 and 2050 simulated head surfaces, middle Wilcox (Layer 5).	10-19
Figure 10.2.9	Simulated 2000 (a) and 2050 (b) head surfaces, lower Wilcox (Layer 6).....	10-20
Figure 10.2.10	Difference between 2000 and 2050 simulated head surfaces, lower Wilcox (Layer 6).	10-21
Figure 10.2.11	Simulated 2010 head surface (a) and drawdown from 2000 (b) for the Carrizo (Layer 3).	10-22
Figure 10.2.12	Simulated 2020 head surface (a) and drawdown from 2000 (b) for the Carrizo (Layer 3).	10-23
Figure 10.2.13	Simulated 2030 head surface (a) and drawdown from 2000 (b) for the Carrizo (Layer 3).	10-24
Figure 10.2.14	Simulated 2040 head surface (a) and drawdown from 2000 (b) for the Carrizo (Layer 3).	10-25
Figure 10.2.15	Simulated 2010 (a) and 2020 (b) head surface, upper Wilcox (Layer 4).....	10-26
Figure 10.2.16	Simulated 2030 (a) and 2040 (b) head surface, upper Wilcox (Layer 4).....	10-27
Figure 10.2.17	Simulated 2010 (a) and 2020 (b) head surface, middle Wilcox (Layer 5).....	10-28
Figure 10.2.18	Simulated 2030 (a) and 2040 (b) head surface, middle Wilcox (Layer 5).....	10-29
Figure 10.2.19	Selected hydrographs from predictive simulation to 2050 with the DOR.....	10-30
Figure 10.2.20	Simulated difference in head surfaces for the Carrizo between the average condition 2050 simulation and the drought of record 2050 simulation.....	10-31
Figure 10.2.21	Simulated difference in head surfaces for the middle Wilcox between the average condition 2050 simulation and the drought of record 2050 simulation.	10-32
Figure 10.2.22	Simulated difference in head surfaces for the lower Wilcox between the average condition 2050 simulation and the drought of record 2050 simulation.	10-33
Figure 10.2.23	Simulated saturated thickness in the outcrop at year 2000.....	10-34
Figure 10.2.24	Simulated saturated thickness in the outcrop at year 2050.....	10-35
Figure 10.2.25	Difference between the 2010 base simulation and the 2010 simulation including the Twin Oaks Project in Bexar County.	10-36

LIST OF TABLES

Table 2.1	River basins in the Southern Carrizo-Wilcox GAM study area.....	2-3
Table 3.1	Previous groundwater models of the Carrizo-Wilcox aquifer in the study area.	3-2
Table 4.2.1	Data sources for layer elevations for the southern Carrizo-Wilcox model.	4-9
Table 4.3.1	Summary statistics for horizontal hydraulic conductivity	4-27
Table 4.3.2	Summary of literature estimates of Carrizo-Wilcox specific yield.	4-34
Table 4.4.1	Summary of data used to generate the predevelopment water-level elevation contours for the Carrizo Formation and the Wilcox Group.....	4-53
Table 4.4.2	Summary of data used to generate the predevelopment water-level elevation contours for the Queen City and Bigford formations.	4-54
Table 4.4.3	Data used to generate water-level elevation contours for the start of model calibration (January 1980).	4-55
Table 4.4.4	Data used to generate water-level elevation contours for the end of model calibration (December 1989).	4-61
Table 4.4.5	Data used to generate water-level elevation contours for the end of model verification (December 1999).	4-66
Table 4.5.1	Review of recharge rates for the Carrizo-Wilcox aquifer in Texas (after Scanlon et al., 2002).	4-88
Table 4.5.2	Potential recharge rates for the Carrizo-Wilcox (after LBG-Guyton and HDR, 1998).	4-89
Table 4.6.1	Stream flow gain/loss studies in the study area (after Slade et al., 2002, Table 1).	4-95
Table 4.6.2	Documented springs in the study area.	4-97
Table 4.7.1	Rate of groundwater withdrawal (AFY) from all model layers of the Carrizo-Wilcox aquifer for counties within the study area.....	4-105
Table 8.1.1	Calibrated hydraulic conductivity values for the steady-state model (ft/day).	8-6
Table 8.2.1	Steady-state head calibration statistics.	8-17
Table 8.2.2	Water budget for the steady-state model (AFY).	8-20
Table 8.2.3	Water budget for the steady-state model with values expressed as a percentage of inflow or outflow.	8-20
Table 9.2.1	Calibration statistics for the transient model for the calibration and verification periods.	9-12
Table 9.2.2	Calibration statistics for the hydrographs shown in Figures 9.2.7-9.2.13.	9-13
Table 9.2.3	Comparison of simulated stream leakance to LBG-Guyton and HDR (1998) simulated values (AFY per mile of stream).....	9-14
Table 9.2.4	Water budget for the transient model. All rates reported in AFY.	9-15
Table 10.1	SPI Precipitation Deficit Classification System (Hayes, 2001).	10-3
Table 10.3.1	Water budget for predictive simulations, AFY.	10-38

APPENDICES

Appendix A	Brief Summary of the Development of the Carrizo-Wilcox Aquifer in Each County and List of Reviewed Reports
Appendix B	Standard Operating Procedures (SOPs) for Processing Historical Pumpage Data TWDB Groundwater Availability Modeling (GAM) Projects
Appendix C	Standard Operating Procedures (SOPs) for Processing Predictive Pumpage Data TWDB Groundwater Availability Modeling (GAM) Projects
Appendix D1	Tabulated Groundwater Withdrawal Estimates for the Carrizo-Wilcox for 1980, 1990, 2000, 2010, 2020, 2030, 2040, and 2050
Appendix D2	Post Plots of Groundwater Withdrawal Estimates for the Carrizo-Wilcox for 1980, 1990, 2000, 2010, 2020, 2030, 2040, and 2050
Appendix D3	Carrizo-Wilcox Groundwater Withdrawal Distributions by County
Appendix E	Using SWAT with MODFLOW in a Decoupled Environment
Appendix F	Water Quality
Appendix G	Draft Report Comments and Responses

ABSTRACT

This report documents a three-dimensional groundwater model developed for the southern Carrizo-Wilcox aquifer in southwest and south-central Texas. The model was developed using MODFLOW and includes the Carrizo-Wilcox aquifer, the Reklaw/Bigford Formations, and the Queen City/El Pico Clay Formations. The purpose of this model is to provide a tool for making predictions of groundwater availability. The model has been calibrated to predevelopment conditions (prior to significant resource use) which are considered to be at steady state. The steady-state model reproduces the predevelopment aquifer heads well within the estimated head uncertainty. The model was also calibrated to transient aquifer conditions from 1980 through December 1989 reproducing aquifer heads and available estimates of aquifer-stream interaction. The transient-calibrated model was verified by simulating aquifer conditions from 1990 through December 1999 and comparing to observed aquifer heads and available estimates of aquifer-stream interaction for that time period.

The verified model was used to make predictions of aquifer conditions for the next 50 years based upon projected pumping demands as developed by the Regional Water Planning Groups. The pumping demand estimates developed from the regional water plans predicted a significant decline in Carrizo-Wilcox pumping demand starting in 2000. This decline is approximately 100,000 AFY. As a result of the predicted pumping declines, the model predicts that Carrizo-Wilcox water levels will rebound in the western model region where groundwater pumping was decreased. The eastern portion of the model shows gradual water-level decline as pumping demand generally increases in that part of the model. Pumping associated with potential future Laredo pumping (14,000 AFY) of the Carrizo-Wilcox in Northern Webb County created a local drawdown cone of over 100 feet by 2050.

This model provides an integrated tool for the assessment of water management strategies to directly benefit state planners, Regional Water Planning Groups (RWPGs), and Groundwater Conservation Districts (GCDs). The model is applicable for the assessment of groundwater availability on a regional scale (e.g., tens of miles). The model is not applicable for predicting conditions at an individual well and may not be applicable for determining operational details for particular water resource strategies without refinement. The model is ideally suited for refinement as it has been developed using a constant grid-block spacing of one square mile.

Surface-groundwater interaction has been modeled in a first-order analysis method and this GAM should not be used solely as a surface water assessment tool.

1.0 INTRODUCTION

The Carrizo-Wilcox aquifer is classified as a major aquifer in Texas (Ashworth and Hopkins, 1995) ranking third in the state for water use (430,000 acre-feet per year [AFY]) in 1997 behind the Gulf Coast aquifer and the Ogallala aquifer (TWDB, 2002). The aquifer extends from the Rio Grande in South Texas to East Texas and continues into Louisiana and Arkansas. The Carrizo-Wilcox aquifer provides water to all or parts of 60 Texas counties with the greatest historical use being in and around the Tyler, Lufkin-Nacogdoches, and Bryan-College Station metropolitan centers and in the Wintergarden region of South Texas (Ashworth and Hopkins, 1995).

The Texas Water Code codified the requirement for the development of a State Water Plan that allows for the development, management, and conservation of water resources and the preparation and response to drought, while maintaining sufficient water available for the citizens of Texas (TWDB, 2002). Senate Bill 1 and subsequent legislation directed the TWDB to coordinate regional water planning with a process based upon public participation. Also as a result of Senate Bill 1, the approach to water planning in the state of Texas has shifted from a water-demand based allocation approach to an availability-based approach.

Groundwater models provide a tool to estimate groundwater availability for various water use strategies and to determine the cumulative effects of increased water use and drought. A groundwater model is a numerical representation of the aquifer system capable of simulating historical and predicting future aquifer conditions. Inherent to the groundwater model, are a set of equations which are developed and applied to describe the physical processes considered to be controlling groundwater flow in the aquifer system. It can be argued that groundwater models are essential to performing complex analyses and in making informed predictions and related decisions (Anderson and Woessner, 1992). As a result, development of Groundwater Availability Models (GAMs) for the major Texas aquifers is integral to the state water planning process. The purpose of the GAM program is to provide a tool that can be used to develop reliable and timely information on groundwater availability for the citizens of Texas and to ensure adequate supplies or recognize inadequate supplies over a 50-year planning period.

The Southern Carrizo-Wilcox GAM has been developed using a modeling protocol which is standard to the groundwater model industry. This protocol includes; (1) the

development of a conceptual model for groundwater flow in the aquifer, (2) model design, (3) model calibration, (4) model verification, (5) sensitivity analysis, (6) model prediction, and (7) reporting. The conceptual model is a conceptual description of the physical processes which govern groundwater flow in the aquifer system. We reviewed the available data and reports for the model area in the conceptual model development stage. Model design is the process used to translate the conceptual model into a physical model, in this case a numerical model of groundwater flow. This involved organizing and distributing model parameters, developing a model grid and model boundary conditions, and determining the model integration time scale. Model calibration is the process of modifying model parameters so that observed field measurements (e.g., groundwater levels in wells) can be reproduced. The model was calibrated to predevelopment conditions (prior to significant resource use) which are considered to be at steady-state and to transient aquifer conditions from 1980 through 1990. Model verification is the process of using the calibrated model to reproduce observed field measurements not used in the calibration to test the model's predictive ability. The model was verified against measured aquifer conditions from 1990 through 1999. Sensitivity analyses were performed on both the steady-state and transient models to offer insight on the uniqueness of the model and the uncertainty in model parameter estimates. Model predictions were performed from 2000 to 2050 to estimate aquifer conditions for the next 50 years based upon projected pumping demands developed by the Regional Water Planning Groups. This report documents the modeling process and results from conceptual model development through predictions according to standard requirements specified by the TWDB in their Request for Qualifications. The model and associated data files are publicly available. These files, along with this report, are available at the TWDB GAM website at <http://www.twdb.state.tx.us/GAM>.

Consistent with state water planning policy, the Southern Carrizo-Wilcox GAM was developed with the support of stakeholders through quarterly stakeholder forums. The purpose of this GAM is to provide a tool for Regional Water Planning Groups, Groundwater Conservation Districts, River Authorities, and state planners for the evaluation of groundwater availability and to support the development of water management strategies and drought planning. The South Central Texas Regional Water Planning Group (Region L) area coincides with a large percent of the model area. Region L seeks to meet 25% of their water needs in 2050

by newly developed groundwater supplies with the bulk of these new supplies originating from the Carrizo-Wilcox aquifer. The GAM provides a tool for use in assessing these strategies.

2.0 STUDY AREA

The Carrizo-Wilcox aquifer is comprised of hydraulically connected sands from the Wilcox Group and the Carrizo Formation of the Claiborne Group (Ashworth and Hopkins, 1995). The Carrizo-Wilcox aquifer extends across Texas from the Rio Grande in the southwest to the Sabine River in the northeast and beyond into Louisiana and Arkansas. The Carrizo-Wilcox aquifer is classified as a major aquifer in Texas providing groundwater resources to all or part of 60 Texas counties (Ashworth and Hopkins, 1995).

Because of its large size, the Carrizo-Wilcox aquifer was divided by the TWDB for modeling purposes into three areas, with each being modeled separately. The three Carrizo-Wilcox GAMs are the Northern Carrizo-Wilcox GAM, the Central Carrizo-Wilcox GAM, and the Southern Carrizo-Wilcox GAM (Figure 2.1). These models have significant overlap areas as shown in Figure 2.1. This study documents the Southern Carrizo-Wilcox GAM. The model area is shown in Figure 2.2 and includes all or parts of Atascosa, Bastrop, Bee, Bexar, Caldwell, DeWitt, Dimmit, Duval, Fayette, Frio, Gonzales, Guadalupe, Karnes, La Salle, Lavaca, Live Oak, Maverick, McMullen, Medina, Uvalde, Webb, Wilson, and Zavala counties. Figure 2.3 shows the surface outcrop and downdip subcrop of the major aquifers in the study area.

Groundwater model boundaries are typically defined on the basis of surface or groundwater hydrologic boundaries. The model area for the Southern Carrizo-Wilcox GAM is bounded laterally on the northeast by the surface water basin divide between the Guadalupe and Colorado rivers and to the southwest by the Rio Grande. The basin divide serves as a model boundary in the outcrop (presumed groundwater flow divide) and was extended into the subsurface to the down-dip boundary of the model. The upper model boundary was defined by the ground surface in the outcrop of the Carrizo-Wilcox aquifer extending south to the extent of the Queen City/El Pico outcrop. The lower-model boundary is the base of the Wilcox Group representing the top of the Midway Formation. The down-dip boundary of the Carrizo-Wilcox aquifer extends past the limits of fresh water to the updip limit of the Wilcox growth fault zone (Bebout et al., 1982).

The study area encompasses all or part of five regional water-planning areas (Figure 2.4): (1) the Lower Colorado Region (Region K), (2) the South Central Texas Region (Region L), (3) the Rio Grande Region (Region M), (4) the Coastal Bend Region (Region N), and the

(5) Lavaca Region (Region P). The study area includes all or parts of the following Groundwater Conservation Districts (Figure 2.5): (1) the Bee Groundwater Conservation District, (2) the Edwards Aquifer Authority, (3) the Evergreen Underground Water Conservation District, (4) Fayette County Groundwater Conservation District, (5) the Gonzales County Underground Water Conservation District, (6) the Guadalupe County Groundwater Conservation District, (7) the Lavaca County Groundwater Conservation District, (8) the Live Oak Underground Water Conservation District, (9) the Lost Pines Groundwater Conservation District, (10) the McMullen Groundwater Conservation District, (11) the Medina County Groundwater Conservation District, (12) Pecan Valley Groundwater Conservation District, (13) the Plum Creek Conservation District, (14) the Uvalde County Underground Water Conservation District, and (15) the Wintergarden Groundwater Conservation District. The model study area also contains the southernmost extension of the Bexar Metropolitan Water District.

The study area also intersects six river authorities; (1) Lower Colorado River Authority, (2) Guadalupe-Blanco River Authority, (3) Lavaca-Navidad River Authority, (4) Nueces River Authority, (5) Rio Grande River Authority, and the (6) San Antonio River Authority. Figure 2.6 shows the major river basins in the study area.

The model area intersects six major river basins from west to east: (1) the Rio Grande, (2) the Nueces, (3) the San Antonio, (4) the Guadalupe, (5) the Colorado, and the Lavaca. Of these, the Rio Grande and the Colorado River originate outside of Texas. Climate is a major control on flow in rivers and streams. The primary climactic factors are precipitation and evaporation. In general flow in rivers in the western portion of the model area is episodic with extended periods of low flow, or no flow conditions. These rivers tend to lose water to the underlying formations on average. In contrast, in the eastern portion of the study area, rivers and streams are perennial and tend to gain flow from the underlying geology.

Table 2.1 provides a listing of the river basins in the study area along with the river length in Texas, the river basin area in Texas, and the number of major reservoirs within the river basin in Texas (BEG, 1976).

Table 2.1 River basins in the Southern Carrizo-Wilcox GAM study area.

River Basin	Texas River Length (mi)	Texas River Basin Drainage Area (square miles)	Number of Major Reservoirs
Rio Grande	1,250	48,259	3
Nueces	315	16,950	2
San Antonio	225	4,180	2
Guadalupe	250	6,070	2
Colorado	600	39,893	11
Lavaca	74	2,309	1

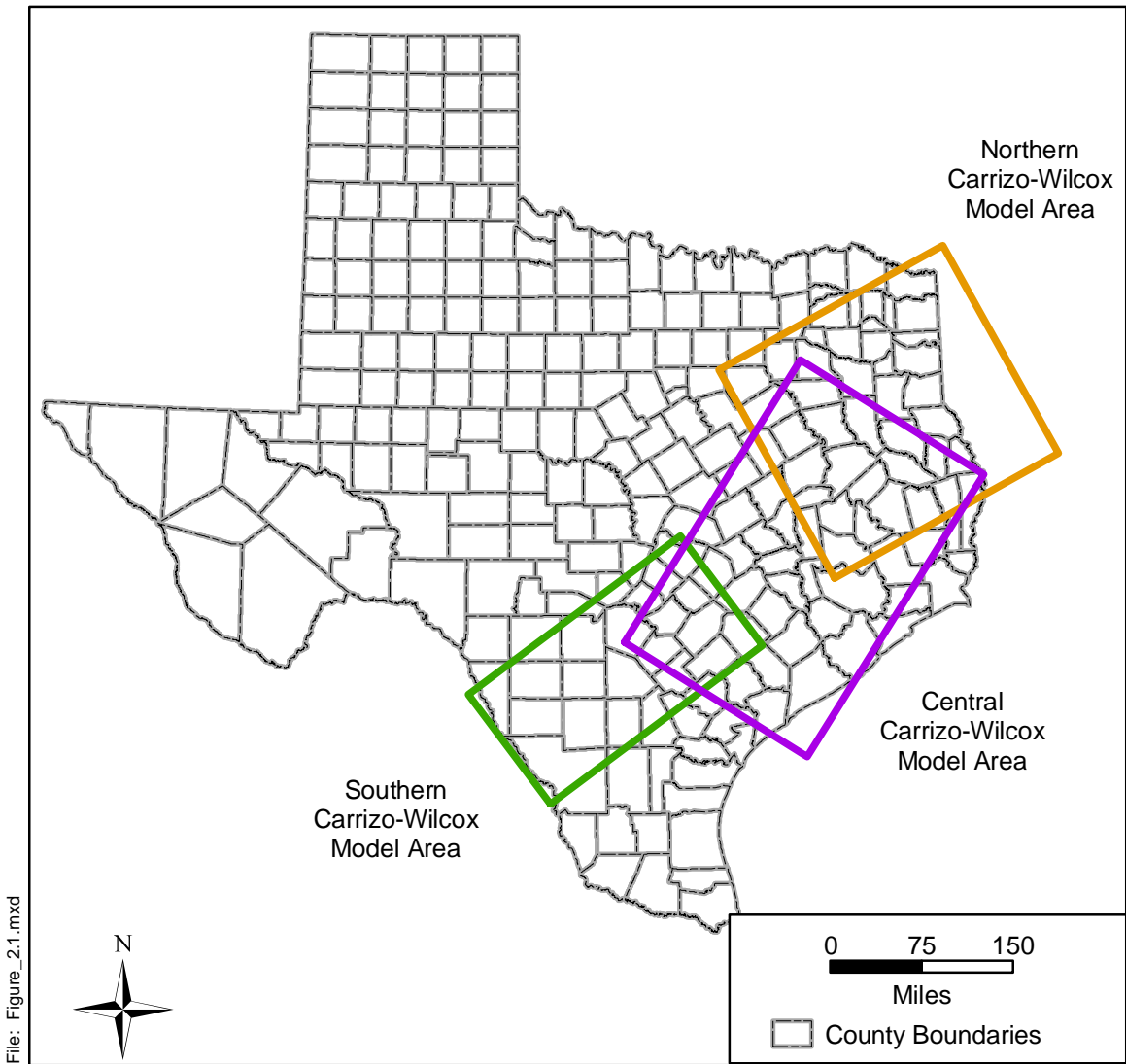


Figure 2.1 Location of the three Carrizo-Wilcox GAMs.

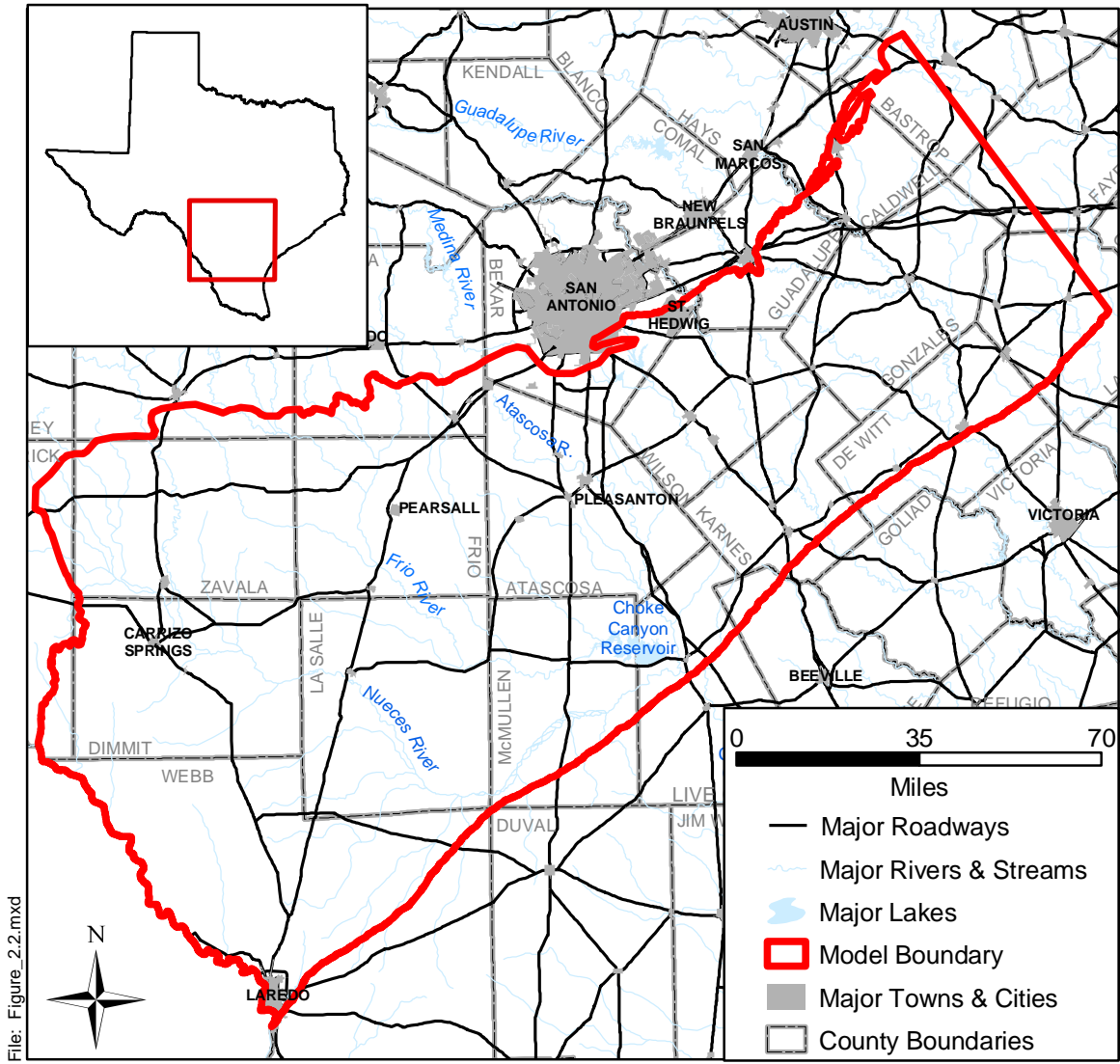


Figure 2.2 Location of study area showing county boundaries, cities, lakes, and rivers.

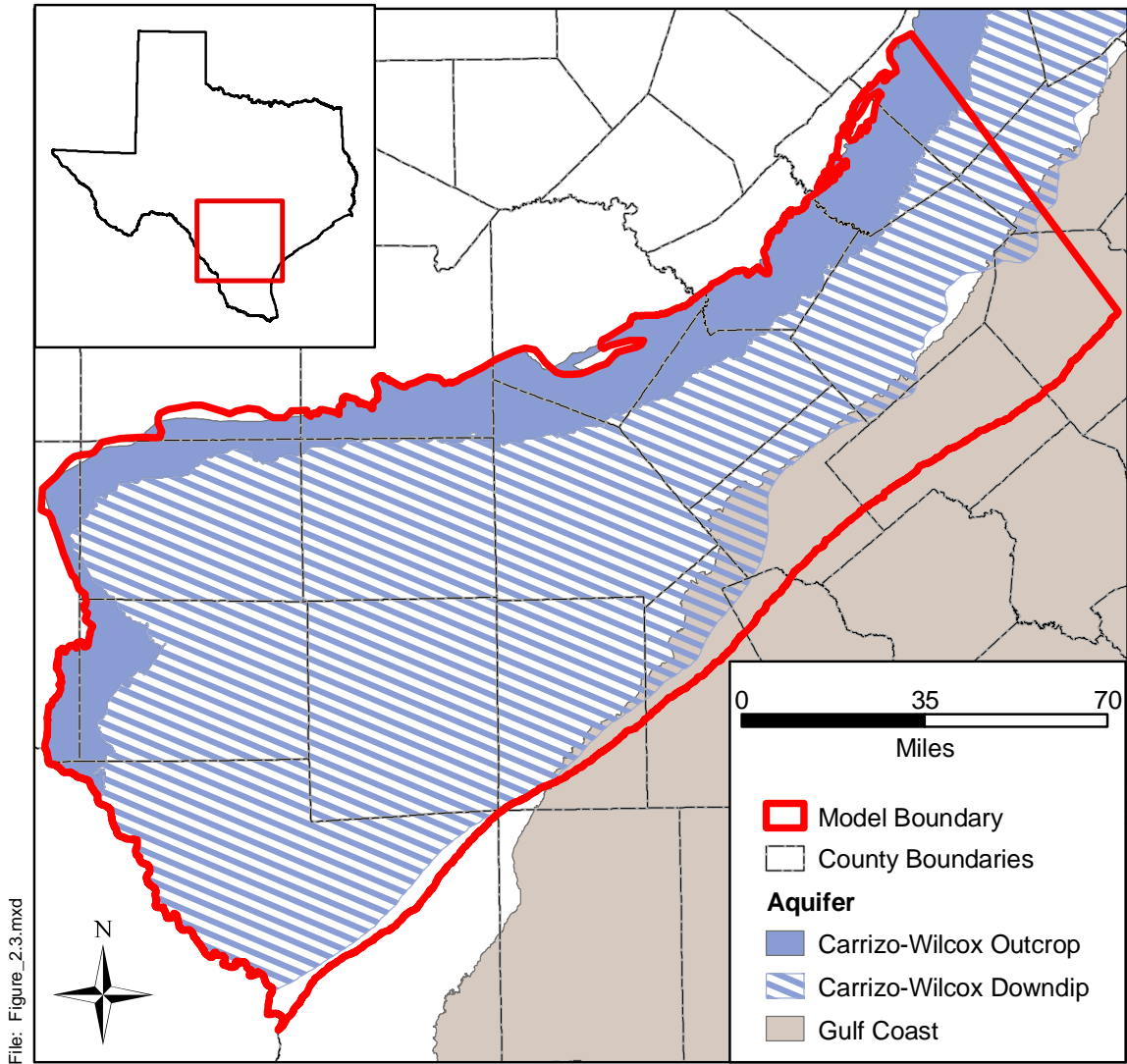
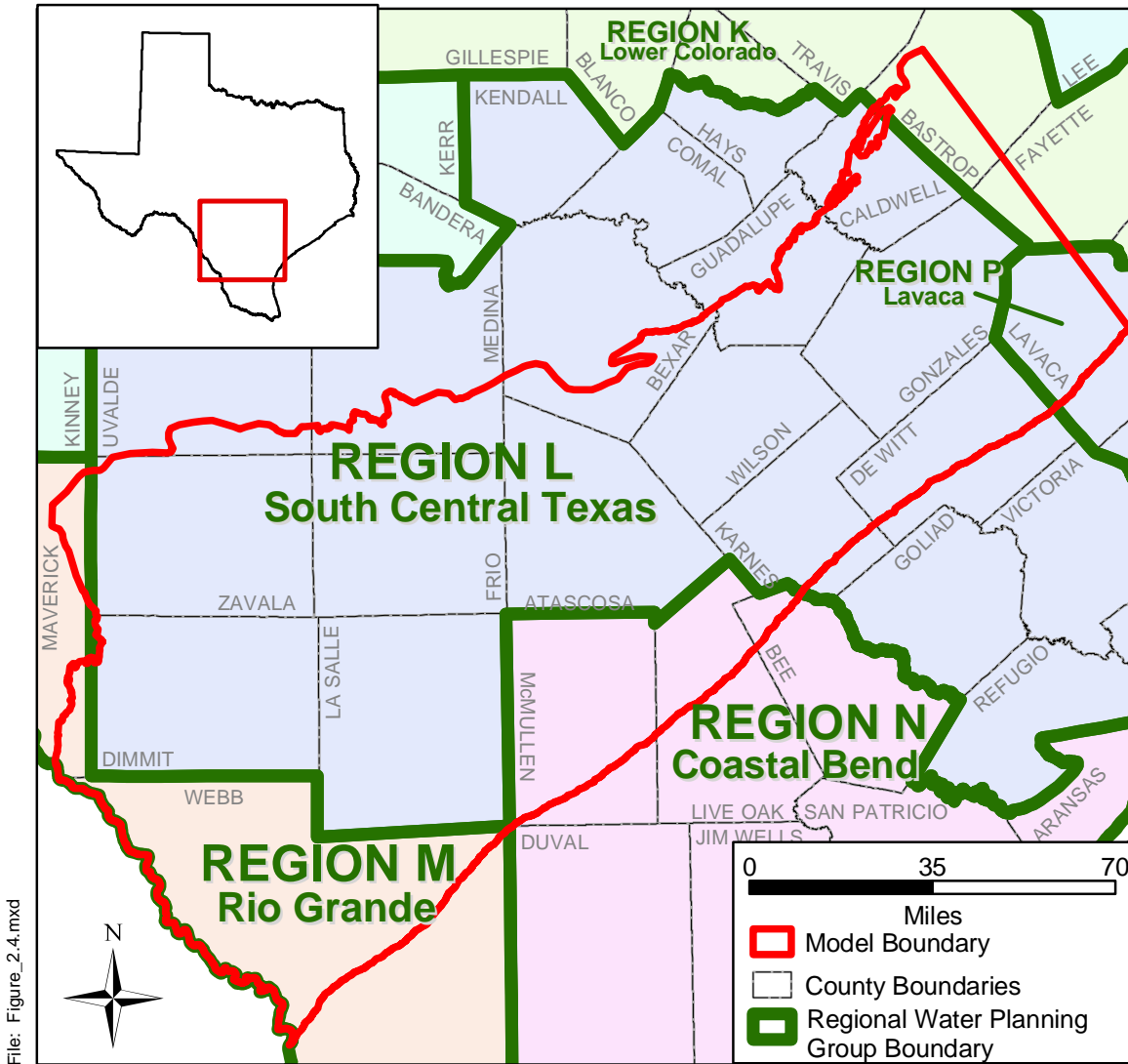


Figure 2.3 Areal extent of the major aquifers in the study area.



Source: Online: Texas Water Development Board, September 2002

Figure 2.4 Location of Regional Water Planning Groups in the study area.

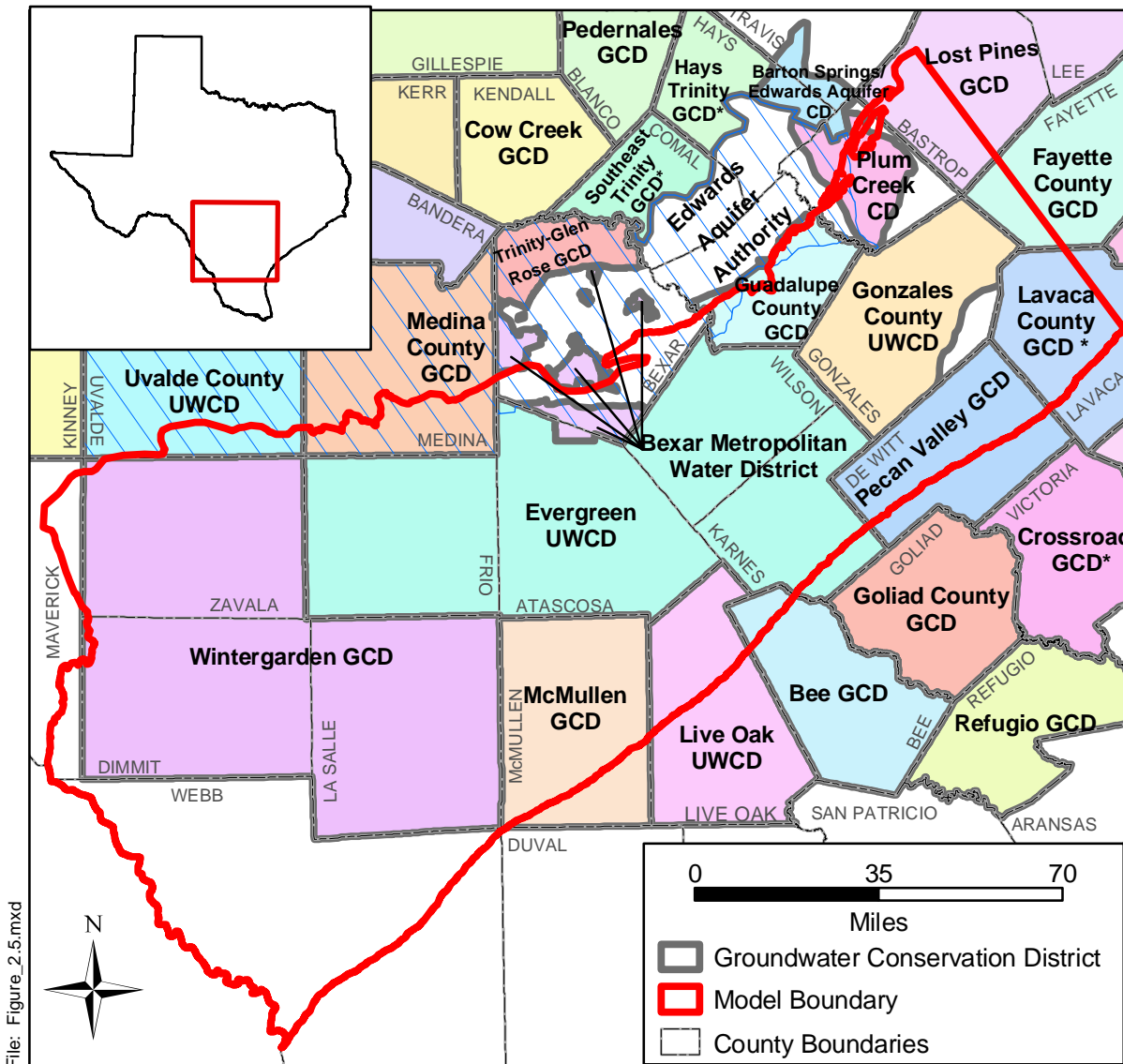


Figure 2.5 Location of Groundwater Conservation Districts in the study area.

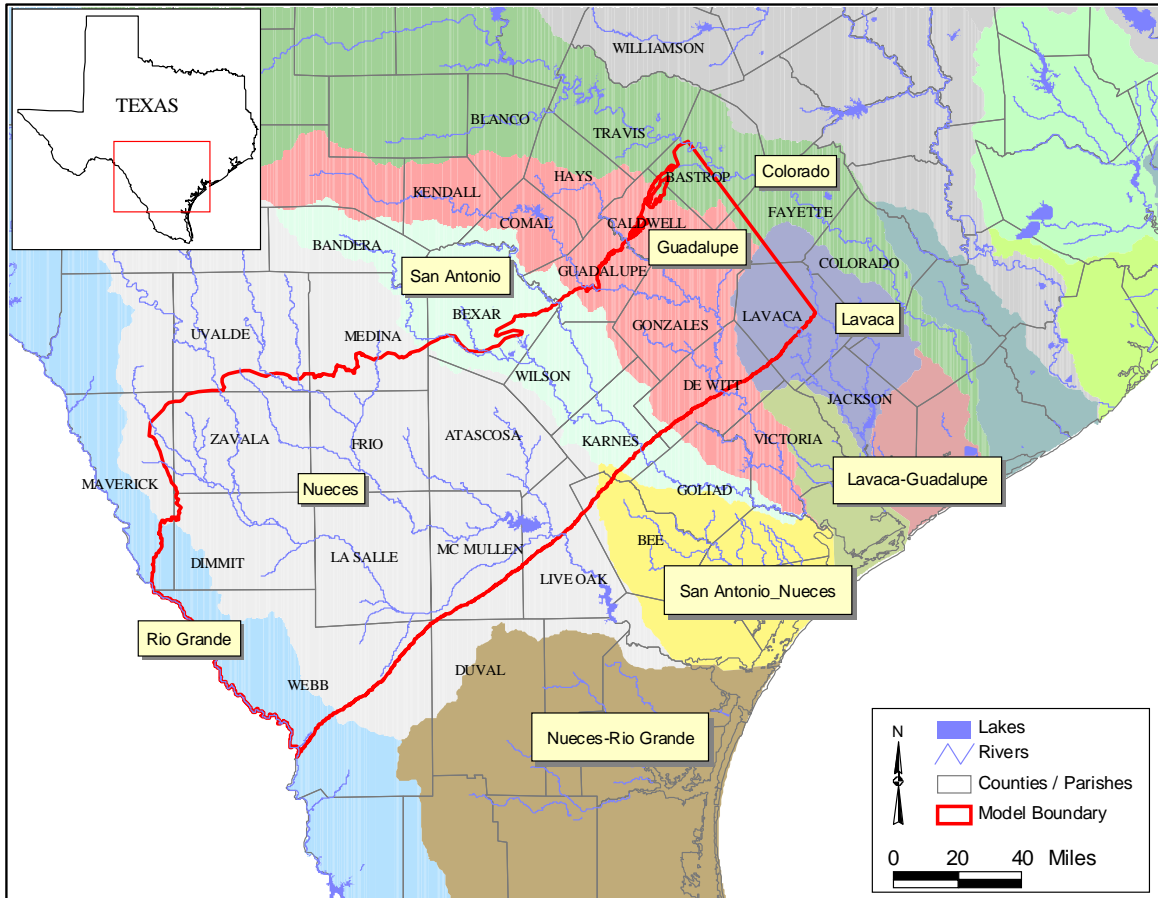


Figure 2.6 Major river basins in the study area.

2.1 Physiography and Climate

The study area is located in the Western Gulf Coastal Plain physiographic province (Alexander et al., 1964) in the Rio Grande Embayment of South Texas. The study area includes portions of the Rio Grande, Nueces, San Antonio, Guadalupe, Colorado, and Lavaca river basins. The region is characterized as having low relief with ground surface elevations gently decreasing from the southwest to the northeast and southeast. Figure 2.7 provides a topographic map of the study area. Ground surface elevation varies from nearly 300 feet above sea level in the western study area to less than 100 feet above sea level in river valleys and in the southeastern most regions of the study area. The gentle gulfward decrease in ground surface elevation is interrupted by resistant Tertiary sandstone outcrops, most prominently the Carrizo and the Catahoula-Oakville outcrops (Hamlin, 1988). The river valleys are broadly incised with terraced valleys that are hundreds of feet lower than the surface basin divide elevations (Hamlin, 1988). The model study area falls within the Gulf Coastal Plains, Blackland Prairies, and Coastal Prairies physiographic provinces. These physiographic provinces are further subdivided into ecological regions. Figure 2.8 shows the ecological regions which fall within the study area.

The study area intersects three climatic divisions in Texas: the Edwards Plateau division; the South Central division; and the South Texas division. The climate in the study area ranges from dry subhumid in the eastern part of the study area to semiarid in the west (Hamlin, 1988). Summers are usually hot and humid, while winters are often mild and dry. The hot weather persists from late May through September, accompanied by prevailing southeasterly winds (TWDB, 2002, Region L Plan). There is little change in the day-to-day summer weather except for the occasional thunderstorm, which produces much of the annual precipitation within the region. The cool season, beginning about the first of November and extending through March, is typically the driest season of the year as well. Winters are typically short and mild. Average daily temperature in the model region generally varies from a low in the low 40s to upper 30s in January to highs of the upper 90s in July (TWDB, 2002, Region L Plan). In the study region, the average annual temperature decreases from the south to the north from 73°F to 70°F (Hamlin, 1988).

The average annual net pan evaporation depth in the study area is high relative to available moisture ranging from a low of 49.9 inches per year in the far southeast portion of the model area to a high of 65.9 inches per year in the southwest corner of the model study area (Figure 2.9). For the study area, historical daily precipitation data is available at approximately 100 stations (Figure 2.10) from 1900 through 1999. The spatial distribution is relatively dense in the model domain across the period of record. However, the number of available gages in any given year is quite variable with a general chronological increase in the number of gages available. Most gages began measuring precipitation in the 1930s or 1940s. There are only eight precipitation gages in the study area that have records extending back to the first decade of the 1900's. Approximately 40 precipitation gages have records extending as far back as 1941.

Based upon the available precipitation records, the average annual precipitation in the study area is 29.4 inches. Historical average annual precipitation varies from a low of 20.9 inches at Eagle Pass to a high of 37.4 inches at Hallettsville. The PRISM (Parameter-elevation Regressions on Independent Slopes Model) precipitation data set developed and presented online by the Oregon Climate Service at Oregon State University provides a good distribution of average annual precipitation across the model area based upon the period of record from 1961 to 1990. Figure 2.11 provides a raster data post plot of average annual precipitation across the model study area. Generally, the average annual precipitation is greater in the east and towards the coastal areas. Figure 2.12 shows annual precipitation recorded at five precipitation gages with long periods of record within the model area and located in San Antonio (Bexar Co.), Flatonia (Fayette, Co.), Dilley (Frio Co.), Runge (Karnes Co.), and Encinal (Webb Co.). Also plotted in these plots is the long-term period of record average annual precipitation depth for each gage.

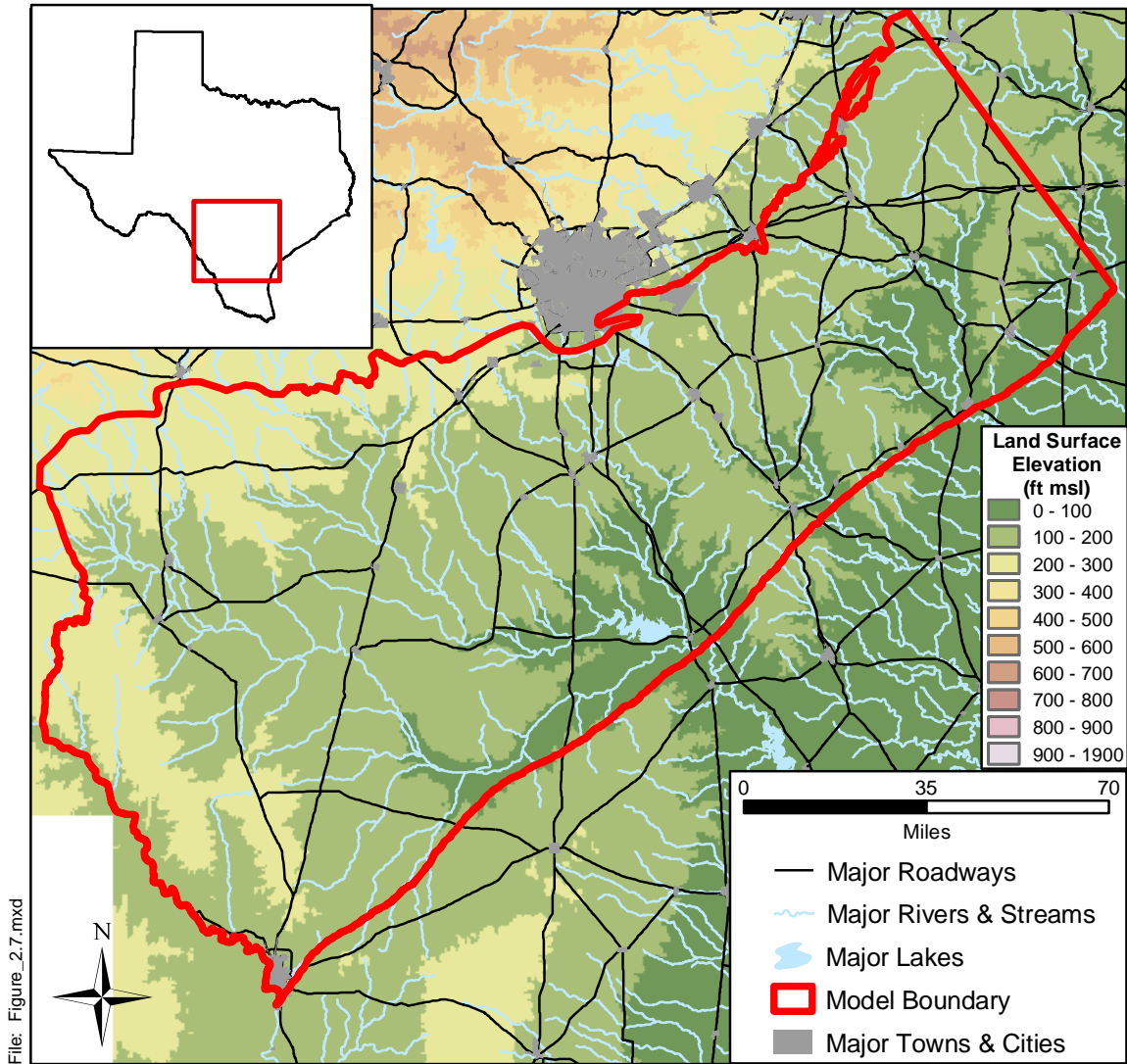


Figure 2.7 Topographic map of the study area.

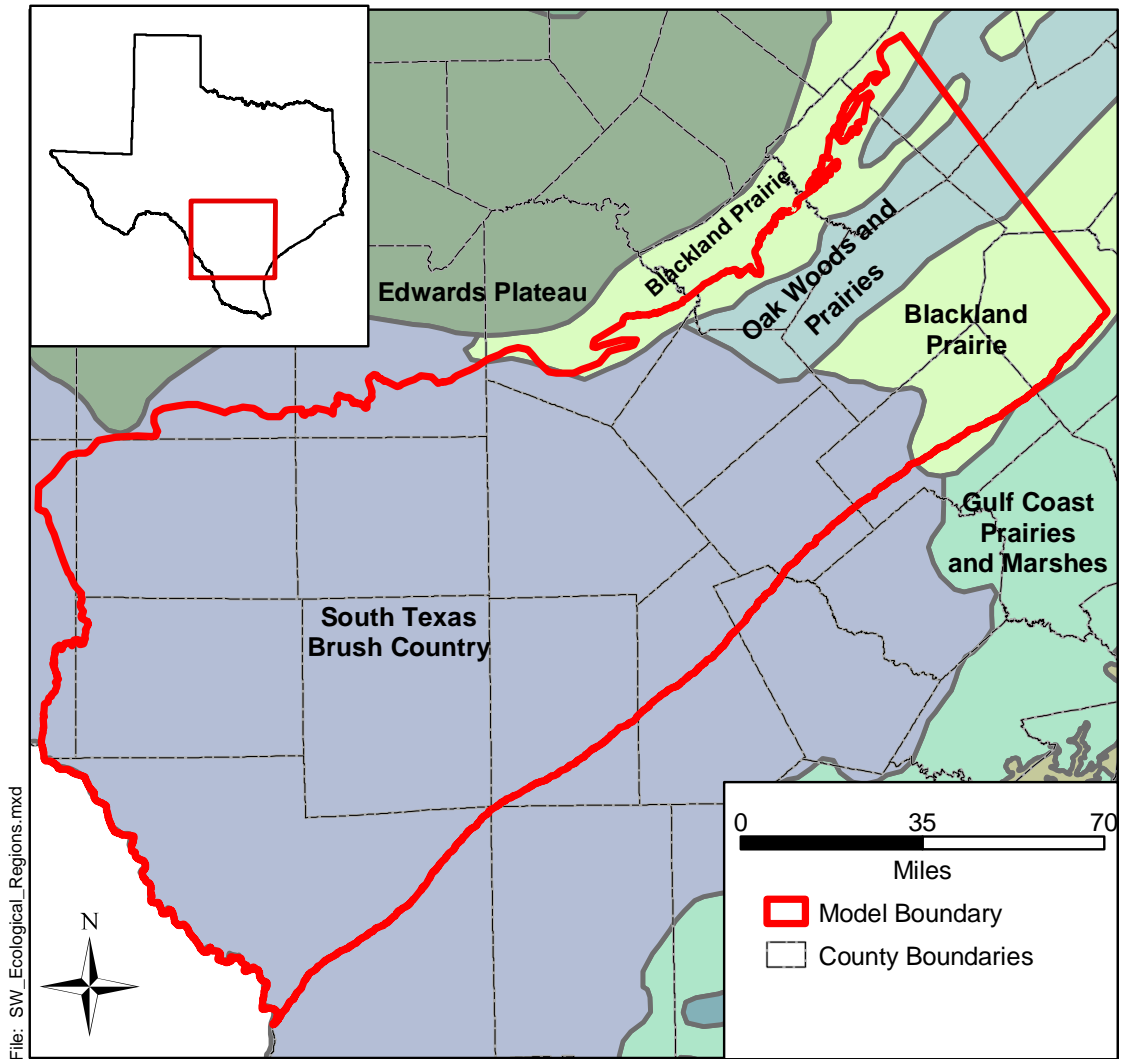
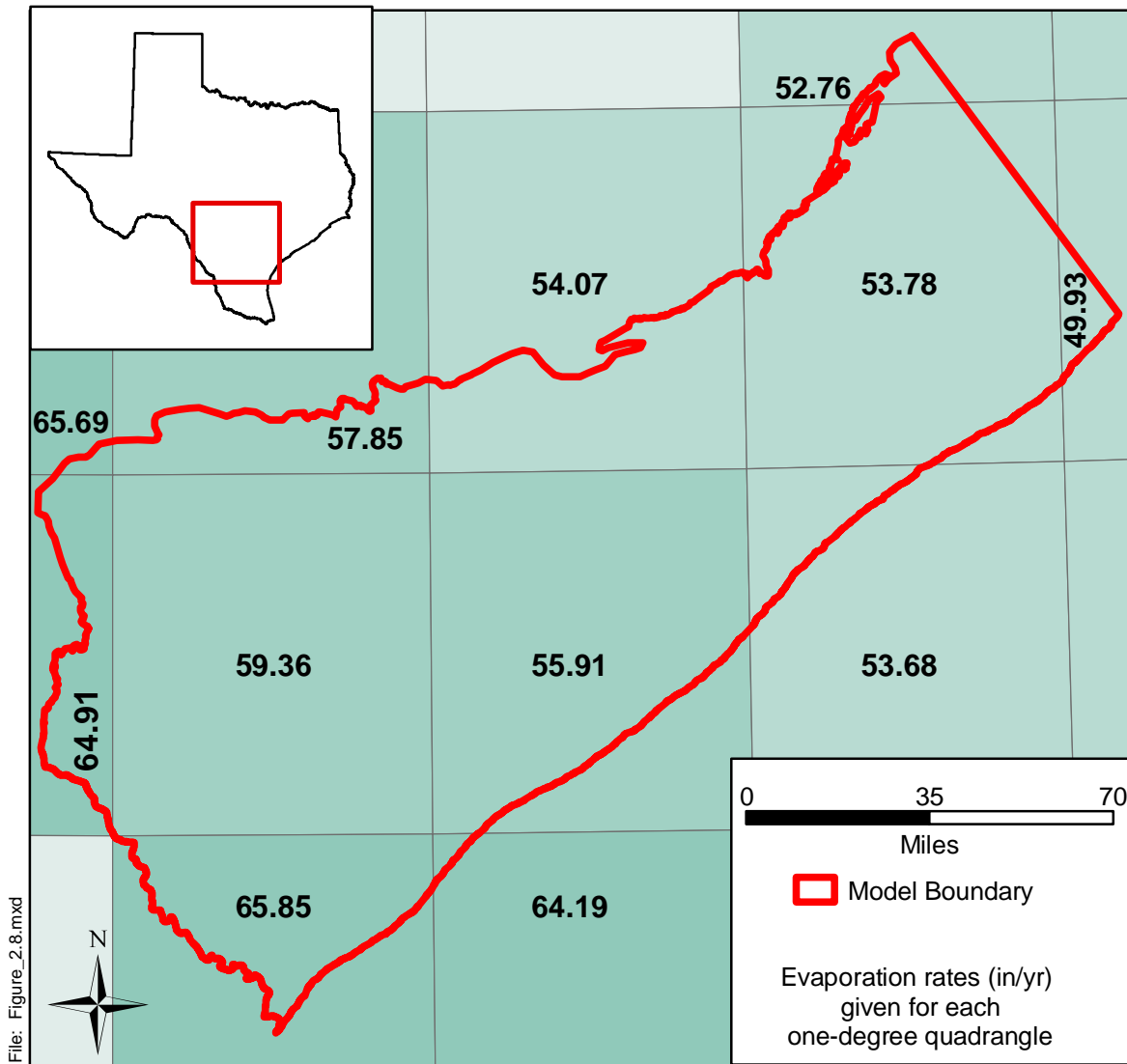


Figure 2.8 Ecological regions within the study area.



Source: Online: Texas Water Development Board, September 2002

Figure 2.9 Average annual net pan evaporation rate in inches per year.

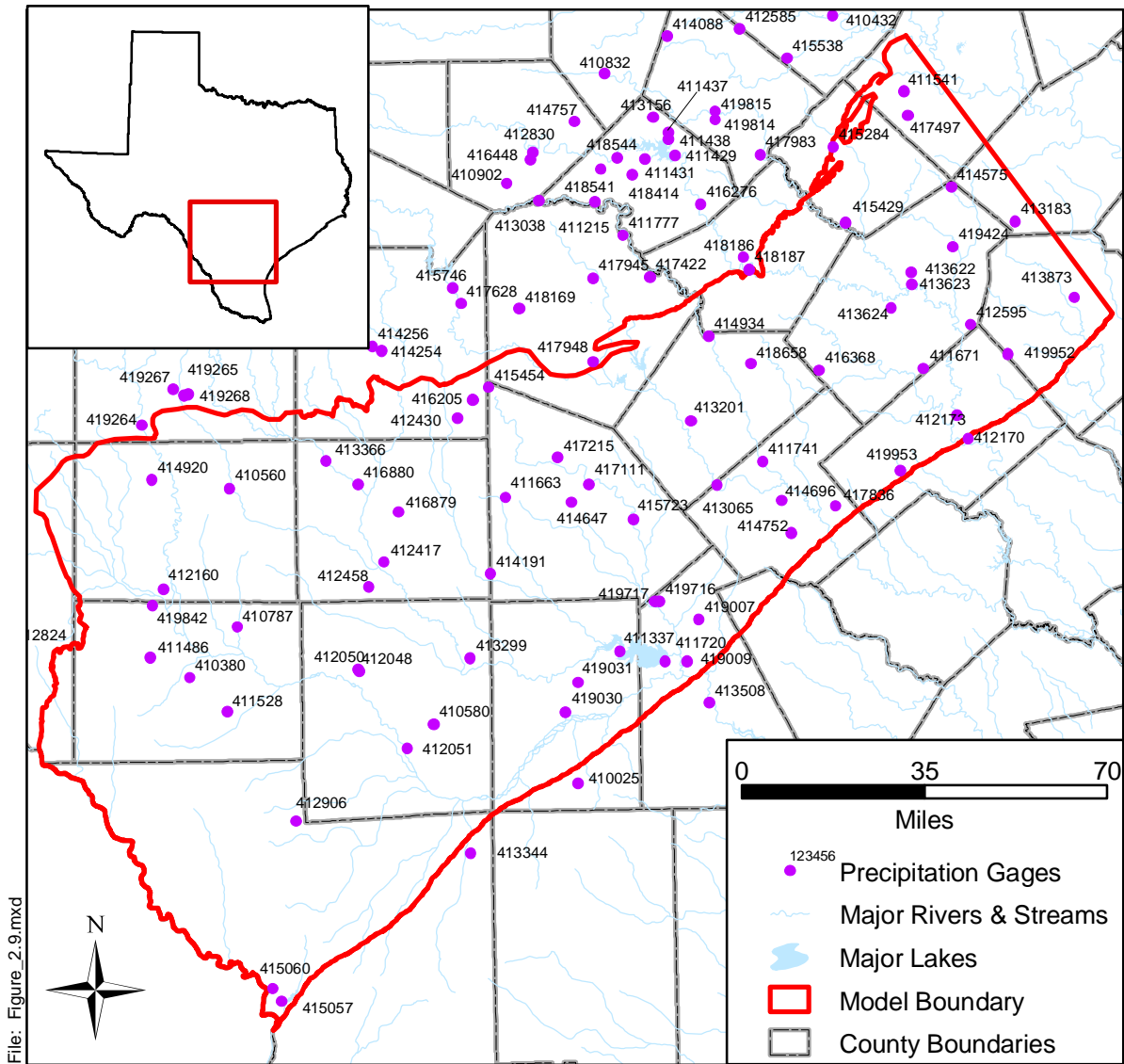


Figure 2.10 Location of precipitation gages in the study area (Period of Record is 1900 to 1999).

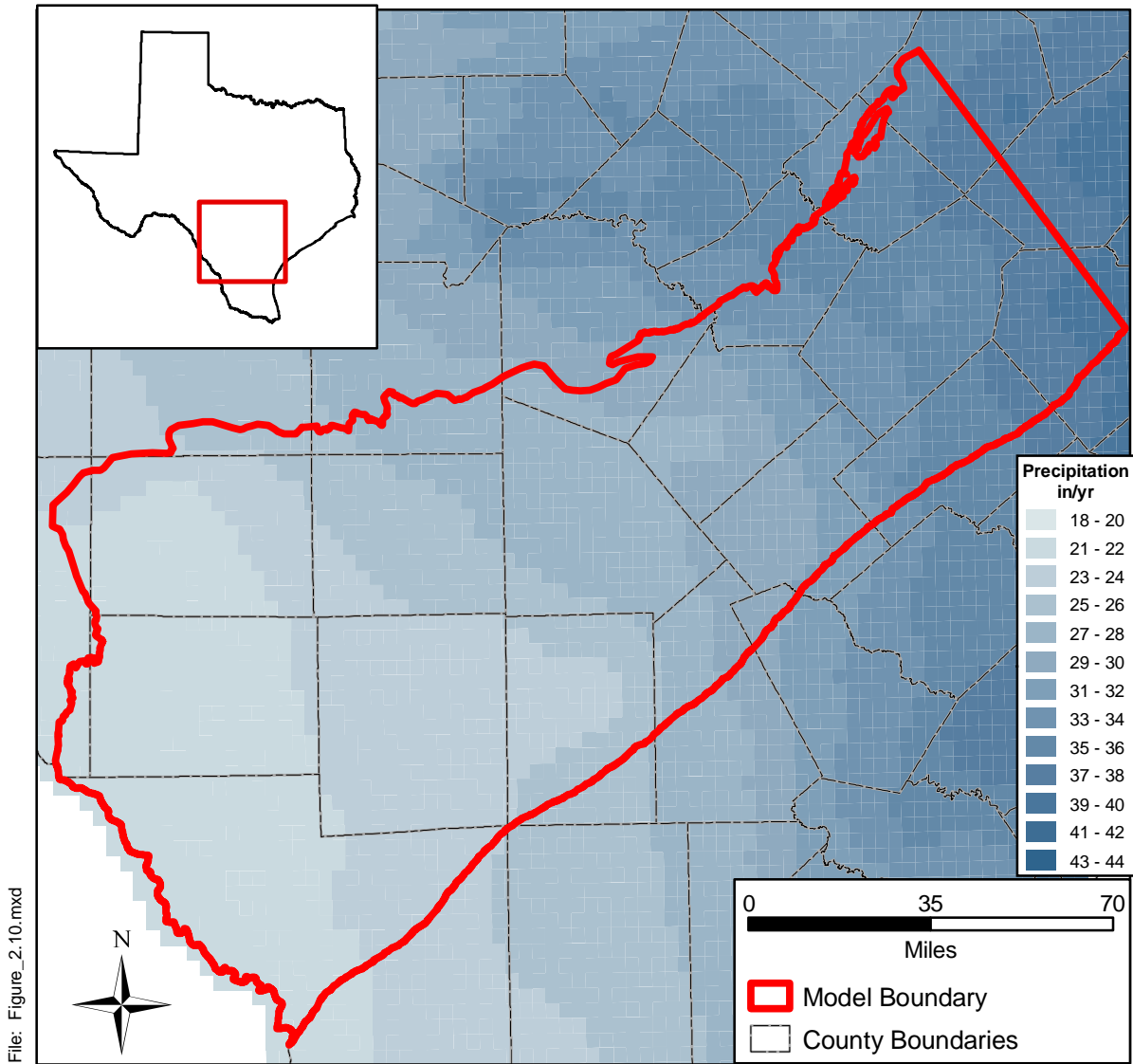


Figure 2.11 Average annual precipitation (1961-1990) over the study area in inches per year (Source: Oregon Climate Service, Oregon State University, PRISM data set).

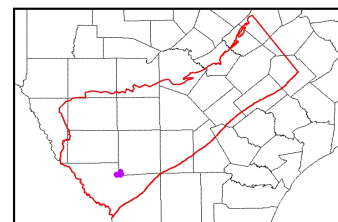
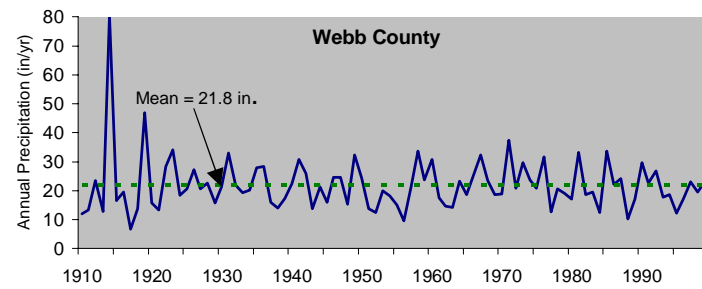
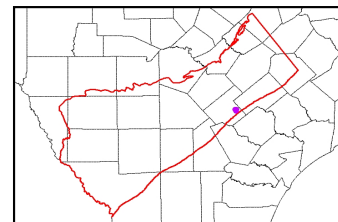
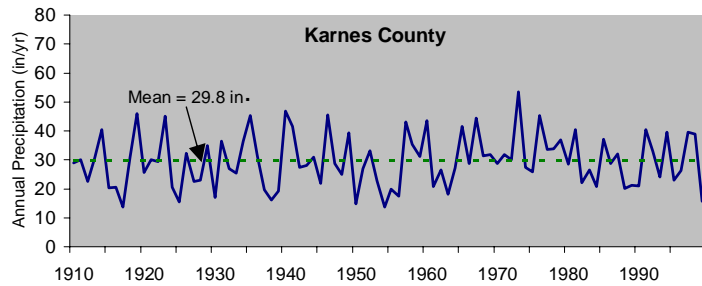
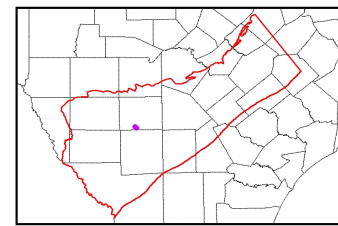
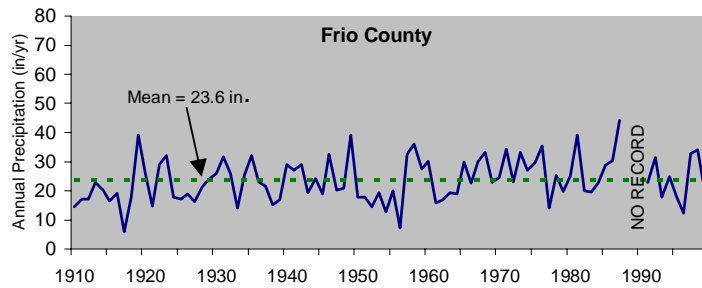
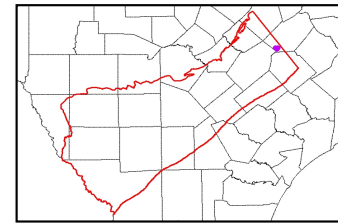
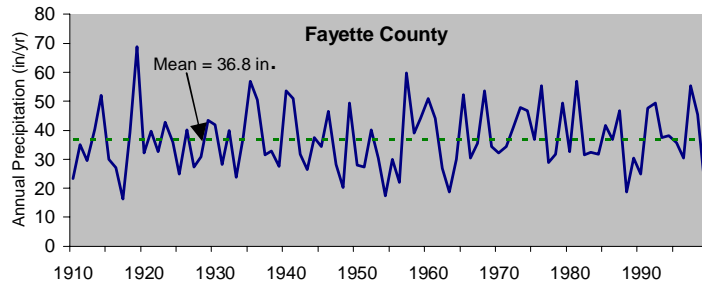
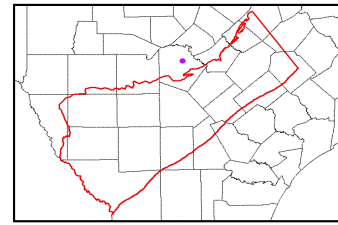
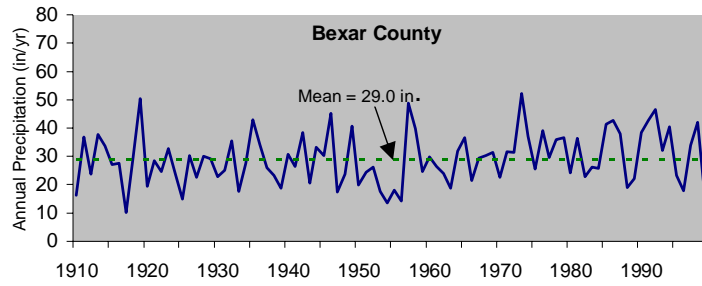


Figure 2.12 Annual precipitation time series for gages in Bexar, Fayette, Frio, Karnes, and Webb counties.

2.2 Geology

The sediments that form the aquifer in the study area are part of a gulfward thickening wedge of Cenozoic sediments deposited in the Rio Grande Embayment of the northwest Gulf Coast Basin. Deposition in the Rio Grande Embayment was influenced by regional crust subsidence, episodes of sediment inflow from areas outside of the Gulf Coastal Plain, and eustatic sea-level change (Grubb, 1997). Galloway et al. (1994) characterized Cenozoic sequences in the Gulf Coast in the following three ways. Deposition of Cenozoic sequences is characterized as an offlapping progression of successive, basinward thickening wedges. These depositional wedges aggraded the continental platform and prograded the shelf margin and continental slope from the Cretaceous shelf edge to the current Southwest Texas coastline. Deposition occurred along sand-rich, continental margin deltaic depocenters within embayments (Rio Grande, Houston, and Mississippi Embayments) and was modified by growth faults and salt dome development.

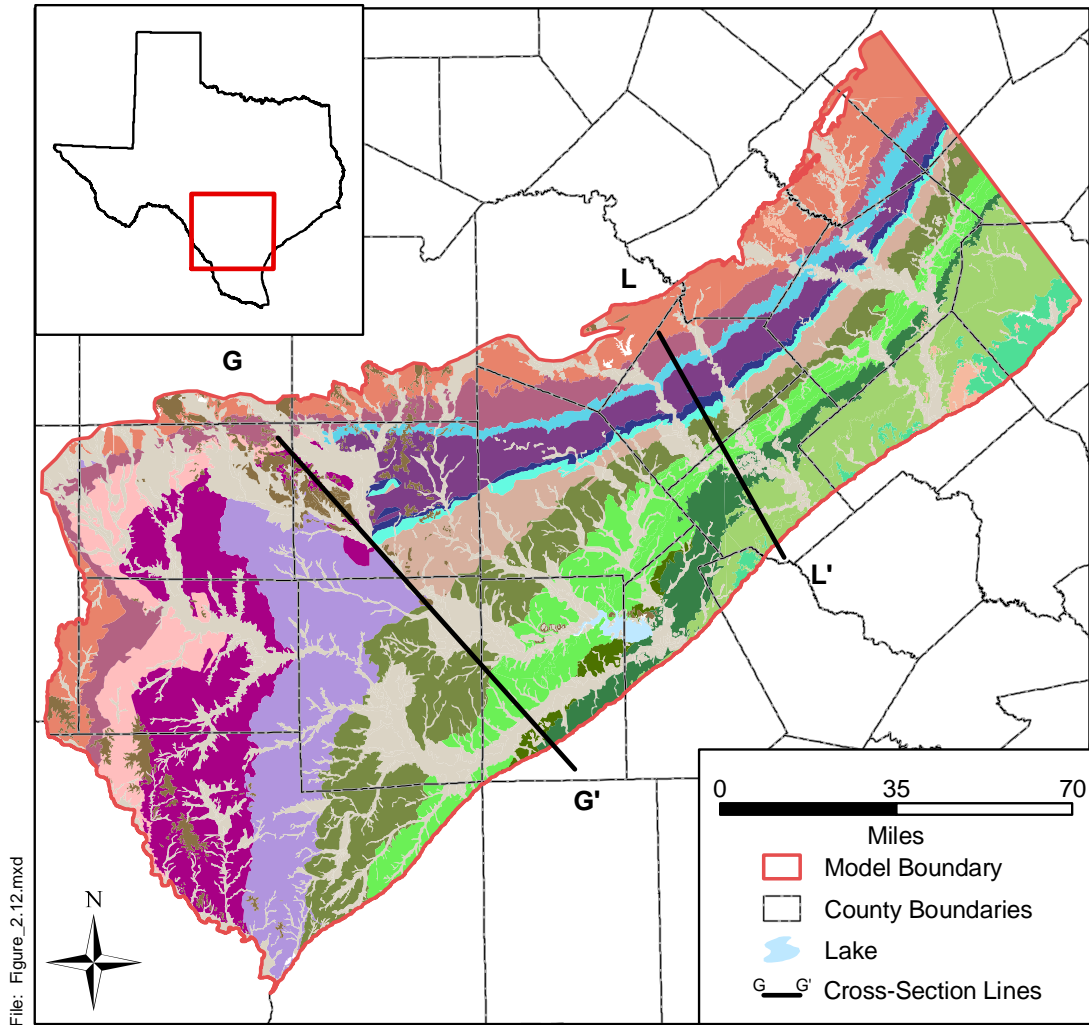
The primary Paleogene depositional sequences in ascending stratigraphic order are the lower Wilcox, the upper Wilcox, the Carrizo, the Queen City, the Sparta, the Yegua-Cockfield, the Jackson, and the Vicksburg-Frio (Galloway et al., 1994). Each of these depositional sequences is bounded by marine shales and finer grained sediments representing transgressions (e.g., Reklaw and Weches formations).

Figure 2.13 shows a geologic map of the area showing the Tertiary sediments comprising the aquifers of interest in this study as well as the Quaternary undivided sediments. Inspection of the surface geology shows the general outcrop pattern from southwest to northeast coincident with depositional strike, the Balcones Fault Zone, and normal to basin subsidence. Also important to note are the stratigraphic changes that occur from east of the Frio River to west of the Frio River. Many of the Tertiary formations change lithologic character in the vicinity of the Frio River coincident with the axis of the Rio Grande Embayment.

Figure 2.14 shows a representative stratigraphic section for the study area. The southern Carrizo-Wilcox aquifer overlies the Midway Group which is composed of marine clays. The southern Carrizo-Wilcox aquifer consists of fluvial-deltaic sediments of the upper Paleocene and lower Eocene Wilcox Group and Carrizo Sand. In the study area, the Wilcox Group is

subdivided into a lower, middle, and upper unit. The lower Wilcox is composed of sands and clays deposited in a barrier bar and lagoon-bay system (Fisher and McGowen, 1967). The middle Wilcox is not generally subdivided in the study area but is generally described as a lower energy depositional sequence representative of a minor transgression. The Carrizo Sand in the outcrop and shallow subsurface correlates with the upper part of the Wilcox Group in the deeper subsurface (Hamlin, 1988; Bebout et al., 1982). The Carrizo-upper Wilcox predominantly consists of a fluvial sand facies that grades into more deltaic and marine facies farther downdip (Bebout et al., 1982). South and west of the Frio River, the Wilcox is sometimes referred to as the Indio Formation and is composed of irregularly bedded sandstone and shale. Figure 2.15 shows two structural cross-sections (for location see Figure 2.13) after Hamlin (1988) in the study area. Cross-section G-G' of Hamlin shows that the Carrizo-Wilcox dips less in the southwestern portion of the study area and the fresh water line extends into McMullen County in the Carrizo. By contrast, section L-L' shows that the aquifer dips much more steeply in the east (Wilson & Karnes counties) with the extent of fresh water closer to the outcrop.

The Carrizo-Wilcox aquifer is bounded from above by the Reklaw Formation, representing a semi-confining unit between the Carrizo Sand and the shallow aquifer of the Queen City Formation. The Reklaw Formation consists of variable amounts of mud and sand and is considered the upper confining stratum of the Carrizo-upper Wilcox aquifer in the northeastern part of the study area. To the southwest in the study area, the Bigford Formation is the equivalent of the Reklaw, which consists mainly of sands, silts, and shales and is considered a minor aquifer compared to the underlying Carrizo-upper Wilcox aquifer. In the western part of the study area, the Bigford Formation is overlain by the El Pico Clay composed mainly of clays with few sand lenses. In the northeast portion of the study area, the Queen City Sand and clayey Weches Formation overlie the Reklaw and interfinger laterally with the El Pico Clay in the southwest. In the southwestern part of the model area, sands and sandstones of the Laredo aquifer overlie the El Pico Clay. The Laredo aquifer correlates with the interbedded sands and clays of the Sparta aquifer and with the clays and fine sands of the Cook Mountain Formation in the northeast. Both the Laredo and Sparta aquifers produce small to moderate quantities of water.



Source: Bureau of Economic Geology

West of Frio River	East of Frio River
	Quaternary Undivided
	Willis Formation
	Uvalde Gravel
	Goliad Formation
	Fleming Formation; Oakville Sandstone
	Catahoula Formation
	Frio Formation
	Jackson Group
	Yegua Formation
Laredo Formation	Cook Mountain Formation
El Pico Clay	Sparta Sand
Bigford Formation	Weches Formation
	Queen City Sand
	Reklaw Formation
	Carrizo Sand
	Wilcox Group
	Midway Group

Figure 2.13 Surface geology of the study area.

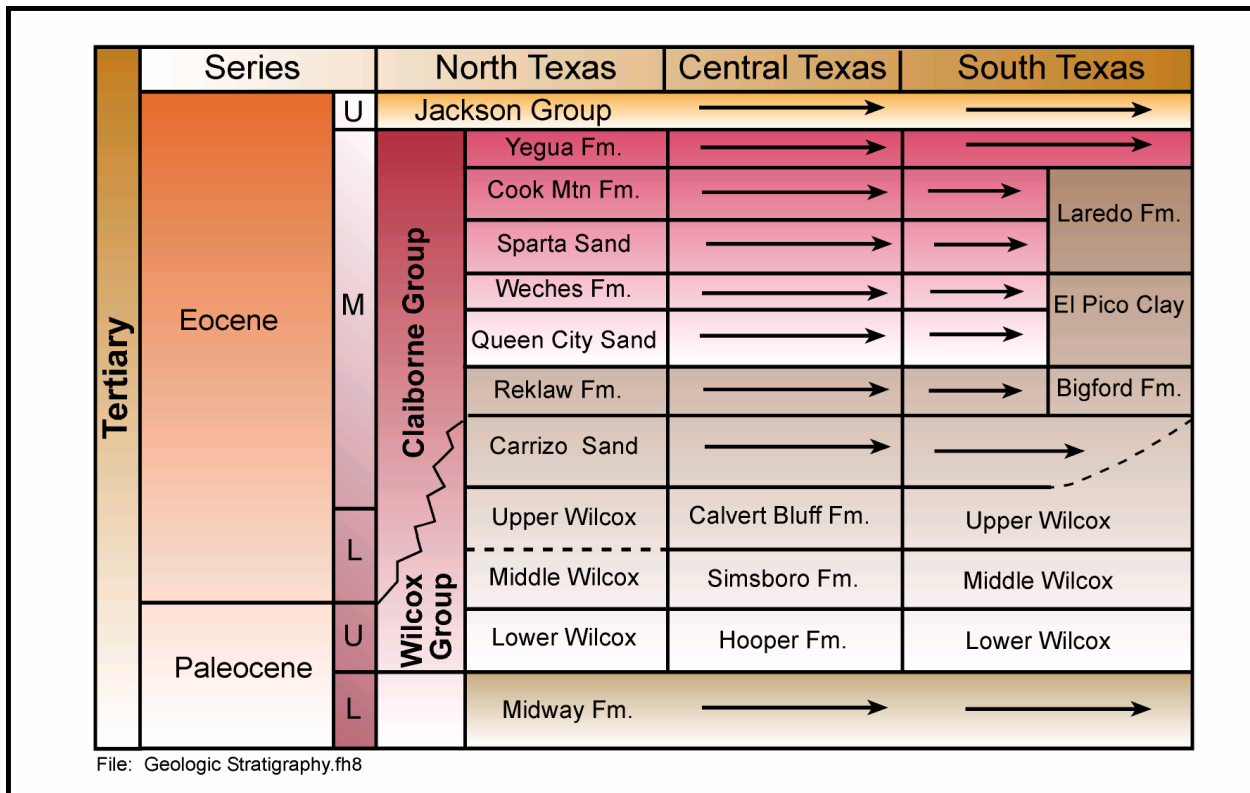


Figure 2.14 Generalized stratigraphic section for the Carrizo-Wilcox aquifer in Texas (after Ayers and Lewis, 1985; Hamlin, 1988; Kaiser et al., 1978).

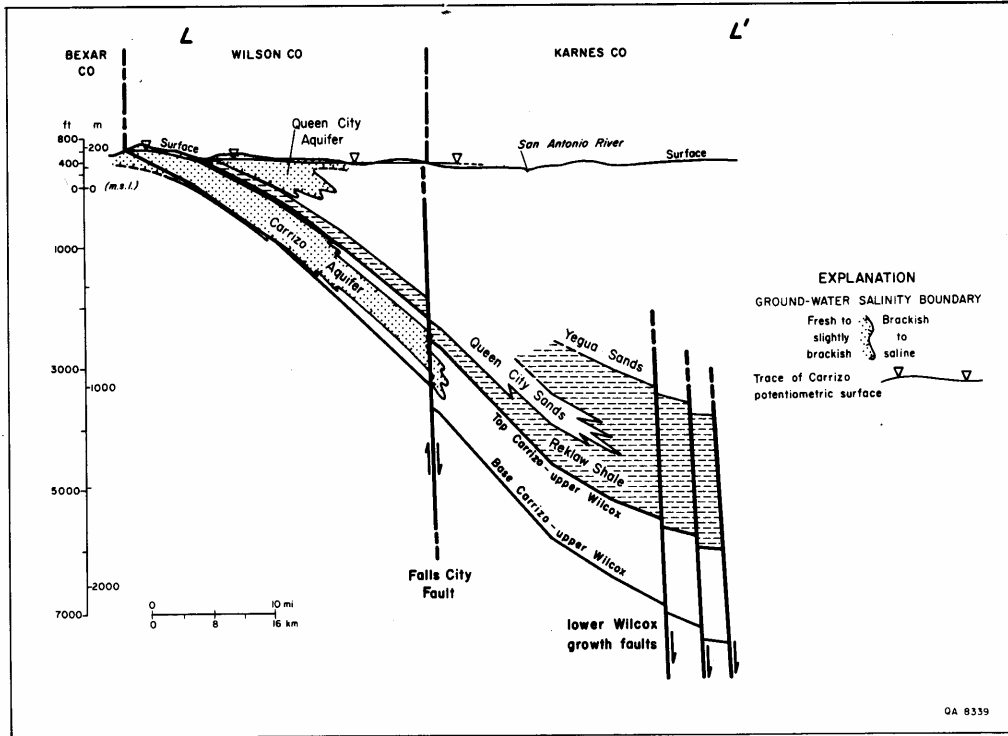
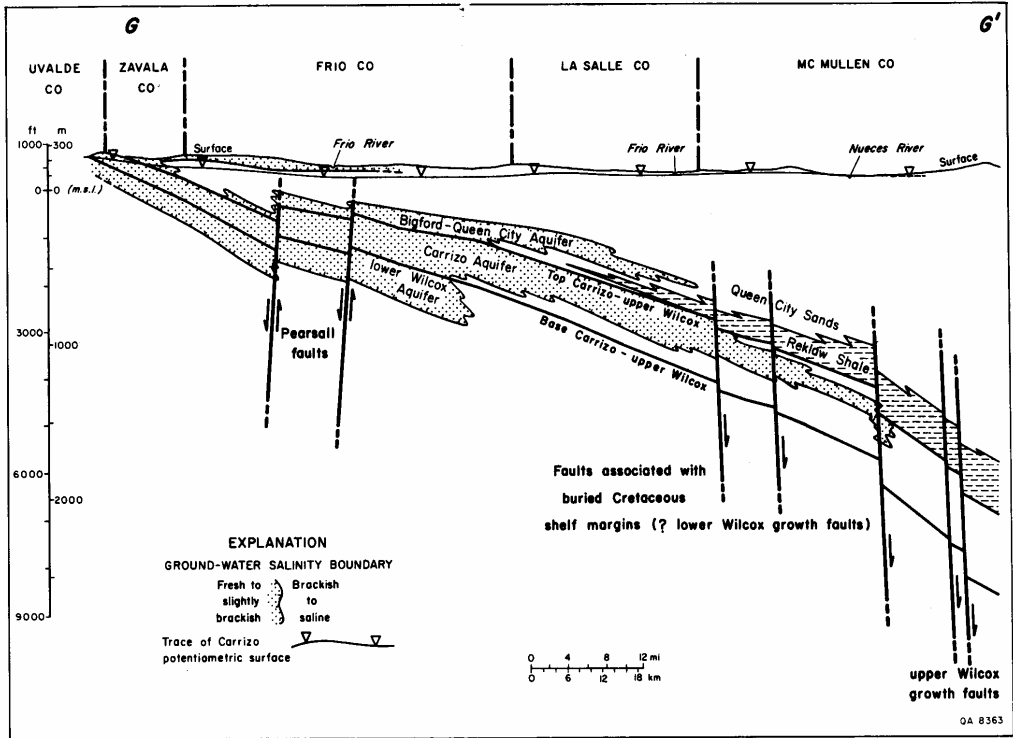


Figure 2.15 Structural cross-sections in the study area (after Hamlin, 1988).

3.0 PREVIOUS INVESTIGATIONS

The southern Carrizo-Wilcox aquifer has been studied by many investigators and numerous groundwater bulletins have been developed by the Texas Water Development Board for the counties in the study area. The two major hydrogeologic investigations in the model area are Klemt et al. (1976) and Hamlin (1988). Klemt et al. (1976) studied the groundwater resources of the Carrizo aquifer in the Wintergarden area. Klemt et al. (1976) included a comprehensive review of the available data concerning the aquifer including recharge, discharge, hydraulic conductivity, water quality, and groundwater availability. The study was a seminal study of groundwater in Texas because it included a groundwater model of the Carrizo aquifer in the Wintergarden region.

Hamlin (1988) focused on the depositional and sequence stratigraphy of the Carrizo and upper Wilcox in South Texas. Hamlin (1988) investigated the lithostratigraphy of the Carrizo and upper Wilcox and he mapped net sand thickness and sand percent within the study area which will be discussed further in Section 4 of this report. Hamlin (1988) also studied structure, hydraulic heads, flow patterns and geochemistry of the Carrizo and upper Wilcox in the study area. Both of these studies have been used and borrowed from extensively for the development of the Southern Carrizo-Wilcox GAM.

In addition to these groundwater flow studies, there have been several groundwater models developed with model domains that overlap this GAM study area. Figure 3.1 shows the model boundaries for the Southern Carrizo-Wilcox GAM as it relates to previous modeling study boundaries. Table 3.1 lists these previous investigations along with some basic model characteristics to provide a basis for the following discussion.

As previously mentioned, Klemt et al. (1976) developed a single-layer model of the Carrizo aquifer in the Wintergarden area to investigate future declines in water levels in the Carrizo aquifer. They performed three sets of simulations based on three criteria for future pumpage from the aquifer. The objective of the modeling was to assess the ability of the Carrizo aquifer to meet future demands. As one can see from Figure 3.1, the model area is nearly coincident with the GAM boundaries. From Table 3.1 it is important to note that the model was developed with a TWDB in-house simulator which was typical in the 1970s. The model was a single-layer model of the Carrizo and likely included much of the upper-Wilcox as it might be

defined by Hamlin (1988). The details regarding the calibration of this model are unknown. The model was used in a predictive mode to: (1) simulate regional water level declines 1970-2020, (2) determine the potential for Wilson County to provide up to 40,000 AFY of groundwater for municipal needs, and (3) see what pumping rate per unit area would be required to create a 400 foot decline in water levels throughout the Wintergarden area.

Table 3.1 Previous groundwater models of the Carrizo-Wilcox aquifer in the study area.

Model	Code	No. of Carrizo-Wilcox Layers	Calibration	Predictive Simulations
Klemt et al. (1976)	Research	1	unknown	1970 to 2020
Ryder (1988)	Research	2	Steady-state	No
Williamson et al. (1990)	Research	2	Steady-state (1980)	No
Thorkildsen et al. (1989)	MODFLOW	4	Steady-state (1985)	1985-2029
Ryder & Ardis (1991)	Research	2	Steady-state (1910) Transient (1910-1982)	Yes
Thorkildsen & Price (1991)	Unknown	4	Unknown	Unknown
LBG-Guyton & HDR (1998)	MODFLOW	2	Steady-state (1910); Transient (1910-1994)	1994-2050

Thorkildsen et al. (1989) modeled the Carrizo-Wilcox aquifer in the Colorado River Basin using MODFLOW. Their objective was to “provide a management tool for the Lower Colorado River Authority to evaluate the regional water-supply capabilities of the Carrizo-Wilcox aquifer within the Colorado River Basin”. Their three-dimensional model extended from the ground surface to the base of the Wilcox Group. The model was calibrated as a steady-state model to aquifer conditions in 1985. The model was used to predict future conditions in the aquifer from 1985 through 2029 based on estimated future pumping as documented in the TWDB 1984 State Water Plan.

Thorkildsen and Price (1991) report that a three-dimensional model of the Carrizo-Wilcox aquifer in central Texas was constructed as part of their study. Little is known regarding the details of this model, but it is expected that it was an extension of the 1989 model. The model was designed to evaluate the occurrence, availability, and quality of ground water in the Carrizo-Wilcox aquifer.

In 1998, LBG-Guyton Associates and HDR Engineering, Inc. developed a groundwater model with a focus on the interaction between surface water and groundwater in the

Wintergarden area (LBG-Guyton & HDR, 1998). The model was an extension of the Klemt et al. (1976) Carrizo model and modeled from the base of the Wilcox through the Yegua Formation. The model was developed with MODFLOW and results from the groundwater model were used to predict changes in surface water flows using proprietary surface water models of the area's river basins developed by HDR Engineering, Inc. Two model calibrations were performed: a steady-state calibration to predevelopment conditions (1910) and a transient calibration from 1910 through 1994. The calibrated model was then used to predict future conditions from 1994 through 2050 for three future pumping scenarios; (1) 1994 pumping (249,890 AFY), (2) 2050 pumping from 1994 through 2050 (264,715 AFY), and (3) 2050 plus (449,952 AFY including 185,237 additional AFY in Atascosa, Dimmit, Gonzales, and Wilson counties). Rick Hay at Texas A&M-Corpus Christi is currently (2002) using this model for the Evergreen Underground Water Conservation District to investigate future water resource strategies currently being considered by the Region L Planning Group and the San Antonio Water Supply.

In addition to these regional models, the United States Geological Survey (USGS) has developed super-regional models which incorporate the entire Carrizo-Wilcox aquifer in Texas (Ryder, 1988; Ryder and Ardis, 1991) and in the entire Gulf Coast Region (Williamson et al., 1990) as part of the RASA (Regional Aquifer-System Analysis) studies. Their analyses modeled from the Midway Formation through the Gulf Coast aquifer systems. The Carrizo-Wilcox aquifer was modeled as two layers, generally a lower and middle Wilcox aquifer and an upper Wilcox and Carrizo aquifer. Ryder (1988) reported that the model objectives were to define the hydrogeologic framework and hydraulic characteristics of the Texas coastal plain aquifer systems, delineate the extent of freshwater and density of saline water in the various hydrogeologic units, and describe the regional groundwater flow system. A steady-state calibration to predevelopment conditions was performed using a research code developed by Kuiper (1985).

The entire U.S. Gulf Coast aquifer system above the Midway Formation was modeled by Williamson et al. (1990) using the research code developed by Kuiper (1985). The model consisted of a steady-state calibration to predevelopment conditions, a steady-state calibration to 1980 water-level data, and transient simulations from 1935 to 1980. The model objectives were "to help in the development of quantitative appraisals of the major ground-water systems of the

United States, and to analyze and develop an understanding of the ground-water flow system on a regional scale, and to develop predictive capabilities that will contribute to effective management of the system”.

Ryder and Ardis (1991) extended the work performed by Ryder (1988) and developed another model of the coastal plain aquifers in Texas. The model, developed using the research code developed by Kuiper (1985), was calibrated to both steady-state predevelopment conditions and transient conditions from 1910 to 1982. In addition, transient predictive simulations were performed using the calibrated model. The objectives for the modeling study consisted of: (1) defining the hydrogeologic framework and hydraulic characteristics of the aquifer systems, (2) delineating the extent of fresh to slightly saline water in various hydrogeologic units, (3) describing and quantifying the groundwater flow system, (4) analyzing the hydrologic effects of man’s development on the flow system, and (5) assessing the potential of the aquifer systems for further development.

Each of these models provides information which is both relevant and useful to the study of groundwater availability in the southern Carrizo-Wilcox aquifer study area. However, many traits of the previous investigations have made development of the current GAM necessary to meet the GAM specifications defined by the TWDB. Specifically, GAM models are expected to (1) be well documented and publicly available, (2) utilize standard modeling tools which are non proprietary (MODFLOW), and (3) be calibrated both steady-state and transiently and capable of adequately simulating a verification period to a pre-defined calibration criteria.

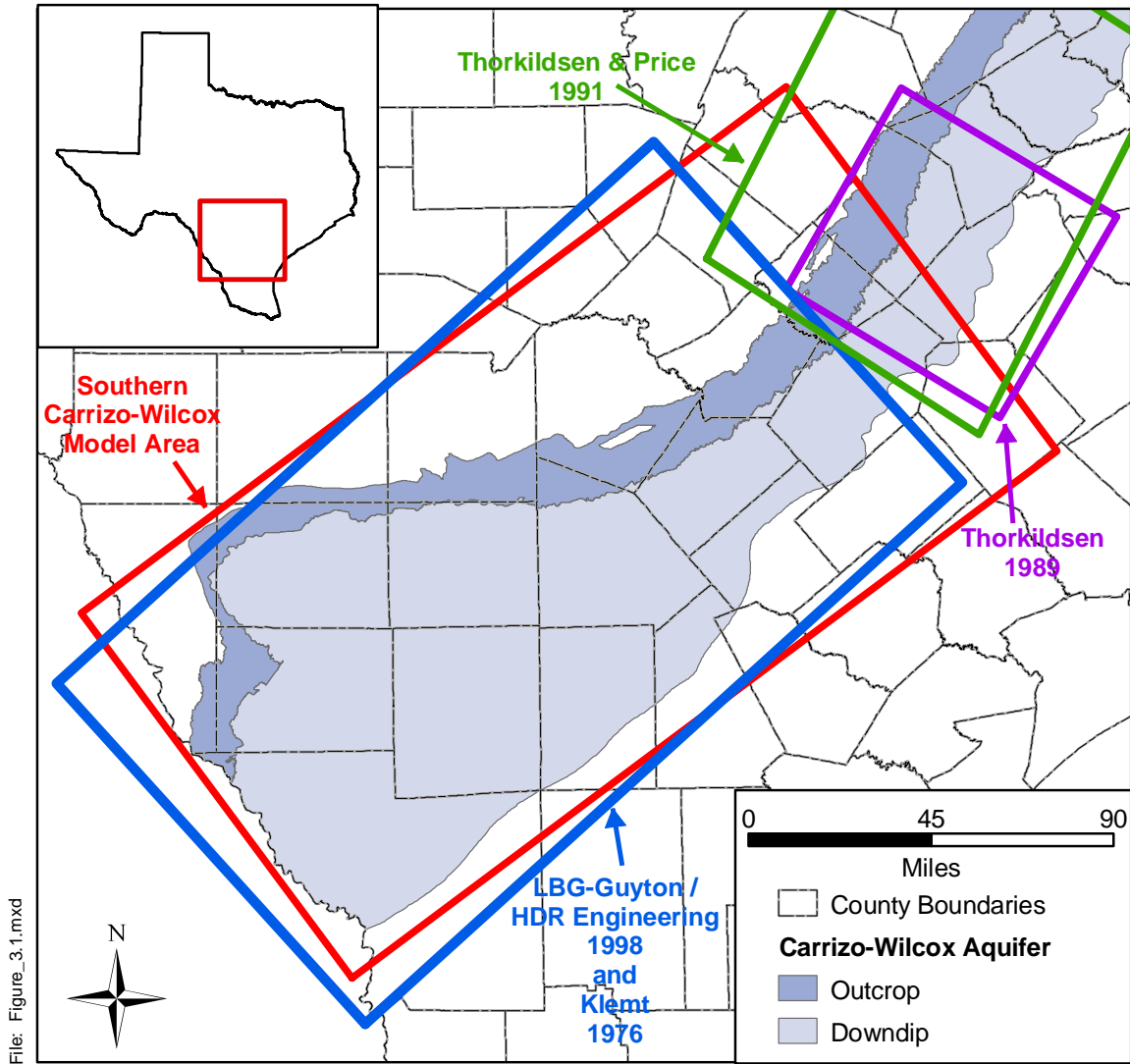


Figure 3.1 Southern Carrizo-Wilcox GAM model boundary with previous modeling study boundaries which have included the Carrizo-Wilcox aquifer.

4.0 HYDROGEOLOGIC SETTING

The hydrogeologic setting of the Carrizo-Wilcox aquifer is defined by the hydrostratigraphy, hydraulic properties, structure, regional groundwater flow, surface and groundwater interaction, and recharge and discharge. The characterization of the hydrogeologic setting is based on previous geologic and hydrologic studies in the area and a detailed compilation and analysis of structure maps, hydraulic properties, water-level data, spring and stream flow data, and climatic information.

4.1 Hydrostratigraphy

The Carrizo-Wilcox aquifer extends from South Texas northeastward through East Texas into Arkansas and Louisiana. The aquifer consists of fluvial-deltaic sediments of the upper Paleocene and lower Eocene Wilcox Group and Carrizo Sand. The aquifer is bounded below by marine deposits of the Midway Group and above by the Reklaw and Bigford formations, representing a semi-confining unit between the Carrizo Sand and the shallow aquifer, the Queen City Formation.

The Southern Carrizo-Wilcox GAM model area extends from the groundwater divide between the San Marcos and Colorado rivers to the Rio Grande to the south. In this area, the Wilcox Group is subdivided into a lower, middle, and upper Wilcox. The upper Wilcox in the deeper subsurface is correlated to the Carrizo Formation in the outcrop (Bebout et al., 1982; Hamlin, 1988). Bebout et al. (1982) mapped the lower contact of the upper Wilcox based on the lower regional marker identified in geophysical logs by Fisher and McGowen (1967). Hamlin (1988) also combined the Carrizo and upper Wilcox and mapped the base of the upper Wilcox as a distinct facies change from a fluvial (bed-load channel system) and mixed alluvial facies in the upper Wilcox to a predominantly marine facies (delta, prodelta) in the middle Wilcox.

In comparison, Klemm et al. (1976) lithologically picked the base of the Carrizo aquifer as the top of the Wilcox Group by identifying the base of the major sand units of the Carrizo Formation. Klemm's mapped Carrizo Formation correlates with the Carrizo, as mapped in central Texas (Ayers and Lewis, 1985), and was used as a layer for the southern model. However, the definition of the upper Wilcox required combining two different data sources having somewhat different interpretations. In order to discriminate the sand facies of the upper Wilcox from the

middle Wilcox, the thickness difference between the Carrizo Sand mapped by Klemt et al. (1976) and the Carrizo-upper Wilcox mapped by Hamlin (1988) was used as the upper Wilcox layer. In much of the updip section, Hamlin's base of the upper Wilcox intersects Klemt's base of Carrizo. For layer consistency, we assumed that in this area the upper Wilcox layer thins to a minimum thickness having the same characteristics as the underlying middle Wilcox.

The Carrizo-upper Wilcox in the southern GAM area is characterized by three distinct depositional systems, including a mixed alluvial system, a bed-load channel system, and a deltaic system (Hamlin, 1988). The bed-load channel system comprises the massive sand typically associated with the Carrizo aquifer, but also contains some sandy mud. The mixed alluvial system consists of interbedded sand and mud associated with channel sands and abandoned channel fill, levee and crevasse splay, floodplain, lacustrine, and delta plain sediments. The deltaic system consists of delta-front sand, which changes to prodelta mud basinward. This change to marine facies was considered the boundary between the upper and middle Wilcox (Hamlin, 1988). The middle Wilcox includes several transgressive flooding events and consists of various deltaic facies that form a partial hydrologic barrier between the fluvial-deltaic sediments of the lower Wilcox, and the predominant fluvial system of the Carrizo-upper Wilcox (Galloway et al., 1994).

The Reklaw Formation above the Carrizo corresponds to a more extensive transgressive flooding event and consists predominantly of marine mud, which grades in the southwestern part of the study area to non-marine mud and sands of the Bigford Formation.

The Queen City Formation represents another deltaic depositional system consisting of sands and clays and which is separated from the Sparta Sand by marine clays of the Weches Formation. In the southwest portion of the study area, the lower part of the Queen City grades into the Bigford Formation and the upper part into the El Pico clay. The overlying Sparta sand correlates to the basal sands of the Laredo Formation southwest of the Frio River.

The hydrostratigraphic layers of the Carrizo-Wilcox aquifer for the Southern Carrizo-Wilcox GAM (Figure 4.1.1) include the main depositional facies of the Wilcox Group and the Carrizo Sand. The Reklaw confining unit and Bigford Formation are represented by a single layer, accounting for variations in aquitard thickness and facies change from predominantly marine clay to mixed clay and sand in the southwestern portion of the study area. The Queen

City aquifer is included as the top layer of the model to better simulate the hydraulic gradient across the Reklaw confining unit. This allows for better determination of the leakage between the Carrizo and the shallow Queen City aquifer. Younger formations that lie above the Queen City in the southern part of the model are represented in the model by general head boundary conditions accounting for the hydraulic connection between the Queen City and the shallow water table.

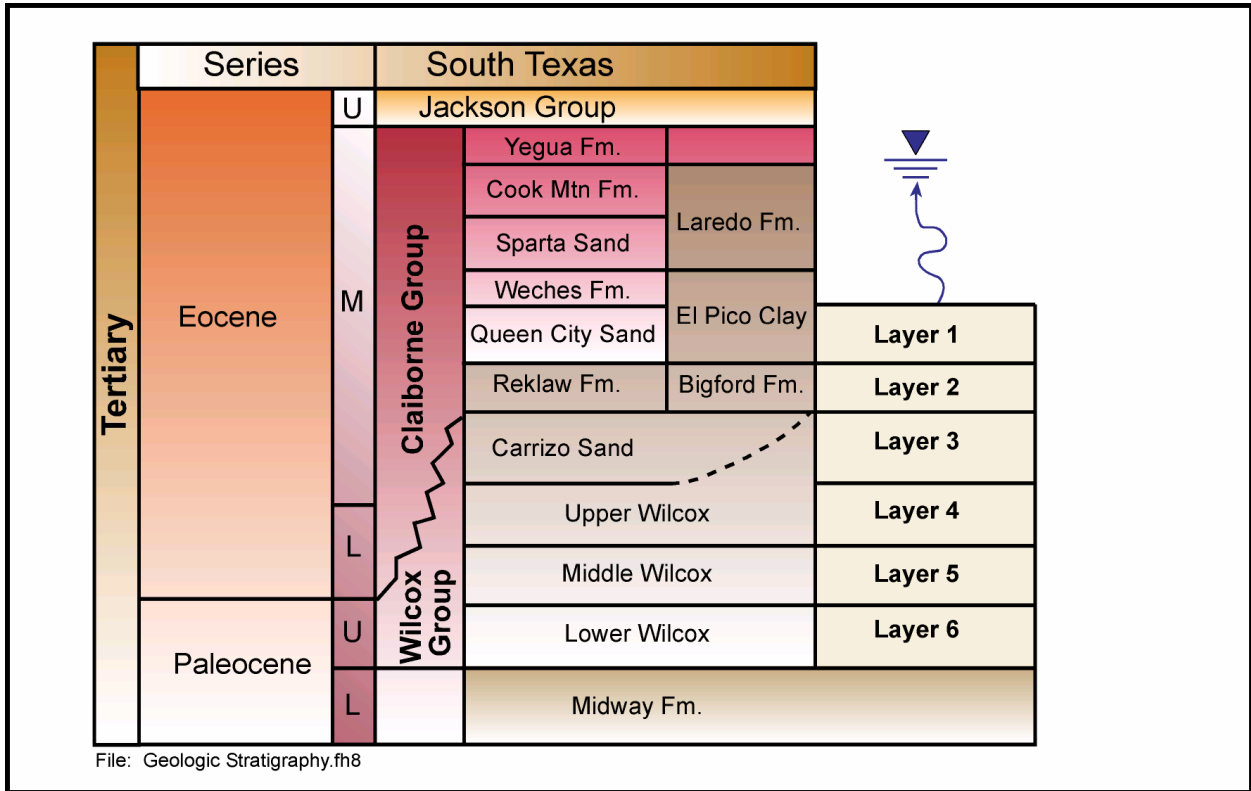


Figure 4.1.1 Hydrostratigraphy and model layers.

4.2 Structure

The structural setting for the Southern Carrizo-Wilcox GAM is dominated by the Rio Grande Embayment, the San Marcos Arch, and the growth faults along the downdip boundary of the model area. (Figure 4.2.1). The Wilcox Group and Carrizo Formation represent the earliest sand/mud sequence within the Gulf Coast Tertiary section. Cenozoic deposition is characterized by an offlapping progression of successive, basinward thickening wedges (Galloway et al., 1994). During deposition of each sediment wedge, deposition focused along sand-rich continental margin deltaic centers. The Rio Grande Embayment is the principal depocenter in the study area. Stable arches occupy the regions between embayments and are areas of lesser subsidence and deposition. In the study area, the San Marcos Arch separates the Rio Grande Embayment to the southwest from the Houston Embayment to the northeast. Growth fault trends exist within the Wilcox Group in areas where Wilcox deltas prograded basinward past the Cretaceous Stuart City Shelf Margin (Bebout et al., 1982). Displacement of sediments occurred across these faults during burial and loading, isolating pore fluids within sands and shales and preventing dissipation of pore fluids during compaction. As a result, pore fluids within the growth fault trends are at pressures above hydrostatic and are poorly connected to the up-dip portions of the aquifers.

Today the Carrizo-Wilcox aquifer outcrops in a band 10 to 20 miles wide that is sub parallel to the present-day coastline. The Carrizo-Wilcox aquifer dips into the subsurface at an average dip of 100 feet per mile. The structure surfaces of the different hydrostratigraphic units used for the Southern Carrizo-Wilcox GAM are based on many different sources, which are summarized in Table 4.2.1.

The processing of the structure data required several steps. The data from the different sources were digitized and converted to GAM coordinates and merged for the individual structure surfaces. The data were initially kriged to identify problems. Problems were solved through a combination of eliminating or adding source data or defining guide data points to constrain the kriging algorithm. The data were kriged again and delimited to the corresponding subcrop areas. The kriged and delimited data were then merged with the outcrop elevation grid, which was developed from U.S. Geological Survey digital elevation model (DEM) data. The

final kriged structure surfaces were then used to calculate layer thicknesses, which were checked to insure that layer thicknesses are not less than 20 ft throughout the model.

Figures 4.2.2 through 4.2.8 show the structure contour maps for the different hydrostratigraphic units. The structure maps identify the data control point locations and identify the data sources. The base of the Wilcox dips southeast toward the gulf coast. The overall dip of the structure surface generally increases from the south to the north (Figure 4.2.2). The top of the Lower Wilcox, shown in Figure 4.2.3, shows a similar structure as the base of the Wilcox. The data base for the bottom and top of the lower Wilcox is primarily from the USGS RASA study (Wilson and Hosman, 1987) and from Bebout et al. (1982), respectively, which both correlate with the structure surfaces in the Central Carrizo-Wilcox GAM area.

The top of the middle Wilcox is largely derived from the base of the upper Wilcox as mapped by Hamlin (1988), with additional data points from Bebout et al. (1982) in the northeastern part (Figure 4.2.4). This layer surface does not correlate with the central GAM area, because the middle Wilcox in the central GAM area is represented by the Simsboro Formation, which is mapped as the major sand layer of the Wilcox Group. South of the Colorado River, the sand thins and the Simsboro is not identifiable in geophysical logs. Figure 4.2.4 also shows the updip limit of the upper Wilcox, where the base of the upper Wilcox as mapped by Hamlin (1988) crosses the base of the Carrizo Formation as mapped by Klemt et al. (1976).

The top of the upper Wilcox corresponds to the base of the Carrizo Sand as mapped by Klemt et al. (1976), which is correlated to the top of the Wilcox in the central Carrizo Wilcox GAM (Figure 4.2.5). Similarly, the top of the Carrizo Sand is based on Klemt et al. (1976) and is correlated with the data from the Central Carrizo-Wilcox GAM (Figure 4.2.6). Additional data from TWDB (1972) were used in the downdip section. The top of the Reklaw and Bigford formations, shown in Figure 4.2.7, was based on multiple data sources (Table 4.2.1) and the top of the uppermost layer, representing the Queen City and El Pico formations (Figure 4.2.8) was based on data used in LBG-Guyton and HDR (1998).

The Gonzales County Underground Water Conservation District also provided structure data based upon boreholes in Gonzales County. Their data agreed well with the structure surfaces developed for the model on a regional basis.

The thickness maps of the various hydrostratigraphic units are shown in Figures 4.2.9 through 4.2.15, which were constructed based on the elevation difference in the structure contour maps (Figures 4.2.2 through 4.2.8). The thickness of the lower Wilcox generally increases downdip to as much as about 1800 ft (Figure 4.2.9). Note that actual data in the downdip section in the northeastern portion of the study area were limited (Figure 4.2.2 and 4.2.3) and the resulting thickness variation in this area is considered to be uncertain. The thickness of the middle Wilcox typically shows more variation reaching as much as 1000 ft in the southern part of the study area and increasing to as much as 1800 ft (Figure 4.2.10) in the northeastern part of the study area.

The upper Wilcox is comparatively thin (Figure 4.2.11) with a typical thickness range of 100 to 600 ft. As mentioned above, the updip limit is somewhat artificial because of the two different interpretations for the base of the Carrizo used by our data sources. In the model, the layer is extended beyond the updip limit with a uniform thickness of 20 ft, having properties identical to the middle Wilcox.

The thickness of the Carrizo Sand corresponds to that of Klemt et al. (1976) and is shown in Figure 4.2.12. The Carrizo is the main aquifer unit of the Southern Carrizo-Wilcox GAM. The thickness increases in the confined section to between 200 and 1100 ft, with a trend of greater thickness in the central and northeast areas as compared to the southwestern portion of the study area.

The thickness of the confining layer, represented by the Reklaw Formation in the northeast and the Bigford Formation in the southwest is shown in Figure 4.2.13. The thickness of the Reklaw is typically less than 300 ft; only toward the downdip boundary does the thickness increase significantly above 300 ft. The Bigford Formation southwest of the Frio River shows a somewhat higher thickness of about 500 ft increasing to over 800 ft near the downdip boundary (Figure 4.2.13). The uppermost model layer represents the Queen City Formation in the northeast and the El Pico Clay in the southwest (Figure 4.2.14). This layer ranges in thickness between 200 and 1500 ft in the confined section. Figure 4.2.15 provides a thickness map of the younger sediments overlying the Queen City. These units are not explicitly modeled in the GAM.

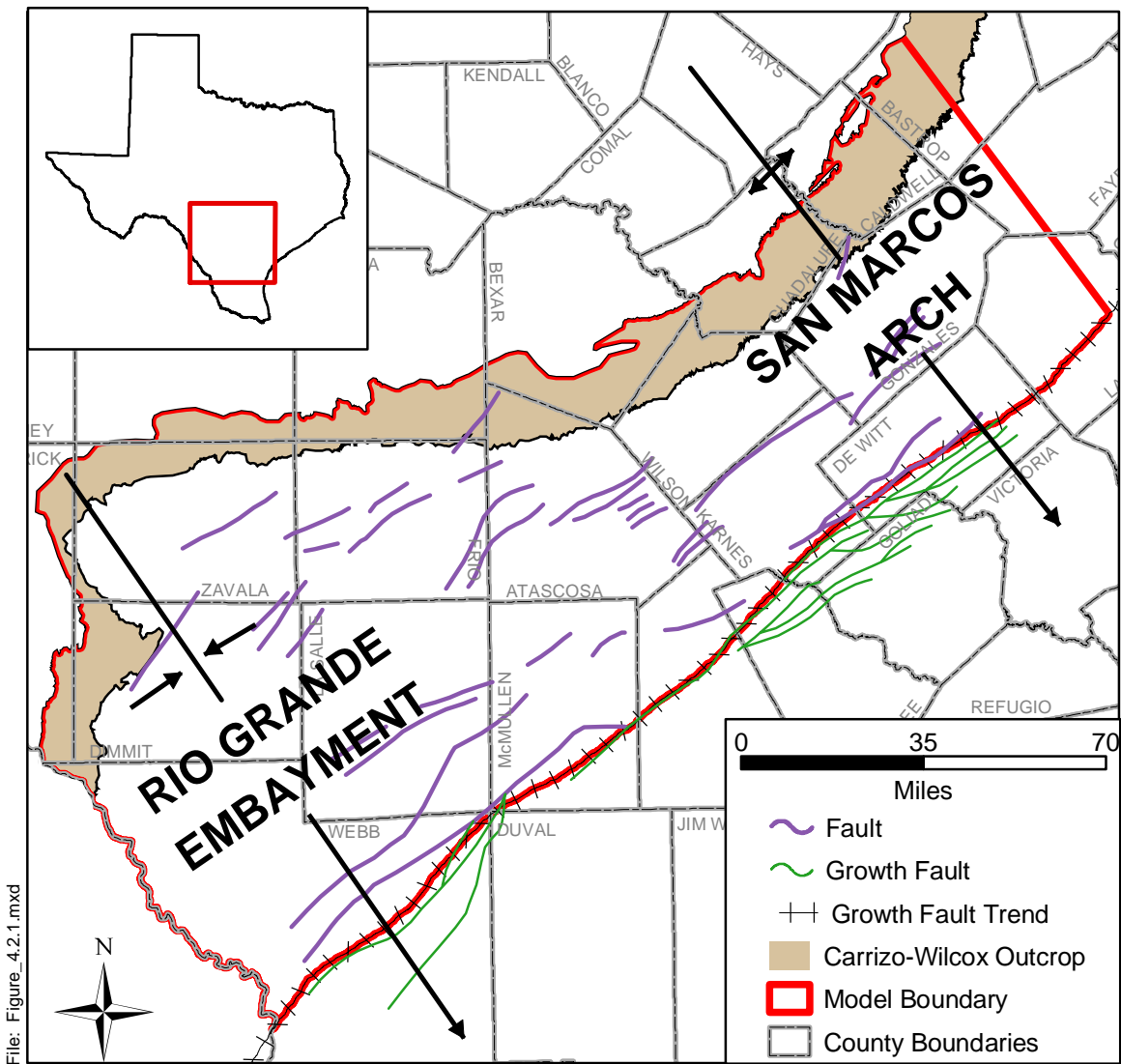
The major growth faults represent the downdip limit of the model area, where the different layers are displaced downward, effectively disconnecting downward flow paths. There are a number of smaller faults farther updip that are generally parallel to the growth fault trend (Figure 4.2.1). These faults may affect local groundwater flow pattern, but most of these faults are relatively small and do not offset the entire thickness of the modeled aquifers.

Table 4.2.1 Data sources for layer elevations for the southern Carrizo-Wilcox model.

Model Layer Boundary	LBG-Guyton and HDR (1998)	Klemt et al. (1976) (TWDB)	Wilson and Hosman (1988) (USGS RASA)	TWDB (1972)	Anders (1960) and Shafer (1965)	Hamlin (1988) (BEG)	Bebout et al. (1982) (BEG)	Central Carrizo-Wilcox GAM Model	Surface Elevations (USGS DEM)
Top of Queen City/El Pico	X								X
Top of Reklaw/Bigford	X		X		X			X	X
Top of Carrizo		X		X				X	X
Top of Wilcox		X						X	X
Top of Middle Wilcox						X	X		X
Top of Lower Wilcox							X	X	X
Base of Wilcox			X				X	X	X

Data format for the data sources:

Data Source	Report Number	Format
Klemt et al. (1976)	TWDB Report 210	Arc Info files of elevation contours provided by the Austin office of the USGS.
Wilson and Hosman (1988) - RASA	USGS Open-File Report 87-677	Printed tables.
TWDB (1972)	TWDB Report 157	Elevation contour map.
Shafer (1965) (Gonzales County)	TWDB Report 4	Geologic sections and a base map.
Anders (1960) (Kames County)	TBWE Bulletin 6007	Geologic sections and a base map.
Hamlin (1988)	BEG RI No. 175	Elevation contour map and isopach map.
Bebout et al. (1982)	BEG RI No. 117	Geologic sections and a base map.
Central Carrizo-Wilcox GAM Model		Text files containing x, y, and elevation.
LBG-Guyton and HDR (1998)		MODFLOW input files
Surface Elevations		DEM files.



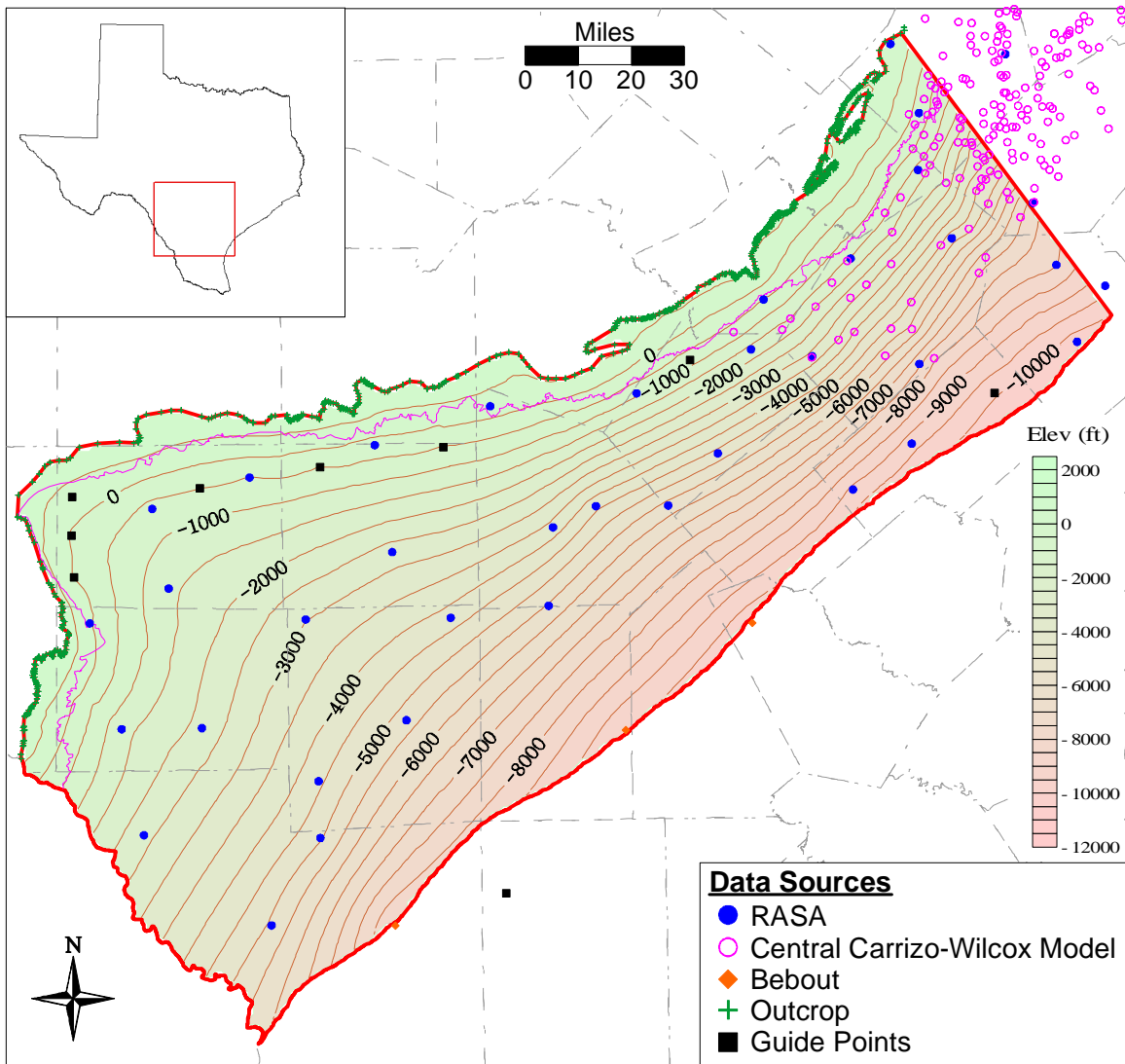


Figure 4.2.2 Structure contour map of the base of the Wilcox Group.

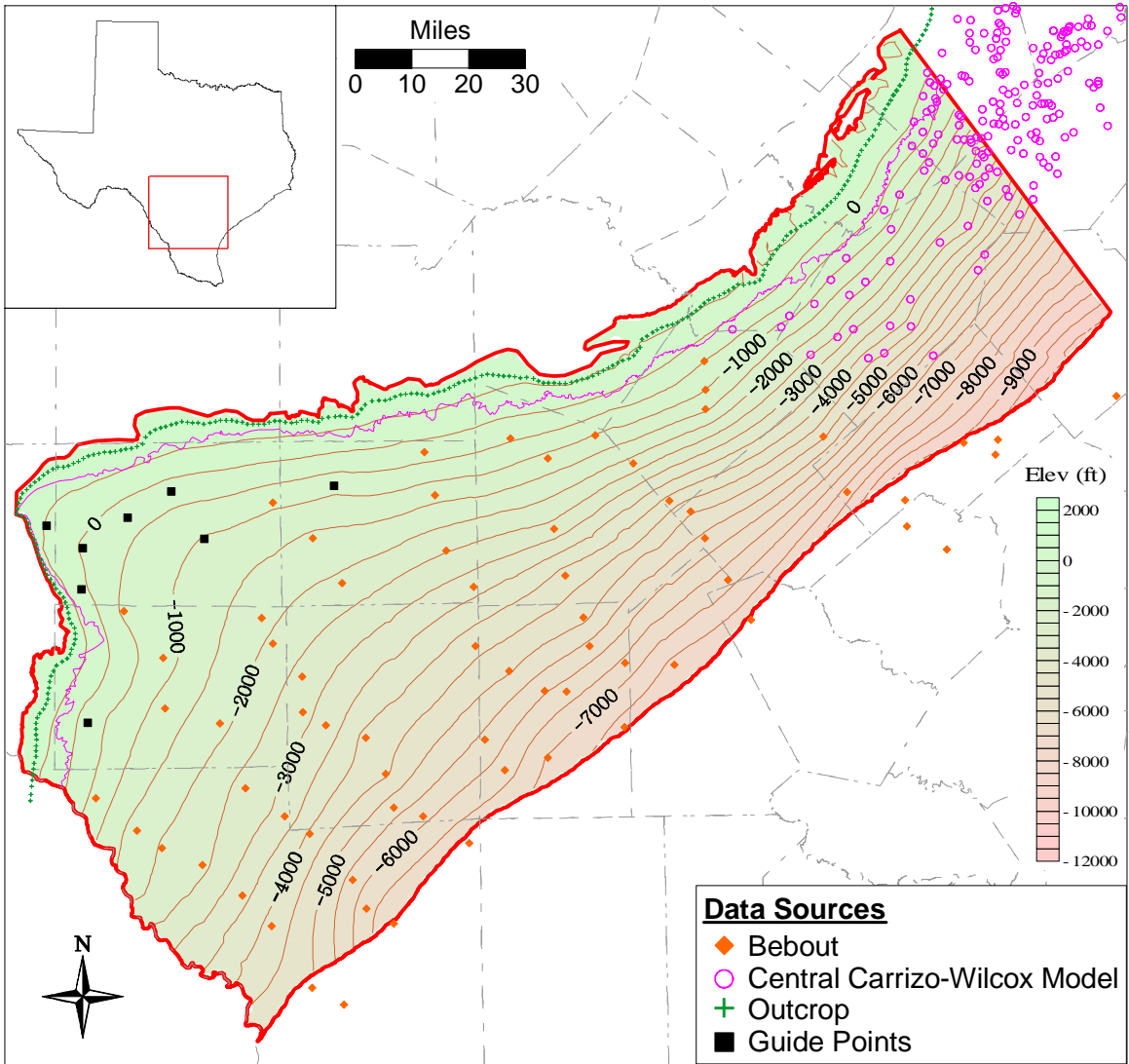


Figure 4.2.3 Structure contour map of the top of the lower Wilcox.

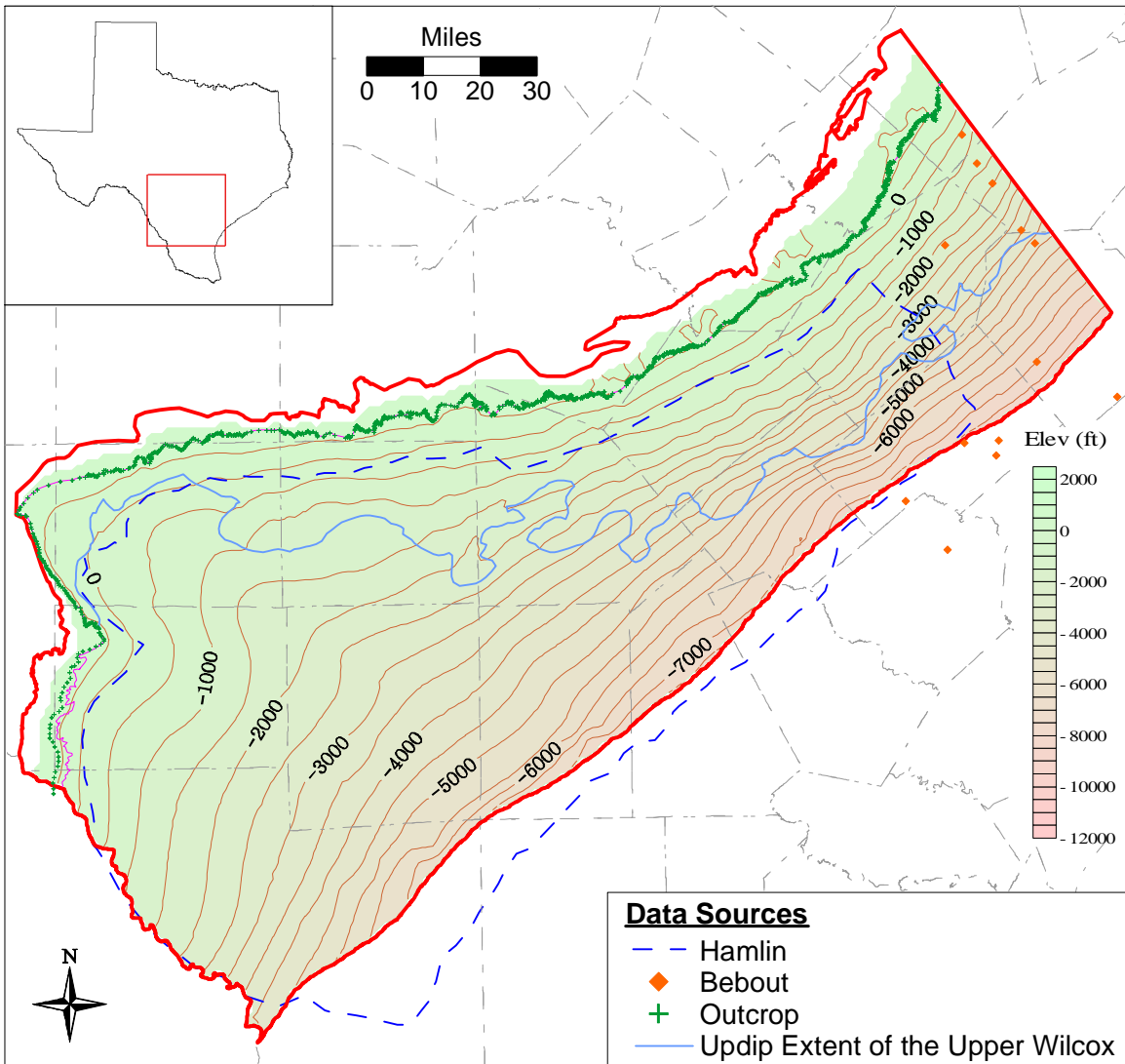


Figure 4.2.4 Structure contour map of the top of the middle Wilcox.

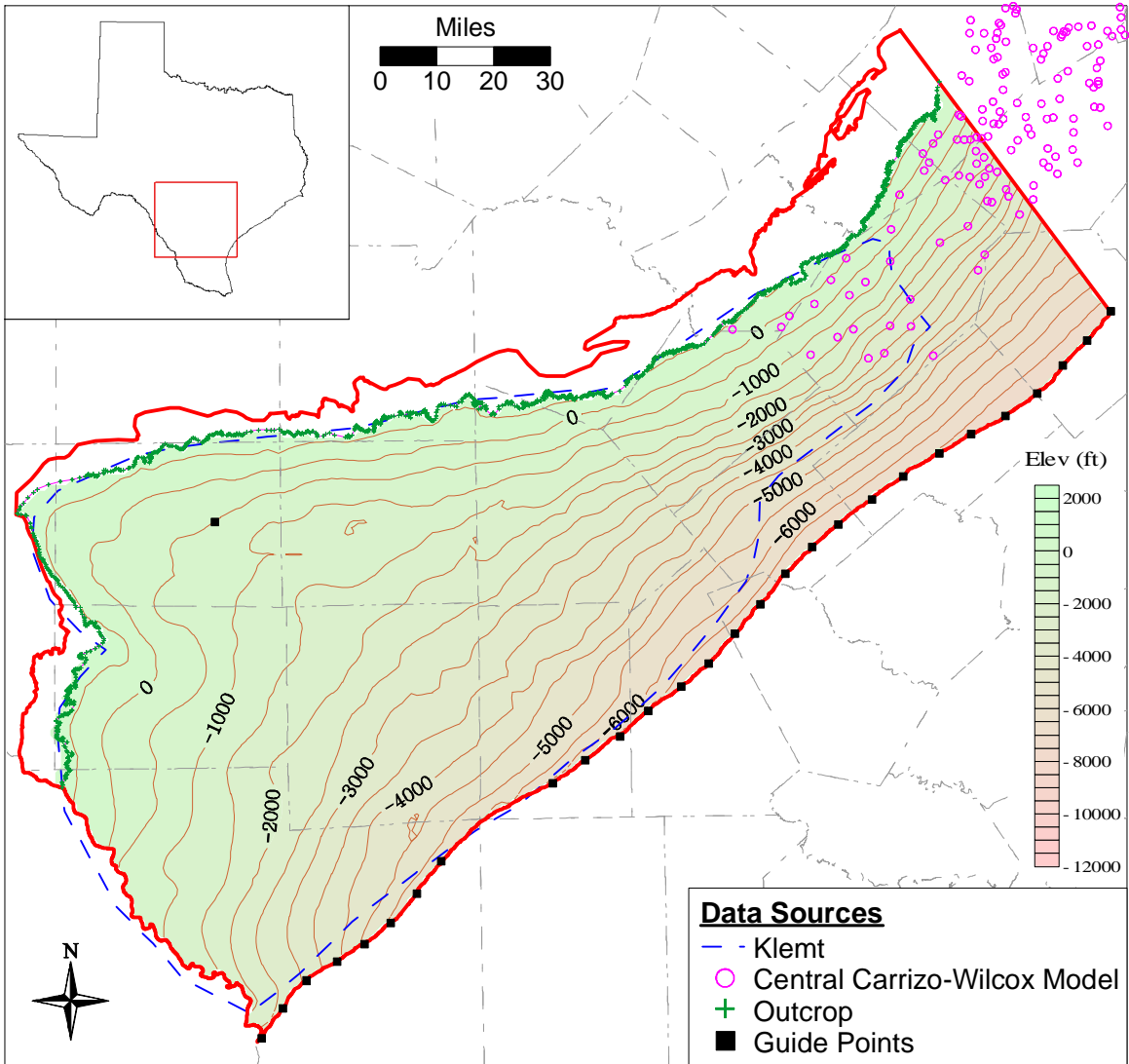


Figure 4.2.5 Structure contour map of the top of the Wilcox Group.

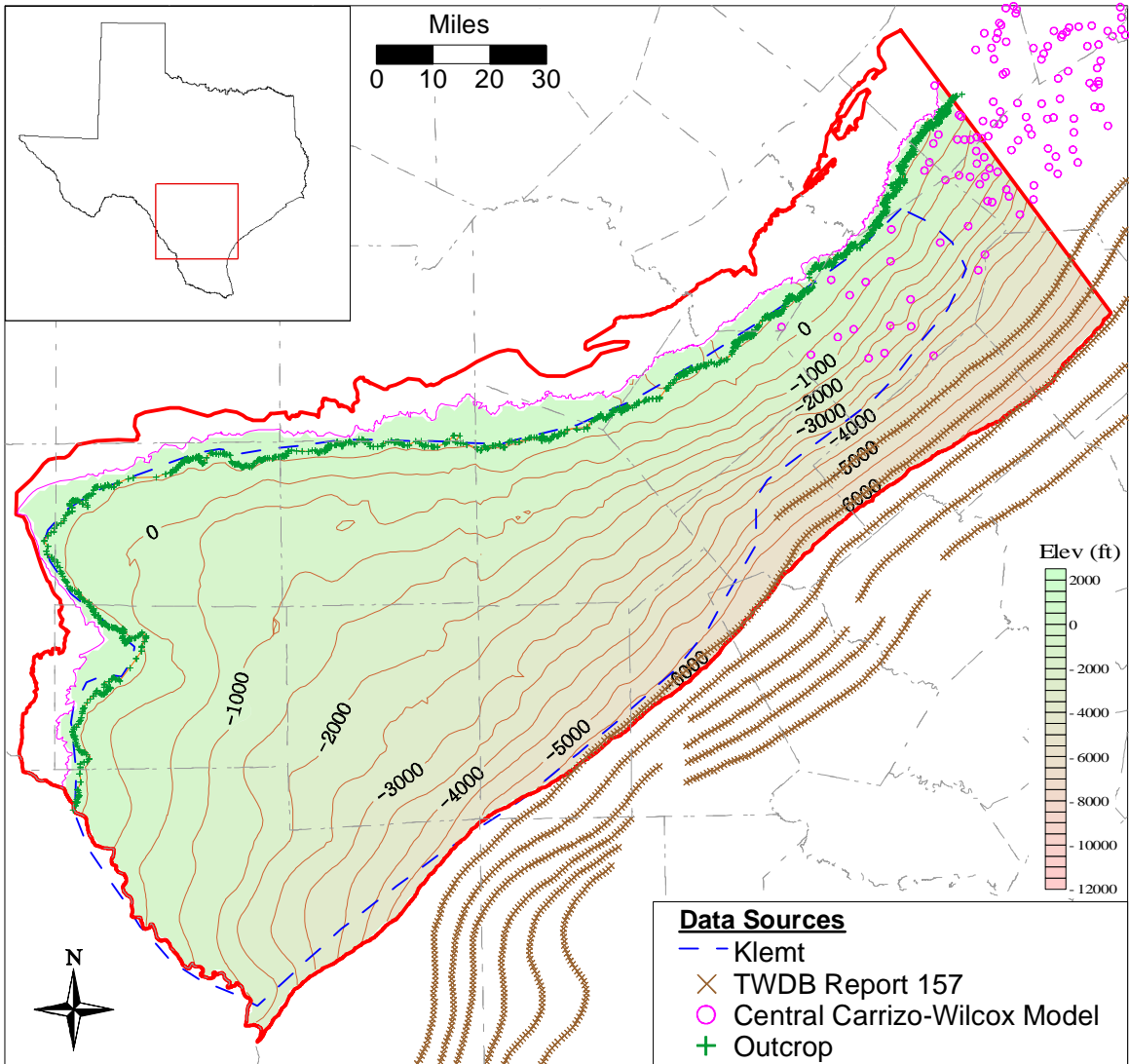


Figure 4.2.6 Structure contour map of the top of the Carrizo.

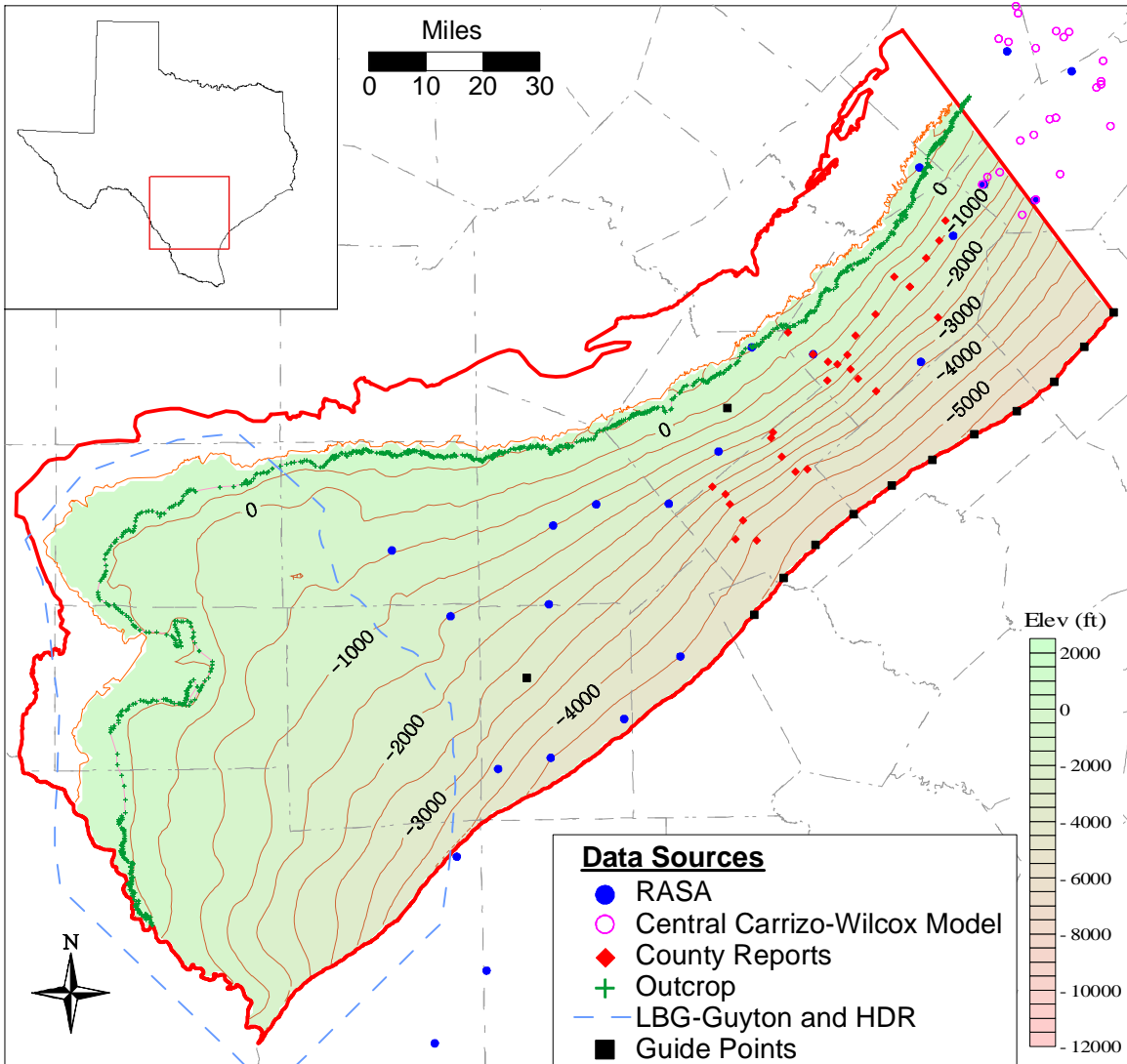


Figure 4.2.7 Structure contour map of the top of the Reklaw/Bigford formations.

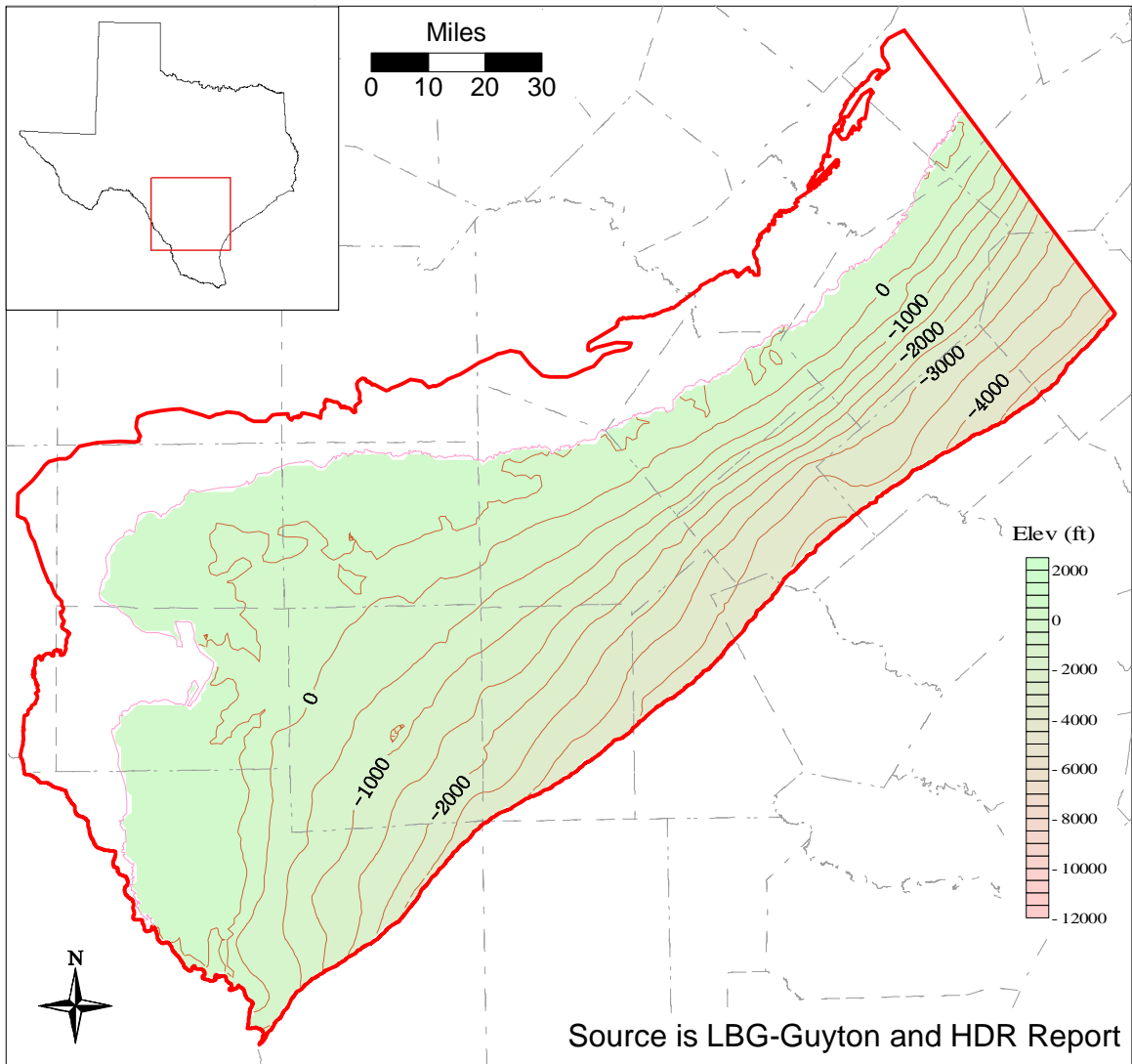


Figure 4.2.8 Structure contour map of the top of the Queen City/El Pico.

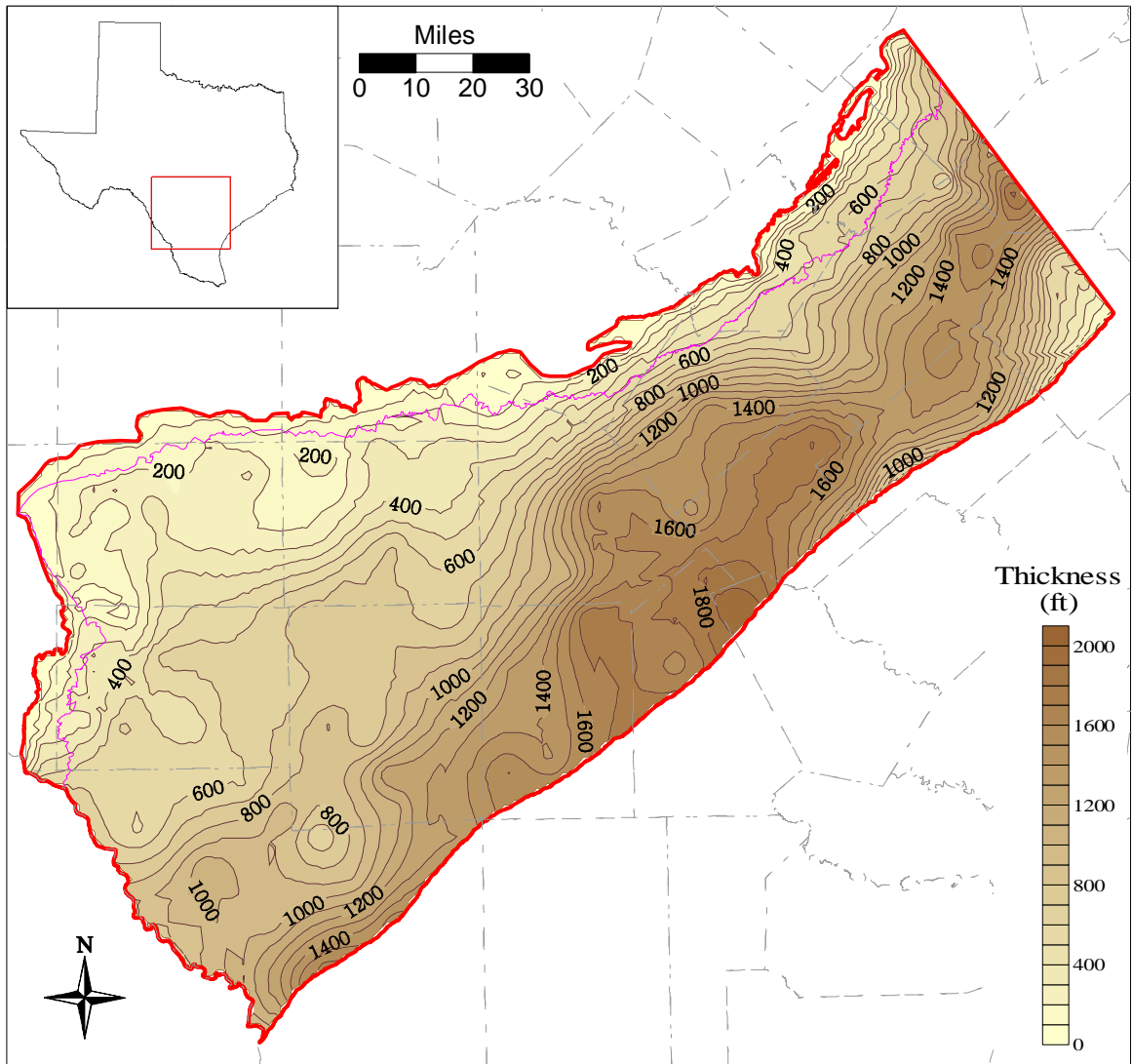


Figure 4.2.9 Thickness map of the lower Wilcox.

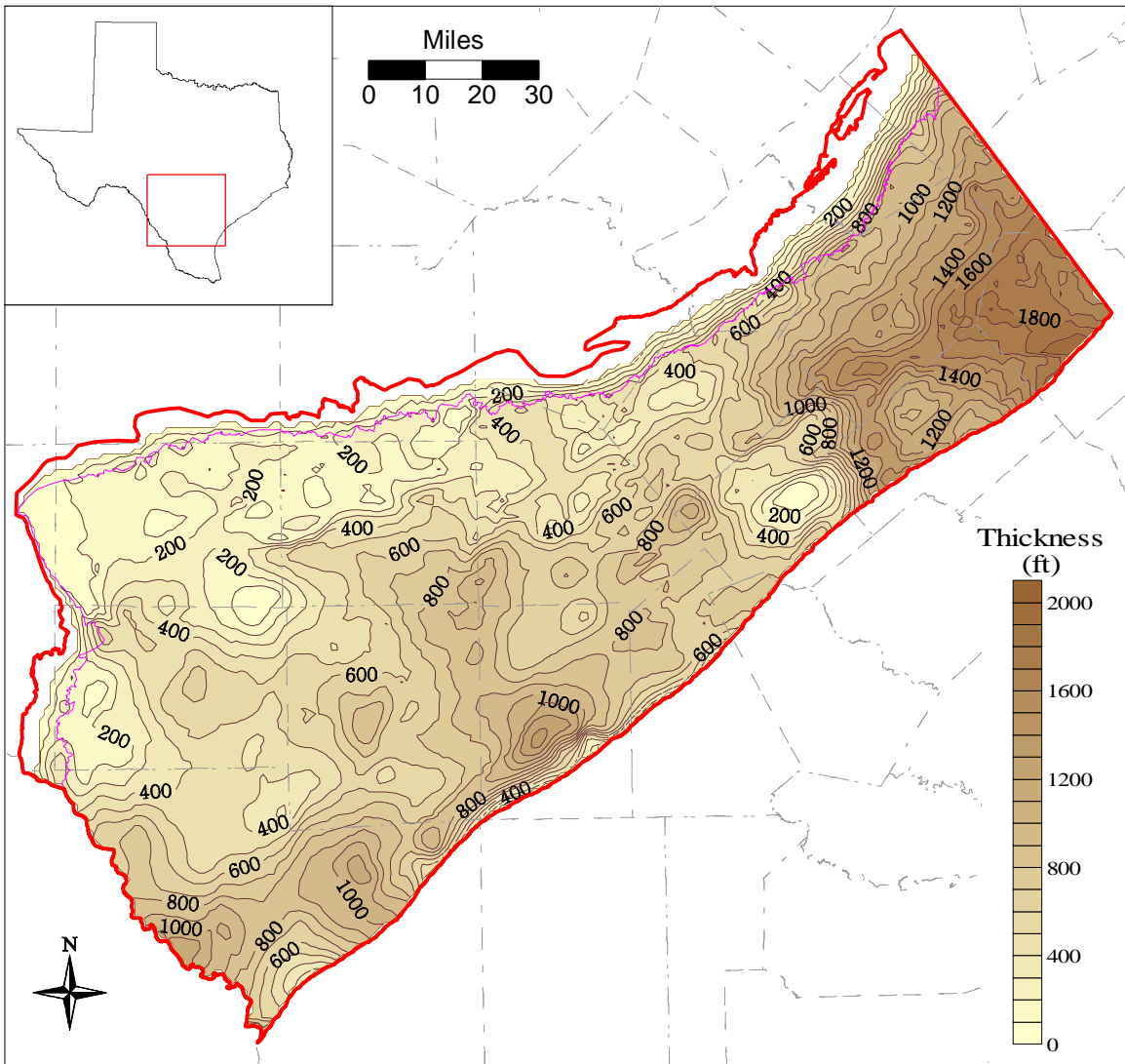


Figure 4.2.10 Thickness map of the middle Wilcox.

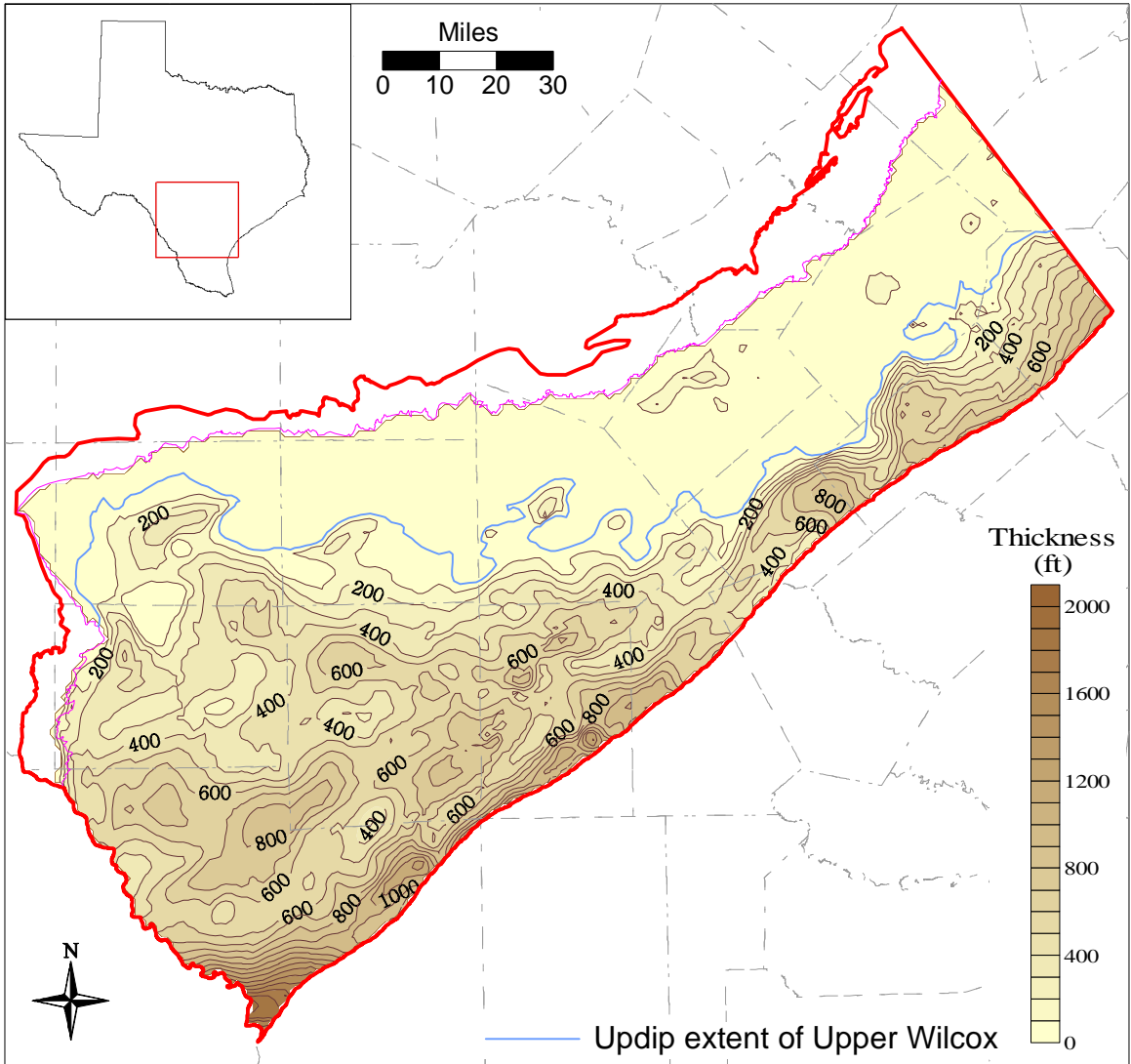


Figure 4.2.11 Thickness map of the upper Wilcox.

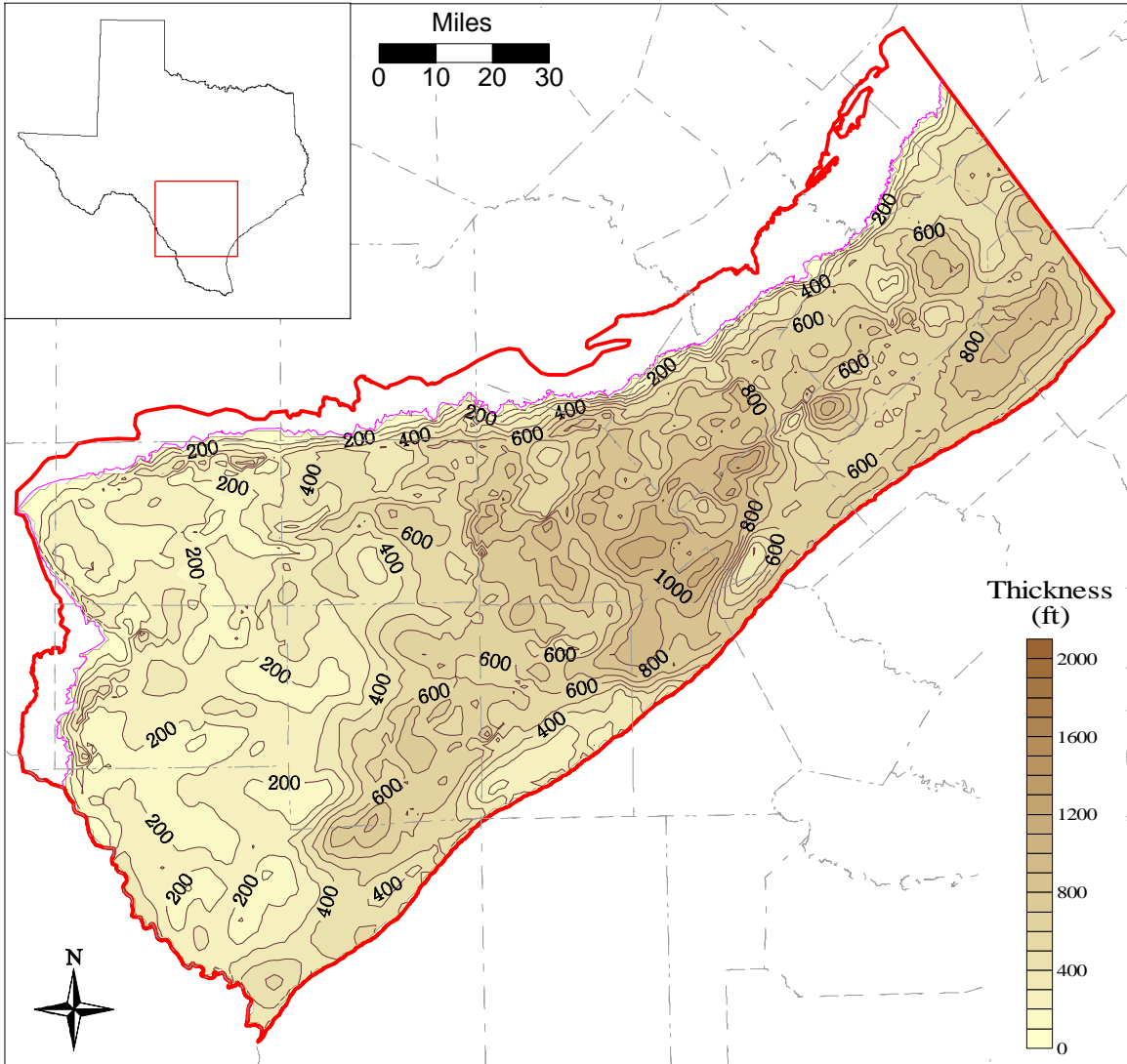


Figure 4.2.12 Thickness map of the Carrizo.

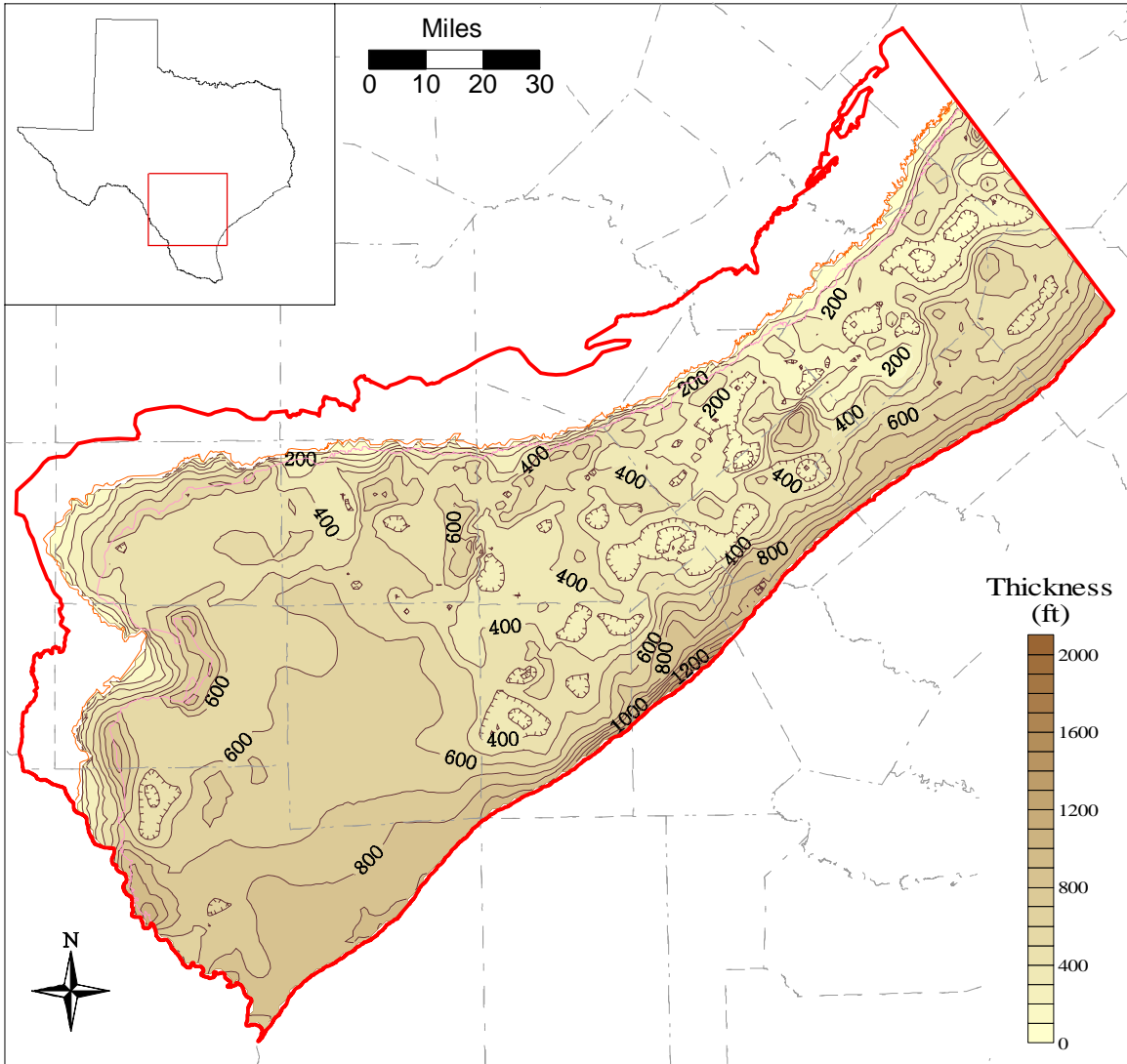


Figure 4.2.13 Thickness map of the Reklaw/Bigford.

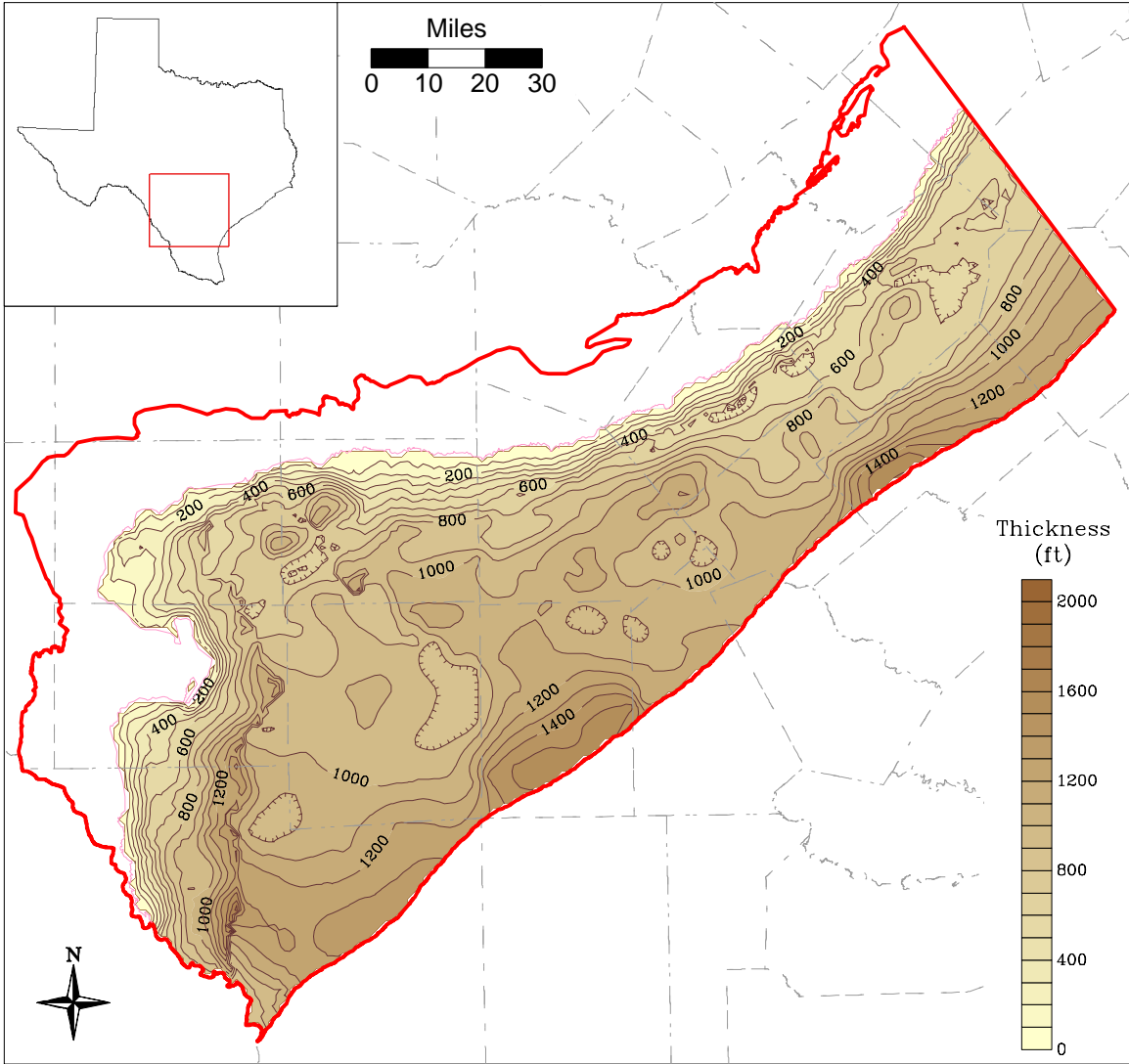


Figure 4.2.14 Thickness map of the Queen City/El Pico.

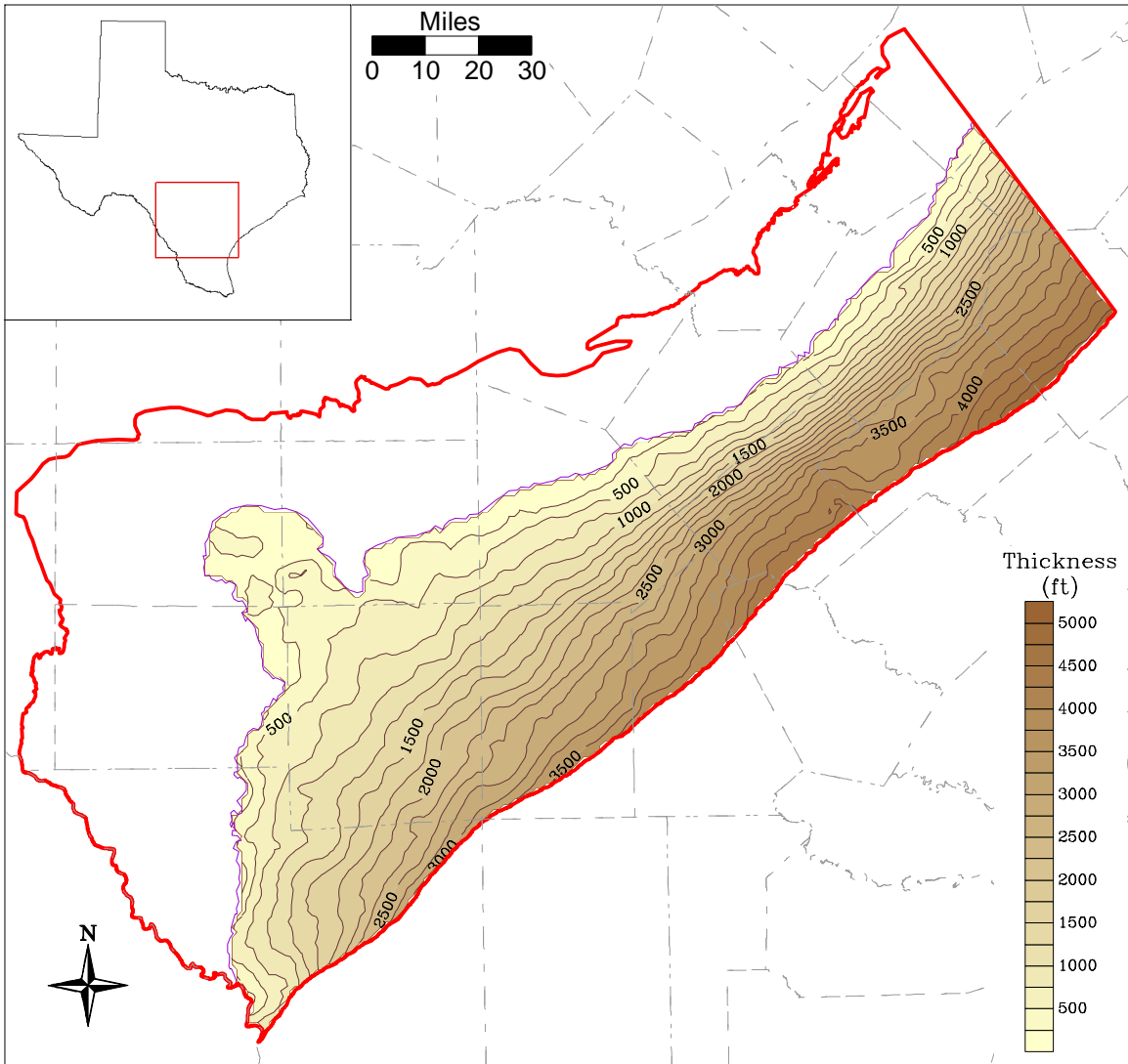


Figure 4.2.15 Thickness map of younger sediments overlying the Queen City.

4.3 Hydraulic Properties

Information on hydraulic properties of the Carrizo-Wilcox aquifer is based largely on data and sources provided by Mace et al. (2000a). INTERA also received aquifer test results for wells in Gonzales County and La Salle County from LBG-Guyton & Associates and URS Corporation, respectively. Mace et al. (2000a) compiled and statistically analyzed transmissivity, hydraulic conductivity, and storativity data from numerous sources for the entire Carrizo-Wilcox aquifer in Texas. They also analyzed spatial distributions of hydraulic properties in the Carrizo Sand and in the Wilcox Group, developing regional kriged maps of transmissivity and hydraulic conductivity. The uneven data coverage and relatively large local-scale variability, expressed in a high nugget in the semivariograms (Mace et al., 2000a), indicate significant uncertainty in the hydraulic properties of the Carrizo-Wilcox. A relationship between hydraulic properties and sand thickness (using sand maps from Bebout et al., 1982) could not be established. However, more detailed small-scale studies have determined correlations between different sand facies and hydraulic conductivities (e.g., Payne, 1975; Henry et al., 1980; Fogg, 1986; Thorkildsen and Price, 1991). The hydraulic conductivities determined through aquifer tests are biased towards higher permeability sands which tends to undermine the correlation of facies and hydraulic conductivity on a regional scale.

The Carrizo aquifer generally consists of fairly homogeneous fluvial sands overlying the multi-aquifer system of the Wilcox Group that is composed of fluvial and deltaic sands distributed among lower permeability interchannel sands and muds. Proper simulation of groundwater flow in such a complex depositional environment requires accurate description of both the subsurface arrangement of the various lithofacies (i.e., sand body distributions) and associated hydraulic properties. As pointed out by Fogg (1986), sensitivity of hydraulic head to heterogeneity or interconnectedness of sands in such a complex 3-D aquifer system is relatively low. This results in potential non-unique solutions in model calibrations and concomitant, inaccurate representations of simulated groundwater flow patterns. Moreover, hydraulic properties have to be representative for the hydrostratigraphic unit that is implemented as a model layer in the numerical model. That is, both the horizontal and vertical distributions of property measurements are important, so information on well locations and screen depths and/or well depths is required.

The evaluation of the hydraulic conductivity data was performed in several steps. Initially, the database from Mace et al. (2000a) was processed in terms of data location relative to the GAM region and to the hydrostratigraphic units. Next, a statistical analysis of the data was performed to evaluate variability between different data sources and different aquifers. A geostatistical analysis was then performed to characterize the spatial structure of the hydraulic conductivity data. Finally, trends in hydraulic properties were compared to depositional trends and/or sand-body distributions.

4.3.1 Processing of the Hydraulic Property Database

For the Southern Carrizo-Wilcox GAM, the original database from Mace et al. (2000a) was imported into an MS Access Database (file: cw_97_xp.mdb). A new data table that contains a link between the well BEG Number and the well location in GAM coordinates was added to the database (the coordinate conversion from decimal degrees to GAM coordinates was completed in ArcView). A new table was added titled “models” which identified the wells within the southern GAM region. This table was created in ArcView by intersecting the GAM outline with the point coverages of the wells. As recommended by Mace et al. (2000a), data from the Texas Railroad Commission (TRRC) and data from slug or bailing tests were excluded in this study, because of a bias toward lower values. The five aquifer tests obtained from URS and LBG-Guyton were also added to this database.

Figure 4.3.1 shows a flow diagram for the screening of hydraulic conductivity data. After discarding the TRRC, slug, and bailing test data, the remaining data were screened for the availability of a horizontal hydraulic conductivity measurement. Some data had a transmissivity measurement, but no estimate of effective thickness (e.g. screen length), and were discarded. If the top and bottom elevations of the well screen were recorded, these were compared to the model layer elevations. The hydraulic conductivity measurement was assigned to the layer that contained the largest fraction of the well screen. If the screen spanned more than three layers, the measurement was discarded. Those data without screen elevation information were checked for the presence of a layer-specific aquifer code. If this code was available, then the hydraulic conductivity measurement was assigned to that layer. Data marked only with general aquifer codes indicating multiple model layers (e.g. Wilcox Combined or Carrizo-Wilcox) were discarded.

4.3.2 Statistical Analysis of the Hydraulic Property Data

A summary of the statistical analysis of the hydraulic properties for the different hydrostratigraphic units is given in Table 4.3.1. The table summarizes the number of data measurements and the mean and median hydraulic conductivities. The hydraulic conductivities are summarized by layer with CDF curves in Figure 4.3.2. These distributions appear to be log-normal. The hydraulic conductivities for the different layers range between 0.1 ft/day to about 900 ft/day.

Table 4.3.1 Summary statistics for horizontal hydraulic conductivity

Layer	Unit	Count	Median K (ft/d)	Mean K (ft/d)
1	Queen City/El Pico	46	9.8	22.9
2	Reklaw/Bigford	74	9.9	16.3
3	Carrizo	605	31.5	55.8
4	Upper Wilcox	19	3.9	11.8
5	Middle Wilcox	215	8.1	28.2
6	Lower Wilcox	173	4.6	16.3

Figure 4.3.2 and Table 4.3.1 indicate that the Reklaw/Bigford Formation, which is considered the upper confining unit for the Carrizo-Wilcox aquifer, has relatively high horizontal hydraulic conductivity for a confining unit. The Reklaw Formation may contain extensive sand layers within muds and pumpage is reported from the Reklaw. However, some of the wells that are designated as Reklaw wells by aquifer code or by the structure data are probably completed in the adjacent Carrizo or Queen-City aquifer. Because the Reklaw is relatively thin, small errors in the structure surfaces can result in misplacement of screened intervals. West of the Frio River, the Bigford Formation is considered a minor aquifer with minor amounts of pumpage from sand layers within the muds. However, for both the Reklaw and Bigford, the more important hydraulic property is the vertical hydraulic conductivity, which is controlled by the hydraulic conductivity of the more continuous muds and shales within the Reklaw and Bigford. The vertical conductivity of the Reklaw/Bigford is not represented by the data set summarized in Table 4.3.1.

4.3.3 Spatial Distribution of Hydraulic Property Data

The spatial distribution of hydraulic properties was characterized by a variogram analysis to quantify spatial correlation and variability (for detailed background information on

geostatistics, refer to Isaaks and Srivastava, 1989). The variogram describes the degree of spatial variability between observation points as a function of distance. Typical hydrogeologic properties show some spatial correlation indicated by low variance for nearby measurements. As the distance between measurements increases, variance increases until it becomes constant, which corresponds to the ensemble variance of the entire data set. At the separation distance where the variance becomes constant, no correlation between measurements exists. The variogram quantifies the spatial variability in terms of the correlation length and variance, and provides information on spatial trends in the data. The variogram can also be used as a tool to characterize horizontal anisotropy in hydraulic conductivity. In an aquifer with horizontal anisotropy, hydraulic conductivity is a function of horizontal direction. We performed a directional-variogram analysis to detect any horizontal anisotropy in hydraulic conductivity. However, our analysis failed to identify anisotropy in horizontal hydraulic conductivity.

Figure 4.3.3 is a variogram for hydraulic conductivity of the lower Wilcox for the study area. The variogram indicates an increase in variance which levels off for distances greater than about 100,000 ft, though exhibiting large variations. A function was fit to the variogram data (experimental variogram), which shows an intercept of 0.22 at zero distance between measurements. The variance of the intercept is referred to as the “nugget”, indicating the local-scale variability of hydraulic conductivity. The nugget amounts to about half of the total variance of 0.42 of the ensemble data (“sill”), suggesting potentially large variability of hydraulic conductivity in nearby well locations and poor spatial correlation between measurements.

Once the model variogram has been developed, the spatial distribution of the hydraulic conductivity data is then produced by ordinary kriging, which uses the variogram information to estimate property values over the area of interest based on the limited number of data points available. Kriging results in some smoothing of the data by taking a weighted average of nearby measurement points. Using the hydraulic conductivity data points for the lower Wilcox, the variogram and corresponding kriged hydraulic conductivity distribution are shown in Figure 4.3.4. The kriged map of hydraulic conductivity shows that most of the data are along the outcrop and shallow confined section in the central and northeastern part of the study area. We did not krig properties past our data limits and past the correlation length. The hydraulic conductivities range from about 1 ft/day to about 30 ft/day.

The variogram for hydraulic conductivities of the middle Wilcox shows a correlation length of about 150,000 ft and a nugget of about 0.16 compared to a sill of about 0.42 (Figure 4.3.5). The hydraulic conductivity data are limited to the outcrop band and shallow subsurface similar to those of the lower Wilcox and showing a similar range in hydraulic conductivities (1 and 30 ft/day). Only 19 measurements were identified (Table 4.3.1) for the upper Wilcox located primarily in the southwestern part of the study area. We concluded that the data coverage was too sparse to construct a kriged map.

The variogram for the Carrizo Sand, shown in Figure 4.3.6, indicates a relatively small correlation length of about 25,000 ft compared to that in the lower and middle Wilcox (Figures 4.3.4 and 4.3.5). Again, the nugget is relatively high (0.16) compared to the sill (0.3), but the sill is significantly lower than those from the lower or middle Wilcox. That is, the overall variability of hydraulic conductivity in the Carrizo is lower than that of the Wilcox which is characterized by a sill of about 0.42. The kriged hydraulic conductivities range from about 1 ft/day to as much as 100 ft/day. Note that actual data coverage in the deeper confined section is limited; however, the kriged map for the Carrizo was extrapolated to the downdip boundary assuming a trend toward lower hydraulic conductivities, particularly in the southern part and the northeastern part of the study area.

The spatial distribution of hydraulic conductivity for the Reklaw and Bigford formations was not explicitly analyzed, because of limited data and uncertainty in the appropriate assignment of the data points to the Reklaw or to adjacent aquifer units. A preliminary evaluation of hydraulic property data for the Queen City Formation was performed, indicating a relatively small correlation length, a lower nugget (0.05), and a lower sill (0.2) as compared to the Carrizo-Wilcox (Figure 4.3.7). The kriged map indicates limited data distribution in the northern half of the area and very few data along the southwestern part of the area. For this particular map, the contours were limited to within a certain radius from the nearest observation point.

In general, the kriged maps of hydraulic conductivity indicate significant variability. These distributions represent horizontal permeabilities of sands within the different hydrostratigraphic units, because most wells tend to be completed and tested in sand intervals. In the Carrizo aquifer, which consists typically of 60 to over 90% sand, the spatial pattern

reflects lithologic variability and potentially depth of burial. The Carrizo kriged map was extended to the southern model boundary by including false data points to produce a decrease in hydraulic conductivity with depth toward the southern boundary consistent with interpretations by Klemt et al. (1976) and Prudic (1991). For the Wilcox, relatively large portions of the study area are not constrained by data. To incorporate the hydraulic property information into the numerical model, an approach is needed to assign properties where no data are available and to produce property values that are representative over the entire layer thickness. This is of particular importance, where the aquifer units consist of significant amounts of muds. In the following section, geologic information is examined for complementing the estimation of hydraulic properties.

4.3.4 Relationship between Hydraulic Property and Sand Distribution

The distribution of sand and muds not only affects the transmissivity of the aquifer but also the groundwater flow. Groundwater preferentially flows through more transmissive zones that consist of well connected sands of relatively high hydraulic conductivity. The hydraulic conductivity data presented in Section 4.3.3 were based on hydraulic tests performed at specific depth intervals which generally do not cover the entire thickness of the aquifer model layer. The data are also representative of the sand encountered in the interval rather than an average value over the entire screened section. The kriged hydraulic conductivity maps assume that the sands tested in adjacent wells at different depth intervals are laterally and vertically connected. This assumption is most likely valid for the Carrizo, which is dominantly sand. For the Wilcox Group, which typically consists of less than 50% sand in the lower and middle Wilcox, sand bodies are embedded in a fine-grained matrix and may not always be connected.

For the combined Carrizo-upper Wilcox unit, Hamlin (1988) produced detailed net-sand, sand-percent, and maximum sand thickness maps. The sand-percent maps by Hamlin (1988) indicated a range from 50 to over 90 percent for the Carrizo-upper Wilcox. The maximum sand thickness map identifies the thickest sand in the interval and shows spatial trends that are characteristic of high-energy bed-load sedimentation in major fluvial channels. The sand thickness is not only important to define the overall transmissivity of the aquifer but also can indicate zones of higher permeability. Intuitively, one would expect that sands in the major fluvial channels generally have higher conductivities than thinner, more isolated sands. Spatial information on sand distributions can be used as soft data to extrapolate the kriged permeability

maps to areas where no hydraulic conductivity data are available. Mace et al. (2000a) compared generalized net sand maps for the upper and lower Wilcox by Bebout et al. (1982) to transmissivity values for the Wilcox Group throughout Texas, but did not find a correlation between sand thickness and transmissivity. However, more local studies have shown relationships between sand thickness or specific channel sands and hydraulic conductivities (Payne, 1975; Fogg, 1986).

For the study area, we examined both the net sand thickness and maximum sands as well as the percent sand of the Carrizo-upper Wilcox (Hamlin, 1988) for comparison with hydraulic conductivity values. For this analysis, only hydraulic conductivity data with a Carrizo aquifer designation and with a known screen interval were used. Maximum sand maps are considered more indicative of the major channel sand, ignoring thinner and less continuous splay and overbank sands. However, the maximum sand maps show only a limited thickness range. Histograms of hydraulic conductivities (log-K) by maximum sand thickness and net sand thickness are shown in Figure 4.3.8. These two histograms show no clear relationships. The maximum sand histograms do not indicate a clear trend, whereas the net-sand histograms indicate generally lower median log-K values for thicker sands. This may be due to the fact that the net sand thickness increases downdip, where data are more limited. The kriged map for the Carrizo indicates that the highest observed conductivities are in the shallow confined section and in the outcrop, where net sand thickness is low. Figure 4.3.9 shows a correlation of increasing hydraulic conductivity with increasing sand percent. This suggests a trend to generally lower permeability downdip, where net-sand increases and sand-percent decreases. A similar trend of decreasing conductivities in the deeper section was indicated by the permeability map constructed by Klemm et al. (1976).

There are some limitations in the analysis. The sand thickness maps are manually contoured taking into account the depositional model. Furthermore, the hydraulic conductivity data points were assigned to the nearest sand thickness contour. For this study, the net-sand map was primarily used to estimate the transmissivity of the model layer. For the Carrizo, we did extrapolate the kriged hydraulic conductivities into the downdip section with limited data coverage, based on an inferred trend toward lower conductivity. This trend is apparent in the southern and northeastern part of the model areas (Figure 4.3.6).

For consistency with Carrizo structure, the net-sand map for the Carrizo was taken from Klemm et al. (1976) and using our total thickness map of the Carrizo, a sand-percent map was generated (Figure 4.3.10). The percent sand for the upper Wilcox (Figure 4.3.11) was derived by subtracting the sand thickness of Klemm et al. (1976) from the combined Carrizo-upper Wilcox sand thickness by Hamlin (1988) and dividing by our total thickness map of the upper Wilcox. Zones of hydraulic conductivity were based upon the derived sand percent map. Similarly, hydraulic properties for the middle and lower Wilcox were based on zones incorporating the kriged hydraulic conductivities in the outcrop and shallow confined section where data were available.

4.3.5 Vertical Hydraulic Conductivity

Specific data on vertical hydraulic conductivity within the Carrizo-Wilcox aquifer and for the Reklaw confining layer are not available at the scale of this study. Previous modeling studies of the Carrizo-Wilcox aquifer derived estimates of vertical permeability from model calibration. Stochastic modeling studies of a generic aquifer system consisting of two contrasting hydraulic conductivity facies (channel sands and finer grained interchannel sediments) having various degrees of vertical interconnection indicate effective vertical conductivities ranging between the geometric and harmonic mean conductivities (Fogg, 1989).

A lower bound estimate of vertical conductivity can be calculated as the lowest vertical conductivity value measured in a hydrostratigraphic section, assuming complete lateral continuity of the low-permeability zone. Measurements of hydraulic conductivity typically focus on high-permeability zones with a few core data available for low-permeability muds within the Wilcox Group (Bob Harden, personal communication). In the Region G model developed by Harden and Associates (2000), core estimates of clay hydraulic conductivity were used to represent clay strata within the Carrizo-Wilcox aquifer ($K = 5.35 \times 10^{-6}$ ft/day). The effective vertical conductivity for the different aquifer layers were estimated based on a harmonic mean of the individual proportions of sand, silt, and clay (Harden and Associates, 2000).

Fogg et al. (1983) inferred a maximum reasonable horizontal to vertical permeability ratio K_h/K_v (anisotropy ratio) on the order of 10,000 to 1,000 to reproduce the vertical head gradients within the Carrizo-Wilcox aquifer in a groundwater flow model near the Oakwood salt

dome in Freestone and Leon counties. A vertical to horizontal anisotropy ratio of 1,000,000 was considered too low to reproduce the general pressure-depth gradients across the model.

The vertical hydraulic conductivity of the Reklaw confining layer can be considered to be less than that of the Wilcox aquifer, because of more continuous fine-grained lithologies. In the southwestern portion of the study area, the Bigford contains more sand layers within the clays, which could increase the effective vertical hydraulic conductivity. On the other hand, the Bigford Formation is thicker, allowing for more continuous clay layers.

Fogg et al. (1983) used a vertical hydraulic conductivity of 2.6×10^{-4} ft/day for the Reklaw in their model, which they considered a maximum value. The USGS RASA model for the Texas Gulf Coast aquifer systems reported a vertical hydraulic conductivity of the lower Claiborne confining unit (equivalent to the Reklaw Formation) of 2×10^{-5} ft/day from their calibrated transient model (Ryder and Ardis, 1991). This value was lower than the calibrated value from an earlier steady-state model by Ryder (1988) of 1×10^{-4} ft/day.

The Carrizo Formation is generally considered to have much lower anisotropy ratios than the Wilcox, because of typically much higher sand content. However, the range in measured hydraulic conductivities for the Carrizo in the study area ranges over four orders of magnitude (Figure 4.3.2). Previous modeling studies reported Carrizo-upper Wilcox anisotropy ratios (K_v/K_h) of 2.5×10^{-3} based on a steady-state calibration (Ryder, 1988) and 8.7×10^{-5} based on a transient model calibration (Ryder and Ardis, 1991).

4.3.6 Storativity

The specific storage of a confined saturated aquifer can be defined as the volume of water that a unit volume of aquifer releases from storage under a unit decline in hydraulic head (Freeze and Cherry, 1979). The storativity is equal to the product of specific storage and aquifer thickness and is dimensionless. For unconfined conditions, the storativity is referred to as the specific yield and is defined as the volume of water an unconfined aquifer releases from storage per unit surface area of aquifer per unit decline in water table (Freeze and Cherry, 1979).

Mace et al. (2000a) compiled 107 estimates of storativity and calculated 64 estimates of specific storage from tests of the Carrizo-Wilcox aquifer where the screen length was known. Storativity ranged in magnitude from 1×10^{-6} to 0.1 with a geometric mean equal to 3×10^{-4} . Specific storage ranged from about 1×10^{-7} to 1×10^{-4} 1/m with a geometric mean of 4.6×10^{-6} 1/m.

The medians were essentially equal to the geometric mean for both distributions demonstrating the lognormal form of both distributions.

Specific yield estimates summarized in Table 4.3.2 are derived from aquifer tests and from model calibrated values. The range of specific yield is from 0.05 to 0.32. Perhaps the most direct estimate of specific yield is from Duffin and Elder (1979). They performed 20 seismic refraction profiles in the Carrizo Sand outcrop in areas west of Gonzales County.

Table 4.3.2 Summary of literature estimates of Carrizo-Wilcox specific yield.

Source	Specific Yield	Reference
TWDB Report 210	0.25 (average)	Klemt et al. (1976)
TDWR Report 229	0.16 to 0.32	Duffin and Elder (1979)
TWDB/LCRA model	0.05 to 0.3	Thorkildsen et al. (1989)
TWDB Report 332	0.1 to 0.3	Thorkildsen & Price (1991)
USGS OFR 91-64	0.15	Ryder & Ardis (1991)
BEG RI 256	0.29 (Simsboro)	Dutton (1999)
Region G Model	0.15	Harden & Assoc. (2000)

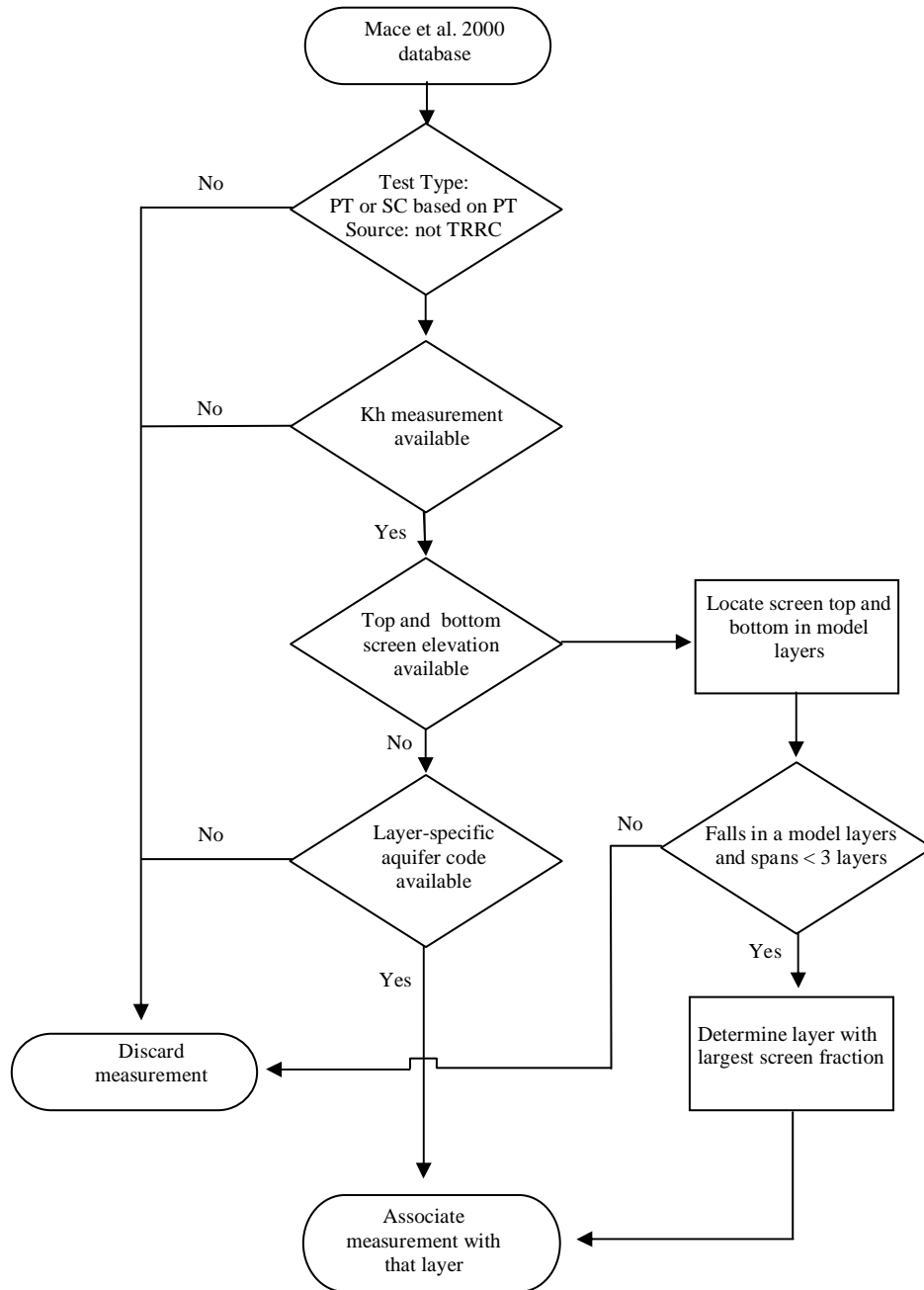


Figure 4.3.1 Screening of hydraulic conductivity data.

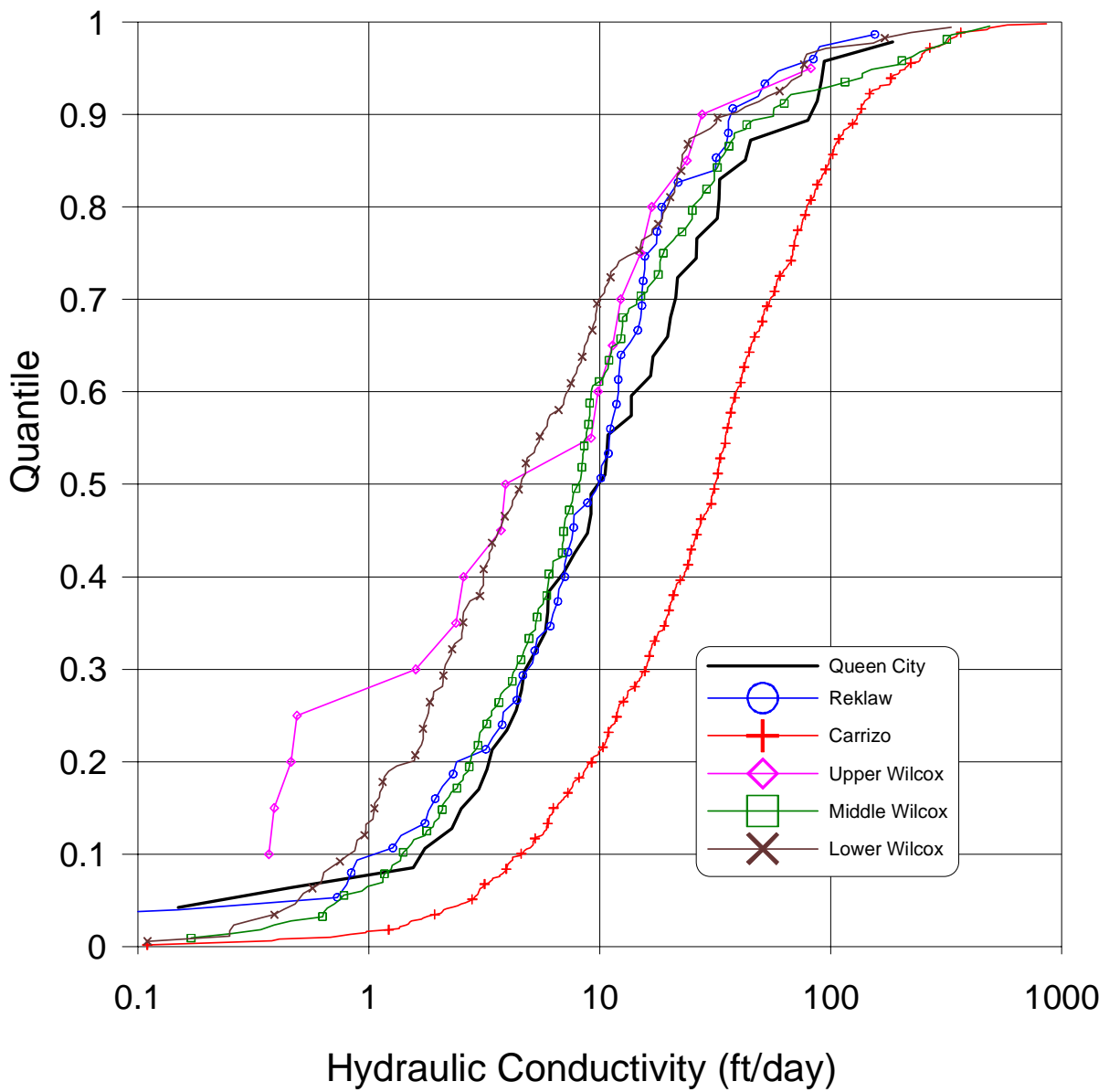


Figure 4.3.2 CDF curves of hydraulic conductivity for the modeled aquifer units.

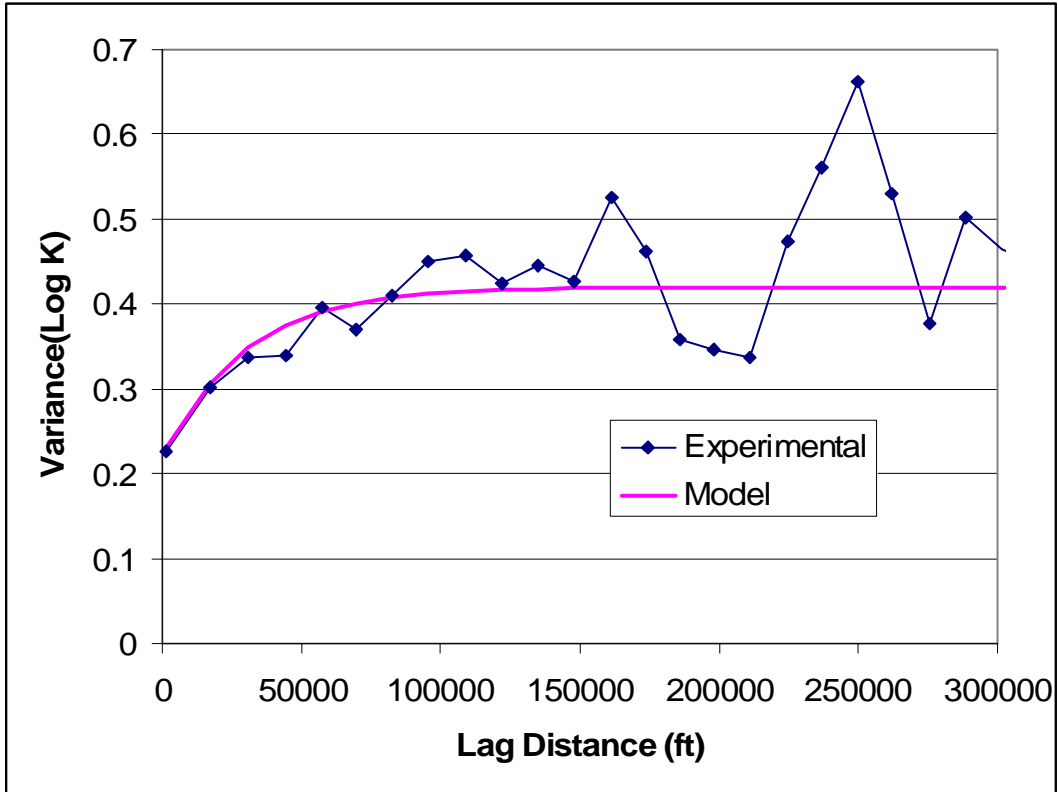


Figure 4.3.3 Variogram for hydraulic conductivity data for the lower Wilcox.

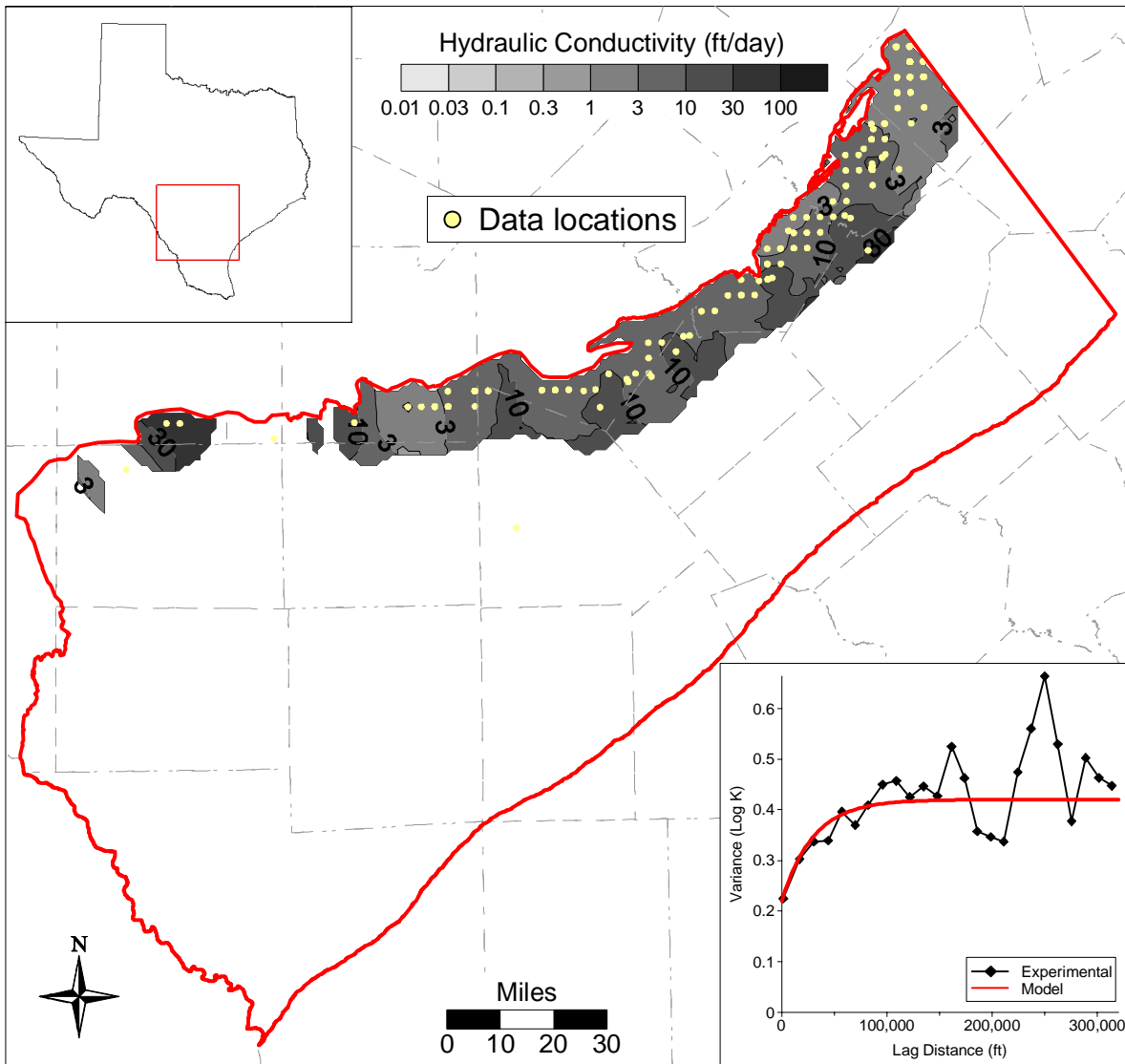


Figure 4.3.4 Variogram and kriged map of hydraulic conductivity for the lower Wilcox.

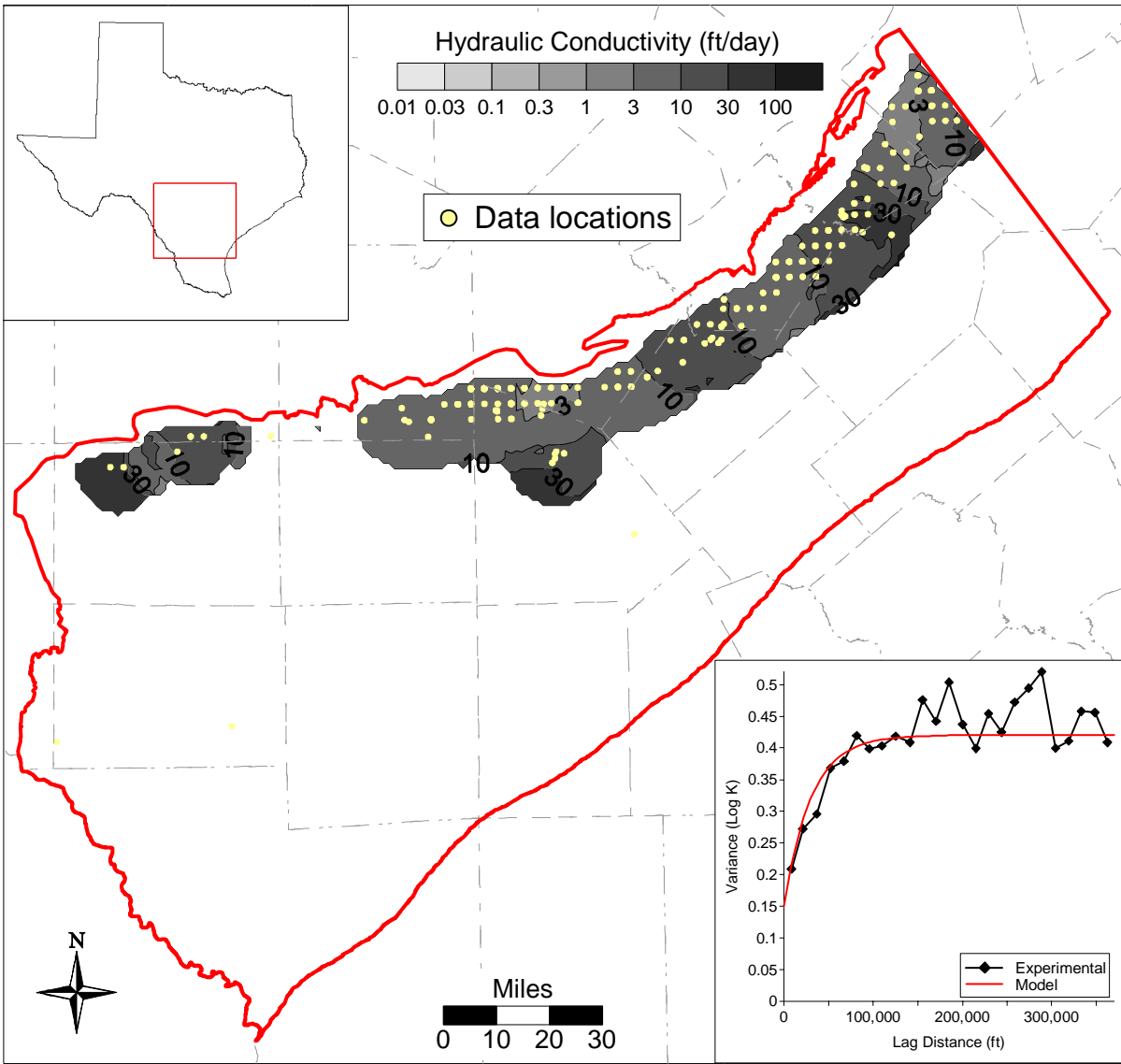


Figure 4.3.5 Variogram and kriged map of hydraulic conductivity for the middle Wilcox.

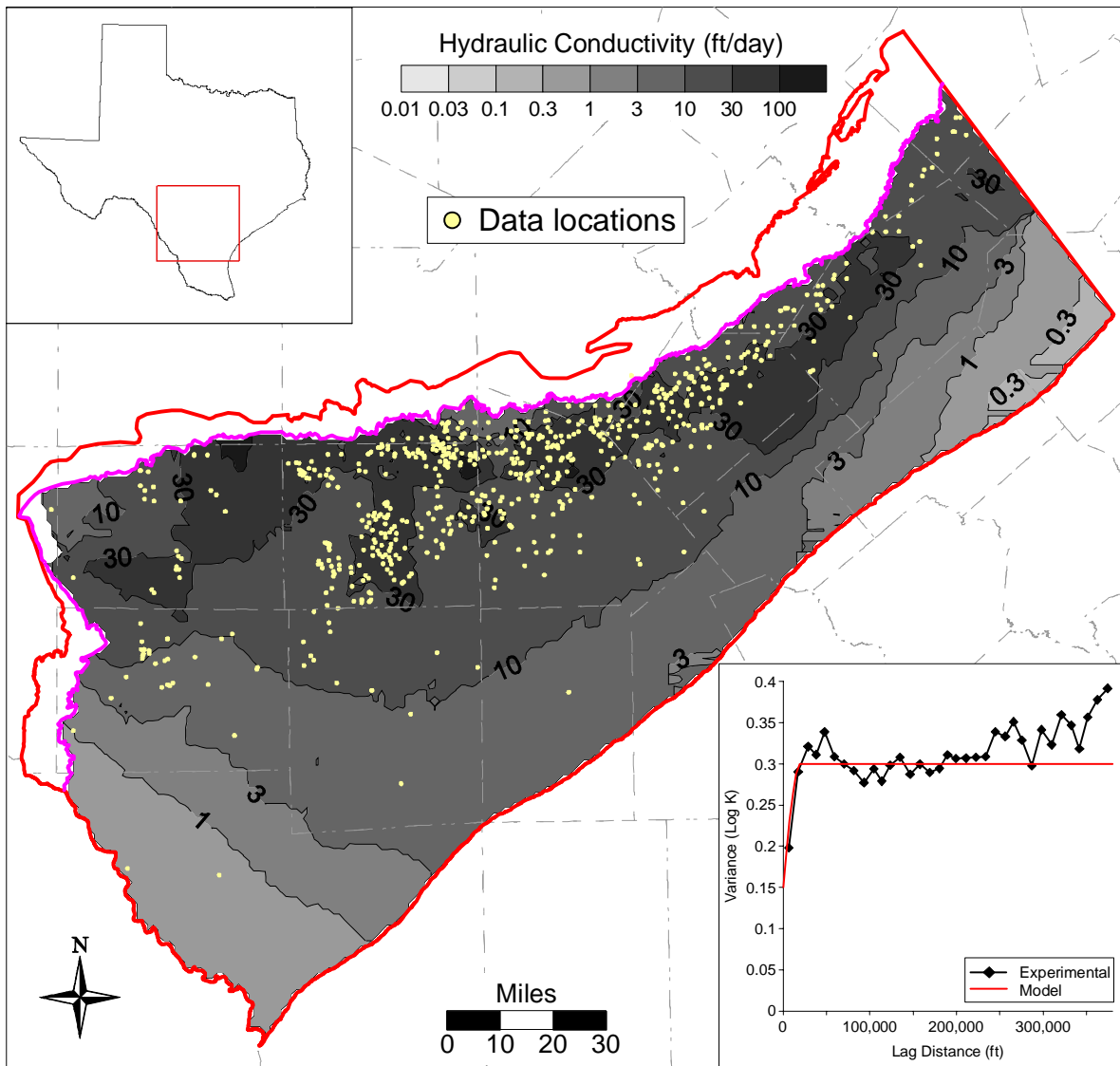


Figure 4.3.6 Variogram and kriged map of hydraulic conductivity for the Carrizo.

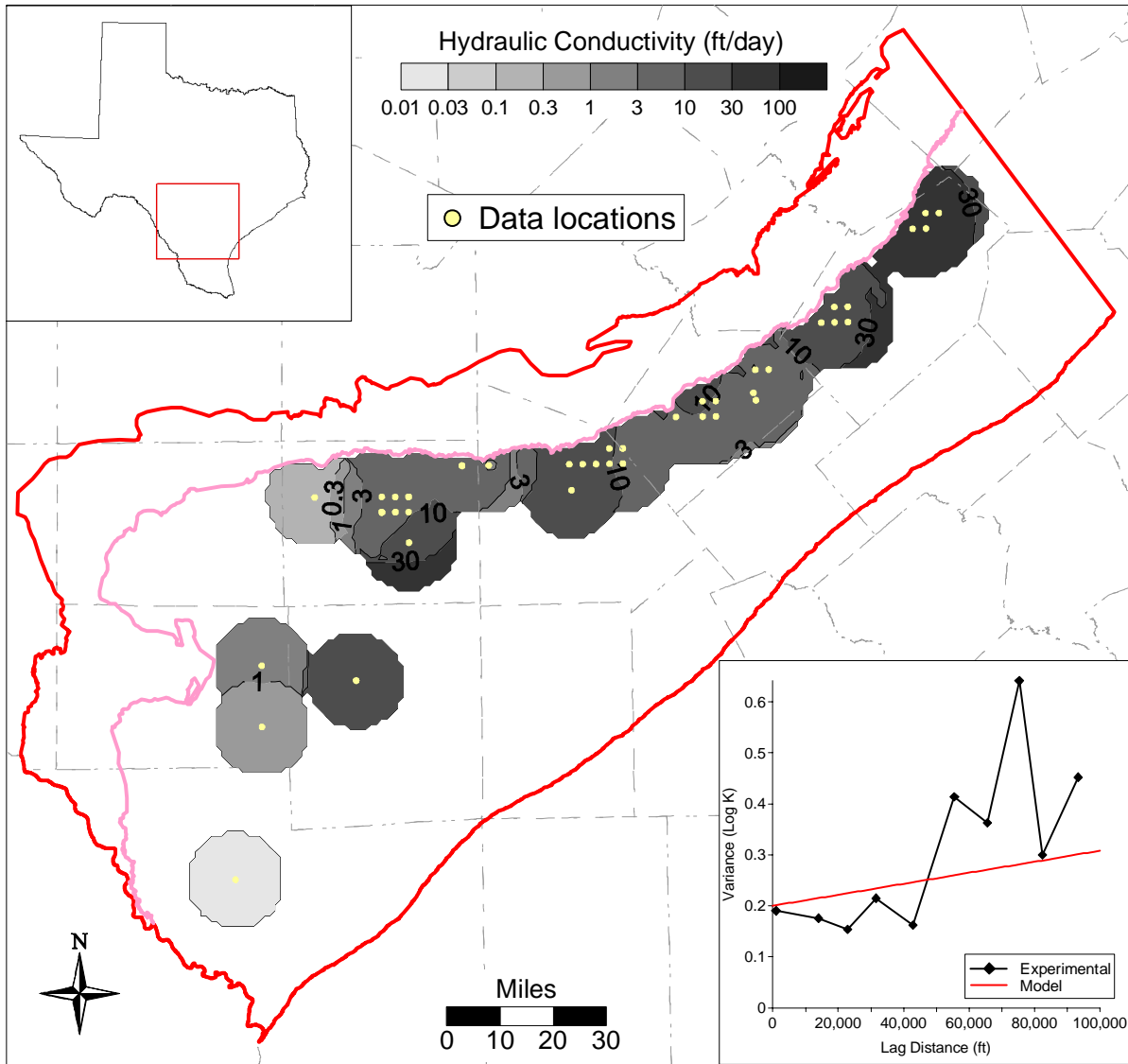


Figure 4.3.7 Variogram and kriged map of hydraulic conductivity for the Queen-City.

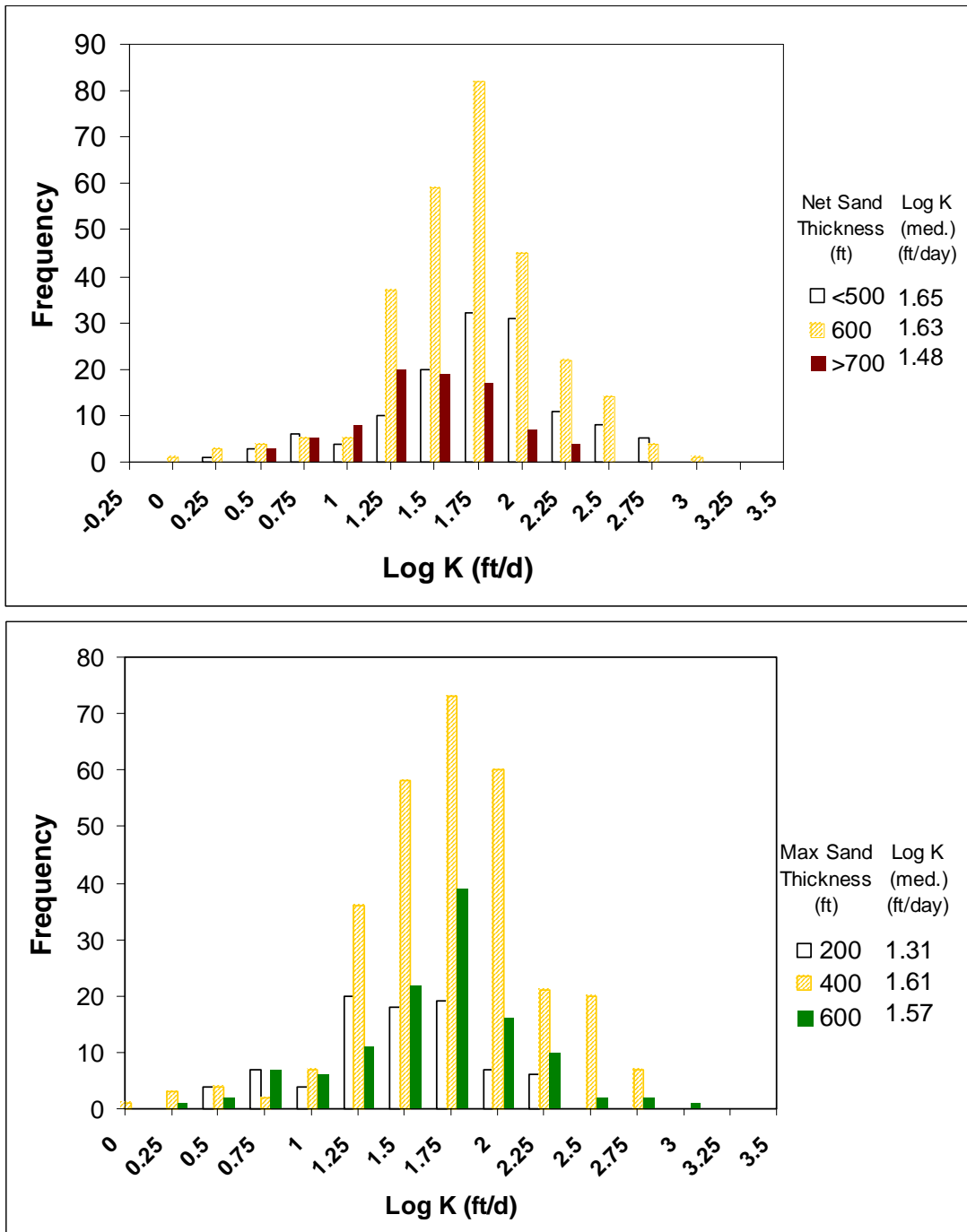


Figure 4.3.8 Histogram of net-sand thickness for the Carrizo-upper Wilcox and maximum sand thickness of the Carrizo-upper Wilcox and hydraulic conductivity (Log K).

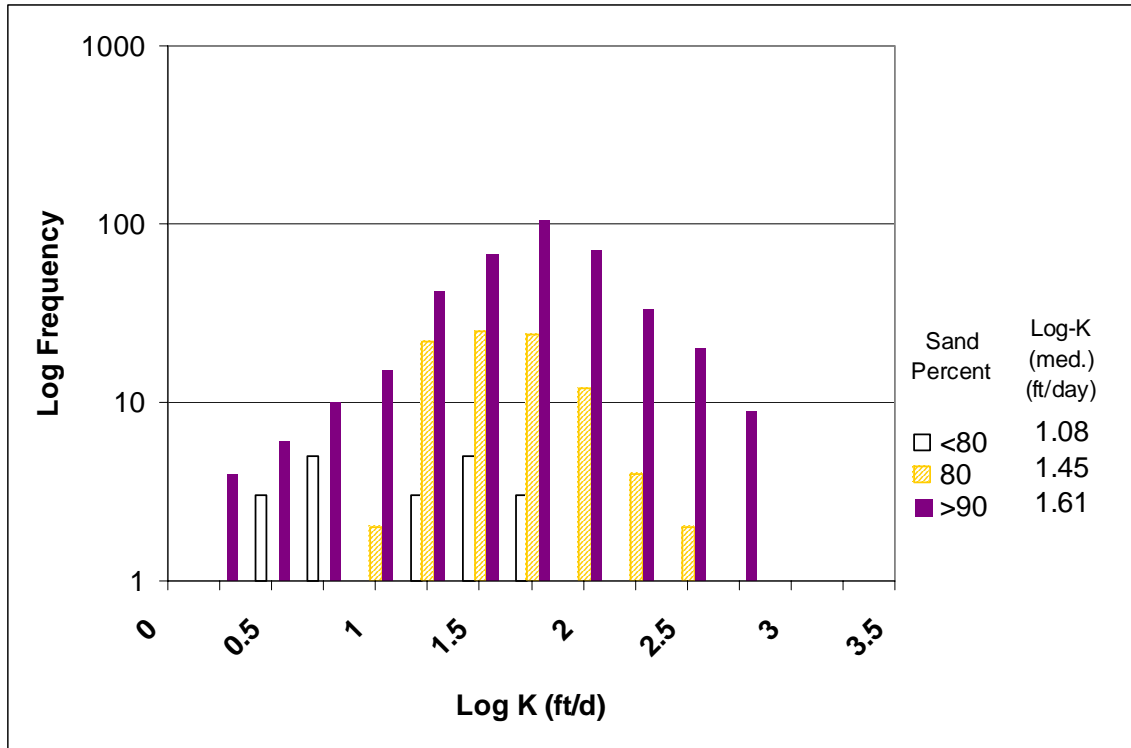


Figure 4.3.9 Histogram of sand percent for the Carrizo- upper Wilcox and the log of hydraulic conductivity (Log K).

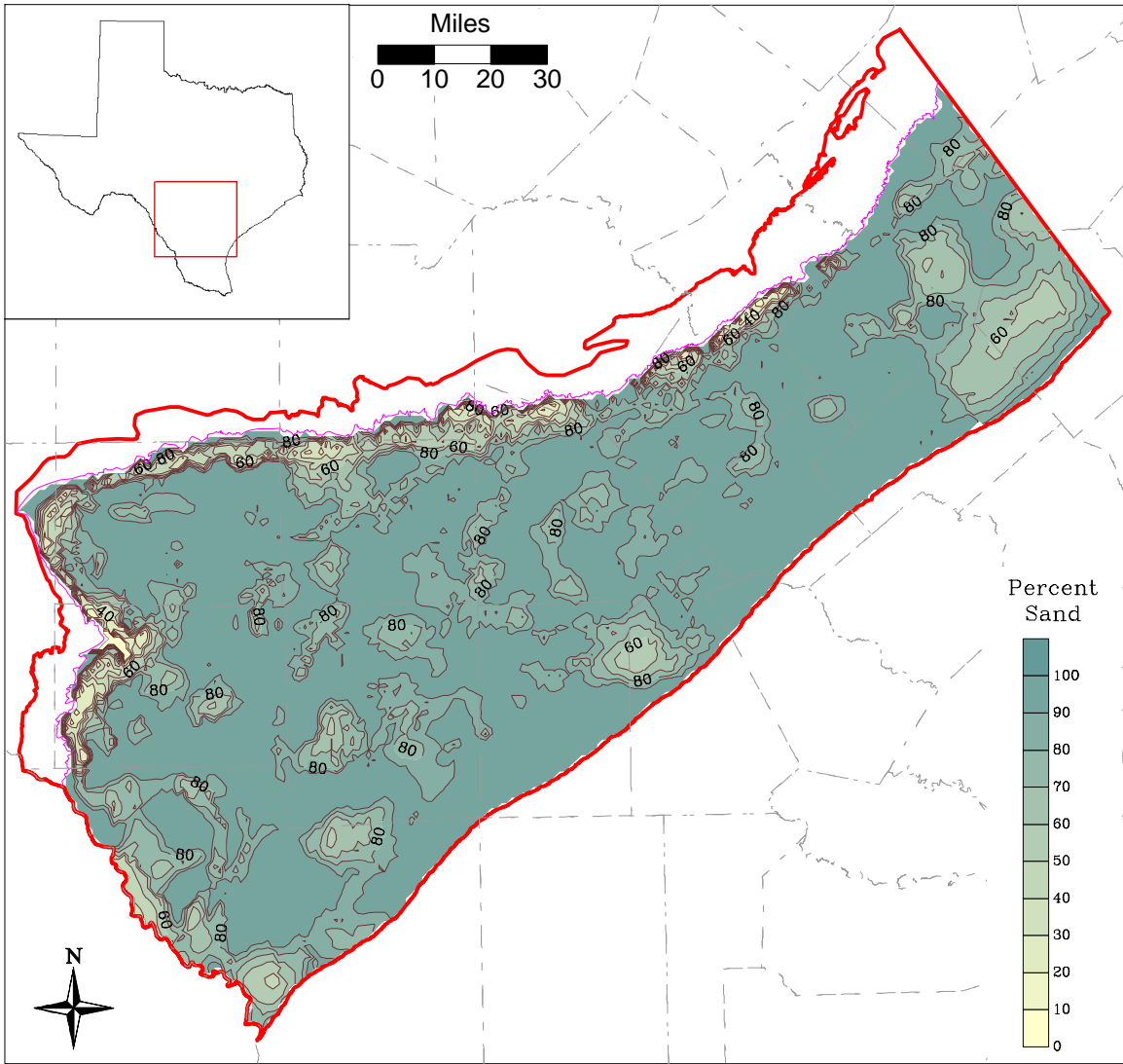


Figure 4.3.10 Percent sand for the Carrizo.

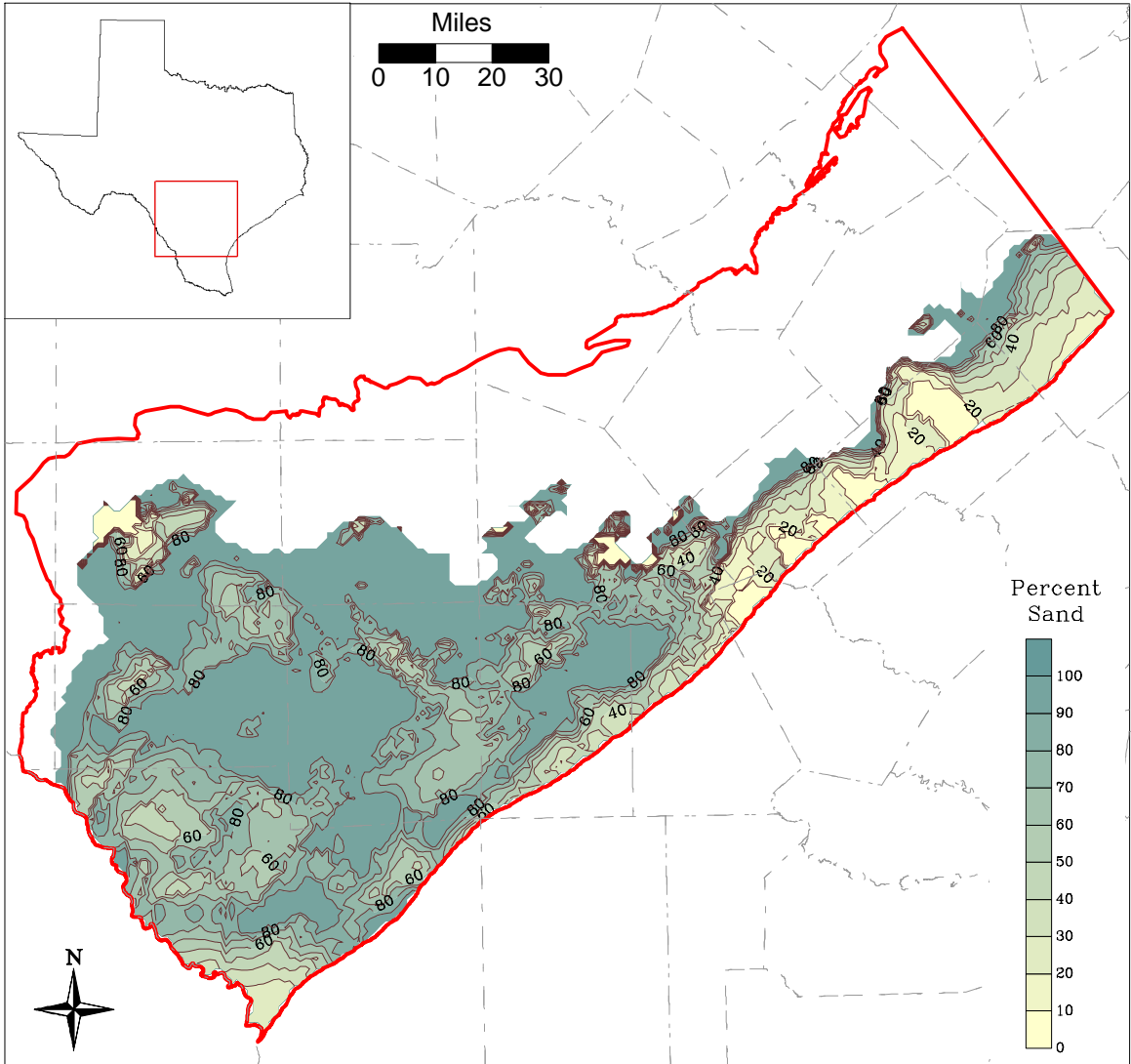


Figure 4.3.11 Percent sand for the upper Wilcox.

4.4 Water Levels and Regional Groundwater Flow

An extensive literature search was conducted to understand (1) regional groundwater flow in the Carrizo Sand and Wilcox Group prior to extensive development of groundwater resources in the area and (2) the history of groundwater usage from the Carrizo Sand and the Wilcox Group. The literature search included a review of the available county reports, historical USGS reports (predominately water-supply papers), and reports by the various Texas state agencies responsible for water resources (i.e., the Texas Board of Water Engineers, the Texas Water Commission, and the Texas Water Development Board). A summary of all reports reviewed can be found in Appendix A. In addition, water-level data provided by the Texas Water Development Board (TWDB) on their website¹ was used to (1) perform a pressure versus depth analysis, (2) investigate pseudo predevelopment conditions for the Queen City Sand/Bigford Formation, (3) investigate transient water level conditions, and (4) develop water-level elevation contours for the start of the calibration period (January 1980), the end of the calibration period (December 1989), and the end of the verification period (December 1999).

The Carrizo Sand is the principal aquifer in most of the Southern Carrizo-Wilcox GAM area. In general, the sands of the Wilcox Group provide fresh to slightly saline water only in and near the outcrop area. Sands of the Wilcox Group are not considered to be an aquifer in Karnes County due to the moderate to high salinity of the water (Anders, 1960). The Wilcox Group is "...not known to yield water..." in LaSalle and McMullen counties (Harris, 1965). The county report for Live Oak County (Anders and Baker, 1961) does not mention the Wilcox Group, suggesting that the sands of the Wilcox Group are not an aquifer in that county. In Caldwell and Bastrop counties, the sands of the Carrizo and Wilcox are hydraulically connected and are considered to act as a single aquifer (Follett, 1966 and Follett, 1970, respectively). Moulder (1957) states that the sands of the Carrizo and Wilcox are hydraulically connected to some extent in Zavala County. The water-level data available in the TWDB database indicates, in general, Carrizo and Wilcox wells in the outcrop areas and Carrizo wells concentrated downdip of the outcrop (Figure 4.4.1).

¹ Found on the web site:
rio.twdb.state.tx.us/publications/reports/GroundWaterReports/GWDatabaseReports/GWdatabaserpt.htm

Water within the Carrizo and Wilcox sands is under water-table conditions in the outcrop areas and under artesian conditions down dip of the outcrop. In many areas, artesian pressures within the aquifer were originally sufficient to drive water above ground surface (Moulder, 1957). Moulder (1957) estimates that the depth to water in the Wintergarden area (Zavala, Frio, Dimmit, La Salle, and Atascosa counties) was originally less than 100 ft.

4.4.1 Predevelopment Conditions for the Carrizo Sand and the Wilcox Group

Development of groundwater resources from the Carrizo Sand and Wilcox Group began in the early 1900s in parts of the study area. The first flowing well was drilled in 1884 at Carrizo Springs in Dimmit County (Turner et al., 1960). Successful crop growth and available transport to market via railroads resulted in the rapid development of Carrizo and Wilcox waters in parts of the Wintergarden District as early as 1910 (Moulder, 1957). Irrigation was greatest in Dimmit and Zavala counties. White and Meinzer (1931) investigated groundwater conditions in southwestern Texas and showed that the original extent of flowing wells was substantially reduced by 1930 in these two counties.

To develop an estimate of water-level conditions in the Carrizo Sand and Wilcox Group prior to significant pumpage, the history of well development and pumpage was compared to the dates of water-level measurements available from literature sources and the TWDB data for each county within the area of interest. In addition, maximum water-level elevations within the counties, regardless of time, were compared to maps showing the locations of originally flowing wells and to ground surface elevations. A brief summary of the development of the Carrizo Sand and the Wilcox Group in each county and the methodology for developing water-level elevations in that county representative of predevelopment conditions can be found in Appendix A.

Actual water-level measurements were used to generate the predevelopment contours for the Carrizo-Wilcox aquifer with the exception of measurements in Dimmit County, northwestern LaSalle County and southern Zavala County. For these locations, all available water-level measurements reflected the effects of pumpage. Map 3 in White and Meinzer (1931) shows the areas in these counties where wells completed to the Carrizo and Wilcox originally flowed. Based on that map, the values for selected water-level elevations measured in those three areas were increased by between 75 and 125 ft. This was done in order to obtain a measurement that was above ground surface and was consistent with the contour lines generated in the other areas

of the model using actual measured values. Water-level elevations in Zavala, Frio, and Atascosa counties used to generate the predevelopment contours were compared to the map from White and Meinzer (1931) to verify that they were higher than ground surface in the areas shown on the map as originally having flowing wells. The predevelopment water-level elevation contours indicate that, under undisturbed conditions, groundwater in the Carrizo Sand and Wilcox Group flows from topographic highs in and near the outcrop areas to topographic lows to the southeast.

The predevelopment water-level elevations represent a combined Carrizo-Wilcox aquifer in and near the outcrop areas and in Caldwell and Bastrop counties, and the Carrizo aquifer only in the remaining areas. The water-level elevation contours generated to represent predevelopment conditions in the Carrizo-Wilcox aquifer are shown in Figure 4.4.2. This figure also shows the ground-surface elevation based on USGS DEM elevations, and the location and value of water-level elevations used to generate the contours. The values shown in black indicate actual measured values, and the values shown in red indicate measured values that were increased as discussed above. Table 4.4.1 summarizes the water-level measurements used in generating the predevelopment water-level elevation contours.

To evaluate the acceptability of increasing the water-level elevations in Dimmit County, northwestern LaSalle County, and southern Zavala County, a comparison was made between contours generated with and without those values increased (Figure 4.4.3). As can be seen in the figure, the contours generated using the values that were not increased bend in northern LaSalle County and are lower than ground surface in areas of Dimmit, LaSalle, and Zavala counties known to originally have flowing wells.

The predevelopment contours were compared to the predevelopment contours of Ryder (1988). In general, the predevelopment contours shown here give the same flow direction but are (1) wider apart than those of Ryder (1988) indicating a shallower gradient, (2) about 50 ft higher than those of Ryder (1988) in the eastern portion of the model region (Wilson County east) and in northern Atascosa and Frio counties, and (3) about 100 ft higher than those of Ryder (1988) in southern Atascosa and Frio counties, and in LaSalle, Dimmit, and Zavala counties. Note, however, that the predevelopment contours of Ryder (1988) are below ground surface in northern LaSalle County, Dimmit County, and southern Zavala County, locations shown by White and Meinzer (1931) to be areas containing wells that originally flowed. Therefore, the

predevelopment contours presented here are considered to be consistent with historical information and data.

4.4.2 Pressure versus Depth Analysis

A study of pressure head versus screen-midpoint depth was conducted using wells having both water-level and screen-depth data on the TWDB website. The analyses used water-level measurements taken prior to 1950. The goal of the study was to evaluate vertical movement between the hydrostratigraphic units. The locations of the wells used and the unit in which they are completed are shown in Figure 4.4.4. This figure shows that most of the wells completed in the Wilcox are located in the outcrop area in Bastrop, Caldwell, and Guadalupe counties. The majority of the wells completed in the Carrizo are located downdip of the outcrop in the Wintergarden area.

Figure 4.4.5 shows the pressure-depth analysis results for water level measurements prior to 1950. The results by hydrostratigraphic unit are shown in the upper plot and the results by county are shown in the lower plot. The screen midpoints for wells completed in the Carrizo Sand range from very shallow depths to depths greater than 1600 ft. The range in screen midpoints is significantly less for the wells completed in the Wilcox Group. A fit through the data for the 44 wells completed in the Carrizo Sand gives a slope of 1.02 indicating near hydrostatic conditions. A fit through the data for the 44 wells analyzed in the Wilcox Group gives a slope of 0.86 indicating downward flow.

The difference in slope between the data for the Carrizo and Wilcox may suggest a lack of hydraulic communication. However, the spatial distribution of the data (Figure 4.4.4), with the Carrizo wells in the southwestern portion of the study area and the Wilcox wells in the northeastern part of the study area, may represent different regimes of the aquifer system. The pressure-depth Wilcox data are from the outcrop in Bastrop and Caldwell counties. Bastrop County data show a slope of 0.91 indicating downward flow in the outcrop area, though the data range is very limited and difficult to interpret. Caldwell County data indicate near hydrostatic conditions. Most of the data in Caldwell County are located in the outcrop near the San Marcos River, where an upward flow component would be expected.

Carrizo data in Zavala and Dimmit counties show pressure-depth slopes of 1.06 and 1.01, indicating upward flow to hydrostatic conditions. Data distributions within the two counties

extend from the outcrop, where a downward flow would be expected, into the confined section, where upward flow would be expected. Visual inspection of data for Dimmit County does suggest that shallow wells in the outcrop indicate a slope of less than 1, suggesting downward flow. By comparison, deeper wells in the confined section indicate a slope greater than 1 suggesting upward flow (Figure 4.4.5). Shallow wells in Zavala County also suggest a downward flow component as compared to deeper wells in that county which show more data scatter and do not indicate a clear upward trend.

4.4.3 Predevelopment Conditions in the Queen City/Bigford Formations

Water-level elevation contours representative of predevelopment conditions in the Queen City Sand/Bigford formations were estimated. Only water-level data on the TWDB website were used. Therefore, the level of detail considered in construction of predevelopment conditions in the Queen City/Bigford formations were less than that considered for the Carrizo and Wilcox. Generation of approximate predevelopment water-level elevations for the Queen City/Bigford formations consisted of investigating maximum water-level elevations in each county, regardless of time. Figure 4.4.6 shows the predevelopment water-level elevation contours estimated for the Queen City/Bigford formations. Water-level measurements in several wells were above ground surface indicating flowing conditions. In several instances, measured water levels were adjusted upward in order for the developed head map to honor the locations of flowing wells. Table 4.4.2 summarizes that water-level data used in generating the predevelopment water-level elevation contours for the Queen City and Bigford formations.

4.4.4 Transient Water Levels

Historically, the greatest water-level declines have occurred in the Wintergarden District. Figure 4.4.7 shows the decline in water level from predevelopment conditions to 1980. The largest drawdowns (exceeding 400 ft) are found in southern Zavala County and northern Dimmit County. Drawdowns of greater than 150 ft are observed throughout the Wintergarden District. Based on the available data, the rate of decline was fastest during the 1940s and 1950s. Outside of the area influenced by pumpage in the Wintergarden District, historical water-level declines have been relatively small (Figure 4.4.7). The drawdown in central Gonzales County could be an artifact of our predevelopment head surface. Historical head maps in central Gonzales County are usually depressed as a result of the Guadalupe River. Appendix A includes select

long-term hydrographs in the study area showing the magnitude of historical head declines. The remainder of this section will focus on the transient calibration period of record.

Figure 4.4.8 shows the locations for which transient water-level data (hydrographs) are available for the last 20 years based on data in the TWDB database. Also shown on the figure is either the model layer in which the midpoint of the well screen is located or, where screen data are not available, the model layer in which the bottom of the well is located. In general, hydrographs show that water levels have remained relatively constant (less than 20 to 30 ft fluctuation) in the eastern portion of the study area (Bastrop, Caldwell, Guadalupe, Gonzales, and middle to northern Wilson counties) (Figure 4.4.9). The water-level spike in the hydrograph for Guadalupe County shown on this figure is not considered to represent actual conditions. All hydrograph data for Guadalupe County for this time period (six wells) show a water-level spike on the same measurement date (December 1, 1993). The increase in water level indicated by the spikes ranges from 61 to 196 ft greater than preceding and subsequent water-level measurements. In Karnes, Live Oak, and southern Wilson counties, the hydrograph data indicate water-level declines ranging from 25 to 45 ft over the last 20 years (Figure 4.4.10). In the outcrop areas of Bexar, Atascosa, Medina, Frio, Zavala, Maverick, and Dimmit counties, water levels have, in general, remained constant or slightly decreased in the last 20 yrs with the exception of one well in Medina County which shows a slight increase (well 68-49-808) (Figure 4.4.11). Notice that the well showing the increase is completed in the Lower Wilcox whereas all of the other wells are completed in the Carrizo Sand.

Over the last 20 years, no consistent trend is observed in the water levels for wells in the downdip areas of Atascosa, McMullen, Frio, LaSalle, Zavala, Dimmit, and Webb counties. Example hydrographs for Atascosa, Frio, and Zavala counties are provided in Figure 4.4.12. In general, water levels have declined up to 50 ft in Atascosa County over this time period (well 78-20-101), but an increase of over 125 ft is observed in one well (well 78-15-805). Most of the wells in Frio County for which hydrograph data are available show an overall decrease in water level over the last 20 yrs (well 77-23-301). Water levels in many of the downdip wells in Zavala County have decreased over the last 20 yrs (well 77-04-431), several have remained constant or increased (well 77-18-516), and many have had large fluctuations (well 77-19-102). Example hydrographs for Dimmit, La Salle, McMullen, and Webb counties are provided in Figure 4.4.13. Water levels in many of the downdip wells in Dimmit County remained relatively

flat over the last 20 yrs, others declined up to 30 ft (well 77-35-601), while still others had an overall increase in water level (well 77-26-605). All of the wells in McMullen County for which hydrograph data are available show an overall decrease in water level over the last 20 yrs. The majority of the hydrographs for wells in La Salle County show declines in water levels in the past 20 yrs (well 77-48-301), but several show substantial increases in water levels (well 77-37-301). Hydrographs for wells in Webb County show, in general, water-level decreases over the past 20 yrs.

4.4.5 Water-Level Elevations for Model Calibration and Verification

Model calibration considered the time period from January 1, 1980 to December 31, 1989 and model verification considered the time period from January 1, 1990 to December 31, 1999. Water-level data found on the TWDB website were used to develop water-level elevation contours for the start of calibration, the end of calibration, and the end of verification. The contours for the start of calibration were used to initialize the transient model. The contours for the end of calibration and verification were used to evaluate the model's ability to reproduce measured water-level data across the model domain.

Water level data on the TWDB website is not available at regular time intervals in every well. Therefore, the coverage of water-level data for a particular month or even a year is very sparse. For example, water levels were measured in three wells in December, 1980, and in a total of eight wells during 1980. Because this is not enough data to develop contours across the entire model area, measured water levels were averaged across two years before the date of interest and two years after the date of interest. For example, the water-level elevation contours for the end of calibration (December 31, 1989) used an average of the water levels measured in 1988, 1989, 1990, and 1991. This provided a total of 227 measurements for use in contouring.

Recall from Figure 4.4.1 that little water-level data are available for wells completed in the Wilcox downdip of the outcrop. Therefore, the water-level elevation contours for model calibration and verification focused on the Carrizo. The water-level elevation contours for the start of calibration are shown in Figure 4.4.14 and tabulated in Table 4.4.3, for the end of calibration in Figure 4.4.15 and Table 4.4.4, and for the end of verification in Figure 4.4.16 and Table 4.4.5. These figures show that there is continued depressurization of the Carrizo Sand in Webb, La Salle, and McMullen counties throughout this time period.

Table 4.4.1 Summary of data used to generate the predevelopment water-level elevation contours for the Carrizo Formation and the Wilcox Group.

State Well Number ^(a)	County ^(a)	Aquifer Code ^(a)	Year of Measurement ^(a)	LSD Elevation ^(a) (ft)	Depth to Water ^(a) (ft)	Water Level Elevation ^(b) (ft)	Adjusted Water Level Elevation ^(c) (ft)	Amount of Adjust-ment ^(d) (ft)
6851802	Atascosa	124CRRZ	1909	637	108	529		
6859502	Atascosa	124CRRZ	1910	547	25	522		
7803401	Atascosa	124CRRZ	1908	555	38	517		
5854901	Bastrop	124CRRZ	1950	545	118	427		
6706701	Bastrop	124CRRZ	1925	515	90	425		
6713801	Caldwell	124CRRZ	1923	469	40	429		
7624903	Dimmit	124WLCX	1929	689	75	614	714	100
7725202	Dimmit	124CRRZ	1929	682	82	600	686	86
7726414	Dimmit	124CRRZ	1913	578	4	574	674	100
7743502	Dimmit	124CRRZ	1933	571	75	496	596	100
7744105	Dimmit	124CRRZ	1920	520	69	451	575	124
6716404	Fayette	124CRRZ	1966	348	-2	350		
6857701	Frio	124CRRZ	1929	578	10	568		
6961605	Frio	124CRRZ	1929	699	84	615		
7723801	Frio	124CRRZ	1928	541	17	524		
7818206	Frio	124CRRZ	1929	401	-80	481		
6737201	Gonzales	124CRRZ	1931	282	-104	386		
6742903	Gonzales	124CRRZ	1940	390	-21	411		
6718903	Guadalupe	124WLCX	1936	592	82	510		
6733206	Guadalupe	124WLCX	1936	555	27	528		
6733401	Guadalupe	124WLCX	1982	561	59	502		
6832801	Guadalupe	124WLCX	2000	625	62	563		
6840101	Guadalupe	124CZWX	1936	575	7	568		
7816601	Karnes	124CRRZ	1956	502	99	403		
7731703	La Salle	124CRRZ	1960	570	151	419	519	100
7850201	La Salle	124CRRZ	1959	395	-41	436		
7828603	McMullen	124CRRZ	1959	309	-114	423		
7836901	McMullen	124CZWX	1959	351	-66	417		
6849918	Medina	124CRRZ	1930	680	43	637		
6858111	Medina	124CRRZ	1930	641	75	566		
6733703	Wilson	124CRRZ	1910	567	110	457		
6958401	Zavala	124CRRZ	1931	770	31	739		
6958601	Zavala	124WLCX	1929	809	78	731		
6959601	Zavala	124CRRZ	1929	789	49	740		
6960501	Zavala	124CRRZ	1929	860	187	673		
7710603	Zavala	124CRRZ	1931	625	43	582	659	77

- (a) source is the TWDB website:
rio.twdb.state.tx.us/publications/reports/GroundWaterReports/GWDatabaseReports/GWdatabaserpt.htm
- (b) calculated as the LSD elevation minus the depth to water
- (c) determined based on scientific judgment
- (d) the difference between the adjusted and not adjusted water-level elevations

Table 4.4.2 Summary of data used to generate the predevelopment water-level elevation contours for the Queen City and Bigford formations.

State Well Number ^(a)	County ^(a)	Aquifer Code ^(a)	Year of Measurement ^(a)	LSD Elevation ^(a) (ft)	Depth to Water ^(a) (ft)	Water Level Elevation ^(b) (ft)	Adjusted Water Level Elevation ^(c) (ft)	Amount of Adjustment ^(d) (ft)
7805604	Atascosa	124QNCT	1944	350	-16	366	416	50
7812105	Atascosa	124QNCT	1944	408	-2	410	445	35
7813702	Atascosa	124QNCT	1971	330	-41	371	421	50
7814203	Atascosa	124QNCT	1944	350	-1	351	406	55
5855305	Bastrop	124QNCT	1965	570	17	553		
5855501	Bastrop	124QNCT	1941	500	3	497		
5855602	Bastrop	124QNCT	1939	585	54	531		
6707401	Bastrop	124QNCT	1964	500	33	467		
6714101	Bastrop	124QNCT	1952	490	30	460		
6714704	Caldwell	124QNCT	1964	520	26	494		
7727709	Dimmit	124BGDF	1977	525	9	516		
7749301	Dimmit	124BGDF	1961	700	161	539		
6708604	Fayette	124QNCT	1979	342	24	318		
6857702	Frio	124QNCT	1952	578	30	548		
6857908	Frio	124QNCT	1963	601	75	526		
7707403	Frio	124QNCT	1964	580	90	490	510	20
7708401	Frio	124QNCT	1958	660	104	556		
7708701	Frio	124QNCT	1956	602	38	564		
7708802	Frio	124QNCT	1932	640	50	590		
7715901	Frio	124QNCT	1932	508	45	463		
7716403	Frio	124QNCT	1932	569	58	511		
6721201	Gonzales	124QNCT	1977	415	5	410		
6728303	Gonzales	124QNCT	1938	365	56	309	409	100
6728702	Gonzales	124QNCT	1938	350	45	305	390	85
6729701	Gonzales	124QNCT	1963	300	-9	309	379	70
6734803	Gonzales	124QNCT	1981	442	39	403		
6735902	Gonzales	124QNCT	1962	374	50	324	364	40
6743401	Gonzales	124QNCT	1959	314	-25	339	379	40
6743406	Gonzales	124QNCT	1959	312	-14	326	376	50
7724801	La Salle	124BGDF	1959	434	0	434	484	50
7746804	La Salle	124BGDF	1942	450	-8	458		
7826502	McMullen	124QNCT	1971	373	-8	381	431	50
7827903	McMullen	124QNCT	1959	336	-36	372		
7828303	McMullen	124QNCT	1959	281	-110	391		
8519201	Webb	124QNCT	1977	543	38	505		
6854902	Wilson	124QNCT	1963	530	78	452	462	10
6856804	Wilson	124QNCT	1996	489	81	408	458	50
6862507	Wilson	124QNCT	1977	500	84	416	466	50
6960401	Zavala	124BGDF	1946	817	50	767		
7702401	Zavala	124BGDF	1952	732	109	623		
7703502	Zavala	124BGDF	1973	782	115	667		
7704207	Zavala	124BGDF	1976	725	45	680		

- (a) source is the TWDB website:
rio.twdb.state.tx.us/publications/reports/GroundWaterReports/GWDatabaseReports/GWdatabaserpt.htm
- (b) calculated as the LSD elevation minus the depth to water
- (c) determined based on scientific judgment
- (d) the difference between the adjusted and not adjusted water-level elevations

Table 4.4.3 Data used to generate water-level elevation contours for the start of model calibration (January 1980).

State Well Number ^(a)	County ^(a)	Aquifer Code ^(a)	LSD Elevation (ft) ^(a)	Average Depth to Water (ft) ^(b)	Average Water-Level Elevation (ft) ^(c)
6851602	Atascosa	124CRRZ	705	120	585
6851701	Atascosa	124CRRZ	610	55	555
6851801	Atascosa	124CRRZ	673	128	545
6852718	Atascosa	124CRRZ	665	195	470
6858204	Atascosa	124CRRZ	646	161	485
6858302	Atascosa	124CRRZ	650	162	488
6858602	Atascosa	124CRRZ	534	91	443
6859303	Atascosa	124CRRZ	580	123	457
6859501	Atascosa	124CRRZ	545	100	445
6859621	Atascosa	124CRRZ	483	50	433
6859804	Atascosa	124CRRZ	496	86	410
6860303	Atascosa	124CRRZ	550	124	426
6860312	Atascosa	124CRRZ	550	125	425
6860401	Atascosa	124CRRZ	515	102	413
6860610	Atascosa	124CRRZ	535	131	404
6860912	Atascosa	124CRRZ	446	61	385
6860913	Atascosa	124CRRZ	430	59	371
6861310	Atascosa	124CRRZ	520	115	405
6861501	Atascosa	124CRRZ	471	67	404
6861602	Atascosa	124CRRZ	475	74	401
6861905	Atascosa	124CRRZ	482	106	376
6862405	Atascosa	124CRRZ	492	118	374
7802303	Atascosa	124CRRZ	592	150	442
7802602	Atascosa	124CRRZ	530	168	362
7803302	Atascosa	124CRRZ	490	96	394
7803509	Atascosa	124CRRZ	575	205	370
7803601	Atascosa	124CRRZ	565	163	402
7804204	Atascosa	124CRRZ	430	53	377
7804803	Atascosa	124CRRZ	480	104	376
7804812	Atascosa	124CRRZ	421	67	354
7805104	Atascosa	124CRRZ	385	26	359
7805116	Atascosa	124CRRZ	373	13	360
7805501	Atascosa	124CRRZ	405	55	350
7806103	Atascosa	124CRRZ	422	56	366
7806503	Atascosa	124CRRZ	392	35	357
7806507	Atascosa	124CRRZ	350	11	339
7810303	Atascosa	124CRRZ	480	126	354
7810606	Atascosa	124CRRZ	450	111	339
7811202	Atascosa	124CRRZ	542	203	339
7811301	Atascosa	124CRRZ	479	107	372
7811501	Atascosa	124CRRZ	495	138	357
7811903	Atascosa	124CRRZ	400	92	308
7812701	Atascosa	124CRRZ	452	117	335
7814801	Atascosa	124CRRZ	241	-92	333
7814802	Atascosa	124CRRZ	233	-94	327
7815805	Atascosa	124CRRZ	469	116	353
7818601	Atascosa	124CRRZ	376	51	325
7820101	Atascosa	124CRRZ	464	144	320
7821106	Atascosa	124CRRZ	305	-20	325
7822201	Atascosa	124CRRZ	228	-96	324

Table 4.4.3 (continued)

State Well Number^(a)	County^(a)	Aquifer Code^(a)	LSD Elevation (ft)^(a)	Average Depth to Water (ft)^(b)	Average Water-Level Elevation (ft)^(c)
7822202	Atascosa	124CRRZ	242	-104	346
6706201	Bastrop	124CRRZ	480	117	363
6706501	Bastrop	124CRRZ	480	83	397
6706502	Bastrop	124CRRZ	460	91	369
6706609	Bastrop	124CRRZ	593	99	494
6706802	Bastrop	124CRRZ	593	97	496
6853703	Bexar	124CRRZ	570	137	433
6853805	Bexar	124CRRZ	535	121	414
6713201	Caldwell	124CRRZ	575	137	438
6713605	Caldwell	124CRRZ	490	75	415
6713801	Caldwell	124CRRZ	469	47	422
6721104	Caldwell	124CRRZ	475	68	407
7648801	Dimmit	124CRRZ	680	25	655
7718904	Dimmit	124CRRZ	573	320	253
7719703	Dimmit	124CRRZ	572	312	260
7726613	Dimmit	124CRRZ	534	221	313
7726708	Dimmit	124CRRZ	602	180	422
7726904	Dimmit	124CRRZ	525	238	287
7728503	Dimmit	124CRRZ	535	290	245
7733301	Dimmit	124CRRZ	705	165	540
7733611	Dimmit	124CRRZ	690	111	579
7734319	Dimmit	124CRRZ	520	223	297
7734402	Dimmit	124CRRZ	628	166	462
7734607	Dimmit	124CRRZ	565	203	362
7734702	Dimmit	124CRRZ	650	171	479
7737101	Dimmit	124CRRZ	475	212	263
7744103	Dimmit	124CRRZ	560	112	448
6716404	Fayette	124CRRZ	348	8	340
6857402	Frio	124CRRZ	667	192	475
6857505	Frio	124CRRZ	605	113	492
6857616	Frio	124CRRZ	660	196	464
6857701	Frio	124CRRZ	578	82	496
6857901	Frio	124CRRZ	631	125	506
6858506	Frio	124CRRZ	611	165	446
6962601	Frio	124CRRZ	698	206	492
6962902	Frio	124CRRZ	610	144	466
6963605	Frio	124CRRZ	632	134	498
6964501	Frio	124CRRZ	711	191	520
7706205	Frio	124CRRZ	660	259	401
7707201	Frio	124CRRZ	586	166	420
7707501	Frio	124CRRZ	555	175	380
7707901	Frio	124CRRZ	600	251	349
7708201	Frio	124CRRZ	700	290	410
7708409	Frio	124CRRZ	660	274	386
7708716	Frio	124CRRZ	618	269	349
7708803	Frio	124CRRZ	652	353	299
7708806	Frio	124CRRZ	642	292	350
7708812	Frio	124CRRZ	648	295	353
7714601	Frio	124CRRZ	510	231	279
7714904	Frio	124CRRZ	522	221	301
7715907	Frio	124CRRZ	485	176	309

Table 4.4.3 (continued)

State Well Number^(a)	County^(a)	Aquifer Code^(a)	LSD Elevation (ft)^(a)	Average Depth to Water (ft)^(b)	Average Water-Level Elevation (ft)^(c)
7716201	Frio	124CRRZ	652	318	334
7716603	Frio	124CRRZ	640	330	310
7716705	Frio	124CRRZ	532	222	310
7716801	Frio	124CRRZ	521	241	280
7722502	Frio	124CRRZ	610	348	262
7723106	Frio	124CRRZ	520	260	260
7723301	Frio	124CRRZ	515	242	273
7723509	Frio	124CRRZ	575	294	281
7723602	Frio	124CRRZ	500	240	260
7723701	Frio	124CRRZ	560	323	237
7723803	Frio	124CRRZ	562	288	274
7724202	Frio	124CRRZ	458	191	267
7801501	Frio	124CRRZ	525	133	392
7801801	Frio	124CRRZ	501	144	357
7802402	Frio	124CRRZ	582	192	390
7802701	Frio	124CRRZ	553	202	351
7802702	Frio	124CRRZ	522	153	369
7809305	Frio	124CRRZ	471	123	348
7809602	Frio	124CRRZ	491	160	331
7818206	Frio	124CRRZ	401	13	388
6721204	Gonzales	124QNCT	430	51	379
6721701	Gonzales	124CRRZ	430	57	373
6721703	Gonzales	124CRRZ	420	68	352
6721903	Gonzales	124CRRZ	390	12	378
6727502	Gonzales	124CRRZ	435	73	362
6727503	Gonzales	124WLCX	433	74	359
6727701	Gonzales	124CRRZ	392	13	379
6727703	Gonzales	124CRRZ	450	115	335
6727801	Gonzales	124CRRZ	429	55	374
6727805	Gonzales	124CRRZ	370	15	355
6727806	Gonzales	124CRRZ	400	39	361
6727903	Gonzales	124CRRZ	345	-3	348
6727909	Gonzales	124CRRZ	400	37	363
6728104	Gonzales	124CRRZ	321	1	320
6729201	Gonzales	124CRRZ	408	46	362
6729602	Gonzales	124CRRZ	375	28	347
6735701	Gonzales	124CRRZ	364	-13	377
6742202	Gonzales	124CRRZ	409	15	394
6742906	Gonzales	124CRRZ	390	29	361
6743104	Gonzales	124CRRZ	360	-18	378
6743901	Gonzales	124CRRZ	322	-43	365
6744201	Gonzales	124CRRZ	288	-62	350
6744701	Gonzales	124CRRZ	290	-107	397
6734302	Guadalupe	124CRRZ	495	58	437
6734402	Guadalupe	124CRRZ	620	176	444
6734704	Guadalupe	124CRRZ	470	35	435
7816601	Karnes	124CRRZ	502	163	339
7730502	La Salle	124CRRZ	580	349	231
7730801	La Salle	124CRRZ	516	295	221
7731703	La Salle	124CRRZ	570	241	329
7737301	La Salle	124CRRZ	448	174	274

Table 4.4.3 (continued)

State Well Number^(a)	County^(a)	Aquifer Code^(a)	LSD Elevation (ft)^(a)	Average Depth to Water (ft)^(b)	Average Water-Level Elevation (ft)^(c)
7738901	La Salle	124CRRZ	449	193	256
7739301	La Salle	124CRRZ	565	334	231
7739407	La Salle	124CRRZ	431	200	231
7739601	La Salle	124CRRZ	458	73	385
7740303	La Salle	124CRRZ	422	159	263
7748301	La Salle	124CRRZ	420	153	267
7764401	La Salle	124CRRZ	395	74	321
7825803	La Salle	124CRRZ	368	101	267
7841301	La Salle	124CRRZ	455	183	272
7823502	Live Oak	124CRRZ	358	27	331
7607901	Maverick	124CRRZ	703	76	627
7607919	Maverick	124CRRZ	700	75	625
7608401	Maverick	124CRRZ	700	61	639
7608704	Maverick	124CRRZ	701	50	651
7821801	McMullen	124CZWX	378	48	330
7826601	McMullen	124CRRZ	365	29	336
7826802	McMullen	124CRRZ	363	59	304
7827303	McMullen	124CRRZ	394	77	317
7827503	McMullen	124CRRZ	380	85	295
7828501	McMullen	124CRRZ	335	25	310
7828702	McMullen	124CRRZ	342	60	282
7836902	McMullen	124CRRZ	350	25	325
7842902	McMullen	124CRRZ	332	35	297
6849902	Medina	124CRRZ	655	72	583
6850702	Medina	124CRRZ	725	136	589
6857210	Medina	124CZWX	655	144	511
6857307	Medina	124CRRZ	643	106	537
6858101	Medina	124CRRZ	650	138	512
6858109	Medina	124CRRZ	620	113	507
6858110	Medina	124CRRZ	618	134	484
7749601	Webb	124CRRZ	795	272	523
7758701	Webb	124CRRZ	700	215	485
8504401	Webb	124CRRZ	620	177	443
8511302	Webb	124CRRZ	625	110	515
6741102	Wilson	124CRRZ	590	173	417
6741401	Wilson	124CRRZ	536	115	421
6741801	Wilson	124CRRZ	547	144	403
6749201	Wilson	124CRRZ	470	93	377
6750203	Wilson	124CRRZ	434	53	381
6847903	Wilson	124CRRZ	590	164	426
6848502	Wilson	124CRRZ	430	31	399
6848601	Wilson	124CRRZ	490	92	398
6848802	Wilson	124CRRZ	416	8	408
6848812	Wilson	124CRRZ	426	28	398
6848907	Wilson	124CRRZ	502	95	407
6854301	Wilson	124CRRZ	492	99	393
6854602	Wilson	124CRRZ	525	135	390
6854802	Wilson	124CRRZ	575	195	380
6854901	Wilson	124CRRZ	515	89	426
6855202	Wilson	124CRRZ	507	113	394
6855407	Wilson	124CRRZ	456	51	405

Table 4.4.3 (continued)

State Well Number ^(a)	County ^(a)	Aquifer Code ^(a)	LSD Elevation (ft) ^(a)	Average Depth to Water (ft) ^(b)	Average Water-Level Elevation (ft) ^(c)
6855601	Wilson	124CRRZ	513	123	390
6855704	Wilson	124CRRZ	430	37	393
6855706	Wilson	124CRRZ	440	60	380
6855901	Wilson	124CRRZ	396	24	372
6855902	Wilson	124CRRZ	390	44	346
6855903	Wilson	124CRRZ	390	24	366
6856101	Wilson	124CRRZ	490	85	405
6856201	Wilson	124CRRZ	428	32	396
6856302	Wilson	124CRRZ	431	33	398
6856401	Wilson	124CRRZ	565	175	390
6856704	Wilson	124CRRZ	489	113	376
6856902	Wilson	124CRRZ	460	78	382
6862104	Wilson	124CRRZ	590	209	381
6862202	Wilson	124CRRZ	496	102	394
6862205	Wilson	124CRRZ	532	149	383
6862902	Wilson	124CRRZ	437	72	365
6863101	Wilson	124CRRZ	448	66	382
6863302	Wilson	124CRRZ	430	66	364
6863802	Wilson	124CRRZ	456	105	351
6864401	Wilson	124CRRZ	400	32	368
6864402	Wilson	124CRRZ	403	26	377
6864902	Wilson	124CRRZ	358	28	330
6958701	Zavala	124CRRZ	772	131	641
6958704	Zavala	124CRRZ	784	164	620
6958707	Zavala	124CRRZ	789	154	635
6958715	Zavala	124CRRZ	768	83	685
6958801	Zavala	124CRRZ	750	58	692
6959911	Zavala	124CRRZ	765	249	516
6959913	Zavala	124CRRZ	811	280	531
6961502	Zavala	124CRRZ	717	194	523
6961525	Zavala	124CRRZ	719	178	541
6961818	Zavala	124CRRZ	703	225	478
7608406	Zavala	124CRRZ	712	67	645
7624201	Zavala	124CRRZ	608	129	479
7624906	Zavala	124CRRZ	631	231	400
7701101	Zavala	124CRRZ	762	113	649
7701311	Zavala	124CRRZ	776	89	687
7701404	Zavala	124CRRZ	735	110	625
7701501	Zavala	124CRRZ	771	299	472
7701605	Zavala	124CRRZ	739	291	448
7701702	Zavala	124CRRZ	698	103	595
7702103	Zavala	124CRRZ	757	297	460
7702403	Zavala	124CRRZ	748	347	401
7702606	Zavala	124CRRZ	688	280	408
7702706	Zavala	124CRRZ	729	340	389
7703401	Zavala	124CRRZ	731	322	409
7704431	Zavala	124CRRZ	708	291	417
7704601	Zavala	124CRRZ	704	310	394
7704706	Zavala	124CRRZ	680	292	389
7709201	Zavala	124CRRZ	679	375	304
7709704	Zavala	124CRRZ	621	278	343

Table 4.4.3 (continued)

State Well Number^(a)	County^(a)	Aquifer Code^(a)	LSD Elevation (ft)^(a)	Average Depth to Water (ft)^(b)	Average Water-Level Elevation (ft)^(c)
7710604	Zavala	124CRRZ	624	302	322
7711703	Zavala	124CRRZ	634	332	302
7711715	Zavala	124CRRZ	636	325	311
7711718	Zavala	124CRRZ	641	321	320
7717707	Zavala	124CZWX	603	216	387
7719102	Zavala	124CRRZ	614	326	288
Dummy-1 ^(d)					350
Dummy-2 ^(d)					350
Dummy-3 ^(d)					350

- (a) source is the TWDB website:
rio.twdb.state.tx.us/publications/reports/GroundWaterReports/GWDatabaseReports/GWdatabaserpt.htm
- (b) calculated as the LSD elevation minus the average water-level elevation
- (c) calculated from the 1978-1981 data on the TWDB website
- (d) included to define water level in areas with little data

Table 4.4.4 Data used to generate water-level elevation contours for the end of model calibration (December 1989).

State Well Number ^(a)	County ^(a)	Aquifer Code ^(a)	LSD Elevation (ft) ^(a)	Average Depth to Water (ft) ^(b)	Average Water-Level Elevation (ft) ^(c)
6851602	Atascosa	124CRRZ	705	122	583
6851701	Atascosa	124CRRZ	610	56	555
6852713	Atascosa	124CRRZ	665	179	486
6852718	Atascosa	124CRRZ	665	202	463
6858302	Atascosa	124CRRZ	650	177	473
6858602	Atascosa	124CRRZ	534	110	424
6859312	Atascosa	124CRRZ	580	129	451
6859501	Atascosa	124CRRZ	545	116	429
6859517	Atascosa	124CRRZ	578	177	401
6859633	Atascosa	124CRRZ	500	105	395
6859804	Atascosa	124CRRZ	496	107	389
6860312	Atascosa	124CRRZ	550	139	411
6861310	Atascosa	124CRRZ	520	139	381
6861602	Atascosa	124CRRZ	475	78	397
6861905	Atascosa	124CRRZ	482	124	359
6862405	Atascosa	124CRRZ	492	136	357
7802303	Atascosa	124CRRZ	592	187	405
7803509	Atascosa	124CRRZ	575	238	337
7803601	Atascosa	124CRRZ	565	186	379
7804204	Atascosa	124CRRZ	430	77	353
7804612	Atascosa	124CRRZ	420	95	325
7804812	Atascosa	124CRRZ	421	89	332
7805116	Atascosa	124CRRZ	373	34	339
7805501	Atascosa	124CRRZ	405	72	333
7806103	Atascosa	124CRRZ	422	84	339
7806507	Atascosa	124CRRZ	350	14	336
7810303	Atascosa	124CRRZ	480	147	333
7810606	Atascosa	124CRRZ	450	153	297
7811202	Atascosa	124CRRZ	542	229	313
7811218	Atascosa	124CRRZ	445	242	203
7811301	Atascosa	124CRRZ	479	148	331
7811903	Atascosa	124CRRZ	400	127	273
7814801	Atascosa	124CRRZ	241	-63	304
7814802	Atascosa	124CRRZ	233	-64	297
7815301	Atascosa	124CRRZ	475	113	363
7815805	Atascosa	124CRRZ	469	116	353
7820101	Atascosa	124CRRZ	464	170	294
7821106	Atascosa	124CRRZ	305	25	280
7822201	Atascosa	124CRRZ	228	-77	305
7822202	Atascosa	124CRRZ	242	-90	332
5863103	Bastrop	124CRRZ	370	15	355
5863606	Bastrop	124CRRZ	380	60	320
6706501	Bastrop	124CRRZ	480	92	389
6707204	Bastrop	124CRRZ	390	48	343
6852903	Bexar	124CRRZ	608	180	428
6852905	Bexar	124CRRZ	589	165	424
6853703	Bexar	124CRRZ	570	149	421
6854402	Bexar	124CRRZ	435	39	397
6713201	Caldwell	124CRRZ	575	136	439
6720603	Caldwell	124CRRZ	472	77	395

Table 4.4.4 (continued)

State Well Number^(a)	County^(a)	Aquifer Code^(a)	LSD Elevation (ft)^(a)	Average Depth to Water (ft)^(b)	Average Water-Level Elevation (ft)^(c)
6721104	Caldwell	124CRRZ	475	72	403
7624801	Dimmit	124CRRZ	665	110	556
7648801	Dimmit	124CRRZ	680	24	656
7718704	Dimmit	124CRRZ	580	271	309
7725604	Dimmit	124CRRZ	612	232	380
7726101	Dimmit	124CRRZ	590	250	340
7726605	Dimmit	124CRRZ	525	254	271
7726613	Dimmit	124CRRZ	534	212	322
7726708	Dimmit	124CRRZ	602	195	407
7728503	Dimmit	124CRRZ	535	273	262
7733301	Dimmit	124CRRZ	705	173	532
7733322	Dimmit	124CRRZ	665	101	565
7733611	Dimmit	124CRRZ	690	119	571
7733701	Dimmit	124CRRZ	810	229	581
7734606	Dimmit	124CRRZ	553	222	331
7734607	Dimmit	124CRRZ	565	194	371
7734702	Dimmit	124CRRZ	650	170	480
7735601	Dimmit	124CRRZ	540	235	305
7737101	Dimmit	124CRRZ	475	207	268
7737501	Dimmit	124CRRZ	485	225	260
7742801	Dimmit	124CRRZ	613	168	445
7744101	Dimmit	124CRRZ	480	180	300
6857402	Frio	124CRRZ	667	204	464
6857701	Frio	124CRRZ	578	101	478
6858506	Frio	124CRRZ	611	183	428
6962902	Frio	124CRRZ	610	171	439
6963605	Frio	124CRRZ	632	144	488
7706205	Frio	124CRRZ	660	273	387
7706301	Frio	124CRRZ	605	207	398
7707201	Frio	124CRRZ	586	214	372
7707501	Frio	124CRRZ	555	219	336
7707901	Frio	124CRRZ	600	278	322
7708201	Frio	124CRRZ	700	308	393
7708409	Frio	124CRRZ	660	310	351
7708716	Frio	124CRRZ	618	311	308
7708806	Frio	124CRRZ	642	321	321
7708812	Frio	124CRRZ	648	310	338
7714601	Frio	124CRRZ	510	245	265
7714904	Frio	124CRRZ	522	246	276
7715907	Frio	124CRRZ	485	153	333
7716603	Frio	124CRRZ	640	333	307
7716705	Frio	124CRRZ	532	243	289
7716801	Frio	124CRRZ	521	250	271
7721301	Frio	124CRRZ	620	370	250
7722502	Frio	124CRRZ	610	382	228
7723301	Frio	124CRRZ	515	253	263
7723602	Frio	124CRRZ	500	249	251
7723701	Frio	124CRRZ	560	318	242
7723807	Frio	124CRRZ	535	417	118
7723808	Frio	124CRRZ	561	329	232
7724202	Frio	124CRRZ	458	207	252

Table 4.4.4 (continued)

State Well Number ^(a)	County ^(a)	Aquifer Code ^(a)	LSD Elevation (ft) ^(a)	Average Depth to Water (ft) ^(b)	Average Water-Level Elevation (ft) ^(c)
7801501	Frio	124CRRZ	525	154	371
7801801	Frio	124CRRZ	501	161	340
7802402	Frio	124CRRZ	582	226	357
7802501	Frio	124CRRZ	572	182	391
7802701	Frio	124CRRZ	553	216	337
7802702	Frio	124CRRZ	522	187	336
7809305	Frio	124CRRZ	471	141	330
7809507	Frio	124CRRZ	490	165	325
7818206	Frio	124CRRZ	401	18	383
6721703	Gonzales	124CRRZ	420	73	347
6721903	Gonzales	124CRRZ	390	51	339
6727502	Gonzales	124CRRZ	435	76	359
6727805	Gonzales	124CRRZ	370	19	351
6728104	Gonzales	124CRRZ	321	3	319
6729303	Gonzales	124CRRZ	410	53	357
6729602	Gonzales	124CRRZ	375	34	341
6729603	Gonzales	124CRRZ	375	38	337
6742202	Gonzales	124CRRZ	409	20	390
6726311	Guadalupe	124CRRZ	490	90	400
6734402	Guadalupe	124CRRZ	620	181	439
6734406	Guadalupe	124CRRZ	540	85	455
6734704	Guadalupe	124CRRZ	470	39	431
7816601	Karnes	124CRRZ	502	173	329
7730502	La Salle	124CRRZ	580	349	231
7730801	La Salle	124CRRZ	516	274	242
7731703	La Salle	124CRRZ	570	182	388
7737301	La Salle	124CRRZ	448	52	396
7738201	La Salle	124CRRZ	468	232	236
7738901	La Salle	124CRRZ	449	207	242
7739301	La Salle	124CRRZ	565	337	228
7739407	La Salle	124CRRZ	431	205	226
7739408	La Salle	124CRRZ	415	189	226
7739601	La Salle	124CRRZ	458	72	386
7740303	La Salle	124CRRZ	422	155	268
7740305	La Salle	124CRRZ	402	70	332
7747802	La Salle	124CRRZ	398	37	361
7748301	La Salle	124CRRZ	420	160	260
7764401	La Salle	124CRRZ	395	88	307
7823502	Live Oak	124CRRZ	358	58	300
7607901	Maverick	124CRRZ	703	71	632
7607919	Maverick	124CRRZ	700	71	629
7608401	Maverick	124CRRZ	700	71	629
7615303	Maverick	124CRRZ	707	58	649
7826802	McMullen	124CRRZ	363	88	275
7827503	McMullen	124CRRZ	380	116	264
7828501	McMullen	124CRRZ	335	60	276
7828602	McMullen	124CRRZ	288	18	270
7828702	McMullen	124CRRZ	342	77	266
7837103	McMullen	124CRRZ	345	78	267
6849902	Medina	124CRRZ	655	75	580
6850717	Medina	124CRRZ	690	149	541

Table 4.4.4 (continued)

State Well Number^(a)	County^(a)	Aquifer Code^(a)	LSD Elevation (ft)^(a)	Average Depth to Water (ft)^(b)	Average Water-Level Elevation (ft)^(c)
6857307	Medina	124CRRZ	643	116	527
6858101	Medina	124CRRZ	650	146	504
6858110	Medina	124CRRZ	618	143	475
6956903	Medina	124CRRZ	750	120	630
6960201	Uvalde	124CRRZ	891	199	692
7749501	Webb	124CRRZ	862	310	552
7750601	Webb	124CRRZ	655	226	429
7750603	Webb	124CRRZ	655	199	457
7759401	Webb	124CRRZ	720	283	437
7760201	Webb	124CRRZ	668	365	303
8504401	Webb	124CRRZ	620	196	424
6741102	Wilson	124CRRZ	590	180	411
6741801	Wilson	124CRRZ	547	143	405
6749201	Wilson	124CRRZ	470	99	371
6846903	Wilson	124CRRZ	520	105	415
6846904	Wilson	124CRRZ	520	110	410
6847601	Wilson	124CRRZ	652	201	452
6847903	Wilson	124CRRZ	590	172	418
6848402	Wilson	124CRRZ	547	90	457
6848502	Wilson	124CRRZ	430	32	398
6848507	Wilson	124CRRZ	473	68	405
6848601	Wilson	124CRRZ	490	96	394
6848812	Wilson	124CRRZ	426	30	396
6848907	Wilson	124CRRZ	502	106	397
6854506	Wilson	124CRRZ	419	36	383
6854602	Wilson	124CRRZ	525	145	380
6854802	Wilson	124CRRZ	575	215	360
6854901	Wilson	124CRRZ	515	137	378
6855202	Wilson	124CRRZ	507	116	391
6855206	Wilson	124CRRZ	525	120	405
6855407	Wilson	124CRRZ	456	50	406
6855704	Wilson	124CRRZ	430	49	382
6855706	Wilson	124CRRZ	440	53	387
6856101	Wilson	124CRRZ	490	79	411
6856201	Wilson	124CRRZ	428	37	391
6856302	Wilson	124CRRZ	431	40	391
6856409	Wilson	124CRRZ	560	176	384
6856902	Wilson	124CRRZ	460	87	373
6862205	Wilson	124CRRZ	532	163	369
6862902	Wilson	124CRRZ	437	99	338
6862906	Wilson	124CRRZ	422	67	355
6863101	Wilson	124CRRZ	448	72	376
6863802	Wilson	124CRRZ	456	123	333
6864401	Wilson	124CRRZ	400	38	362
6958701	Zavala	124CRRZ	772	131	641
6958707	Zavala	124CRRZ	789	166	623
6958715	Zavala	124CRRZ	768	82	686
6958801	Zavala	124CRRZ	750	60	690
6959401	Zavala	124CRRZ	815	100	715
6959904	Zavala	124CRRZ	743	267	477
6961502	Zavala	124CRRZ	717	203	514

Table 4.4.4 (continued)

State Well Number ^(a)	County ^(a)	Aquifer Code ^(a)	LSD Elevation (ft) ^(a)	Average Depth to Water (ft) ^(b)	Average Water-Level Elevation (ft) ^(c)
6961525	Zavala	124CRRZ	719	183	536
7608406	Zavala	124CRRZ	712	70	642
7608503	Zavala	124CRRZ	728	92	636
7624906	Zavala	124CRRZ	631	233	398
7701311	Zavala	124CRRZ	776	88	689
7701404	Zavala	124CRRZ	735	117	619
7701501	Zavala	124CRRZ	771	300	471
7701702	Zavala	124CRRZ	698	121	577
7702103	Zavala	124CRRZ	757	305	452
7702414	Zavala	124CRRZ	747	338	409
7702606	Zavala	124CRRZ	688	290	399
7703401	Zavala	124CRRZ	731	311	420
7704202	Zavala	124CRRZ	751	304	447
7704431	Zavala	124CRRZ	708	338	370
7704603	Zavala	124CRRZ	688	282	406
7704718	Zavala	124CRRZ	686	327	359
7709101	Zavala	124CRRZ	668	275	393
7709704	Zavala	124CRRZ	621	244	377
7711703	Zavala	124CRRZ	634	300	334
7711718	Zavala	124CRRZ	641	306	335
7712702	Zavala	124CRRZ	641	325	317
7718516	Zavala	124CRRZ	574	278	296
7719102	Zavala	124CRRZ	614	328	286

- (a) source is the TWDB website:
rio.twdb.state.tx.us/publications/reports/GroundWaterReports/GWDatabaseReports/GWdatabaserpt.htm
- (b) calculated as the LSD elevation minus the average water-level elevation
- (c) calculated from the 1988-1991 data on the TWDB website

Table 4.4.5 Data used to generate water-level elevation contours for the end of model verification (December 1999).

State Well Number ^(a)	County ^(a)	Aquifer Code ^(a)	LSD Elevation (ft) ^(a)	Average Depth to Water (ft) ^(b)	Average Water-Level Elevation (ft) ^(c)
6851701	Atascosa	124CRRZ	610	59	552
6852713	Atascosa	124CRRZ	665	172	494
6852718	Atascosa	124CRRZ	665	199	466
6858302	Atascosa	124CRRZ	650	185	465
6858602	Atascosa	124CRRZ	534	116	419
6859212	Atascosa	124CRRZ	603	132	471
6859312	Atascosa	124CRRZ	580	139	441
6859316	Atascosa	124CRRZ	593	113	480
6859317	Atascosa	124CRRZ	565	137	428
6859501	Atascosa	124CRRZ	545	125	420
6859517	Atascosa	124CRRZ	578	158	420
6859633	Atascosa	124CRRZ	500	104	396
6859804	Atascosa	124CRRZ	496	105	391
6860852	Atascosa	124CRRZ	472	118	354
6860912	Atascosa	124CRRZ	446	101	345
6861602	Atascosa	124CRRZ	475	75	401
6861905	Atascosa	124CRRZ	482	136	346
6862405	Atascosa	124CRRZ	492	137	355
7804612	Atascosa	124CRRZ	420	95	326
7805116	Atascosa	124CRRZ	373	38	336
7805124	Atascosa	124CRRZ	385	54	331
7805212	Atascosa	124CRRZ	405	76	329
7805802	Atascosa	124CRRZ	410	85	325
7806103	Atascosa	124CRRZ	422	82	340
7810315	Atascosa	124CRRZ	489	192	297
7811202	Atascosa	124CRRZ	542	243	300
7811301	Atascosa	124CRRZ	479	173	306
7814801	Atascosa	124CRRZ	241	-13	254
7814802	Atascosa	124CRRZ	233	-17	250
7815805	Atascosa	124CRRZ	469	-18	487
7820101	Atascosa	124CRRZ	464	172	292
7822201	Atascosa	124CRRZ	228	-22	250
5863103	Bastrop	124CRRZ	370	13	358
5863606	Bastrop	124CRRZ	380	53	327
6706501	Bastrop	124CRRZ	480	89	391
6707204	Bastrop	124CRRZ	390	44	347
6853907	Bexar	124CRRZ	565	210	355
7624801	Dimmit	124CRRZ	665	108	557
7648801	Dimmit	124CRRZ	680	25	655
7718704	Dimmit	124CRRZ	580	276	304
7726605	Dimmit	124CRRZ	525	254	271
7726708	Dimmit	124CRRZ	602	195	407
7728503	Dimmit	124CRRZ	535	283	252
7733301	Dimmit	124CRRZ	705	176	529
7733309	Dimmit	124CRRZ	665	122	543
7733322	Dimmit	124CRRZ	665	107	558
7733611	Dimmit	124CRRZ	690	132	558
7733701	Dimmit	124CRRZ	810	236	574
7734607	Dimmit	124CRRZ	565	213	352
7734702	Dimmit	124CRRZ	650	175	475

Table 4.4.5 (continued)

State Well Number^(a)	County^(a)	Aquifer Code^(a)	LSD Elevation (ft)^(a)	Average Depth to Water (ft)^(b)	Average Water-Level Elevation (ft)^(c)
7737501	Dimmit	124CRRZ	485	183	302
7742801	Dimmit	124CRRZ	613	176	437
7744101	Dimmit	124CRRZ	480	202	278
6716404	Fayette	124CRRZ	348	0	348
6857701	Frio	124CRRZ	578	110	468
6858506	Frio	124CRRZ	611	214	397
6962902	Frio	124CRRZ	610	191	420
7707201	Frio	124CRRZ	586	215	372
7707501	Frio	124CRRZ	555	244	311
7707901	Frio	124CRRZ	600	318	282
7708409	Frio	124CRRZ	660	344	317
7708716	Frio	124CRRZ	618	304	314
7708803	Frio	124CRRZ	652	354	298
7708806	Frio	124CRRZ	642	269	373
7708812	Frio	124CRRZ	648	257	392
7714904	Frio	124CRRZ	522	361	161
7716603	Frio	124CRRZ	640	319	322
7716705	Frio	124CRRZ	532	257	276
7716801	Frio	124CRRZ	521	257	265
7721301	Frio	124CRRZ	620	320	300
7722401	Frio	124CRRZ	605	338	268
7723205	Frio	124CRRZ	553	370	183
7723301	Frio	124CRRZ	515	297	219
7723602	Frio	124CRRZ	500	312	188
7723807	Frio	124CRRZ	535	366	170
7724202	Frio	124CRRZ	458	210	248
7801501	Frio	124CRRZ	525	157	369
7802702	Frio	124CRRZ	522	186	336
7802815	Frio	124CRRZ	534	209	325
7809305	Frio	124CRRZ	471	163	308
7809506	Frio	124CRRZ	550	283	267
7809507	Frio	124CRRZ	490	206	285
7818206	Frio	124CRRZ	401	24	377
6721703	Gonzales	124CRRZ	420	75	345
6727502	Gonzales	124CRRZ	435	0	435
6727805	Gonzales	124CRRZ	370	22	349
6727903	Gonzales	124CRRZ	345	-2	347
6728104	Gonzales	124CRRZ	321	3	319
6729602	Gonzales	124CRRZ	375	40	336
6729603	Gonzales	124CRRZ	375	34	342
6742202	Gonzales	124CRRZ	409	22	387
6742906	Gonzales	124CRRZ	390	-44	434
6742913	Gonzales	124CRRZ	341	-9	350
6734704	Guadalupe	124CRRZ	470	40	430
6734706	Guadalupe	124CRRZ	515	98	417
7808301	Karnes	124CRRZ	330	-32	362
7808302	Karnes	124CRRZ	325	-40	365
7808306	Karnes	124CRRZ	315	-117	432
7816601	Karnes	124CRRZ	502	175	327
7729603	La Salle	124CRRZ	515	303	212
7730502	La Salle	124CRRZ	580	405	175

Table 4.4.5 (continued)

State Well Number^(a)	County^(a)	Aquifer Code^(a)	LSD Elevation (ft)^(a)	Average Depth to Water (ft)^(b)	Average Water-Level Elevation (ft)^(c)
7730801	La Salle	124CRRZ	516	330	186
7731703	La Salle	124CRRZ	570	189	381
7738201	La Salle	124CRRZ	468	266	202
7738901	La Salle	124CRRZ	449	117	332
7739301	La Salle	124CRRZ	565	364	201
7739407	La Salle	124CRRZ	431	253	178
7740303	La Salle	124CRRZ	422	195	227
7740305	La Salle	124CRRZ	402	66	337
7747802	La Salle	124CRRZ	398	23	375
7748301	La Salle	124CRRZ	420	195	225
7748801	La Salle	124CRRZ	345	106	239
7764401	La Salle	124CRRZ	395	115	280
7607901	Maverick	124CRRZ	703	72	631
7607919	Maverick	124CRRZ	700	70	630
7828501	McMullen	124CRRZ	335	81	254
7828602	McMullen	124CRRZ	288	37	252
7837103	McMullen	124CRRZ	345	106	239
6849902	Medina	124CRRZ	655	78	577
6857307	Medina	124CRRZ	643	126	517
6858101	Medina	124CRRZ	650	159	491
6960201	Uvalde	124CRRZ	891	200	691
7750603	Webb	124CRRZ	655	248	407
7759501	Webb	124CRRZ	714	280	434
8401601	Webb	124CRRZ	380	-60	440
8503905	Webb	124CRRZ	595	161	434
8504401	Webb	124CRRZ	620	211	409
6741102	Wilson	124CRRZ	590	178	412
6741304	Wilson	124CRRZ	519	118	401
6749201	Wilson	124CRRZ	470	100	371
6848401	Wilson	124CRRZ	547	73	474
6848502	Wilson	124CRRZ	430	31	399
6848509	Wilson	124CRRZ	430	32	398
6848601	Wilson	124CRRZ	490	93	398
6848812	Wilson	124CRRZ	426	33	393
6848907	Wilson	124CRRZ	502	114	388
6853902	Wilson	124CRRZ	585	211	375
6854506	Wilson	124CRRZ	419	42	377
6854602	Wilson	124CRRZ	525	154	372
6854901	Wilson	124CRRZ	515	111	404
6855111	Wilson	124CRRZ	483	116	367
6855407	Wilson	124CRRZ	456	46	410
6855505	Wilson	124CRRZ	450	73	377
6855704	Wilson	124CRRZ	430	60	370
6855901	Wilson	124CRRZ	396	40	356
6855902	Wilson	124CRRZ	390	108	282
6856101	Wilson	124CRRZ	490	94	396
6856201	Wilson	124CRRZ	428	41	387
6856302	Wilson	124CRRZ	431	43	388
6862108	Wilson	124CRRZ	572	220	352
6862902	Wilson	124CRRZ	437	104	333
6862906	Wilson	124CRRZ	422	62	360

Table 4.4.5 (continued)

State Well Number ^(a)	County ^(a)	Aquifer Code ^(a)	LSD Elevation (ft) ^(a)	Average Depth to Water (ft) ^(b)	Average Water-Level Elevation (ft) ^(c)
6863101	Wilson	124CRRZ	448	54	394
6863802	Wilson	124CRRZ	456	145	311
6864402	Wilson	124CRRZ	403	48	355
7806302	Wilson	124CRRZ	415	60	355
6958701	Zavala	124CRRZ	772	138	634
6958707	Zavala	124CRRZ	789	153	636
6958715	Zavala	124CRRZ	768	85	683
6958801	Zavala	124CRRZ	750	60	690
6959904	Zavala	124CRRZ	743	284	459
6961502	Zavala	124CRRZ	717	221	497
6961525	Zavala	124CRRZ	719	205	514
7608406	Zavala	124CRRZ	712	24	688
7624906	Zavala	124CRRZ	631	237	394
7701101	Zavala	124CRRZ	762	96	666
7701311	Zavala	124CRRZ	776	89	687
7701404	Zavala	124CRRZ	735	117	618
7701702	Zavala	124CRRZ	698	109	589
7702414	Zavala	124CRRZ	747	338	409
7702606	Zavala	124CRRZ	688	303	385
7703401	Zavala	124CRRZ	731	336	396
7704431	Zavala	124CRRZ	708	355	353
7704603	Zavala	124CRRZ	688	350	338
7709101	Zavala	124CRRZ	668	289	379
7711718	Zavala	124CRRZ	641	317	324
7712702	Zavala	124CRRZ	641	335	306
7718516	Zavala	124CRRZ	574	219	355
7719102	Zavala	124CRRZ	614	305	309

- (a) source is the TWDB website:
rio.twdb.state.tx.us/publications/reports/GroundWaterReports/GWDatabaseReports/GWdatabaserpt.htm
- (b) calculated as the LSD elevation minus the average water-level elevation
- (c) calculated from the 1998-2001 data on the TWDB website

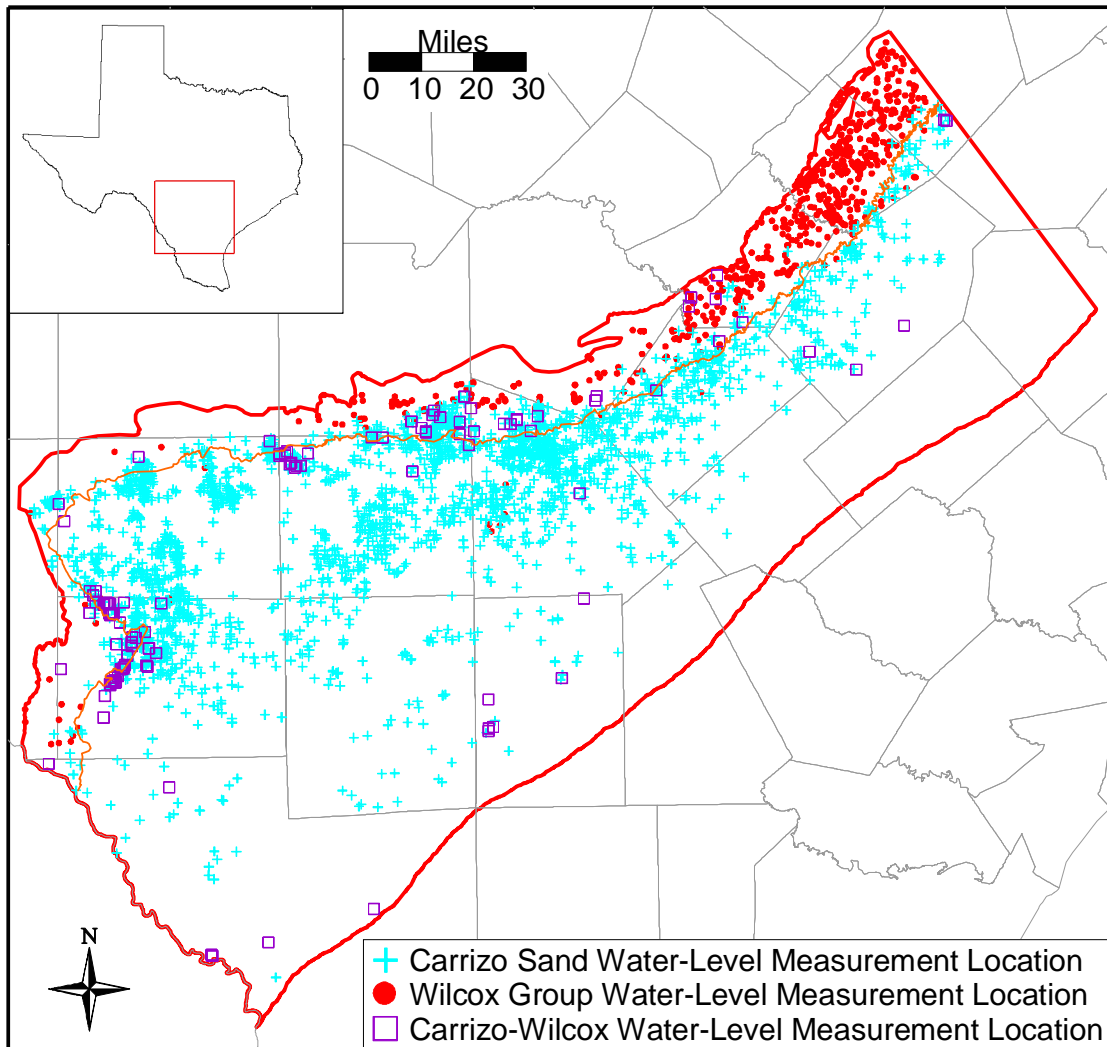


Figure 4.4.1 Water-level measurement locations for the Carrizo-Wilcox aquifer.

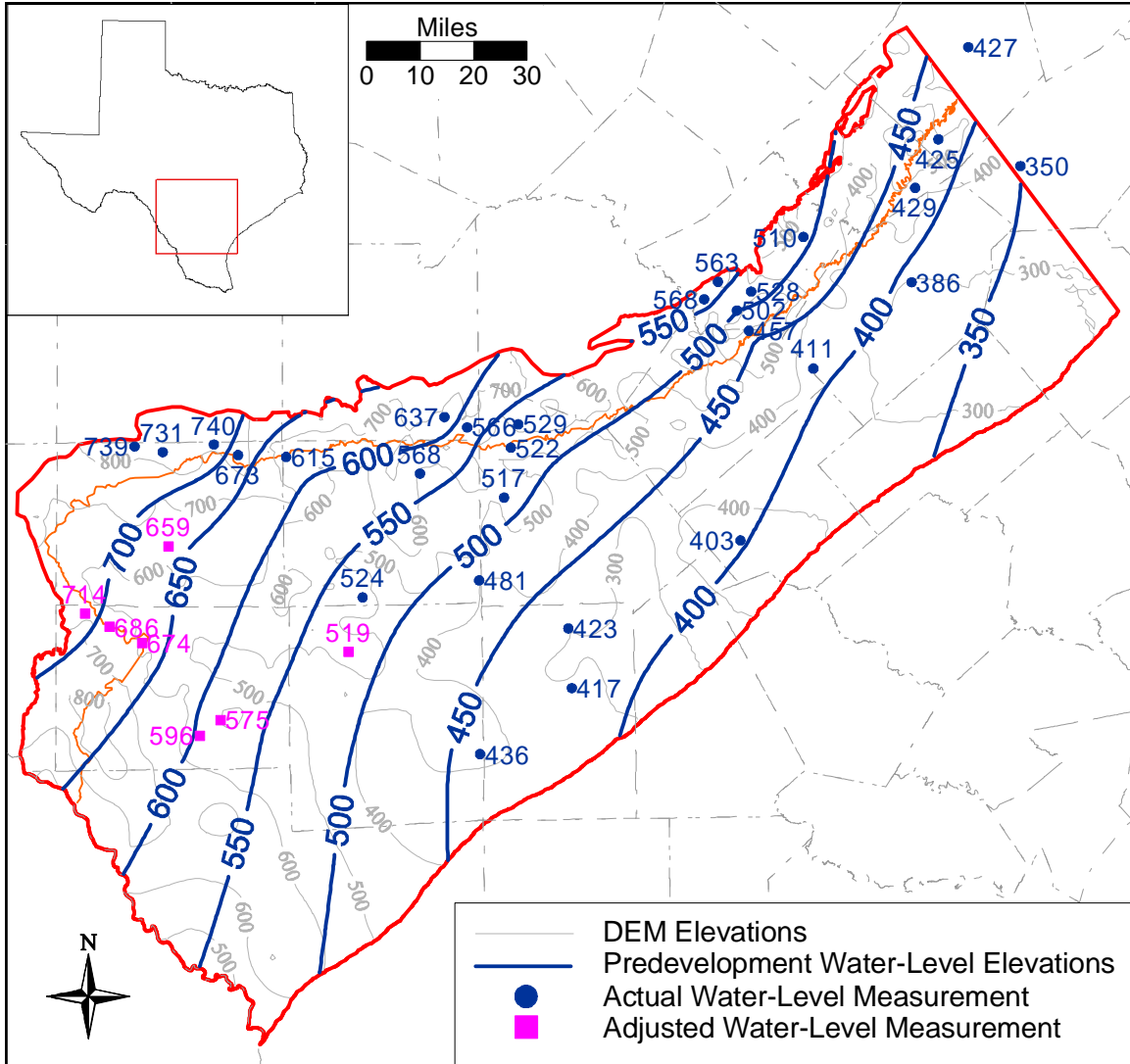


Figure 4.4.2 Predevelopment water-level elevations for the Carrizo-Wilcox aquifer.

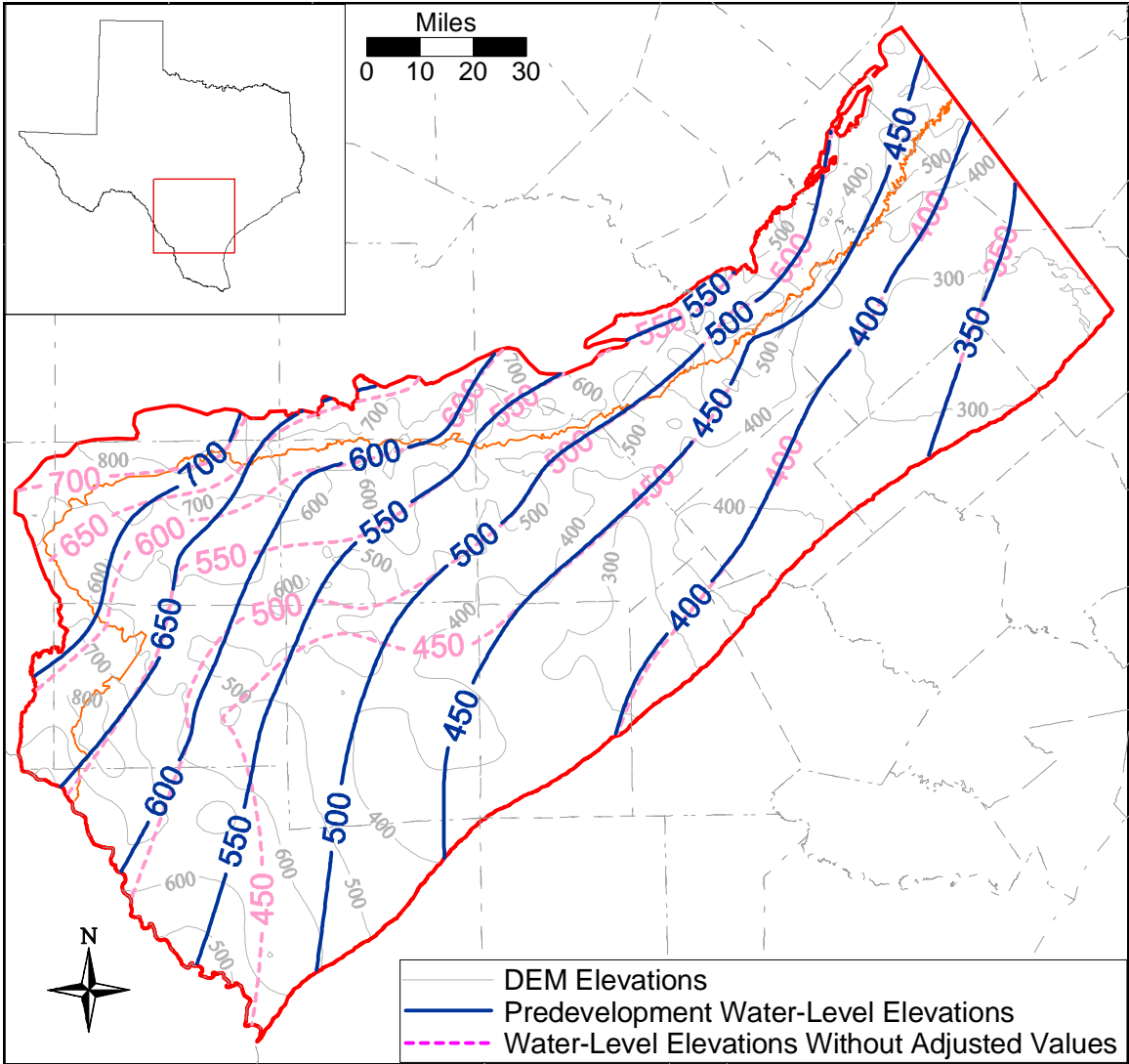


Figure 4.4.3 Difference in predevelopment water-level elevation contours between adjusted and not adjusted water levels.

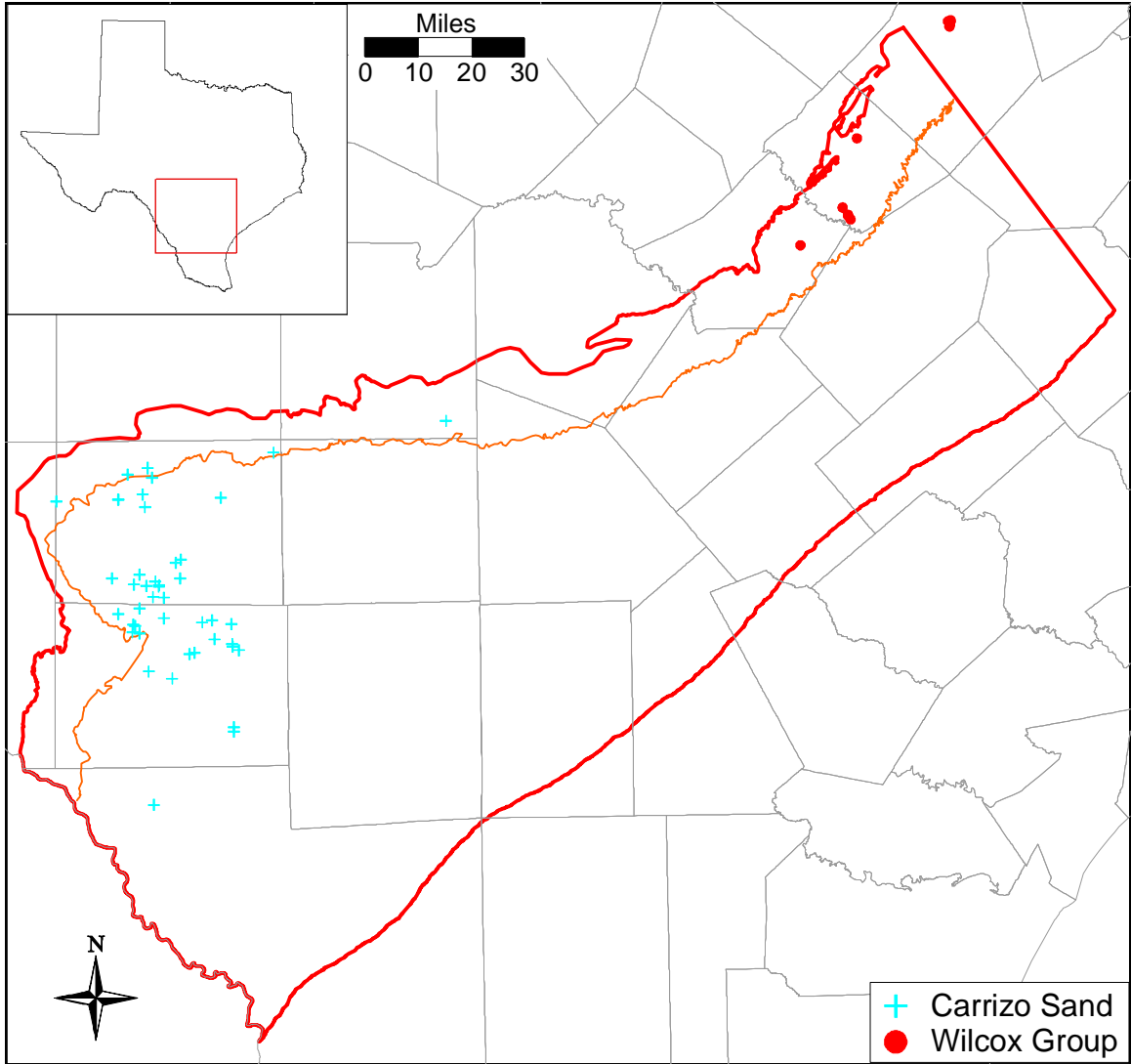


Figure 4.4.4 Water-level measurement locations used for pressure-depth analysis.

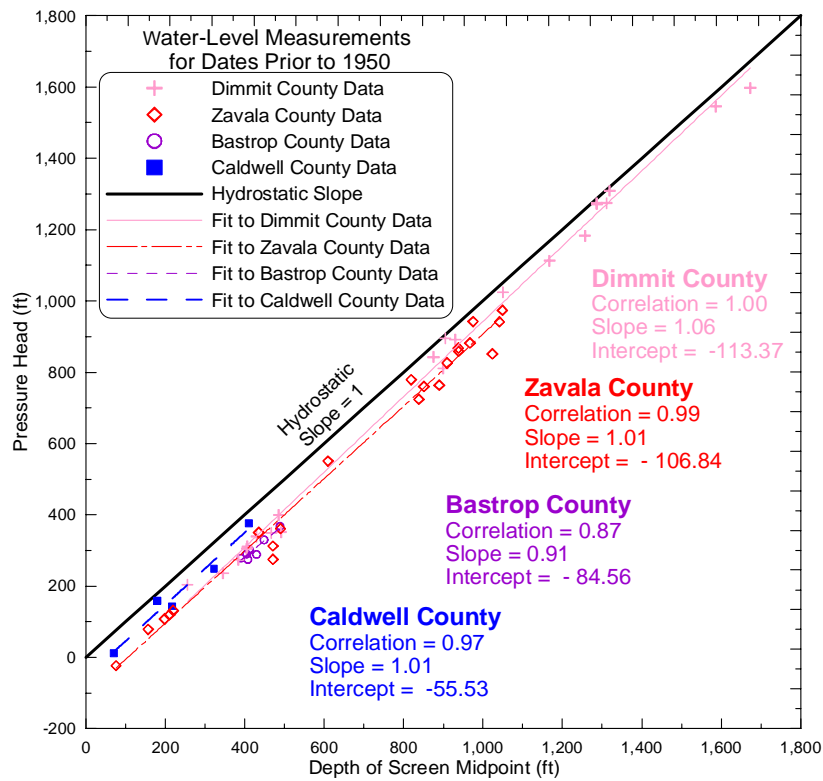
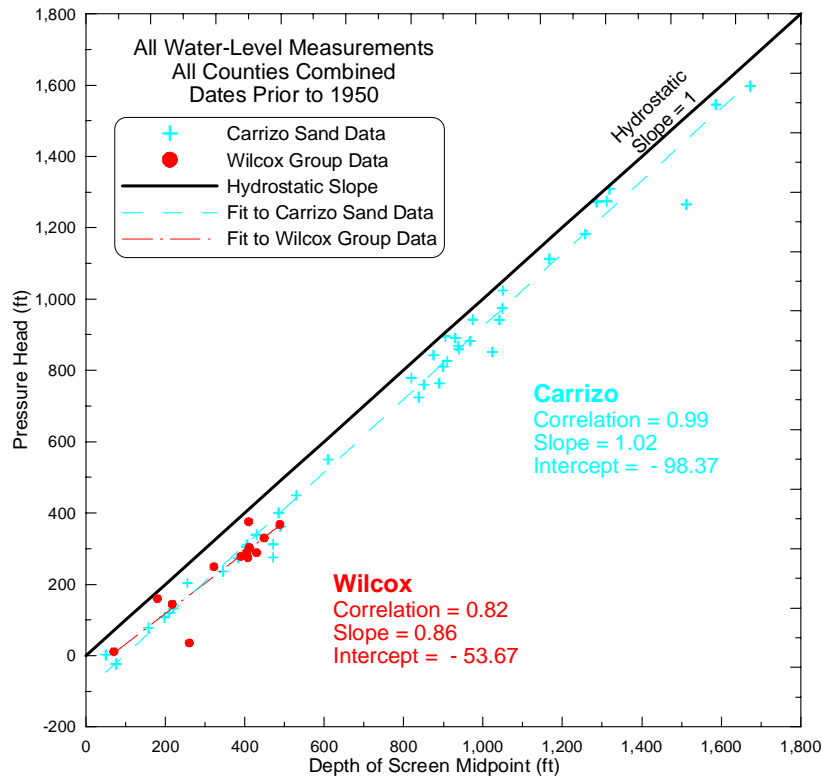


Figure 4.4.5 Pressure versus depth analysis results.

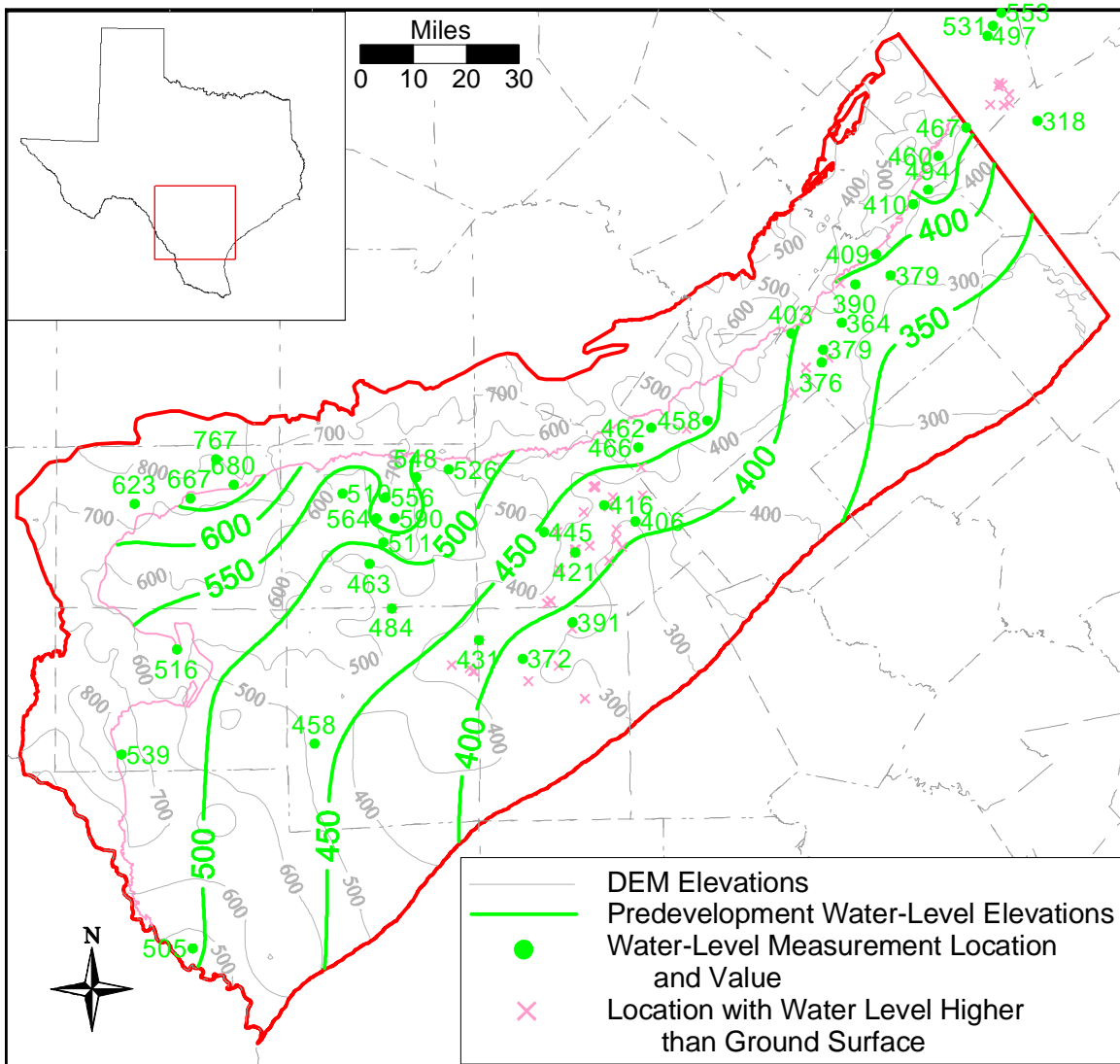


Figure 4.4.6 Predevelopment water-level elevation contours for the Queen City/Bigford formations.

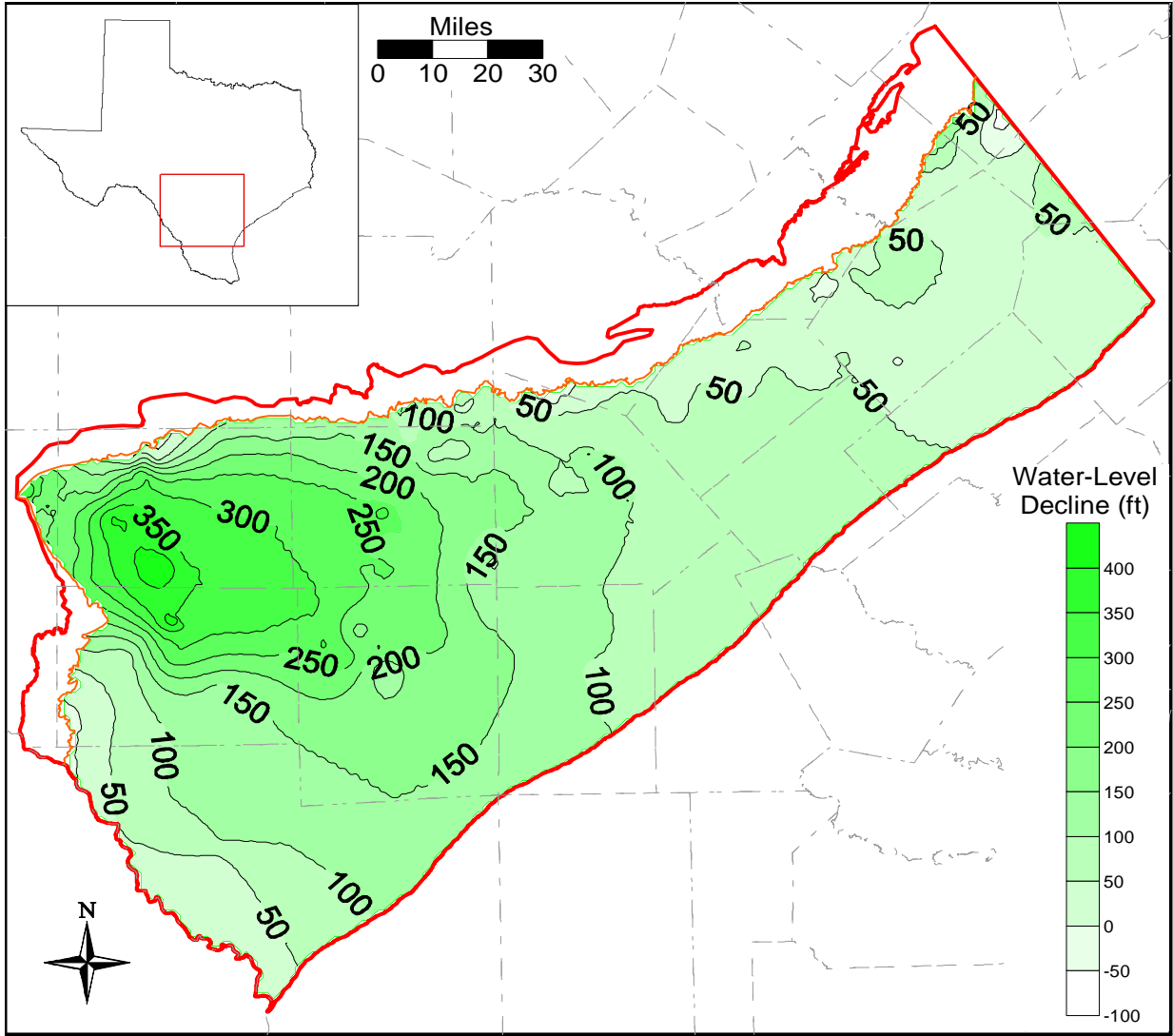


Figure 4.4.7 Water-level decline in the Carrizo –upper Wilcox from predevelopment to 1980.

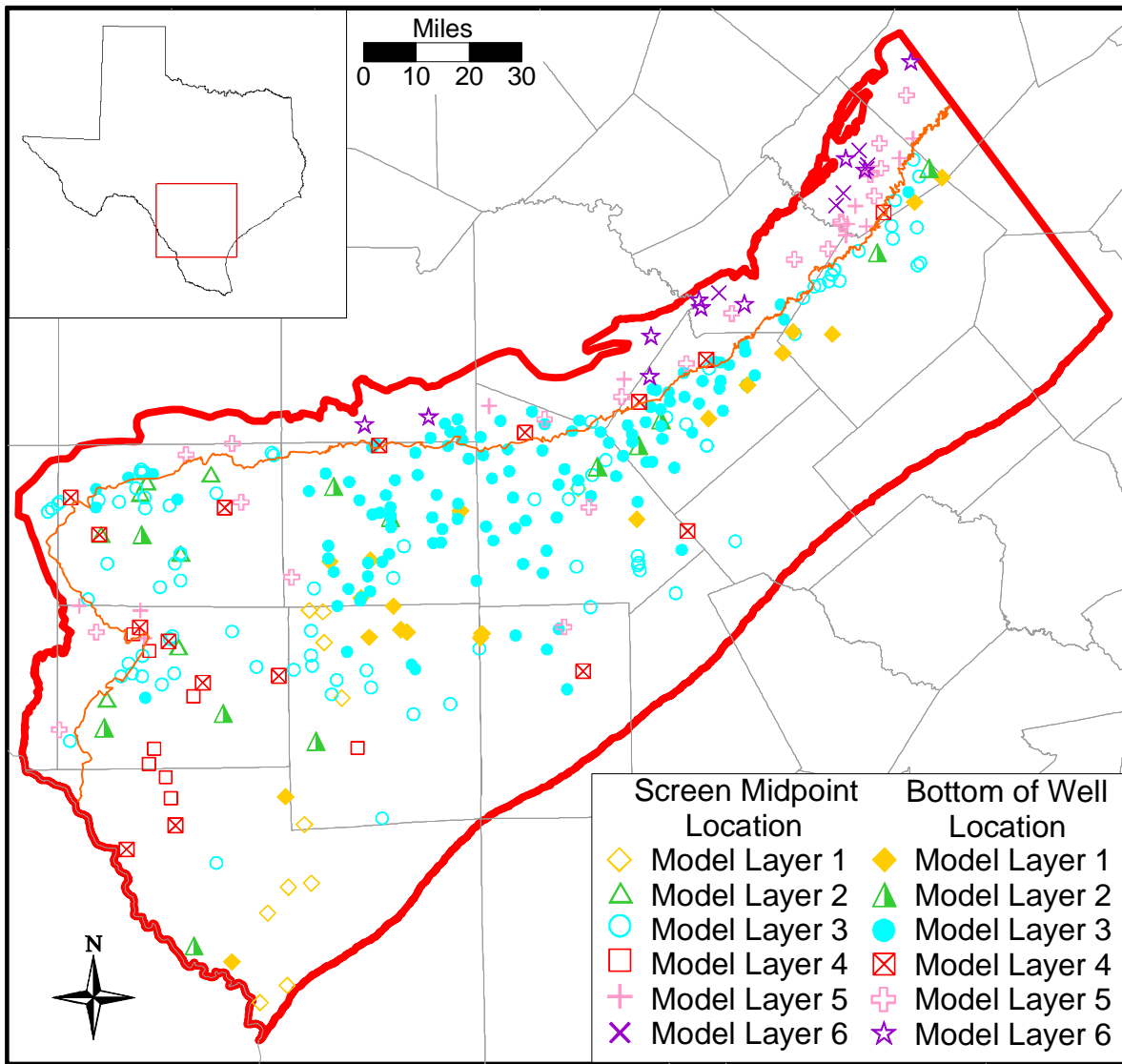


Figure 4.4.8 Model layer for locations with transient water-level data.

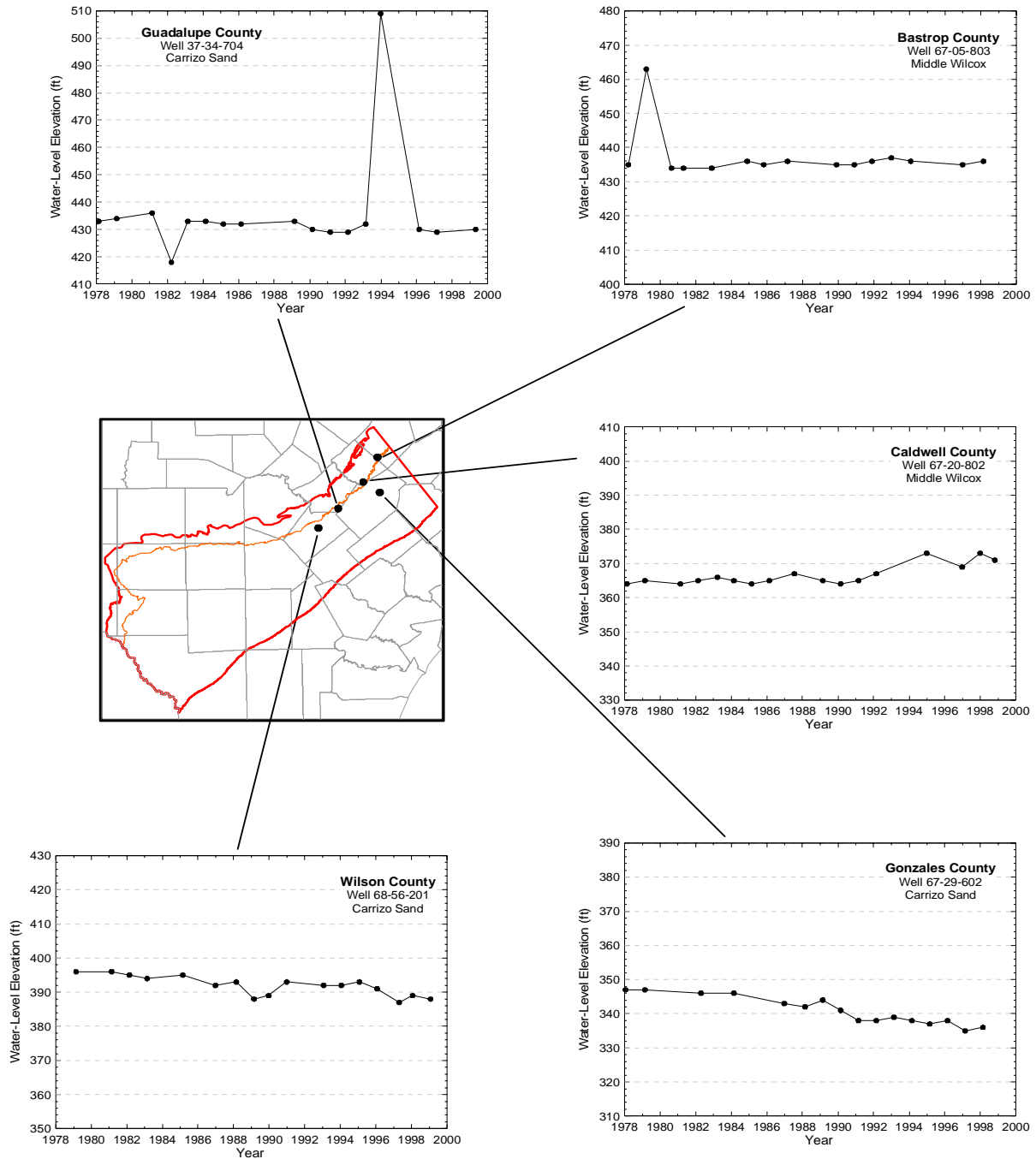


Figure 4.4.9 Example hydrographs for wells located in Bastrop, Caldwell, Gonzales, Guadalupe, and northern Wilson counties.

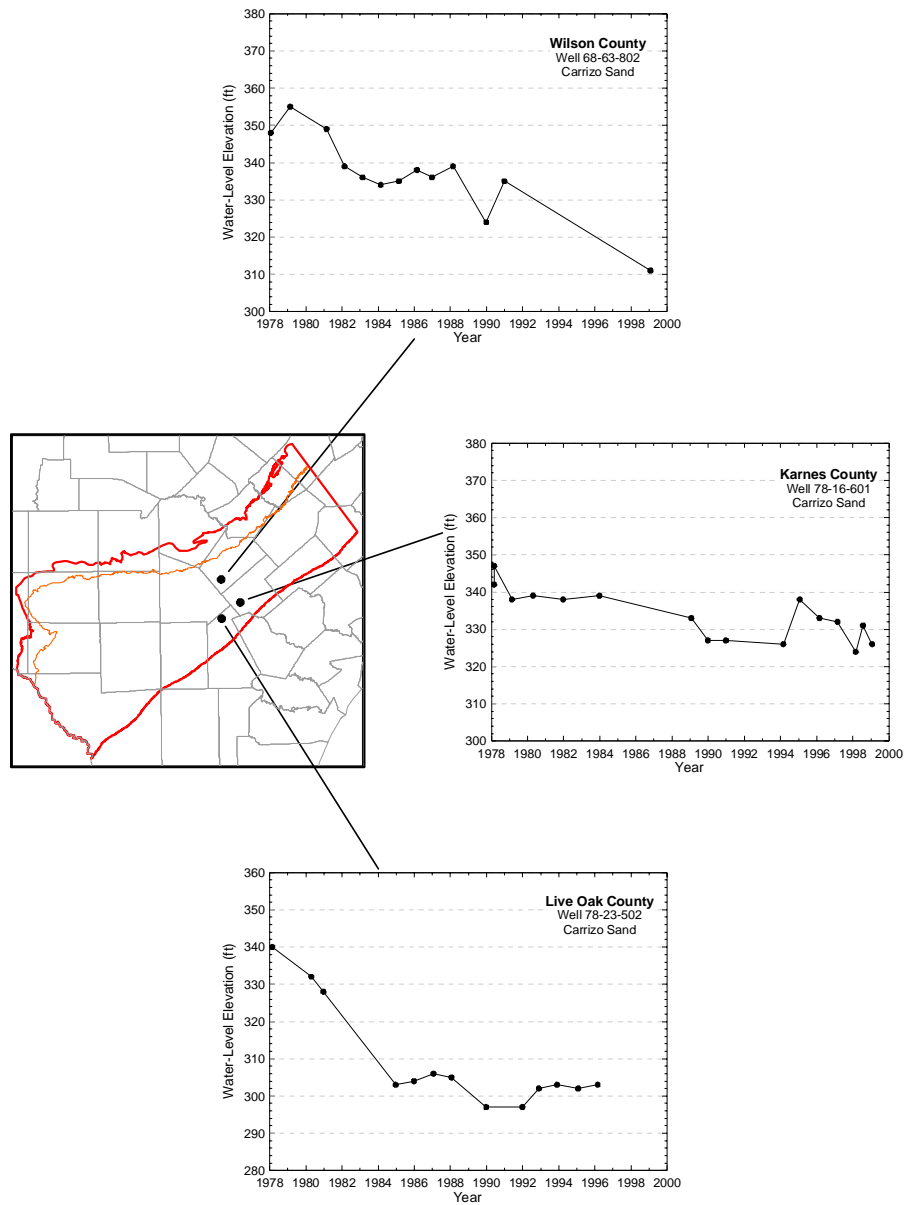


Figure 4.4.10 Example hydrographs for wells in southern Wilson County and Karnes and Live Oak counties.

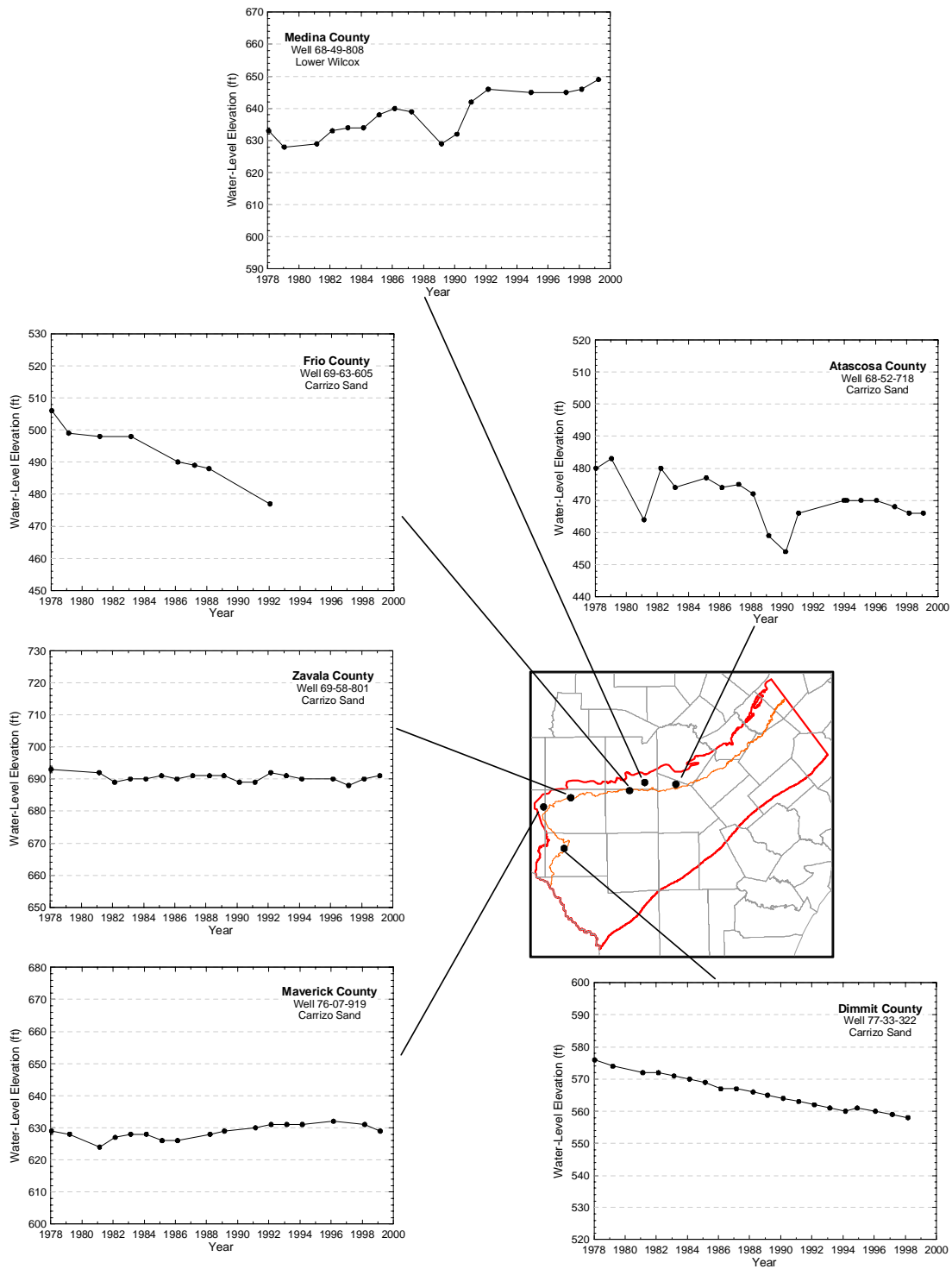


Figure 4.4.11 Example hydrographs for wells in the outcrop areas of Atascosa, Medina, Frio, Zavala, Maverick, and Dimmit counties.

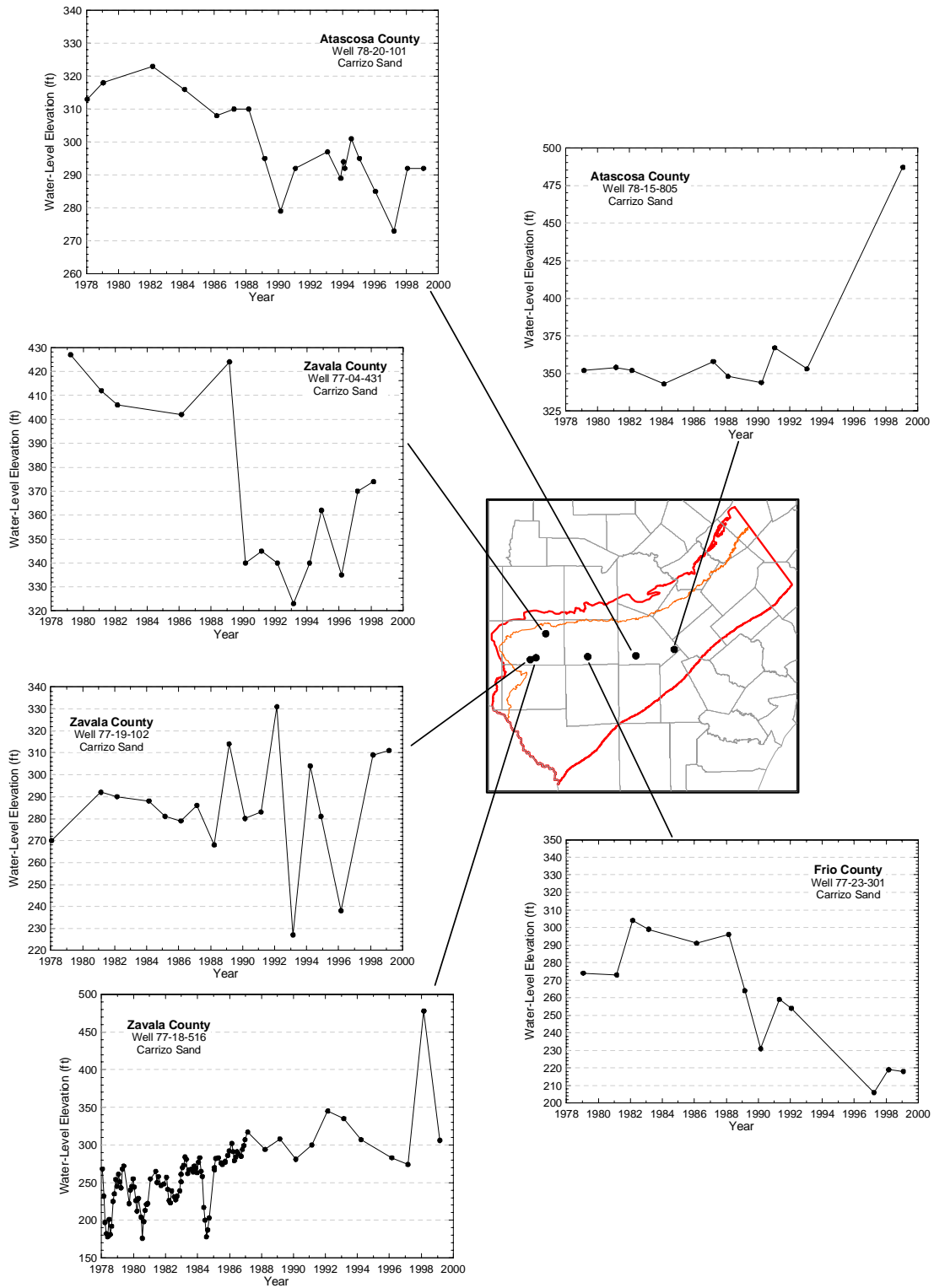


Figure 4.4.12 Example hydrographs for wells in the down-dip areas of Atascosa, Frio, and Zavala counties.

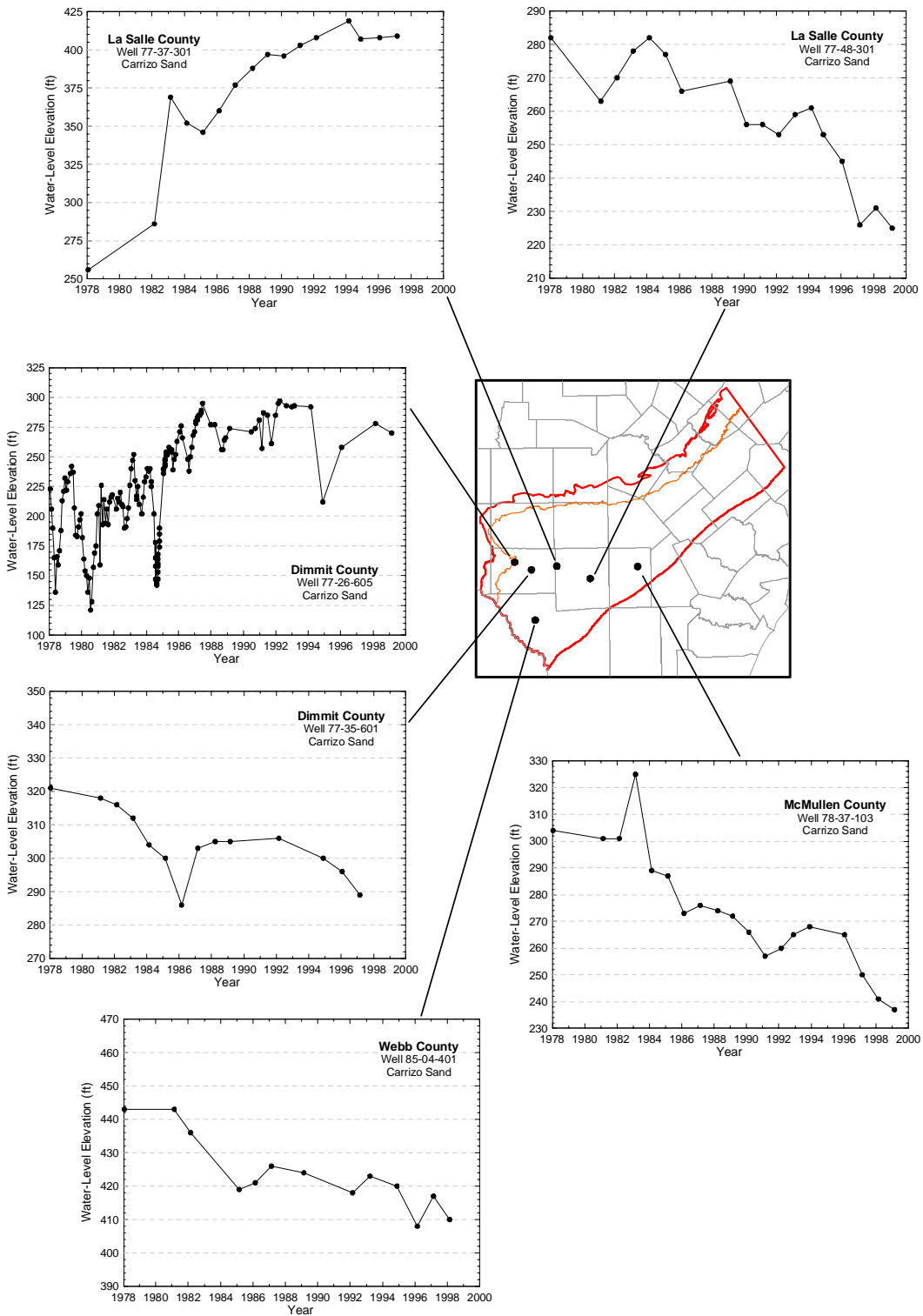


Figure 4.4.13 Example hydrographs for wells in McMullen, La Salle, Webb, and the downdip area of Dimmit counties.

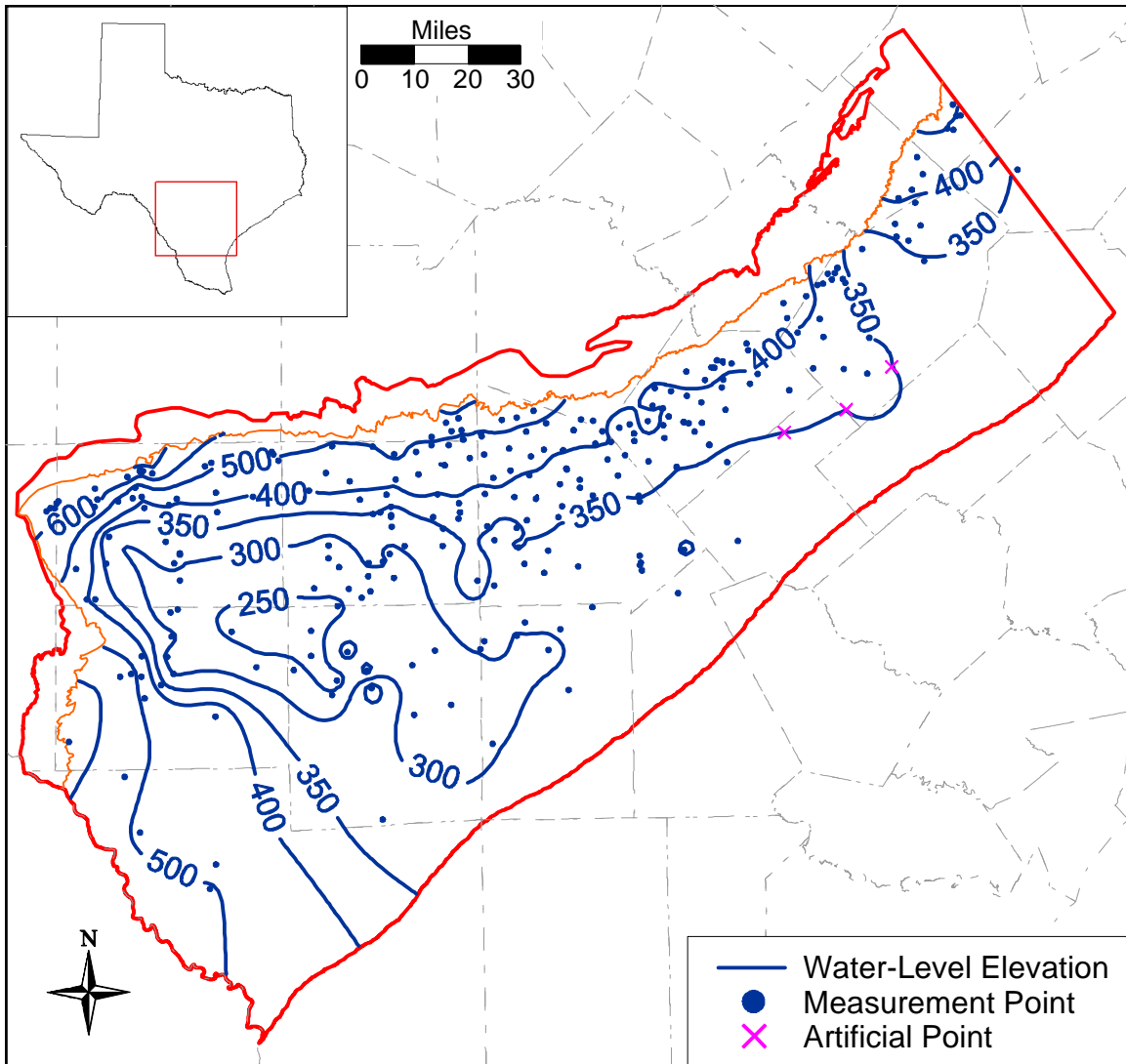


Figure 4.4.14 Water-level elevation contours for the Carrizo-Wilcox aquifer at the start of model calibration (January 1980).

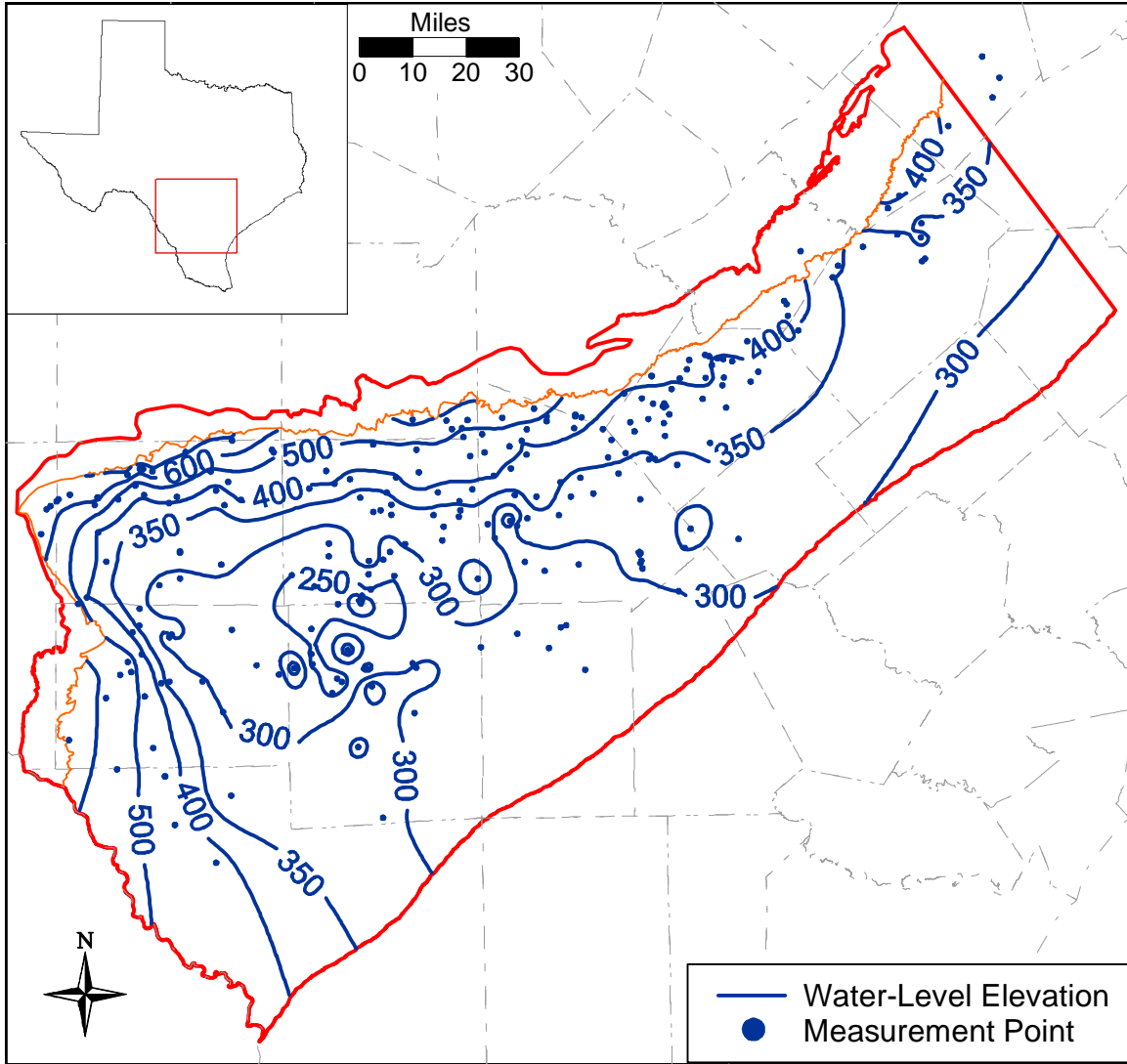


Figure 4.4.15 Water-level elevation contours for the Carrizo-Wilcox aquifer at the end model calibration (December 1989).

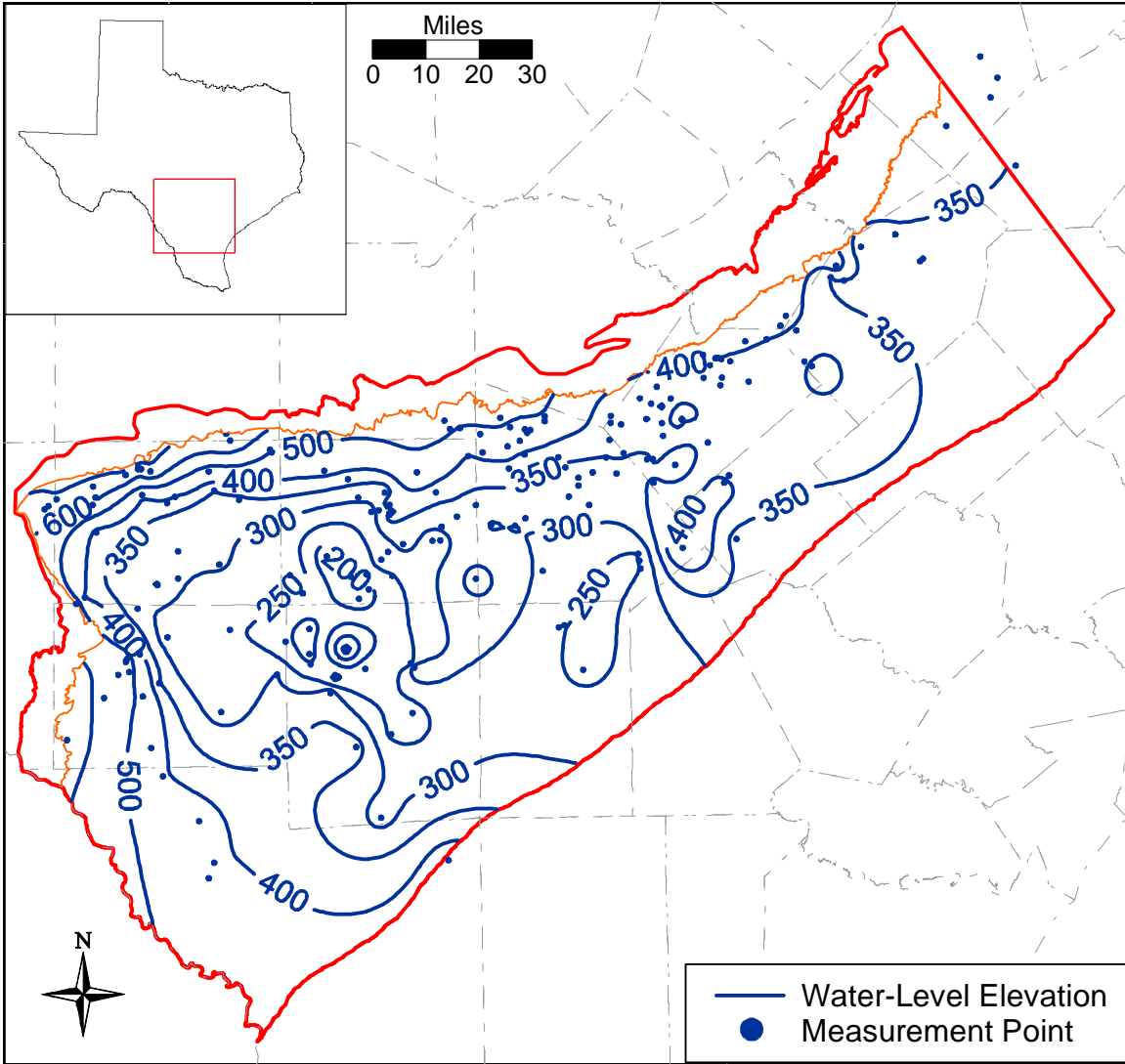


Figure 4.4.16 Water-level elevation contours for the Carrizo-Wilcox aquifer at the end model verification (December 1999).

4.5 Recharge

Recharge can be defined as water which enters the saturated zone at the water table (Freeze, 1969). Potential sources for recharge to the water table include precipitation, stream or reservoir leakage, or irrigation return flow. In the Southern Carrizo-Wilcox GAM area, recharge is conceptualized to occur as diffuse recharge in the inter-stream areas as a result of precipitation and irrigation return flow and as focused recharge in the stream valleys and in the vicinity of reservoirs (Scanlon et al, 2002). In the Southern Carrizo-Wilcox GAM region, the streams tend to be losing which makes them areas for potential recharge.

The cleaner and more massive sands of the Carrizo Formation have commonly been assumed to be the preferentially recharged unit in the Carrizo-Wilcox aquifer system. This is likely the result of the formation's increased ability to move water away from the water table (Freeze, 1969) relative to other hydrostratigraphic units adjacent to and within the Carrizo-Wilcox. However, recharge is a complex function of precipitation rate and volume, soil type, water level and soil moisture, topography, and evapotranspiration (ET) (Freeze, 1969). Because of its large outcrop area and relatively high sand content, the Wilcox Group also has a good potential for diffuse recharge in the study area. When recharge rates exceed the saturated hydraulic conductivity of the underlying soils and aquifer, then the transmission capability of the underlying formation becomes a limiting factor. These conditions may be expected to occur in locations of focused recharge near streams during high flow conditions and around reservoirs. Because precipitation, ET, and soil moisture vary as a function of time, recharge is also expected to vary as a function of time. Recharge will be highest in times of significant rainfall when soil moisture content is high. In drier times, redistribution and ET may effectively prevent significant recharge.

Several investigators have studied recharge in the Carrizo-Wilcox aquifer in Texas and these studies have been summarized by Scanlon et al. (2002) and are reproduced in Table 4.5.1. Those studies which are limited to the Southern Carrizo-Wilcox GAM model area are grouped as the top five entries in Table 4.5.1 because of their direct relevance to this study. For all studies, recharge rates range from a low of 0.1 inches estimated for Rains and Van Zandt counties (White, 1973) using a Darcy's Law approach to a high of 5.8 inches per year in Atascosa County (Opfel and Elder, 1978) using neutron probe measurements in the vadose zone. The range

specific to the study area is similar in magnitude ranging from a low of 0.2 inches per year (LBG-Guyton Associates and HDR 1998) in the Winter Garden Area to a high of 5.8 inches per year (Opfel and Elder, 1978) in Atascosa County as described above.

The most recent recharge study in the GAM model area is a groundwater model developed using MODFLOW and proprietary surface water models developed by HDR Engineering (LBG-Guyton and HDR, 1998). In that study, recharge was estimated for three components, diffuse recharge, main-channel stream recharge, and flood-flow recharge. The estimation of recharge was based upon an iterative methodology that partitioned the three types of recharge for each basin modeled based upon potential aquifer recharge estimates from unpublished TWDB transmission capacity estimates. The potential recharge estimates from LBG-Guyton and HDR (1998) are summarized in Table 4.5.2 for counties that intersect the Southern Carrizo-Wilcox GAM area. To estimate these recharge potentials in terms of inches per year, we intersected the Carrizo-Wilcox outcrop with the county boundaries to get a contributing recharge area per county.

Their range in recharge potential based upon transmission capacity ranged from 0.2 to 7.2 inches per year in the GAM model area. LBG-Guyton and HDR (1998) estimated that total recharge to their model (including the Queen City, Sparta and Younger units) partitioned into 66.7% diffuse recharge, 24.8% flood-flow recharge, and 8.5% main-channel stream recharge. There are no natural lakes in the model study area. There are two reservoirs that intersect one or more of the active outcrop grid cells in the GAM area, Calaveras Lake and Victor Braunig Lake, which are both located in Southern Bexar County. Figure 4.5.1 shows the locations of these two reservoirs and includes lake stage elevations for the historical simulation period from 1980 to 1999.

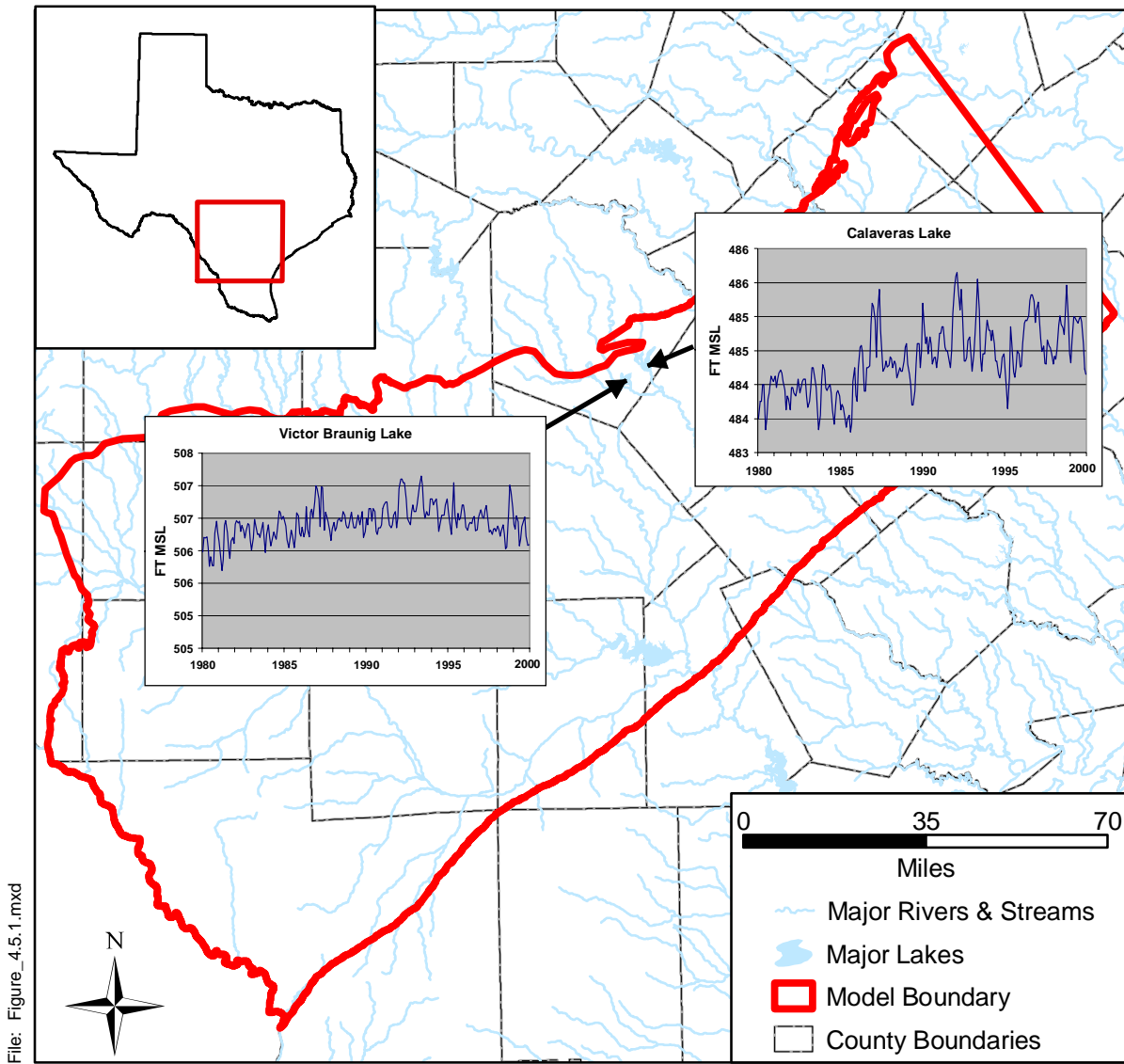
Table 4.5.1 Review of recharge rates for the Carrizo-Wilcox aquifer in Texas (after Scanlon et al., 2002).

Major Aquifer	Location (County/Area)	Aquifer	Recharge rate (mm/yr)	Recharge rate (in/yr)	Total recharge (af/yr)	Reference	Technique
Carrizo Wilcox	Atascosa, Frio	Carrizo sand	45.7	1.8		Alexander and White, 1966	¹⁴ C, Darcy's Law
	Winter Garden Area	undifferentiated	5-127	0.2-5		LBG-Guyton & Assoc. and HDR, 1998	modeling, water budget
	Bexar	Hooper, Simsboro, Calvert Bluff	45.7	1.8		HDR Engineering, 2000	groundwater modeling
	Atascosa	Carrizo	147	5.8		Opfel and Elder, 1978	neutron probe logging
	Atascosa, Bexar, Dimmit, Frio, Gonzales, Guadalupe, Medina, Uvalde, Wilson, Zavala	undifferentiated			25,000	Turner, et al., 1960	Darcy's Law
	Sabine, San Augustine	undifferentiated	50.8	2.0		Anders, 1967	Darcy's Law
	Sabine, San Augustine	undifferentiated	25.4	1.0		Anders, 1967	baseflow discharge
	Camp, Franklin, Morris, Titus	Carrizo Wilcox			12,000	Broom et al., 1965	baseflow discharge
	Harrison	Cypress	7.9	0.3	15,000	Broom and Myers, 1966	Darcy's Law
	Harrison	Cypress	7.9	0.3	40,000	Broom and Myers, 1966	baseflow discharge
	Wood	Carrizo	12.7	0.5	3,000	Broom, 1968	Darcy's Law
	Bastrop, Lee, Milam	Simsboro, Carrizo	51-102	2.0-4.0		Dutton, 1999	groundwater modeling
	Bastrop	Carrizo, Wilcox sand	38	1.5		Follett, 1970	Darcy's Law
	Bastrop, Lee, Milam, Robertson, Falls, Limestone, Freestone, Navarro	Carrizo, Simsboro	76-127	3.0-5.0		Harden and Associates, 2000	groundwater modeling
	Bastrop, Lee, Milam, Robertson, Falls, Limestone, Freestone, Navarro	Calvert Bluff, Hooper	12.7	0.5		Harden and Associates, 2000	groundwater modeling
	Winter Garden area	undifferentiated			100,000	Klemt et al., 1976	groundwater modeling
	Rusk	Carrizo	<25.4	<1.0		Sandeen, 1987	Darcy's Law
	Navarro	Carrizo Wilcox	12.7	0.5		Thompson, 1972	estimate
	Caldwell, Bastrop, Lee, Milam, Robertson, Limestone, Freestone	undifferentiated	25.4	1.0		Thorkildsen and Price, 1991	groundwater modeling
	Bastrop, Lee, Fayette	undifferentiated	25.4	1.0		Thorkildsen et al., 1989	groundwater modeling
Rains, Van Zandt	Carrizo Wilcox	3	0.1	5,000	White, 1973	Darcy's Law	

Table 4.5.2 Potential recharge rates for the Carrizo-Wilcox (after LBG-Guyton and HDR, 1998).

County	Recharge Potential (acre feet per year) ⁽¹⁾	Recharge Potential (inches per year) ⁽²⁾
Atascosa	21,582	2.65
Bexar	10,552	0.57
Caldwell	3,063	0.19
Dimmit	6,095	0.45
Frio	5,677	2.64 ⁽³⁾
Gonzales	9,840	7.15 ⁽³⁾
Guadalupe	19,947	1.04
Maverick	1,803	0.18
Medina	18,265	1.04
Uvalde	1,614	0.29
Wilson	33,551	4.05
Zavala	11,058	0.78
Total	143,047	1.06

- (1) As reported by LBG-HDR (1998)
- (2) Calculated by estimating outcrop areas by county
- (3) Small outcrop areas may lead to large error in calculated recharge



File: Figure_4.5.1.mxd

Source: City of San Antonio Public Service, 2001

Figure 4.5.1 Hydrographs for reservoirs in the Carrizo-Wilcox outcrop.

4.6 Natural Aquifer Discharge

Under steady-state conditions (predevelopment), groundwater flow in the aquifer is elevation driven from the higher elevation outcrops to the confined sections of the aquifer. In the predevelopment condition, recharge occurring as a result of diffuse and focused recharge is balanced by discharge in stream valleys and springs, and through cross-formational flow. Under predevelopment conditions, prior to 1900, western streams such as the Nueces and Frio rivers were likely gaining streams based upon historical occurrence of flowing wells. By 1904 there were thirty artesian wells in the Carrizo Springs area alone, with average flows ranging from 40 to 300 gallons per minute. From early times, the Dimmit County area was famous for spring fed creeks that supported travelers and wildlife. Within 40 years of the drilling of the first well, virtually all of the springs and creeks they fed were dry. By 1910, farmers in some areas had to pump their wells (<http://historicdistrict.com/Genealogy/Dimmit/history.htm>). Hamlin (1988) reports that, prior to significant production (before 1900), Carrizo wells flowed at elevations up to 700 ft amsl. By the 1930s, flowing wells were limited to elevations below 500 ft amsl and, by 1972, only certain wells flowed at elevations below 360 ft amsl. In the eastern portion of the model area, flowing Carrizo wells still exist in areas such as Gonzales County. Participants in the Southern Carrizo-Wilcox GAM Stakeholder Advisory Forums have indicated that portions of Cibolo Creek that run through their property in Wilson County have ceased to be perennial gaining streams in recent history.

As a result of precipitation rates, recharge rates, natural depth to water, and pumping induced water level declines, streams tend to change from being perennial and gaining to being non-perennial and losing from east to west across the model study area. LBG-Guyton and HDR (1998) performed an analysis of important stream segments within their model area which closely coincides with this GAM model area. They estimated base flow in summer and winter for stream segments having gages located above and below the Carrizo-Wilcox outcrop. Their analysis indicated that the Nueces and the Frio rivers are dominantly losing in both winter and summer. Cibolo Creek was found to be gaining in both winter and summer. The San Antonio River and the Guadalupe River were found to be gaining in the winter months and losing in the summer months when evapotranspiration was assumed to exceed base flow.

The LBG-Guyton-HDR (1998) model was calibrated to transient heads from 1910 through 1994. Their analysis predicted the gain/loss on a ten-year moving average basis for each major river in the model study area from 1942 through 1994. Their analysis predicted that San Miguel Creek, the Nueces River, and the Frio River were losing streams throughout their analysis period (1942-1994). Through the historical period of interest in this GAM, their results predicted that the Nueces and Frio rivers lose, on average, approximately 500 acre feet per year per mile of outcrop. Conversely, the San Marcos and Guadalupe rivers were shown to be gaining streams throughout the predictive period, gaining less than 100 acre feet per year per mile of outcrop from 1980 through 1994. The San Antonio River changed from strongly gaining (over 400 acre feet per year per mile) to losing greater than 400 acre feet per year per mile of outcrop by 1990. The change from gaining to losing occurred in the late 1960s. The Atascosa River also changed from gaining conditions to losing in the early 1970s to becoming slightly losing (less than 50 acre feet per year per mile) from 1980 through 1994. Cibolo Creek also changed from gaining 200 acre feet per year per mile in the 1940s to losing upwards of 100 acre feet per year per mile in the late 1970s through 1994.

Slade et al (2002) summarized the results of 366 gain/loss studies involving 249 unique reaches of streams throughout Texas since 1918. They documented 33 individual gain/loss studies in the model area in the Carrizo-Wilcox outcrop for the Rio Grande River, the Nueces River, the Leona River, the Medina River and Cibolo Creek. Figure 4.6.1 shows the locations and survey numbers of the gain/loss studies in the model area. Table 4.6.1 provides the characteristics of the gain/loss studies reported by Slade et al. (2002) in the study area. The survey numbers in Figure 4.6.1 correspond to the survey numbers in Table 4.6.1.

Most of the relevant gain/loss studies in the model area have been performed on the Nueces River. Studies 182 through 185 were performed on the same stretch of the Nueces in four surveys from April 1940 through September 1940. The average and median loss estimates for that time period were -814 and -898 (negative indicated a losing stream) acre feet per year per mile of stream, respectively. Studies 194-202 and 206, 207, and 210 were performed as early as 1925 and as late as 1933. The Nueces was predominantly losing during this period with average and median gain/loss estimates of -653 and -959 acre feet per year per mile, respectively. Studies 165 through 175 were performed on the Leona River in Zavala and Uvalde counties from as early as 1925 and as late as 1947. The Leona River was predominantly gaining

over this period with average and median gain/loss estimates of 221 and 50 acre feet per year per mile, respectively. There does seem to be a weak correlation between season and interaction with stream loss occurring more in summer and stream gain occurring more in winter. Study 104 investigated Cibolo Creek across a 62 mile length in September of 1949. The creek was found to be gaining at an average rate of 163 acre feet per year per mile. Study 130 on the Medina River in May of 1925 estimated an average loss rate of -42 acre feet per year per mile of stream. Three studies (325,327,328) were performed on the Rio Grande River yielding widely varying results from an average loss of -1453 to an average gain of 495 acre feet per year per mile.

Discharge also occurs in areas where the water table intersects the surface at springs or weeps. These springs usually occur in topographically low areas in river valleys or in areas of the outcrop where hydrogeologic conditions preferentially reject recharge. We performed a literature survey of springs with location and flow rate data available for the model area (Figure 4.6.2 and Table 4.6.2). The available measured spring flow rates range from a low of 0.01 cubic feet per second (7 acre feet per year) to a high of 3.5 cubic feet per second (2,534 acre feet per year) measured at Mitchell Lake Springs and representing reservoir leakage. Discarding this value as unrepresentative of natural springs in the area, the next highest measurement is at Martinez Springs in Bexar County which is 1.6 cubic feet per second (1,158 acre feet per year) representing a baseflow measurement in a stream. Carrizo Springs flowed constantly until 1929 (Brune, 1975). Because of free-flowing wells in Dimmit County from the late 1800s through the 1930s, Carrizo Springs quit flowing in 1929 and has flowed only intermittently since.

Cross-formational flow is also a natural mechanism for discharge of groundwater from the Carrizo-Wilcox aquifer. Investigators have determined that heads within the Carrizo-Wilcox aquifer of south Texas are higher than heads in the overlying younger strata (Harris, 1965; Kreitler, 1979). This is consistent with our own analysis which found that pre-development head differences between the Carrizo and the Queen City increase with depth of confinement to magnitudes as high as 60 feet. Water chemistry data support the proposed upward flow from the Carrizo Sand to overlying sands (Hamlin, 1988). Our analysis also found that the upward gradient continued between the Queen City aquifer and the estimated regional water table in the confined section. Cross-formational flow occurring in the Carrizo-Wilcox aquifer is not directly measurable and is best determined through modeling studies such as this GAM.

With development of the Carrizo-Wilcox aquifer system, the natural balance of deep section recharge and cross-formational flow has changed. In areas experiencing extensive groundwater pumping, hydraulic gradients between the Carrizo and the overlying units have reversed creating potential for cross-formation flow from younger units to the Carrizo (Hamlin, 1988; Klemt et al., 1976; Mason, 1960). Klemt et al. (1976) estimated that in the central and southwestern portions of the study area cross-formational flow recharging the Carrizo from younger units was approximately 10,000 acre feet per year.

Table 4.6.1 Stream flow gain/loss studies in the study area (after Slade et al., 2002, Table 1).

Streamflow Study No.	Major River Basin	Stream Name	Reach Identification	Date of Study	Reach Length (river mi)	Total No. of Measurement Sites	No. of Measurement Sites on Main Channel	Major Aquifer Outcrop(s) Intersected by Reach	Total Gain or Loss (-) In Reach (ft ³ /s)	Gain or Loss per Mile of Reach (ft ³ /s-mi)	Gain or Loss per AFY-mi
104	Guadalupe	Cibolo Cr	Schertz to San Antonio R near Falls City (08183500)	9/12-13/1949	62	10	7	Carrizo-Wilcox	13.95	0.225	163.0
130	Guadalupe	Medina R	Medina Co Irrigation Co. diversion dam to Losoya	5/26-28/1925	55.1	19	14	Carrizo-Wilcox, Edwards	-3.2	-0.058	-42.0
135	Lavaca	Lavaca R	East of Hallettsville (08163500) to southeast of Edna	12/14-17/1970	65.4	18	14	Gulf Coast	18.23	0.279	202.1
140	Nueces	Atascosa, Frio, and Nueces R	3 mi southwest of Poteet to near Mathis	1/23-26/1951	103.8	29	14	Gulf Coast	4.83	0.047	34.0
141	Nueces	Atascosa, Frio, and Nueces R	Campbellton to near Mathis	4/19-21/1951	60.2	30	15	Gulf Coast	1.13	0.019	13.8
142	Nueces	Atascosa, Frio, and Nueces R	Campbellton to near Mathis	4/27-5/1/1951	58.3	23	13	Gulf Coast	-0.22	-0.004	-2.9
154	Nueces	Frio R	Choke Canyon Reservoir to Shamrock Refinery	11/12-13/1991	8.59	5	4	Gulf Coast	0.12	0.014	10.1
159	Nueces	Frio R	near Fowler to mouth	12/18-21/1967	62.9	13	6	Gulf Coast	10.63	0.169	122.4
165	Nueces	Leona R	1.7 mi southeast of Uvalde to 0.2 mi east of Zavalla-Frio Co line	2/5-8/1946	49.4	35	32	Carrizo-Wilcox	2.0	0.04	29.0
166	Nueces	Leona R	1.7 mi southeast of Uvalde to 35 mi southeast of Uvalde	6/11-12/1931	37.5	15	12	Carrizo-Wilcox	-3.1	-0.083	-60.1
167	Nueces	Leona R	1.7 mi southeast of Uvalde to 7.1 mi southeast of Batesville	8/7-9/1946	36.3	22	21	Carrizo-Wilcox	0.3	0.008	5.8
168	Nueces	Leona R	1.7 mi southeast of Uvalde to 9.5 mi southeast of Uvalde	3/1/1947	9.8	5	5	Carrizo-Wilcox	14.91	1.521	1101.9
169	Nueces	Leona R	1.7 mi southeast of Uvalde to below Batesville	6/21-22/1934	34.6	13	10	Carrizo-Wilcox	-3.1	-0.09	-65.2
170	Nueces	Leona R	1.7 mi southeast of Uvalde to below Batesville	10/18-20/1934	34.6	14	11	Carrizo-Wilcox	2.4	0.069	50.0
171	Nueces	Leona R	1.7 mi southeast of Uvalde to below Batesville	7/5-6/1939	23	14	11	Carrizo-Wilcox	4.3	0.187	135.5
172	Nueces	Leona R	1.7 mi southeast of Uvalde to near Batesville	11/7/1932	17	6	4	Carrizo-Wilcox	21.2	1.247	903.4
173	Nueces	Leona R	10 mi below Uvalde to below Batesville	6/8-10/1939	26	10	8	Carrizo-Wilcox	-3.8	-0.146	-105.8
174	Nueces	Leona R	below Kincaid Dam to 9.5 mi southeast of Uvalde	2/19/1946	5.2	7	7	Carrizo-Wilcox	0.7	0.135	97.8
175	Nueces	Leona R	Uvalde-Friortown Hwy to near Batesville	4/25-28/1925	33.5	14	11	Carrizo-Wilcox	15.89	0.474	343.4
182	Nueces	Nueces R	above Laguna (08190000) to 4.8 mi southeast of La Pryor	5/2-3/1940	46.9	14	13	Carrizo-Wilcox, Edwards	-63.8	-1.36	-985.3
183	Nueces	Nueces R	above Laguna (08190000) to 4.8 mi southeast of La Pryor	7/9-10/1940	46.9	14	13	Carrizo-Wilcox, Edwards	-66.7	-1.422	-1030.2

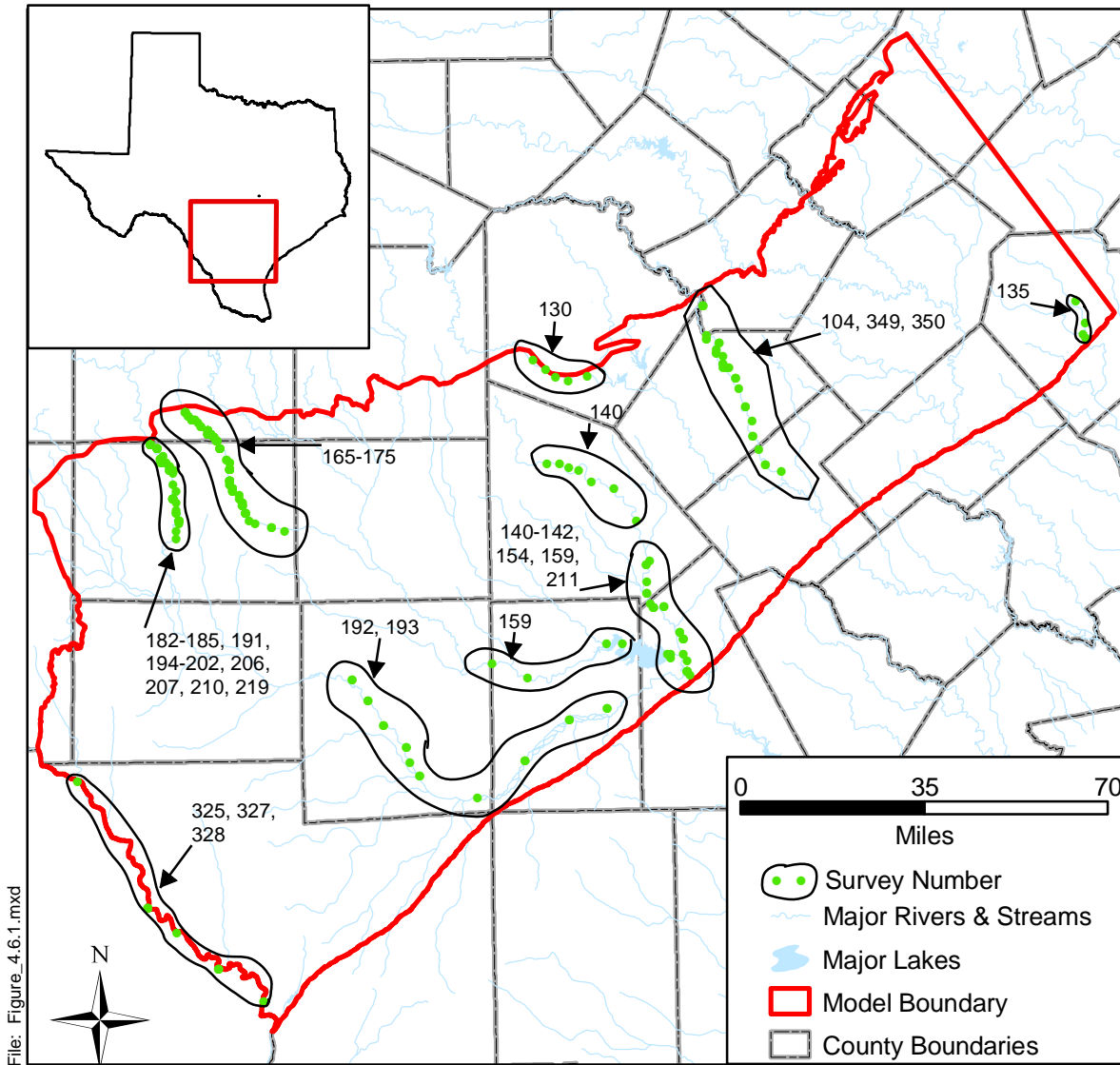
Table 4.6.1 (continued)

Streamflow study no.	Major river basin	Stream name	Reach identification	Date of study	Reach length (river mi)	Total no. of measurement sites	No. of measurement sites on main channel	Major aquifer outcrop(s) intersected by reach	Total gain or loss (-) in reach (ft ³ /s)	Gain or loss per mile of reach (ft ³ /s-mi)	Gain or loss per AFY-mi
184	Nueces	Nueces R	above Laguna (08190000) to 4.8 mi southeast of La Pryor	8/28-29/1940	46.8	14	13	Carrizo-Wilcox, Edwards	-52.3	-1.118	-809.9
185	Nueces	Nueces R	above Laguna (08190000) to 4.8 mi southeast of La Pryor	9/26-27/1940	46.9	14	12	Carrizo-Wilcox, Edwards	-27.9	-0.595	-431.1
191	Nueces	Nueces R	below Odley Cr near Vance to La Pryor	3/17-26/1924	74.4	21	18	Carrizo-Wilcox, Edwards, Edwards-Trinity (Plateau)	19.8	0.266	192.7
192	Nueces	Nueces R	Cotulla (08194000) to Simmons (08194600)	7/28-30/1981	108.1	13	10	Gulf Coast	7.6	0.07	50.7
193	Nueces	Nueces R	Cotulla (08194000) to Simmons (08194600)	8/11-13/1981	108.1	13	10	Gulf Coast	9.29	0.086	62.3
194	Nueces	Nueces R	Laguna (08190000) to 3.8 mi southeast of Cinonia	6/14-30/1939	61.6	27	25	Carrizo-Wilcox, Edwards	-23.7	-0.385	-278.9
195	Nueces	Nueces R	Laguna (08190000) to 5 mi northeast of La Pryor	11/14-16/1931	39.6	10	10	Carrizo-Wilcox, Edwards	-60.2	-1.52	-1101.2
196	Nueces	Nueces R	Laguna (08190000) to 5 mi northeast of La Pryor	1/24-25/1932	39.6	11	11	Carrizo-Wilcox, Edwards	-59.5	-1.503	-1088.9
197	Nueces	Nueces R	Laguna (08190000) to Cinonia	4/30-5/8/1925	54.9	14	14	Carrizo-Wilcox, Edwards	-29.9	-0.545	-394.8
198	Nueces	Nueces R	Laguna (08190000) to Cinonia	5/16-17/1931	56.5	11	11	Carrizo-Wilcox, Edwards	-76.0	-1.345	-974.4
199	Nueces	Nueces R	Laguna (08190000) to Cinonia	6/4-6/1931	53	10	10	Carrizo-Wilcox, Edwards	-84.0	-1.585	-1148.3
200	Nueces	Nueces R	Laguna (08190000) to Cinonia	6/15-17/1931	56.5	12	12	Carrizo-Wilcox, Edwards	-73.6	-1.303	-944.0
201	Nueces	Nueces R	Laguna (08190000) to Cinonia	6/22-24/1931	56.5	12	12	Carrizo-Wilcox, Edwards	-91.9	-1.627	-1178.7
202	Nueces	Nueces R	Laguna (08190000) to Cinonia	7/2-4/1931	56.5	12	12	Carrizo-Wilcox, Edwards	-82.5	-1.46	-1057.7
206	Nueces	Nueces R	Laguna (08190000) to near Cinonia	11/1-4/1932	56.5	14	14	Carrizo-Wilcox, Edwards	28.0	0.496	359.3
207	Nueces	Nueces R	Laguna (08190000) to near Cinonia	7/23-25/1933	56.5	14	14	Carrizo-Wilcox, Edwards	-8.7	-0.154	-111.6
210	Nueces	Nueces R	Uvalde (08204000) to Cinonia	7/13/1931	33.8	7	7	Carrizo-Wilcox	4.0	0.118	85.5
211	Nueces	Nueces R	Miller's Ranch to Nueces R at Highway 59	11/12-13/1991	16.45	7	6	Gulf Coast	65.89	4.005	2901.5
219	Nueces	Nueces R	US 90 to near Crystal City	11/23-25/1964	52.2	19	10	Carrizo-Wilcox	13.4	0.257	186.2
325	Rio Grande	Rio Grande	Eagle Pass to Laredo	2/22-4/12/1928	128	6	6	--	-10.0	-0.078	-56.5
327	Rio Grande	Rio Grande	Eagle Pass to Laredo	4/3-22/1928	128	6	6	--	-75.0	-0.586	-424.5
328	Rio Grande	Rio Grande	Eagle Pass to San Ygnacio	2/12-22/1926	167.5	22	17	Carrizo-Wilcox	336.0	-2.006	-1453.3
349	San Antonio	Cibolo Cr	near Randolph AFB to mouth	3/5-7/1963	79.3	18	13	Carrizo-Wilcox, Gulf Coast	16.68	0.21	152.1
350	San Antonio	Cibolo Cr	Selma (08185000) to mouth	3/4-8/1968	87.1	52	27	Carrizo-Wilcox, Gulf Coast	59.53	0.683	494.8

Table 4.6.2 Documented springs in the study area.

ID	WELL ID	COUNTY	Spring	Aquifer	Flow Rate LPS	Flow Rate GPM	Flow rate CFS	Date of Measurement	Measurement	Notes and Historical Information	Source
1	-	Dimmit	Carrizo Springs	Carrizo Sands	7.36	116.70	0.26	1/1/1892	1 of 3	Flowed constantly until 1929	Brune (1975)
2	-	Dimmit	Carrizo Springs	Carrizo Sands	37.00	586.46	1.31	12/30/1901	2 of 3	Flowed constantly until 1929	Brune (1975)
3	-	Dimmit	Carrizo Springs	Carrizo Sands	0.32	5.07	0.01	1/1/1979	3 of 3	Flowed constantly until 1929	Brune (1975)
4	-	Bexar	Martinez Springs	Wilcox Sands	45.31	718.13	1.60	3/5/1963		Baseflow in gravel streambed	Brune (1975)
5	-	Bexar	Mitchell Lake Springs	Wilcox Sands	99.11	1570.91	3.50	5/28/1925		Represents seepage from reservoir	Brune (1975)
6	-	Wilson	Sutherland Springs	Carrizo Sands	42.48	673.25	1.50	1/1/1949	1 of 3	Includes White Sulphur, Cold, Sour and Alligator Springs. ~100 springs	Brune (1975)
7	-	Wilson	Sutherland Springs	Carrizo Sands	0.28	4.49	0.01	1/1/1954	2 of 3	Includes White Sulphur, Cold, Sour and Alligator Springs. ~100 springs	Brune (1975)
8	-	Wilson	Sutherland Springs	Carrizo Sands	4.25	67.32	0.15	3/6/1968	3 of 3	Includes White Sulphur, Cold, Sour and Alligator Springs. ~100 springs	Brune (1975)
9	6733905	Guadalupe	King Hill Spring	Carrizo Sands	0.63	10.00	0.02			Reported numerous openings in quick sand. Flows about 10 gpm into pond.	TWDB Well Database
10	-	Webb	Sullivan Springs	Tertiary Eocene Sand	0.32	5.07	0.01	2/8/1979			GNIS, Brune (1975)

1 cubic feet per second (cfs) = 724 acre feet per year (AFY)



Source: Online: U.S.G.S. Report by Slade, Bentley and Michaud (2000)

Figure 4.6.1 Stream gain/loss studies in the study area (after Slade et al. 2002).

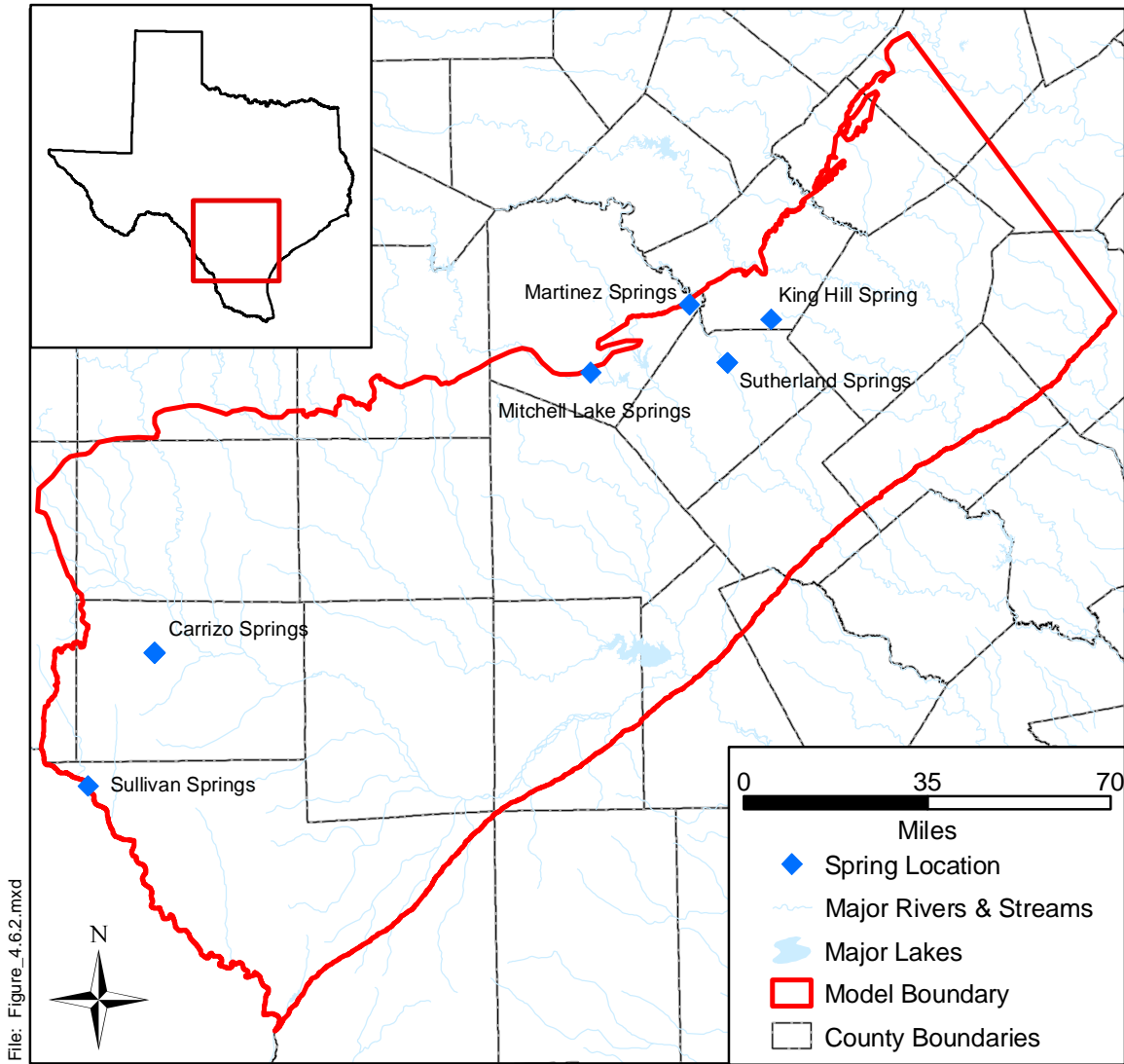


Figure 4.6.2 Documented spring locations in the study area.

4.7 Aquifer Discharge Through Pumping

Pumping discharge from the model required estimations for both the historical modeling period (1980 to 1999) and for the predictive period (2000 to 2050). Historical estimates of groundwater pumpage from the Carrizo-Wilcox aquifer were based on the water use survey database provided by the Texas Water Development Board. The seven water use categories utilized were municipal (MUN), manufacturing (MFG), power generation (PWR), mining (MIN), livestock (STK), irrigation (IRR), and county-other (C-O), which consists primarily of unreported domestic water use. The methodology used to distribute those pumpage estimates is described briefly below, and in detail in the “Standard Operating Procedure for Processing Historical Pumpage Data”, Appendix B to this report.

Municipal, manufacturing, mining, and power pumpage estimates were actual monthly water use records reported by the water user, which were available for 1980 through 1999. In cases where only the total annual pumpage was reported, the average monthly distribution of annual pumpage for the same water use category in the same county-basin, or an adjacent county-basin, was used. A county-basin is a geographic unit created by the intersection of county and river basin boundaries. For example, a county partly crossed by two river basins comprises two county-basins.

The water use survey also included historical annual pumpage estimates for livestock, irrigation, and county-other water use for the years 1980 and 1984 through 1997 for each county-basin. Annual pumpage estimates for the years 1981, 1982, 1983, 1998, and 1999 were developed by linear regression based on significant relationships between reported pumpage and (1) average annual temperature, (2) total annual rainfall measured at the nearest weather station, and (3) the year, for each water use category.

The monthly distribution of county-other water use was assumed to be similar to that of municipal use. The average monthly distribution of municipal water use for a given year within the same (if possible) or an adjacent county-basin was used to estimate how much of the annual total county-other usage was pumped in each month.

Annual livestock water use was distributed uniformly across all twelve months. While this may not accurately reflect seasonality of livestock use, it was not expected to have much impact because livestock is a relatively minor use in the study area.

The procedures for temporal distribution of annual irrigation water use differed for rice and non-rice crops. For rice, monthly irrigation pump electricity consumption use records were used to indicate how much water was pumped in each month for rice irrigation. For non-rice crops, annual irrigation water use was distributed among months using predicted monthly water deficits, based on the rainfall deficit and crop evapotranspiration estimates for each Texas Crop Reporting District, using the approach of Borrelli et al. (1998).

Reported historical pumpage for municipal, manufacturing, mining, and power water uses were matched to the specific wells from which it was pumped to identify the location in the aquifer from which it was drawn (latitude, longitude, and depth below mean sea level) based on the well's reported properties. The well properties were obtained by compiling data from the TWDB's state well database, the Texas Commission on Environmental Quality's Public Water System database, the U.S. Geological Survey's National Water Information System, the TWDB's follow up survey with water users, and various other minor sources as described in the "Standard Operating Procedure for Processing Historical Pumpage Data", Appendix B to this report. When more than one well was associated with a given water user, groundwater withdrawals were divided evenly among those wells.

Livestock pumpage totals within each county-basin were distributed uniformly over the rangeland within the county-basin, based on land use maps, using the categories "herbaceous rangeland", "shrub and brush rangeland", and "mixed rangeland". Vertical assignment of livestock pumpage to model flow layers was performed by interpolating an average well depth and screened interval for all Carrizo-Wilcox livestock watering wells in the TWDB state well database, using the inverse distance method to enhance the influence of nearby wells.

County-other pumpage was distributed within each county-basin based on population density (Figure 4.7.1), after excluding urban areas which would generally be served by municipal water suppliers, using the 1990 federal block-level census data for the years 1980-1990, and the 2000 census data for the years 1991-1999. Vertical assignment of county-other pumpage to model flow layers was performed by interpolating an average well depth and screened interval

for all Carrizo-Wilcox county-other wells in the TWDB state well database, using the inverse distance method to enhance the influence of nearby wells.

Irrigation pumpage within each county-basin was spatially distributed across the land use categories “row crops”, “orchard/vineyard”, and “small grains”. However, the pumpage was not uniformly distributed across these land uses, but weighted based on proximity to irrigated farms mapped from the irrigated farmlands surveys performed in 1989 and 1994 by the Natural Resource Conservation Service of the U.S. Department of Agriculture. The 1989 irrigation survey was used for pumpage between 1980 and 1989, while the 1994 survey was used for pumpage from 1990 to 1999. Further details of the procedure are available in the “Standard Operating Procedure for Processing Historical Pumpage Data”, Appendix B to this report. Vertical assignment of irrigation pumpage to model flow layers was performed by interpolating an average well depth and screened interval for all Carrizo-Wilcox irrigation wells in the TWDB state well database, using the inverse distance method to enhance the influence of nearby wells.

Predicted groundwater pumpage from the Carrizo-Wilcox aquifer for the period 2000 through 2050 was estimated based on projected water demand reported by Regional Water Planning Groups as part of Senate Bill 1 planning (TWDB, 2002). The methodology used to distribute pumpage estimates is described briefly here, and in detail in the “Standard Operating Procedure for Processing Predictive Pumpage Data”, Appendix C to this report. The RWPG water demand projections were available for the years 2000, 2010, 2020, 2030, 2040, and 2050; intervening year projections were developed by linear interpolation. In some cases, the RWPGs identified new well field locations for developing new water supplies. In such instances, the specific locations of the future well fields were used to spatially distribute the groundwater pumpage forecasts. However, in the absence of any data indicating otherwise, it was assumed that the most recent past spatial distribution of groundwater pumpage represented the best available estimate of the locations of future groundwater withdrawals.

Predicted municipal water use totals for each public water supplier were matched to the same wells used for that water user in 1999. Similarly for manufacturing, mining, and power generation, predicted future water pumpage totals by county-basin were distributed among the same wells and locations used by those water users in 1999. Irrigation, county-other, and

livestock pumpage estimates for each county-basin from 2000 to 2050 also utilized the same spatial distribution within county-basins as was used in 1999.

Groundwater withdrawal estimates from the Carrizo-Wilcox aquifer for the years 1980 and 1990, and predictions for 2000, 2010, 2020, 2030, 2040, and 2050 in those counties, or portions of counties, within the model area are provided in Tables D1.1 through D1.6 in Appendix D1. It should be noted that these estimates are the sums of model grid cells. Because the 1 square mile grid cells often cross county boundaries, and are added to that county total in which the center of the grid cell occurs, these county-level estimates are not exact. County-level estimates also may not match the original TWDB estimate because a portion of the county occurred outside the model domain or in inactive model cells, because the location of groundwater withdrawal could not be identified, or because the groundwater was found to have been pumped from a different aquifer based on well properties.

Based on this analysis, approximately 313,000 acre-feet of groundwater were withdrawn from the modeled portion of the Carrizo-Wilcox aquifer in 1980 (Table 4.7.1). The amount of groundwater withdrawn declined by approximately 10% to roughly 282,000 acre-feet by 1990. Based upon regional water planning databases, it is estimated that only approximately 181,000 acre-feet were withdrawn in the year 2000. Based upon the regional water plans, groundwater withdrawals from the modeled aquifers are expected to increase slightly through the year 2020, then decline through 2030. From 2030 to 2050, withdrawals are expected to increase with groundwater withdrawals in 2050 expected to total approximately 160,000 acre-feet, roughly half of the 1980 level. Figures 4.7.2 through 4.7.7 show the 1990 pumping demand for the six model layers. These figures show that the predominant aquifer being used in the model area is the Carrizo (layer 3). Moderate quantities of groundwater are produced from aquifers younger than the Carrizo-Wilcox in the study area (Figure 4.7.2). The pumping analysis indicates that there is some production from permeable sands in the Reklaw east of the Frio River and in the Bigford west of Frio River. The upper and middle Wilcox layers show their greatest use in the Wintergarden area. The lower Wilcox layer (Figure 4.7.7) only provides adequate supplies of potable water in the outcrop and the shallow confined section in Zavala County.

Historically, agricultural irrigation has been responsible for the largest withdrawals from the Carrizo-Wilcox aquifer in the study area, particularly in Atascosa, Zavala, and Frio counties.

However, irrigation water use from the Carrizo-Wilcox in this area is expected to decline substantially. Municipal use of water from the Carrizo-Wilcox is expected to continue to increase, particularly in Bexar, Atascosa, Guadalupe, and Webb counties.

Appendix D2 provides post plots for the pumping distribution in AFY for each model layer for years 1980, 1990, 2000, and 2050. Appendix D3 provides bar charts of total pumping in AFY by year from 1980 through 2050 organized by county.

Table 4.7.1 Rate of groundwater withdrawal (AFY) from all model layers of the Carrizo-Wilcox aquifer for counties within the study area.

COUNTY	1980	1990	2000	2010	2020	2030	2040	2050
ATASCOSA	72676	56463	18938	19388	19916	8905	11365	18926
BASTROP	830	1233	5612	6655	7698	8829	10259	12793
BEE	0	0	80	81	80	82	84	88
BEXAR	7658	6681	36709	37699	37688	32316	32882	31340
CALDWELL	2184	3163	7245	7608	7972	8312	8363	8390
DEWITT	9	10	0	0	0	0	0	0
DIMITT	22321	9350	10360	10070	10111	10476	10562	10704
FAYETTE	87	105	8	8	7	7	6	6
FRIO	77550	83623	20587	20680	20736	5614	5723	5808
GONZALES	3516	4589	3174	2998	2837	2688	2640	2607
GUADALUPE	2060	2680	12761	14176	15769	18001	19879	21254
KARNES	1650	841	3266	2932	2782	2591	2556	2532
LA SALLE	9068	7320	4922	4752	4552	4116	3979	3839
LAVACA	4	2	0	0	0	0	0	0
LIVE OAK	115	80	171	171	171	171	171	171
MAVERICK	1203	3625	576	1061	1601	1505	1367	1244
MCMULLEN	433	1560	578	510	470	440	414	395
MEDINA	8433	1630	6556	6612	6650	2422	2476	2570
UVALDE	4740	366	4442	4388	4345	1544	1533	1512
WEBB	347	712	2580	7430	9096	12597	12599	12628
WILSON	10031	15879	13679	13570	12370	11276	11901	12613
ZAVALA	85741	80449	26771	26789	26744	7465	7704	8005
Total	312636	282351	181015	189588	193615	141387	148503	159475

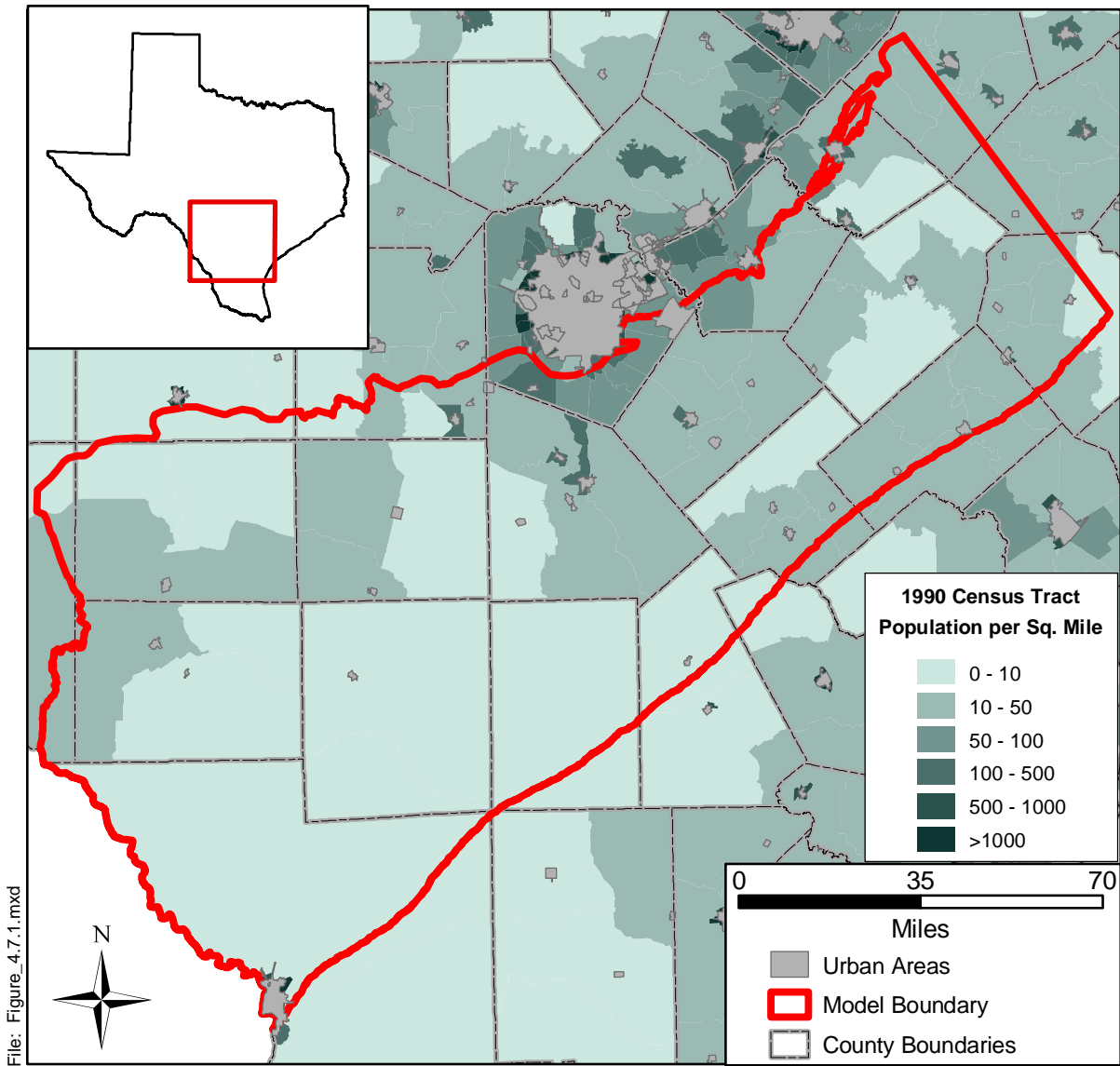


Figure 4.7.1 Rural population density in the study area.

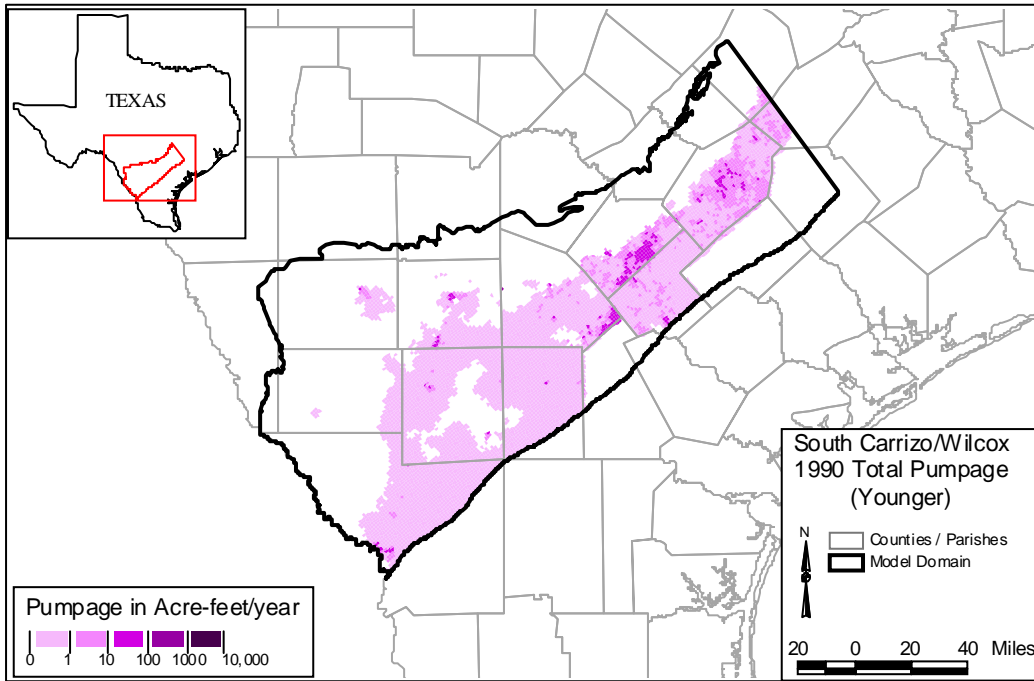


Figure 4.7.2 Younger (Layer 1) Pumpage, 1990 (AFY).

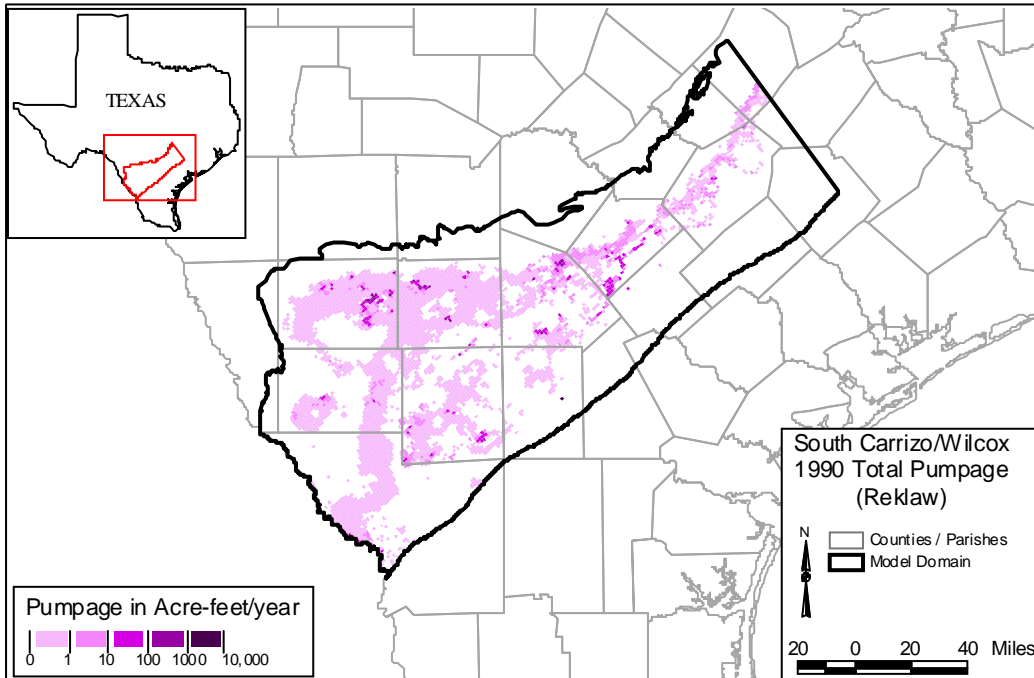


Figure 4.7.3 Reklaw (Layer 2) Pumpage, 1990 (AFY).

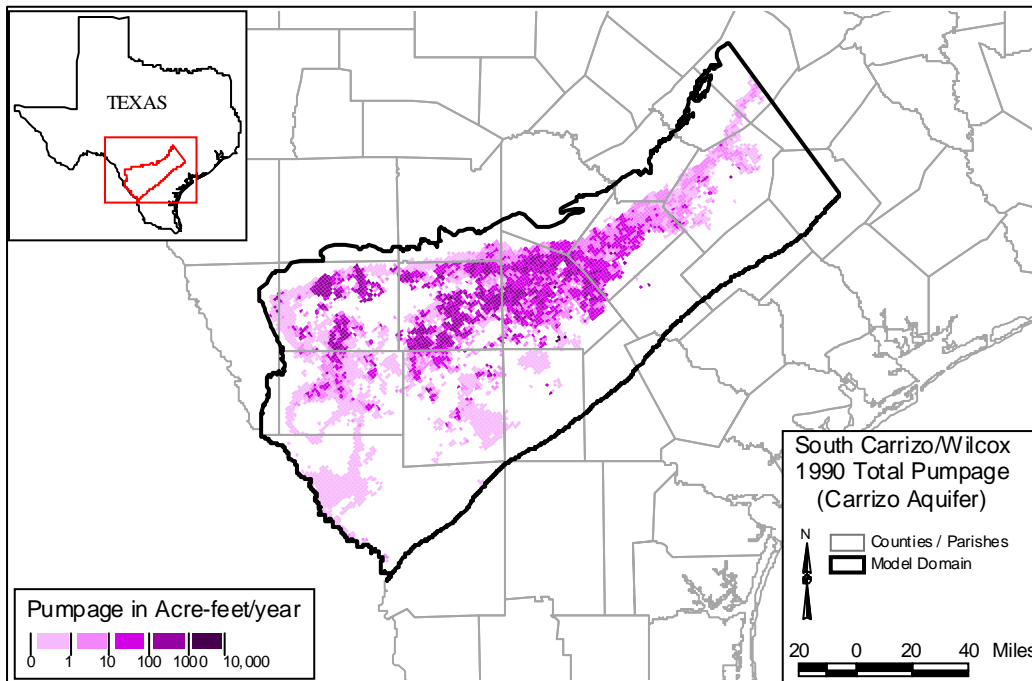


Figure 4.7.4 Carrizo (Layer 3) Pumpage, 1990 (AFY).

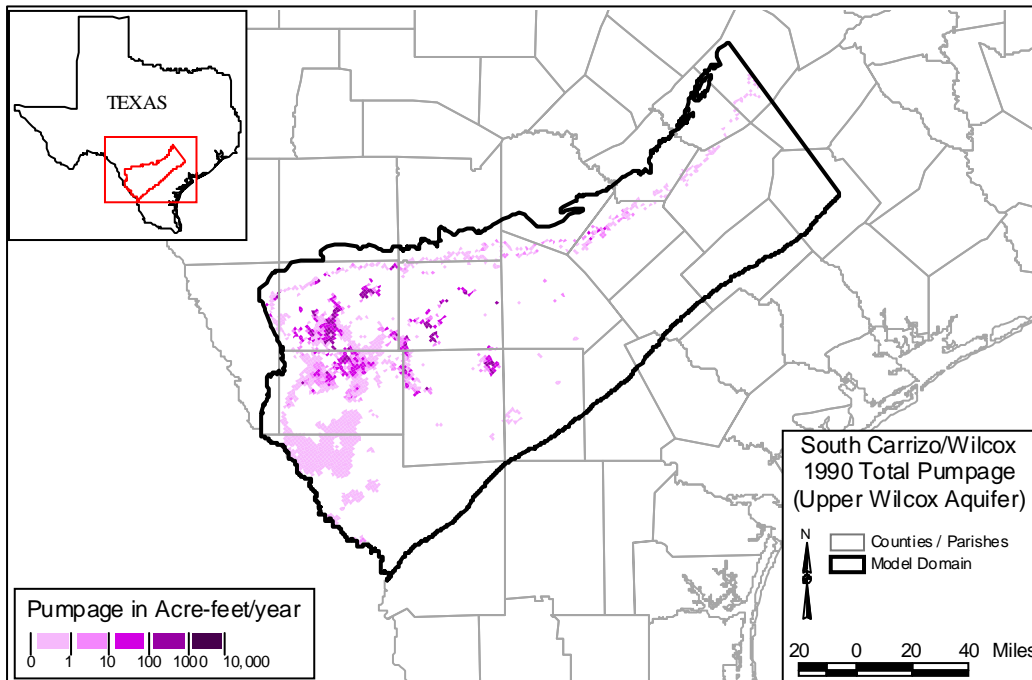


Figure 4.7.5 Upper Wilcox (Layer 4) Pumpage, 1990 (AFY).

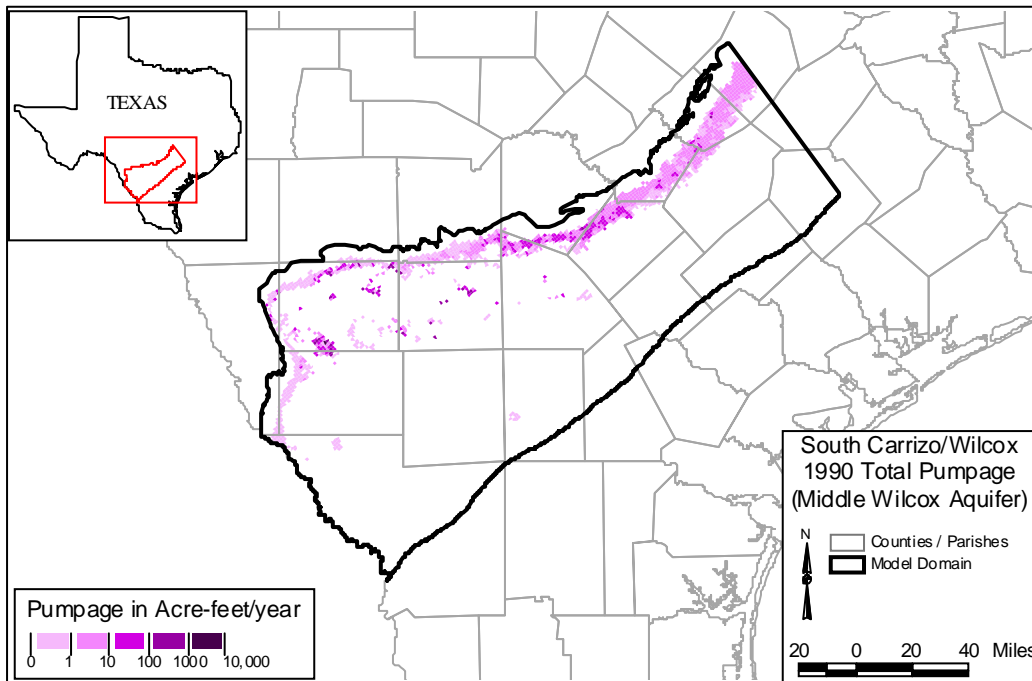


Figure 4.7.6 Middle Wilcox (Layer 5) Pumpage, 1990 (AFY).

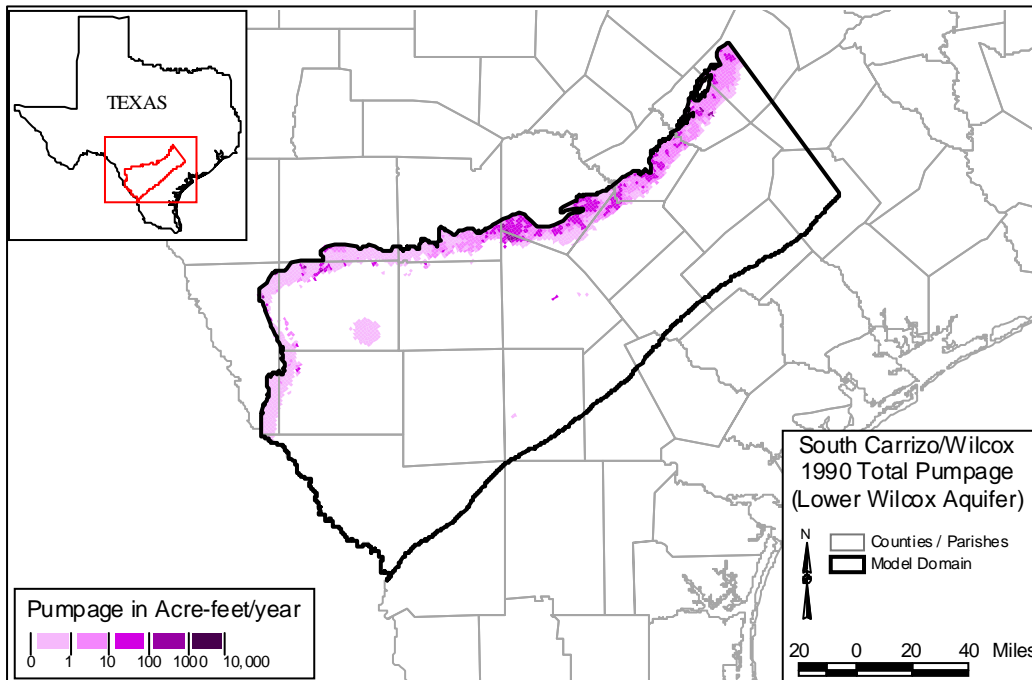


Figure 4.7.7 Lower Wilcox (Layer 6) Pumpage, 1990 (AFY).

4.8 Water Quality

Water quality data for the southern Carrizo-Wilcox aquifer were examined in terms of drinking water quality, irrigation water quality, and industrial water quality, which are described in detail in Appendix F. For the water-quality assessment, available water quality measurements derived from various databases were compared to screening levels for specific constituents (Table F.1 and F.2). Screening levels for drinking water supply are based on the maximum contaminant levels (MCLs) established in National Primary and Secondary Drinking Water Regulations. Irrigation water quality is evaluated based on the concentrations of specific constituents, such as boron, chloride, and TDS, as well as the salinity hazard, owing to their limited tolerance for crop irrigation. Groundwater suitability for industrial purposes is indicated by the content of dissolved solids, as well as its corrosiveness and tendency to form scale and sediments (Table F.1 and F.2). Table F.1 indicates for each constituent the percent of wells in the Carrizo-Wilcox aquifer exceeding the screening levels, and Table F.2 list the percentage of wells in individual counties exceeding one or more screening levels. The spatial concentration distributions of selected constituents in the southern Carrizo-Wilcox aquifer are shown in Figures F.1 through F.7. Note that these water quality data have been reported to the different state agencies and are typically from operational wells. Wells that were drilled and subsequently abandoned due to insufficient yield or unsuitable water quality are typically not reported and may not be included in the available databases.